



University of HUDDERSFIELD

University of Huddersfield Repository

Sadiq, Sohaib

Characterization of Bacterial Exopolysaccharides

Original Citation

Sadiq, Sohaib (2015) Characterization of Bacterial Exopolysaccharides. Doctoral thesis, University of Huddersfield.

This version is available at <http://eprints.hud.ac.uk/id/eprint/23888/>

The University Repository is a digital collection of the research output of the University, available on Open Access. Copyright and Moral Rights for the items on this site are retained by the individual author and/or other copyright owners. Users may access full items free of charge; copies of full text items generally can be reproduced, displayed or performed and given to third parties in any format or medium for personal research or study, educational or not-for-profit purposes without prior permission or charge, provided:

- The authors, title and full bibliographic details is credited in any copy;
- A hyperlink and/or URL is included for the original metadata page; and
- The content is not changed in any way.

For more information, including our policy and submission procedure, please contact the Repository Team at: E.mailbox@hud.ac.uk.

<http://eprints.hud.ac.uk/>

CHARACTERIZATION OF BACTERIAL **EXOPOLYSACCHARIDES**

SOHAIB SADIQ BSEd, MSc

University of
HUDDERSFIELD
Inspiring tomorrow's professionals

A thesis submitted to the University of Huddersfield in partial fulfilment of the
requirements for the degree of Doctor of Philosophy

Department of Chemical and Biological Sciences

School of Applied Sciences

The University of Huddersfield

February 2015

ABSTRACT:

The present study investigated the structural characterization of exopolysaccharides (EPS) produced by *Campylobacter jejuni*, *Bifidobacterium animalis* subsp. *lactis* and a number of *Bifidobacterium breve* strains. Nuclear magnetic resonance (NMR) spectroscopy, size exclusion chromatography coupled with multiangle laser light scattering (SEC-MALLS), anion exchange chromatography, HPAEC-PAD analysis, monomer and linkage analysis employing GC-MS have been used to characterise the EPS structures.

Monomer analysis of the EPS produced by *Campylobacter jejuni* showed the presence of glucose, linkage analysis showed the presence of an α -(1 \rightarrow 6) glycosidic linked repeating monomer unit and NMR (1D- and 2D- experiments) showed that the EPS is an α -dextran.

NMR and size exclusion chromatography analysis for *B. animalis* subsp. *lactis* shows the presence of a complex mixture of EPS. Monomer analysis for different batches suggests that each contains variable amounts of rhamnose, glucose and galactose along with trace levels of mannose. The results of the linkage analysis indicate that a complex mixture of differently linked sugars is present including : terminal rhamnose, 1,2-linked rhamnose, 1,3-linked rhamnose, terminal hexoses, 1,2,3-linked rhamnose, 1,4-linked hexose, 1,3-linked hexose, 1,6-linked hexose, *N*-acetyl sugars and 1,3,4-linked hexoses. SEC-MALLS showed the presence of different molecular weight EPSs. Uronic acid analysis showed that in 5.0 mg of EPS sample, only 0.28 mg of uronic acid is present.

1D- and 2D-NMR experiments were performed on the EPS samples produced by *B. breve* strains including UCC2003, JCM7017, JCM7019 and NCFB2258. Analysis of EPS extracted from cells using sodium hydroxide (NaOH) showed that complex mixtures of polysaccharides were being recovered. However, a common set of NMR signals was present in all the EPS samples from *B. breve*. Analysis of this set of signals suggests that, on treatment of cells with NaOH, a β -(1 \rightarrow 6)-linked glucan is released from a variety of bifidobacterial strains.

ACKNOWLEDGEMENTS

First of all, I would like to thank the ALMIGHTY, the Creator and the Guardian, and to whom I owe my very existence, for giving me the strength and health to complete my PhD.

I would like to express my deep and sincere gratitude to my supervisor and Director of Research, Prof. Andrew P. Laws. His wide knowledge and his logical way of thinking have been of great value for me. His encouragement, understanding, personal guidance, detailed and constructive comments and for his important support throughout this work have provided a good basis for the present report.

I would also to thank my Institution and my faculty members Dr. Neil McClay (NMR), Dr. Richard Hughes (Chromatography), Dr. Marcus Chadha (MALLS), Mr. Jim Rooney, Ms. Janet Clowery and Ms. Julie Walker for their willingness to help and to give their best suggestions. My research would have been a distant reality without their help.

I would also like to thank my parents, my sister Ms. Rizwana Sadiq, my two brothers Mr. Owais Sadiq and Dr. Soban Sadiq, who have always unselfishly supported, encouraged and believed in me, in all my present and future endeavours.

I would also like to thank my wife for making me a proud father of three beautiful children-Haris, Hamza and Hashir (who was born during my PhD) and her unselfish support throughout my PhD. Najma thank you from the bottom of my heart.

Lastly, this report would not have been possible without the guidance and the help of several individuals who in one way or another contributed and extended their valuable assistance throughout my PhD.

Sohaib Sadiq

Glossary

Chemical terms

Acetyl-CoA	Acetyl coenzyme
ADP	Adenine diphosphate
ATP	Adenine triphosphate
<i>B.</i>	<i>Bifidobacterium</i>
<i>C. jejuni</i>	<i>Campylobacter jejuni</i>
CPS	Capsular polysaccharides
D ₂ O	Deuterium oxide
Da	Daltons
DCM	Dichloromethane
DEAE	<i>N,N</i> -Diethylaminoethyl
Del.	Deletion mutant
D-Gal	D-galactose
D-Glc	D-glucose
DMSO	Dimethyl sulfoxide
DNA	Deoxyribonucleic Acid
<i>E. Coli</i>	<i>Escherichia Coli</i>
EDTA	Ethylenediaminetetraacetic acid
EPM	Extracellular polymeric matrix
EPS	Exopolysaccharide
FOS	Fructooligosaccharides
FQ	Fluoroquinolone
Fuc	Fucose
g/L	Grams per Litre
GalNAc	<i>N</i> -acetyl galactosamine
GDP	Guanosine diphosphate
GIT	Gastrointestinal tract
GlcA	Glucuronic acid
GlcNAc	<i>N</i> -acetyl glucosamine
GOS	Glucooligosaccharides
GPC	Gel permeation chromatography
GRAS	Generally regarded as safe
GUT	Gastrourinogenital tract (Alimentary canal)
He	Helium
HMw	High molecular weight
Hz	Hertz
LAB	<i>Lactic acid bacterium</i>
LMw	Low molecular weight
LOS	Lipooligosaccharides
LPS	Lipopolysaccharides
L-Rha	L-Rhamnose
Mbp	Mega base pairs
MHDP	<i>Meta</i> hydroxydiphenyl

mL	Millilitres
mM	Millimolar
MMw	Medium molecular weight
MRS Agar	de Man, Rogosa and Sharpe Agar
M _w	Molecular weight
M _w /M _n	Weight average/molar mass dispersity
MWCO	Molecular weight cut off
NADH	Nicotinamide adenine dinucleotide
NAG	<i>N</i> -acetylglucosamine
NAM	<i>N</i> -acetylmuramic acid
NDP	Nucleoside diphosphate
NMP	Nucleoside monophosphate
PCP	Polysaccharides copolymerase
pH	Hydrogen ion concentration
pI	Isoelectric point
pK _a	Acid dissociation constant
PMAA	Permethylated alditol acetates
PPM	Parts per million
Rha	Rhamnose
rRNA	Ribosomal ribonucleic acid
SDS/NaDS	Sodium dodecyl sulphate
spp.	species
TDP	Tyrosine diphosphate
TLC	Thin layer chromatography
UAs	Uronic acids
UDP	Uridine diphosphate

Experimental terms

COSY	Correlation spectroscopy
CZE	Capillary zone electrophoresis
Dept	Distortionless enhancement of polarization transfer
dn/dc	Refractive index increment
GC-MS	Gas chromatography-Mass spectrometry
HMBC	Heteronuclear multiple bond correlation spectroscopy
HPAEC-PAD	High performance anion exchange chromatography-pulsed amperometric detector
HPLC	High performance liquid chromatography
HSQC	Heteronuclear single quantum coherence spectroscopy
LC-MS	Liquid chromatography-Mass spectrometry
NMR	Nuclear magnetic resonance
RI	Refractive index
SEC-MALLS	Size exclusion chromatography-Multiangle laser light scattering
TOCSY	Total correlation spectroscopy
UV	Ultra violet

Contents

LIST OF FIGURES.....	viii
LIST OF TABLES.....	x
1. General Introduction.....	1
1.1 Carbohydrates:.....	1
1.1.1 Monosaccharides:.....	1
1.1.2 Monosaccharide derivatives	5
1.1.3 Disaccharides:	9
1.1.4 Oligosaccharides:	10
1.2 Polysaccharides:.....	11
1.2.1 Storage polysaccharides:	12
1.2.2 Structural polysaccharides:.....	14
1.3 Bacterial Polysaccharides:.....	15
1.3.1 Bacterial Capsular Polysaccharides (CPSs):.....	17
1.4 Exopolysaccharides [EPS]:.....	18
1.4.1 Applications of EPS:.....	21
1.4.2 Negative attributes of EPS:	22
1.4.3 EPS Biosynthetic pathway:.....	23
1.4.4 Extraction of EPS:	25
1.4.5 Purification of EPS by Size Exclusion Chromatography (SEC):	27
1.4.6 Purification of EPS by Ion Exchange Chromatography (IEX):	28
1.5 Characterisation of EPS:.....	30
1.5.1 Monomer Analysis:	30
1.5.2 High Performance Anion Exchange Chromatography with Pulsed Amperometric Detection (HPAEC-PAD) analysis:.....	32
1.5.3 Gas Chromatography (GC) Analysis:	33
1.5.4 Capillary Electrophoresis (CE):	34
1.5.5 Linkage Analysis:	35
1.5.6 NMR analysis of Exopolysaccharides:	37
1.5.7 MultiAngle Laser Light Scattering (MALLS):.....	39
1.5.8 Weight – Average Molecular Weight Determination	40
1.5.9 SEC – MALLS Analysis of Exopolysaccharides	40
1.5.10 Uronic acid determination:.....	43
1.6 AIM OF RESEARCH:	44

2.	EXPERIMENTAL	46
2.1	General Reagents:.....	46
2.2	Exopolysaccharides:.....	46
2.3	Structural Characterisation/Analysis of EPS:	47
2.3.1	Nuclear Magnetic Resonance (NMR):.....	47
2.3.2	Monomer analysis:.....	47
2.3.3	Linkage analysis:.....	49
2.3.4	Gas chromatography-Mass spectrometry (GCMS):	51
2.3.5	Size Exclusion Chromatography–Multi Angle Laser Light Scattering (SEC-MALLS)	51
2.3.6	Preparative size exclusion chromatography (SEC):.....	53
2.3.7	Preparative anion exchange chromatography (IEC):	55
2.3.8	DIALYSIS:	56
2.3.9	Uronic acid analysis:.....	57
3.	Analysis of the EPS recovered from <i>Campylobacter jejuni</i>	61
3.1	General Introduction:	61
3.2	<i>Campylobacter jejuni</i> :	62
3.2.1	<i>Campylobacter enteritis</i> :.....	64
3.2.2	Antibiotic resistance:	64
3.3	Present work on <i>Campylobacter jejuni</i> :.....	65
3.4	Aim of the study:.....	65
3.5	Experimental :	66
3.5.1	General Reagents:.....	66
3.5.2	<i>Campylobacter jejuni</i> samples:	66
3.6	Structural Characterisation/Analysis of EPS:	66
3.6.1	Nuclear Magnetic Resonance (NMR):.....	66
3.6.2	Monomer analysis using HPAEC-PAD:	66
3.6.3	Linkage analysis using GC-MS :	66
3.6.4	Gas chromatography–Mass spectrometry (GC-MS):	67
3.7	Results and Discussions:	67
3.7.1	Structural analysis using NMR:	67
3.7.2	Structural analysis using GC-MS and HPAEC - PAD:.....	74
3.7.3	Monomer Analysis by HPAEC - PAD:.....	74
3.7.4	Monomer Analysis by GC - MS:.....	76
3.7.5	Linkage analysis:.....	79

3.8	Conclusion:.....	83
4.	Analysis of the EPS recovered from <i>Bifidobacterium animalis</i> subsp. <i>lactis</i>	85
4.1	Introduction - Bifidobacteria:.....	85
4.1.1	Physiology:	88
4.1.2	Hexose Metabolism:	89
4.1.3	<i>Bifidobacterium</i> spp. - as Probiotics:	91
4.2	Exopolysaccharides (EPS) Samples:	92
4.3	Results and Discussion:	94
4.3.1	NMR Analysis	94
4.3.2	SEC – MALLS Analysis of EPS:.....	96
4.3.3	Preparative Size Exclusion Chromatography:	98
4.3.4	Monosaccharide analysis of EPS by GC - MS:	103
4.3.5	Monosaccharide analysis of EPS by HPAEC-PAD:	105
4.3.6	Uronic Acid Analysis:.....	108
4.3.7	Linkage analysis of EPS by GCMS:	109
4.3.8	Analysis of EPS by Ion Exchange Chromatography (IEX) – using DEAE – Sephacel:....	114
4.4	Conclusion:.....	122
4.5	Future work:.....	122
5.	Analysis of the Exopolysaccharides recovered from <i>Bifidobacterium breve</i> strains	124
5.1	Current work on <i>Bifidobacterium</i> spp.:.....	124
5.2	Identifying the EPS gene cluster in <i>B. breve</i> UCC2003:.....	125
5.3	Aim of the study:.....	127
5.4	Samples provided:.....	128
5.5	Analysis techniques used:	128
5.6	Results and Discussions:	128
5.6.1	NMR analysis of the crude sample:.....	128
5.7	Conclusion:.....	140
5.8	Future Work:.....	140
6.	Overall Conclusion:	130
6.1	Future work:.....	130
7.	References:	144
8.	Publications:.....	145

LIST OF FIGURES

Figure 1: D-Glyceraldehyde.....	1
Figure 2: Aldose and Ketose.....	2
Figure 3: Howarth projections of D-glucose	2
Figure 4: Red coloured bonds are out of page and blue coloured bonds are into the page.....	3
Figure 5: Examples of enantiomers	3
Figure 6: Epimers (D-Glucose & D-Mannose).....	4
Figure 7: Diastereoisomers (D-Glucose & D-altrose).....	4
Figure 8: Howarth projections of α -D-glucopyranose and β -D-glucopyranose.....	5
Figure 9: β -D-glucose-1-phosphate	5
Figure 10: Mannitol.....	6
Figure 11: Structures of D-Ribose, D-2-Deoxyribose and D-Rhamnose.....	6
Figure 12: The rhamnose pathway	7
Figure 13: Structures of D-glucosamine and D-galactosamine.....	8
Figure 14: Structures of D-glucose and D-gluconic acid	8
Figure 15: Structures of D-glucose and D-glucuronic acid.....	9
Figure 16: Structure of Sucrose; β -D-fructofuranosyl-(1 \rightarrow 2)- α -D-glucopyranoside	9
Figure 17: Structure of Maltose; α -D-glucopyranosyl-(1 \rightarrow 4)- β -D-glucopyranose	10
Figure 18: Structure of α -D-galactopyranosyl-(1 \rightarrow 6)- α -D-glucopyranosyl-(1 \rightarrow 2)- β -D-fructofuranoside,	10
Figure 19: Structure of starch showing 4 glucose molecules	13
Figure 20: Structure of cellulose	14
Figure 21: Structure of chitin consists of N-acetyl-D-glucosamine units.....	14
Figure 22: Cell location of polysaccharides produced by Gram-positive and.....	16
Figure 23: Gram positive bacterium has a thick layer of peptidoglycan that contains teichoic acids..	17
Figure 24: Possible health-promoting properties of EPS produced by LAB.....	22
Figure 25: Processes for EPS biosynthesis	24
Figure 26: Schematic representation of EPS extraction process	26
Figure 27: Schematic diagram of SEC.....	28
Figure 28: DEAE-anion exchanger.....	29
Figure 29: Monomer analysis reaction scheme	31
Figure 30: Linkage reaction scheme	37
Figure 31: Laser light scattering scheme.....	39
Figure 32: Schematic diagram for SEC-MALLS system.....	41
Figure 33: Gradient increase steps in anion exchange chromatography system	55
Figure 34: Uronic acid detection-Protocol.....	58
Figure 35: Scanning Electron Microscopy Image of <i>Campylobacter jejuni</i>	63
Figure 36: 11168H Crude Proton NMR spectrum	67
Figure 37: KpsM Crude Proton NMR spectrum	68
Figure 38: NMR spectra comparison of 2 samples of <i>Campylobacter jejuni</i>	68
Figure 39: Structure of α -dextran	69
Figure 40: Comparison of 3 NMR spectra, blue = 11168H, red = α -dextran, green = kpsM.....	70
Figure 41: ^{13}C DEPT 135 NMR spectra of <i>Campylobacter jejuni</i>	71

Figure 42: Comparison of <i>Campylobacter jejuni</i> samples.....	71
Figure 43: Comparison of ¹ H– ¹ H COSY spectrum of an α-dextran.....	72
Figure 44: ¹ H– ¹³ C HSQC spectrum of <i>Campylobacter jejuni</i> sample 11168H	73
Figure 45: After hydrolysis - HPAEC–PAD chromatogram of <i>Campylobacter</i>	75
Figure 46: After hydrolysis - HPAEC–PAD chromatogram of <i>Campylobacter</i>	75
Figure 47: HPAEC – PAD chromatogram of Glucose.....	76
Figure 48: GC trace of monomer analysis of <i>Campylobacter jejuni</i> sample kpsM	77
Figure 49: MS of <i>C.jejuni</i> sample kpsM at 13. 413 min.....	78
Figure 50: MS of <i>C.jejuni</i> sample kpsM at 13.687 min.....	78
Figure 51: GC linkage chromatogram of <i>Campylobacter jejuni</i> sample 11168H.....	79
Figure 52: MS of the GC chromatogram at 16.353 min. of the sample (11168H) from <i>C. jejuni</i>	80
Figure 53: GC linkage chromatogram of an α–dextran.....	81
Figure 54: MS of the GC chromatogram at 16.411 min. of an α – dextran standard	81
Figure 55: Proton NMR of α-amylase (spectrum recorded at room temperature).....	82
Figure 56: Proton NMR of α-lactose (blue) and α-amylase (red)	83
Figure 57: Scanning electron micrographs of <i>B. longum</i> NCC2705 cells.	85
Figure 58: Hexose monosaccharides (glucose and fructose).....	90
Figure 59: A1dOx-Batch 9, Crude Proton NMR.....	94
Figure 60: A1-Batch 5, Crude Proton NMR	95
Figure 61: Comparison of ¹ H NMR spectra of A1dOx-Batch 9 (blue) and A1-Batch 5 (red)	95
Figure 62: Pullulan 1000ppm, flow rate 0.45mL/min., mobile phase 0.1M NaNO ₃ ,	96
Figure 63: SEC-MALLS trace of A1-batch 5.....	97
Figure 64: SEC-MALLS trace of A1dOx-Batch 9	97
Figure 65: Chromatograph obtained after passing A1-batch 5, through the SEC column	98
Figure 66: ¹ H NMR spectra comparison of fractions 18-24 with crude A1-batch 5.....	99
Figure 67: Region B, ¹ H NMR spectra comparison of fractions 18-24 with crude A1-batch 5	100
Figure 68: Region A, ¹ H NMR spectra comparison of fractions 18-24 with crude A1-batch 5.....	100
Figure 69: Chromatograph of A1dOx-batch 9, obtained after passing through the SEC column.....	101
Figure 70: Comparison of 1D-1H NMR spectra of combined fractions	102
Figure 71: GC trace of A1-batch 5 (monomer analysis).....	103
Figure 72: MS at 13.831 min. – Sample A1-batch 5 monomer analysis	104
Figure 73: GC trace of A1dOx-batch 9 (monomer analysis)	104
Figure 74: HPAEC chromatogram of A1-batch 5, after hydrolysis	106
Figure 75: HPAEC chromatogram of A1-dOx batch 9 after hydrolysis.....	107
Figure 76: Calibration graph of uronic acid conc. Vs absorbance at 525nm	109
Figure 77: GC trace generated for the PMAA’s derived during linkage analysis of A1-batch 5	110
Figure 78: GC trace generated for the PMAA’s derived during linkage analysis of A1dOx-batch 9... ..	110
Figure 79: GC trace of linkage analysis of A1- batch 5 with linked hexoses	111
Figure 80: Mass spectra fragmentation: A) Terminal glucose, B) 1→3 Linked galactose.....	112
Figure 81: Mass spectra fragmentation (16.199 min-Peak B) of sample A1-batch 5	113
Figure 82: Chromatograph of A1dOx batch-9, obtained after passing through the IEX	115
Figure 83: UV trace obtained from anion exchange chromatography	115
Figure 84: NMR spectrum of pooled fractions 35-39	116
Figure 85: Comparison of NMR spectra showing some anomeric and rhamnose methyls signals–..	117
Figure 86: ¹ H– ¹ H COSY spectrum of pooled fractions: 35-39	118

Figure 87: TOCSY (80ms) spectra of pooled fractions: 35-39	119
Figure 88: Combined COSY (red) and TOCSY (blue) spectra of pooled fractions: 35-39	120
Figure 89: ^1H - ^{13}C HSQC spectra of pooled fractions: 35-39	121
Figure 90: Schematic diagram of the eps gene cluster of <i>B. breve</i> UCC2003.....	126
Figure 91: Comparison of NMR spectra of <i>B. breve</i> samples labelled as <i>B. breve</i> strain	129
Figure 92: COSY spectrum of <i>B. breve</i> strain JCM7017.....	130
Figure 93: COSY and TOCSY overlaying spectrum of <i>B. breve</i> strain JCM7017	131
Figure 94: ^1H - ^{13}C HSQC spectrum of <i>B. breve</i> strain JCM7017.....	132
Figure 95: Comparison of <i>B. breve</i> UCC2003 EPS +ve sample showing only EPS peaks.....	133
Figure 96: Expanded anomeric region of <i>B. breve</i> UCC2003 EPS +ve sample (V=Signal varies).....	133
Figure 97: Comparison of the <i>B. breve</i> UCC2003 samples (EPS-ve {blue}, EDTA-ve {red}).....	134
Figure 98: ^1H - ^1H COSY spectrum of <i>B. breve</i> UCC2003 EPS -ve strain.....	135
Figure 99: ^1H - ^{13}C HSQC spectra of <i>B. breve</i> UCC2003 EPS -ve confirms the positions of carbons	136
Figure 100: ^1H - ^1H COSY spectrum of <i>B. breve</i> UCC2003 EPS +ve with connectivity	137
Figure 101: Comparison of ^1H - ^{13}C HSQC EPS +ve (blue) with EPS -ve (red)	138
Figure 102: Proton NMR of <i>B. breve</i> UCC2003 (del) showing no EPS peaks.....	139

LIST OF TABLES

Table 1: Some of the roles ascribed to exopolysaccharides in biofilms	19
Table 2: Some human disease associated with bacterial biofilms (red: Gram +ve, blue: Gram -ve)...	20
Table 3: Some of the extensively studied bacterial EPS	20
Table 4: Dissociation constants of some common carbohydrates	33
Table 5: Chemical shifts of carbon and proton atoms.....	73
Table 6: HPAEC – PAD retention times of standards	74
Table 7: Currently recongized <i>Bifidobacterium</i> species.....	86
Table 8: General features of completely sequenced some of the <i>Bifidobacterium</i> genomes	87
Table 9: SEC–MALLS results for Pullulan standard	96
Table 10: Standards with their retention time by HPAEC-PAD.....	105
Table 11: Monosaccharide unit comparison of relative area percentage of GC-MS/HPAEC-PAD	106
Table 12: Monosaccharide unit comparison of relative area percentage of GC-MS/HPAEC-PAD	107
Table 13: Showing retention times of different linked hexoses.....	111
Table 14: Bifidobacterial strain isolated from different human environments.....	124
Table 15: General features of eight complete genomes of <i>Bifidobacterium breve</i>	125
Table 16: ^1H NMR chemical shifts of <i>B. breve</i> strain JCM7017.....	130
Table 17: ^1H - ^{13}C HSQC, Carbon chemical shifts of <i>B. breve</i> strain 7017	132
Table 18: Proton NMR chemical shifts of <i>B. breve</i> UCC2003 EPS-ve.....	135
Table 19: Chemical shifts of ^{13}C and ^1H of <i>B. breve</i> UCC2003 EPS-ve	136

1. GENERAL

INTRODUCTION

1. General Introduction

Polysaccharides are complex carbohydrate polymers which exist as either linear or branched chains. These polysaccharides are produced by a large number of species including plants and bacteria. Bacteria present a range of biomolecules at the surface of the cells. A significant number of these are classified as carbohydrates.

1.1 Carbohydrates:

Carbohydrates are one of the most important classes of biomolecules and are responsible for controlling a wide variety of biological processes including energy generation in cells, they help in improving the immune system and they are involved in development and fertilization. Carbohydrates or *Saccharides*, derived from Latin for sugar – origin “sweet sand”, are simple organic compounds comprising of aldehydes and ketones and which also contain many hydroxyl groups, usually one on each carbon atom¹. Carbohydrates (polyhydroxylated aldehydes or ketones) are often classified according to the number of saccharide units they contain. They are monosaccharides (aldoses or ketoses), oligosaccharides (2-10 monomers) or polysaccharides (large linear or branched molecules containing many monosaccharide units).

1.1.1 Monosaccharides:

Monosaccharides are the simplest carbohydrates that cannot be hydrolyzed to smaller (simpler) carbohydrates (sugars). They may be subcategorized as aldoses (contains aldehyde functional group) or ketoses (contains ketone functional group)². The simplest three carbon sugar is glyceraldehyde.

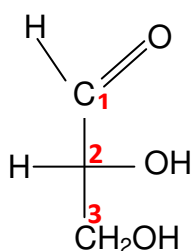


Figure 1: D-Glyceraldehyde

Monosaccharides are often represented as a Fischer projection formula, showing stereochemistry in straight chain organic compounds³. The most common, naturally occurring sugars are glucose (dextrose or blood sugar), galactose (in milk & dairy products) and fructose (in most vegetables & fruits). In their most common forms, monosaccharides contain five (pentoses) or six (hexoses) carbon atoms and they can cyclize to form ring systems where they are referred to as furanose or pyranose.

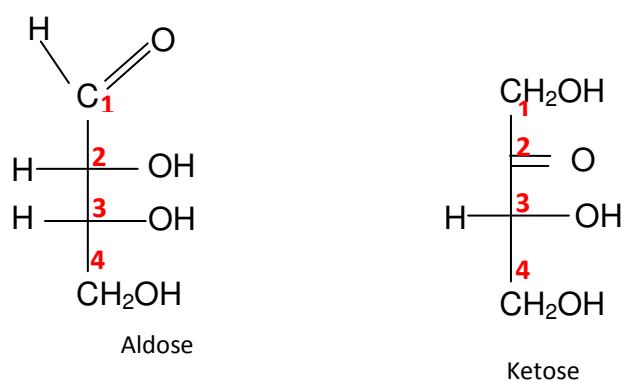


Figure 2: Aldose and Ketose

Pentoses or hexoses can cyclize to form either furanoses (five-membered ring) or pyranoses (six-membered ring)⁴.

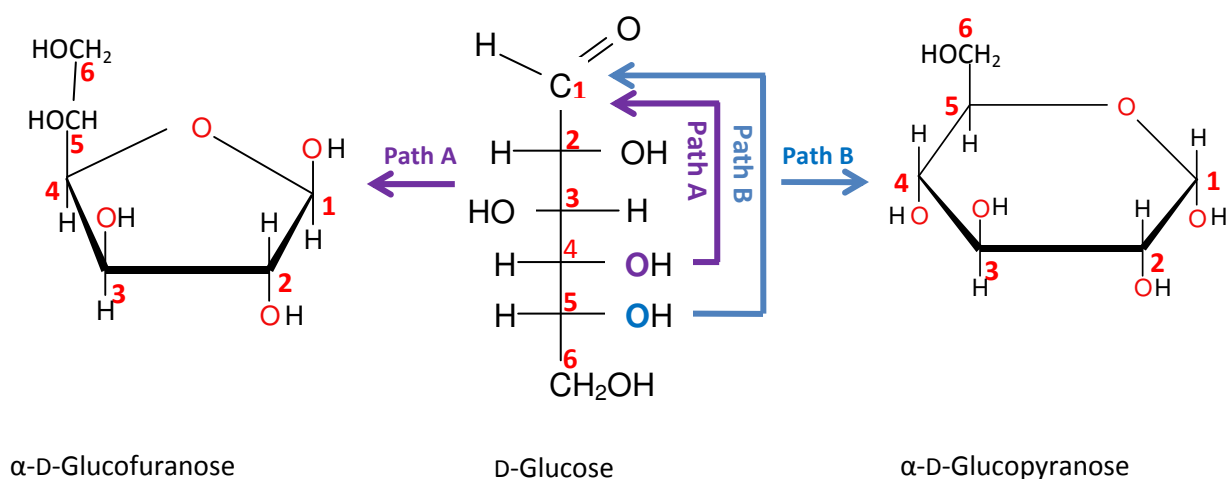


Figure 3: Haworth projections of D-glucose

The pyranose or furanose forms are formed by condensation of an alcohol (OH) with the carbonyl carbon to form a new asymmetric carbon⁵. If monosaccharides have more than one chiral centre, then they are prefixed as D- or L- conformations^{6,7}.

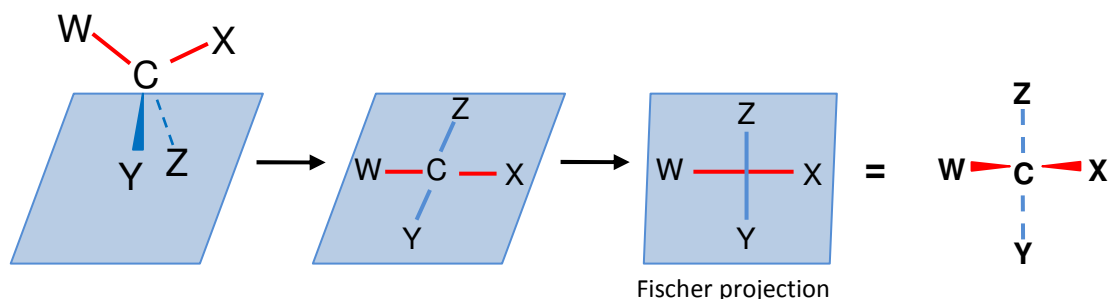


Figure 4: Red coloured bonds are out of page and blue coloured bonds are into the page

Fischer projections represent three-dimensional structures, in which a chiral carbon atom is represented as the intersection of two crossed lines. The aldehyde or ketone carbonyl group of a monosaccharide is always placed toward the top of the page, i.e: **Z** and the longest carbon chain is placed on the vertical axes with the bonds pointing away from the viewer.

Due to the fact that carbohydrates contain multiple stereocenters, many isomers are possible including enantiomers (non-superimposable mirror images, e.g: D and L isomers of glucose), diastereoisomers (chiral carbons are connected to exactly the same substrates but connected with differing configurations {R or S}, e.g: D-glucose and D-altrose) and epimers (are two diastereoisomers that differ only at one stereocentre, e.g: D-glucose and D-mannose)⁷.

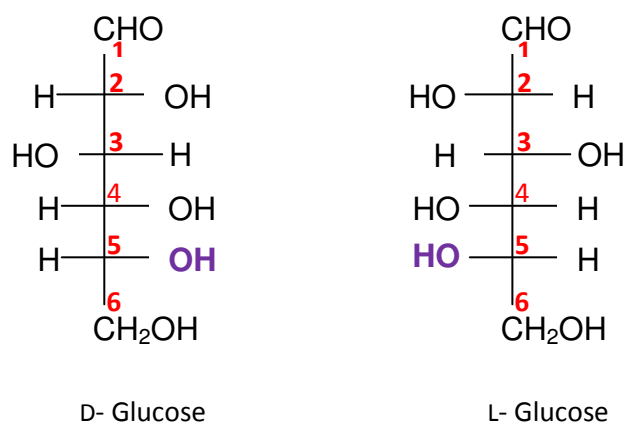


Figure 5: Examples of enantiomers

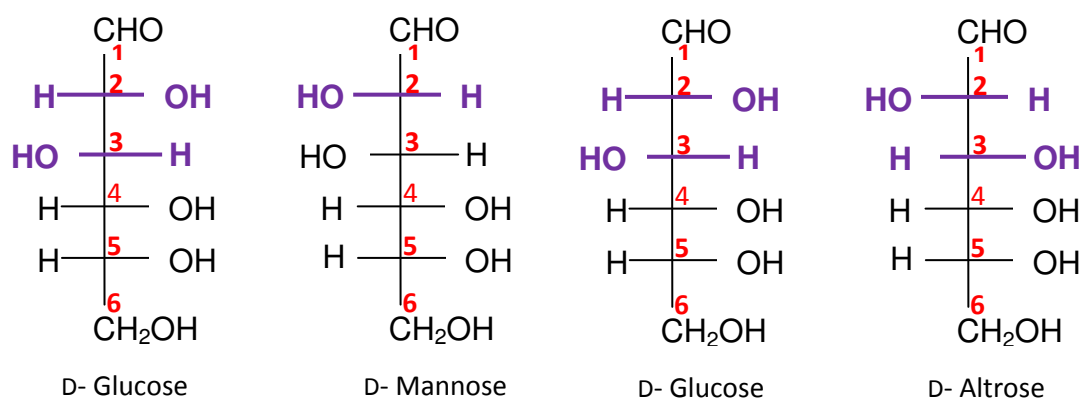


Figure 6: Epimers (D-Glucose & D-Mannose)

Figure 7: Diastereoisomers (D-Glucose & D-altrose)

Pentoses and hexoses can exist in different forms: open chain (Fischer projection), alpha (α)-sugar and beta (β)-sugar. Ring formation tends to be energetically more stable than open chains forms. Pentoses often cyclise into ring form structure called furanose whereas hexoses form cyclic sugars called pyranoses⁸. The two different forms of cyclic sugars (α and β) are referred to as anomers. During cyclization, the carbonyl carbon transforms into a new stereocentre. Cyclization causes the formation of 2 new diastereomers. They differ in the position of the attachment of a certain group relative to the new stereocentre. The new stereocentre is referred to as the anomeric carbon. If the OH group is attached to the anomeric carbon and the functional group is in a *cis* configuration with the highest priority substituent attached at the highest numbered carbon held within the ring, the anomeric carbon is " α -" and if the OH group is attached to the anomeric carbon and the functional group is in a *trans* configuration, the anomeric carbon is " β ". For example, in D-glucose, the hydroxyl group on carbon 5 attacks the carbonyl carbon forming a six membered ring (pyranose) with the carbon that was attacked being known as the anomeric carbon^{8,9}. Depending on the direction of the OH group, the anomeric carbon is either α or β .

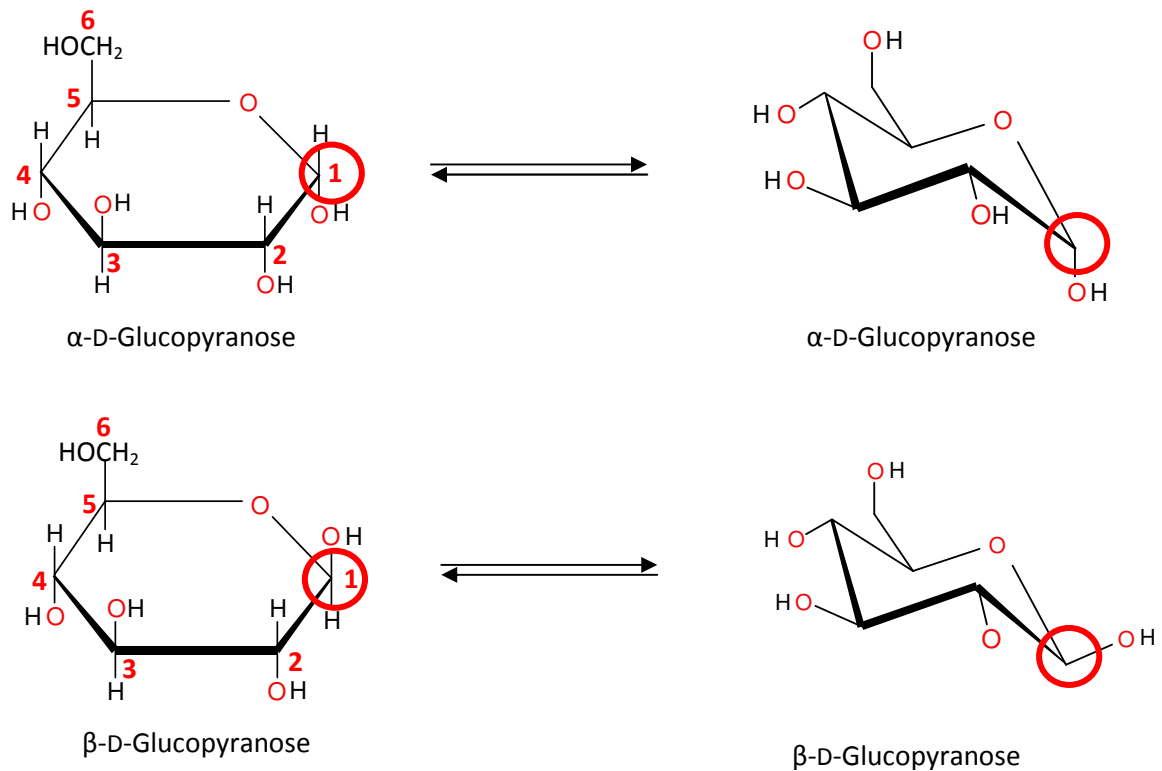


Figure 8: Haworth projections of α -D-glucopyranose and β -D-glucopyranose

1.1.2 Monosaccharide derivatives

In the natural environment, a large number of sugar derivatives are formed including sugar phosphates, alditols (sugar alcohols), amino sugars and deoxy sugars etc. Phosphorylated derivatives are made by the addition of a phosphate group to one of the hydroxyls¹⁰.

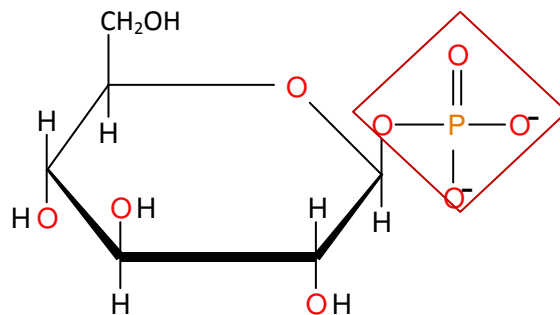


Figure 9: β -D-glucose-1-phosphate

Alditols (sugar alcohols) are made by reducing the carbonyl group of a sugar. The resulting polyhydroxy compounds are called alditols, like erythritol, D-mannitol and D-glucitol (sorbitol)¹⁰.

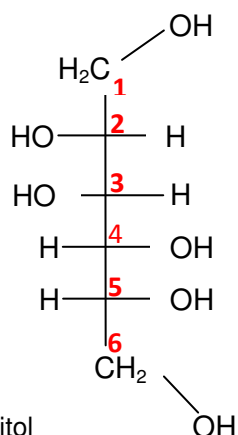


Figure 10: Mannitol

Alditols occur widely in nature, particularly in lower forms of life and they have a number of important physiological functions:

- i) Structural, as in the ribitol phosphate polymers in bacterial cell walls
- ii) Energy storage as in plants containing a large amount of mannitol polymers
- iii) Coenzyme regulation, as in bacteria that excrete large amounts of alditols formed by reduction of sugars in culture media
- iv) They are important intermediate sugar interconversions



Deoxy-sugars are formed when a hydrogen atom replaces one or more of the $-\text{OH}$ groups in the monosaccharide¹⁰.

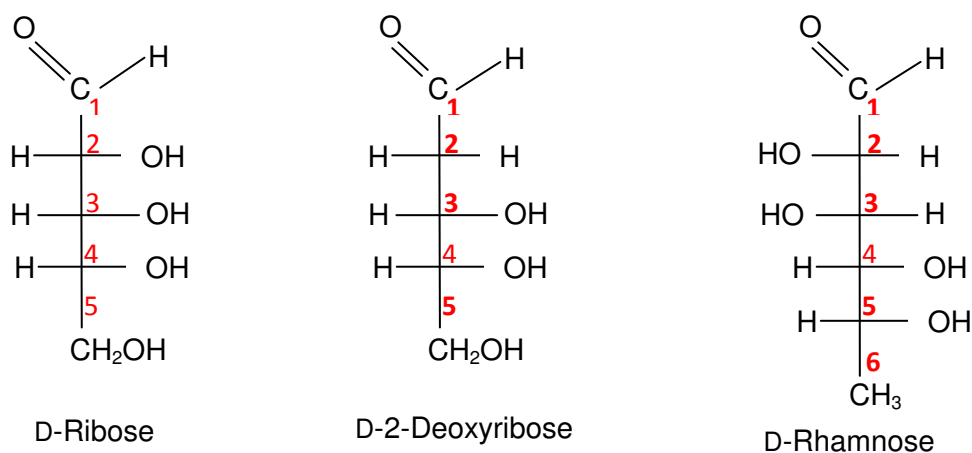


Figure 11: Structures of D-Ribose, D-2-Deoxyribose and D-Rhamnose

Deoxyribose is the most commonly known deoxy-sugar because it is the exact sugar used in DNA double helices. Unlike ribose, deoxyribose doesn't contain an OH group at its "2"-carbon, which would otherwise make it susceptible to hydrogen bonding with other molecules. Rhamnose is naturally present in its L-configuration (L-Rhamnose). Generally it is found in the cells of plants and bacteria rather than animals. It is thought that rhamnose is used in the body in cell proliferation and in the degradation of free radicals¹⁰. Rhamnose is frequently encountered in the polysaccharides presented at the surface of bacterial cells. In Gram-negative bacteria it is one of the important residues of the O-antigen of lipopolysaccharides, a factor that is responsible for the virulence of bacteria.

'Their Synthesis'

L-Rhamnose is a deoxy-sugar that is synthesized by bacteria from glucose-1-phosphate (Glu-1-P), with the help of enzymes: **RmlA** (catalyses the transfer of thymidylmonophosphate nucleotide to Glu-1-P), **RmlB** (catalyses the oxidation of C4 OH group of sugar), **RmlC** (catalyses an epimerisation reaction at positions C3 and C5) and **RmlD** (reduces the C4 keto function to generate the final product-dTDP-L-rhamnose)¹¹.

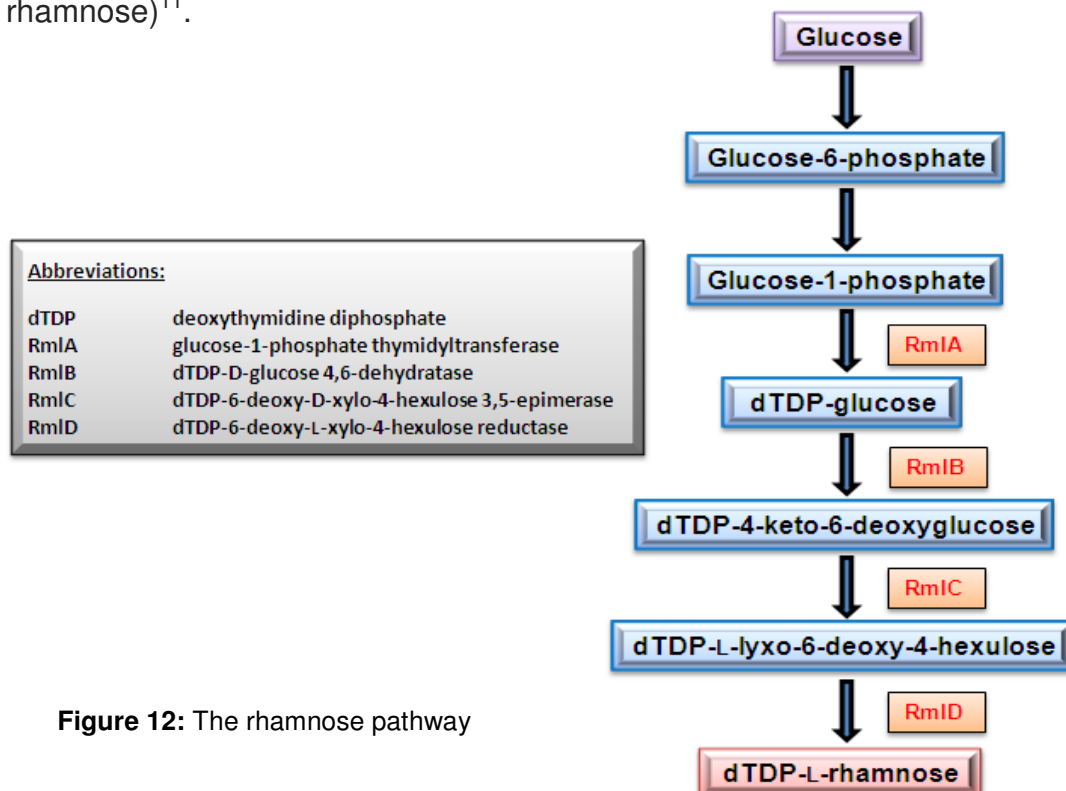


Figure 12: The rhamnose pathway

Amino sugars are the structural units used to make proteins (a short chain called a peptide and a longer chain is called a polypeptides or protein). Amino sugars are made when an -OH group of a monosaccharide has been replaced by an amino (-NH_2) group, e.g: D-glucosamine (present in exoskeletons of crustaceans {chitin}, arthropods and fungi), D-galactosamine (in glycoprotein hormones)¹⁰.

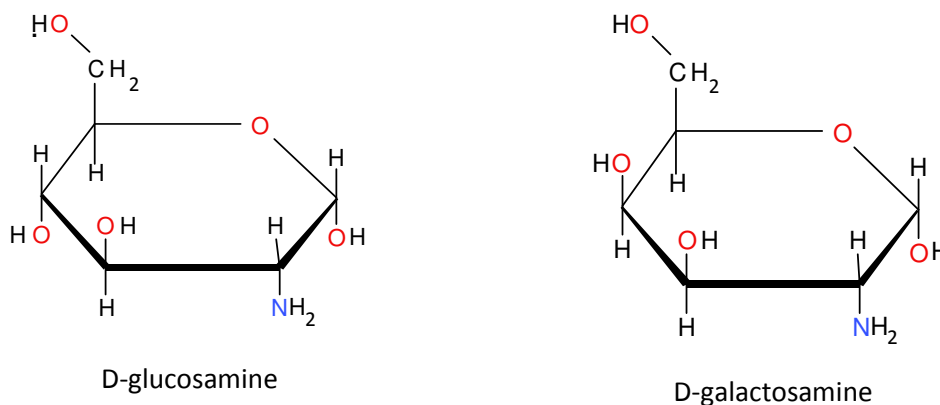


Figure 13: Structures of D-glucosamine and D-galactosamine

Carboxylic acid sugars are made when an aldehyde or alcohol group of a monosaccharide has been oxidized to form a carboxyl group¹⁰.

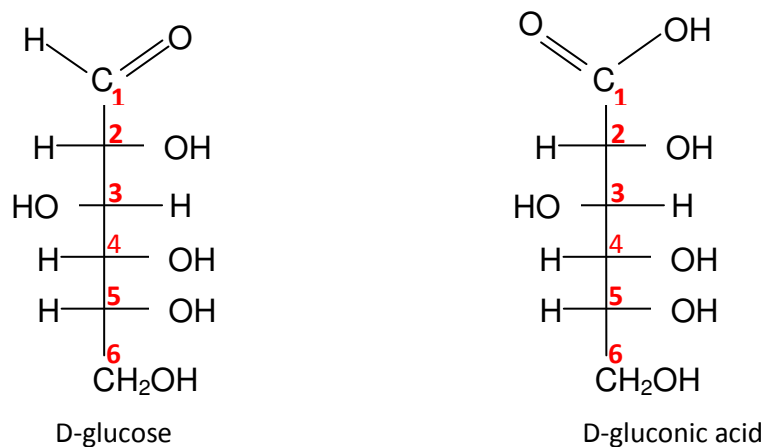


Figure 14: Structures of D-glucose and D-gluconic acid

Uronic acids (glucuronic acids, galacturonic acids) are a class of sugar acids with both carbonyl and carboxylic acid functional groups. They are formed when the terminal carbon's OH group have been oxidized to a carboxylic acid, e.g. pectins (a main component of cell wall and a polymer of galacturonic acid).

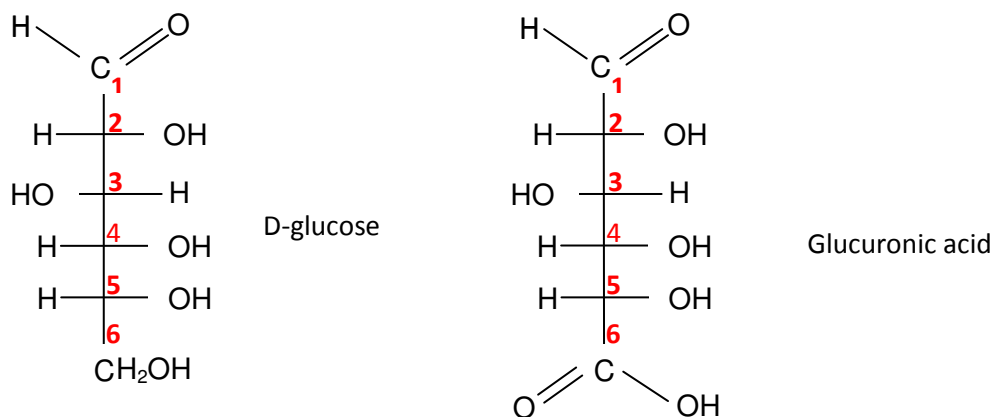


Figure 15: Structures of D-glucose and D-glucuronic acid

1.1.3 Disaccharides:

Disaccharides are sugars made by linking two monosaccharides by a glycosidic bond (OH of one sugar reacts with the anomeric carbon of another sugar) and which can be readily hydrolyzed by acid to give two monosaccharides. Thus disaccharides can be hydrolyzed to yield their free monosaccharide components by heating with dilute acid. e.g: sucrose (table sugar; glucose and fructose units are joined by acetal oxygen bridge in the α -1 on glucose {6 membered ring} and β -2 on fructose {5 membered ring}), maltose (food additive used as sweetener & preservative), lactose (sugar in milk—galactose and glucose units are joined by acetal oxygen bridge in the β -1 on galactose and α -4 on glucose).

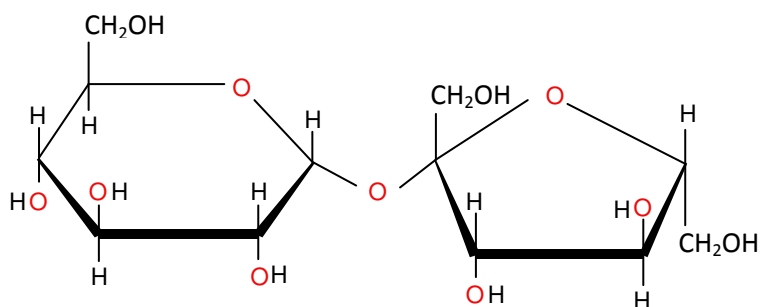


Figure 16: Structure of Sucrose; β -D-fructofuranosyl-(1 \rightarrow 2)- α -D-glucopyranoside

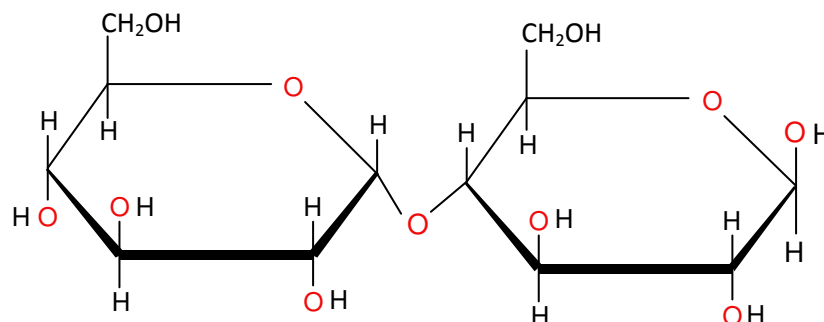


Figure 17: Structure of Maltose; α -D-glucopyranosyl-(1 \rightarrow 4)- β -D-glucopyranose

1.1.4 Oligosaccharides:

Oligosaccharides are low molecular weight carbohydrate polymers which contain between 3 and 10 monosaccharide units linked via O-glycosidic bonds that can be hydrolyzed by acid to give their constituent monosaccharide units, e.g: raffinose, a fructo-oligosaccharide which is found in many vegetables.

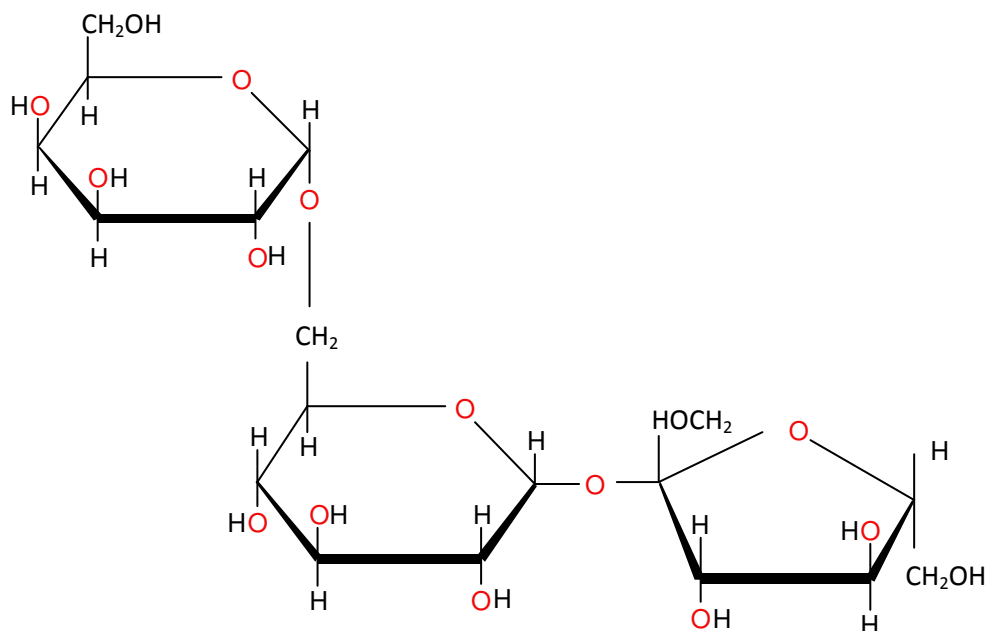


Figure 18: Structure of α -D-galactopyranosyl-(1 \rightarrow 6)- α -D-glucopyranosyl-(1 \rightarrow 2)- β -D-fructofuranoside, Trivial name: **Raffinose**

1.1.4.1 Functional Oligosaccharides:

Lipids and proteins on the cell membrane surface often have associated carbohydrate chains protruding out from the cell surface, known as glycoproteins and glycolipids, and these are often called functional oligosaccharides. They form hydrogen bonds with the water molecules surrounding the cell and thus help to stabilise membrane structure, e.g. fructooligosaccharides (FOS), glucooligosaccharides (GOS) and galactooligosaccharides¹². These oligosaccharides are found in varying concentrations in milk, honey, sugarcane juice, lentils, onions, tomato and bamboo shoots¹³.

1.2 Polysaccharides:

Polysaccharides are polymeric carbohydrate structures, composed of multiple mono- or disaccharide units joined together by glycosidic bonds. These structures are often linear, but may contain various degrees of branching. Polysaccharides are often heterogeneous, containing slight modifications of a repeating unit. Depending on the structure, these macromolecules can have distinct properties acquired from their monosaccharide building blocks. They may be amorphous or insoluble in water^{14,15}.

Polysaccharides can be classified into two separate groups based on their monomeric composition:

- i) When they are composed of a single monosaccharide building block, they are termed as **homopolysaccharides or homoglycans**, e.g: starch, glycogen or cellulose (hundreds of glucose molecules linked by glycosidic bonds)
- ii) When composed of different monosaccharides, they are termed as **heteropolysaccharides or heteroglycans**⁴, e.g: hyaluronic acid (formed of thousands of alternative units of *N*-acetylglucosamine and glucuronic acid).

Polysaccharides are composed of a monosaccharide repeating unit structure and may contain as many as nine different sugar residues in repeating units^{16,17,18}, and may possess substituents like acetyl, pyruvate etc. According to their roles/functions, polysaccharides can be divided into:

- a) Storage polysaccharides (examples include: starch and glycogen);
- b) Structural polysaccharides (examples include: cellulose and chitin).

1.2.1 Storage polysaccharides:

One of the main functions of polysaccharides (macromolecules) in living organisms is as food storage; examples include plant starch which is composed of amylose and amylopectin and glycogen which is a food storage polysaccharide in animals. Starches are polymers in which glucopyranose units are linked by α -linkages. It is made up of a mixture of amylose (15-20%) and amylopectin (80-85%). Amylose consists of a linear chain of several hundred (1,4)-linked glucose molecules and amylopectin consists of a branched structure of several hundred glucose (1,4)-linked units with varying levels of (1,6)-linked branching. These branches provide a mechanism for quick release/storage of glucose units for/from metabolism; a phosphorylase releases glucose-1-P products from amylose or amylopectin chains. They make ideal storage molecules for energy:

- a) as they are large, this makes them insoluble in water and therefore exert no osmotic or chemical effect on the cell;
- b) they change into compact shapes;
- c) they are easily converted into the required sugars whenever needed.

Starches are insoluble in water but can be digested by hydrolysis with the help of an enzyme called amylase, which breaks the α -linkages.

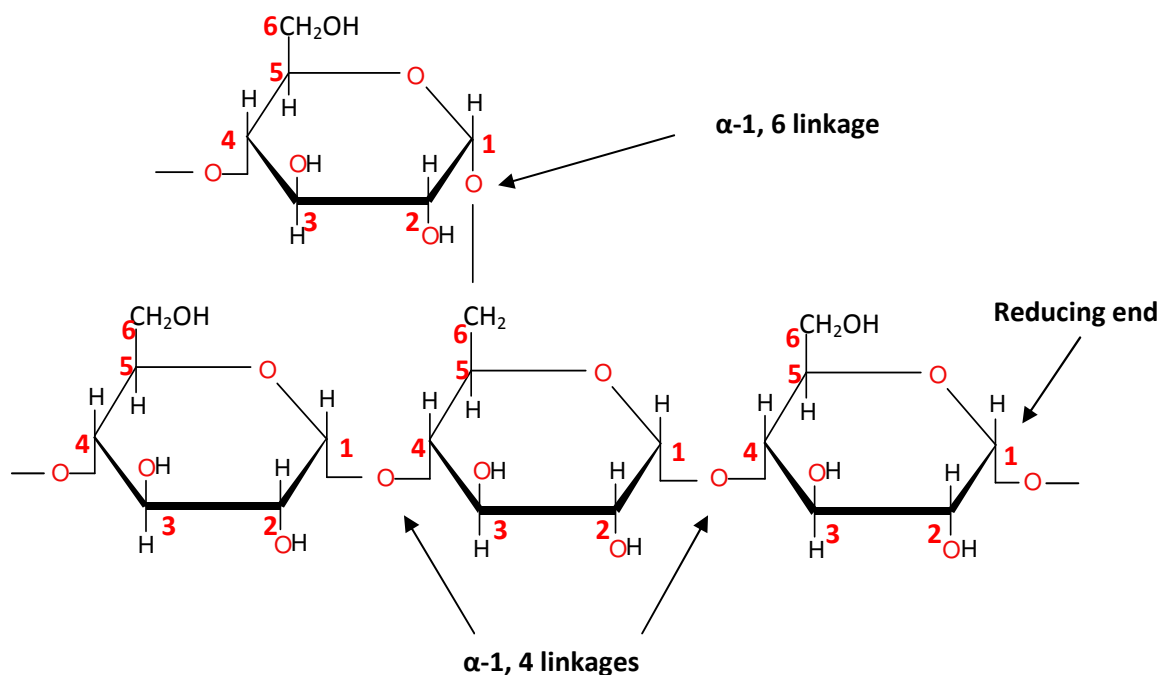


Figure 19: Structure of starch showing 4 glucose moieties¹³

A sugar (like starch) is classified as a reducing sugar only if it has an open chain form with free aldehyde group. This aldehyde group allows the sugar to act as reducing agent, e.g: in Tollen's test (the sugar precipitate as silver metal) or Benedict's reagent. So, in other words a sugar is a reducing sugar if it reduces certain chemicals (via redox reaction). Benedict's reagent and Fehling's solutions are used to test for the presence of a reducing sugar. In these tests the reducing sugar reduced copper (II) ions to copper (I), which then forms a brick red copper (I) oxide precipitate.

Glycogen is the secondary storage form of glucose in animals, with primary energy stores being held in adipose tissue. It is synthesized and stored mainly in the liver (10% liver mass) and the muscles (1-2% muscle mass). It consists of α -(1 \rightarrow 6) glycosidic bonds linked with α -(1 \rightarrow 4) linked branches. Glycogen is a close analogue of starch and is sometimes referred to as animal starch. The structure of glycogen only differs from that of amylopectin in that it is more highly branched with 8 to 12 glucose residues of the α -(1 \rightarrow 4) linked glucan. The degree of polymerization of glycogen is similar to that of amylopectin.

1.2.2 Structural polysaccharides:

Structural polysaccharides compositions are similar to those of storage polysaccharides but with subtle structural differences. Cellulose is the most abundant natural polymer on earth and it is the major component of plant cell walls. It consists of a linear chain of several hundred to over ten thousand $\beta(1\rightarrow4)$ linked D-glucose units. The average values for degree of polymerization (number of monosaccharide units) for cellulose can range from 800 to 1600¹⁹ units. It is the important structural component of the primary cell wall of green plants, many forms of algae and some species of bacteria secrete it to form biofilms^{19,20}.

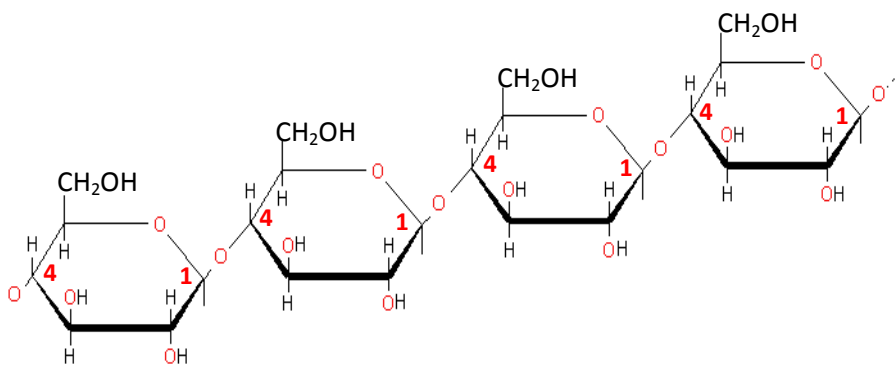


Figure 20: Structure of cellulose

Chitin is the second most abundant polymer on earth. It is the structural component of the exoskeleton of many animals (arthropods like crustaceans – crabs, lobsters, shrimps) and insect exoskeletons. It is a long unbranched chain polymer of a *N*-acetylglucosamine (NAG) formed by covalently joining NAG units using $\beta(1\rightarrow4)$ linkages. Chitin may be regarded as a derivative of cellulose with one OH group on each monomer replaced with an acetamide group.

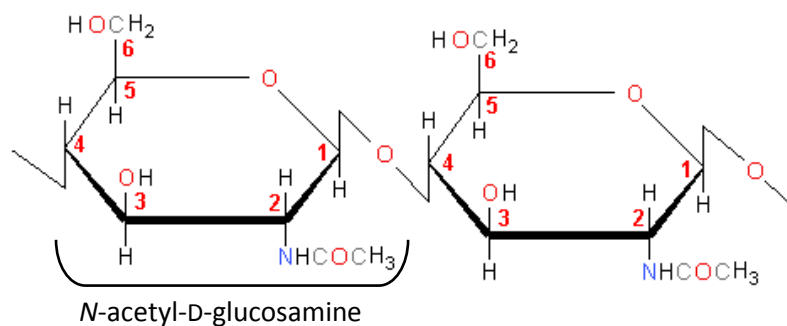


Figure 21: Structure of chitin consists of *N*-acetyl-D-glucosamine units

1.3 ***Bacterial Polysaccharides:***

Bacteria produce a very diverse range of polysaccharides with varied chemical properties via the utilization of simple activated monosaccharide substrates. Some of these polysaccharides have the same function in a number of different bacteria whereas others are specific for certain taxa and serve distinct biological functions^{21,22}.

With respect to their cellular location, polysaccharides can either be intracellular or extracellular. In the current thesis only those polysaccharides that are present on the surface of the cell or which are secreted will be studied. The range of the extracellular polysaccharides are vast and may be grouped into three major classes; capsid, capsular and expolysaccharides^{23,24}. They have been collectively termed as extracellular polymeric substances²³, slime and microcapsular polysaccharides^{25,26} among others. At the cell wall, they serve structural and protective purposes. Outside the cell, they may take the form of a covalently bound cohesive layer; called a capsule²⁶ or they can be completely excreted into the environment as slime²³. Due to their non-toxic nature, some of these extracellular polysaccharides they have found uses in medical applications, as matrices in tissue engineering, drug delivery and as wound dressing; frequently their properties and availability make them more attractive compared to polysaccharides obtained from plants and microalgae^{24,27,28}.

Bacteria produce a variety of polysaccharides as part of their cell walls and the main cell wall component is peptidoglycan. Peptidoglycan consists of sugars and amino acids in a mesh style lattice. The sugars present in peptidoglycan are *N*-acetylglucosamine (NAG or GlcNAc) and *N*-acetylmuramic acid (NAM); peptidoglycan form a mesh-like layer outside the plasma membrane of the bacterial cell.

Bacteria can be divided into two groups; Gram-positive or Gram-negative, based on the structures of their cell wall. The cell walls of Gram-positive bacteria are made up of approximately twenty times as much peptidoglycan than Gram-negative bacteria. Danish scientist Hans Christian Gram devised a method based on the structural differences in their cell walls. According to his test, bacteria that retain the crystal violet dye (thick layer of peptidoglycan) are called Gram-positive bacteria, and

if bacteria do not retain the crystal violet dye, the bacteria is called a Gram-negative bacterium²⁹.

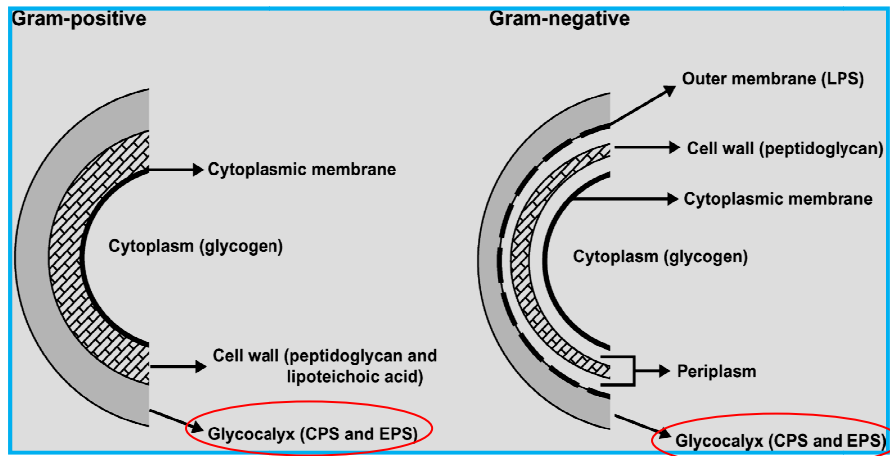


Figure 22: Cell location of polysaccharides produced by Gram-positive and Gram-negative bacteria²⁹

In Gram-negative bacteria the cell wall contains a thin peptidoglycan layer and two membranes-(an outer membrane-lipid layer which contains a phospholipid, protein and lipopolysaccharide layer) and an inner membrane. In Gram-positive bacteria the cell wall contains a thick peptidoglycan layer to which are covalently bonded a second class of polysaccharides known as teichoic acids. Teichoic acids can be linked to *N*-acetylmuramic acid of the peptidoglycan layer. They are fixed to lipids and are referred to as lipoteichoic acids, whereas teichoic acids that are covalently bonded to peptidoglycan layer are referred to as wall teichoic acids³⁰. The main function of teichoic acid is to provide rigidity to the cell wall by attracting cations like magnesium and sodium. Teichoic acids are usually substituted with D-alanine ester residues³¹, giving the molecule zwitterionic properties³². The outer surface of the cell is coated with a slime layer and is frequently composed of polysaccharides and is some times referred to as the bacterial glycocalyx.

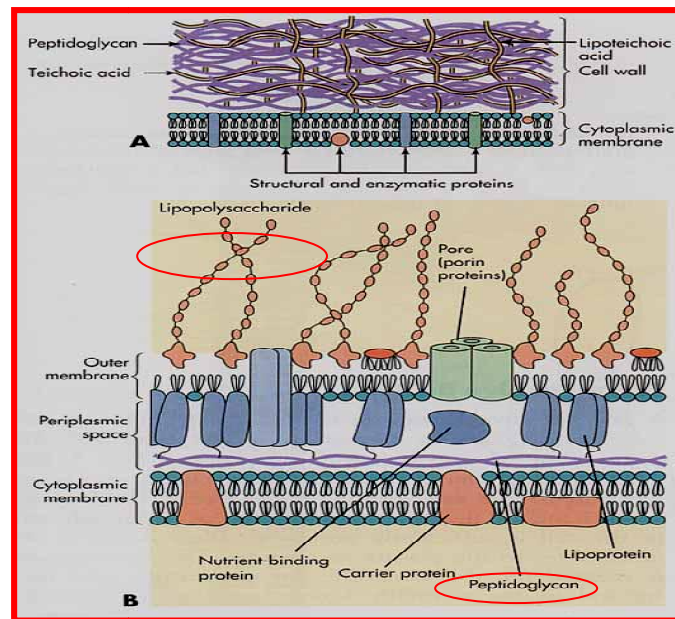


Figure 23: **A.** Gram positive bacterium has a thick layer of peptidoglycan that contains teichoic acids and lipoteichoic acids. **B.** Gram negative bacterium has a thin layer of peptidoglycan and an outer membrane that contains lipopolysaccharide, phospholipids and proteins³³ (adapted from Murray P. R., Medical Microbiology, 2002, 4th Ed.)

This extracellular mucoid layer is comprised of capsular polysaccharides, which form a capsule that is covalently linked to the cell surface, and the exopolysaccharides (**EPS**), which form a slime layer that is loosely attached by absorption to the cell surface or secreted into the environment³⁴. Although it is generally recognized that exocellular polysaccharides are not used as energy and carbon sources by the producer microorganism, the physiological role of these molecules has yet to be established.

1.3.1 Bacterial Capsular Polysaccharides (CPSs):

The outer covering of the bacteria is called as glycocalyx (polypeptide) that surrounds the outside of the cell envelope. If glycocalyx is firmly attached (covalently linked) to the cell it is called as capsule, or called as slime if it is attached loosely to the cell. Bacterial capsule can be viewed by microscope as an extensive layer surrounding the cell³⁵. It is made up of long polysaccharide chains, known as capsular polysaccharides (CPSs) which are typically negatively-charged (due to the presence of uronic acids or ionic non-carbohydrate substituents such as pyruvic acid, phosphoric acid, succinic acid, amino acids and lactic acid and therefore generate a highly hydrated capsular layer³⁶. In some *Escherichia coli* (*E. coli*), this

layer can extend from the cell surface for approximately 100–400 nm³⁶ and is formed by glycan chains more than 200 sugars long³¹. Due to their surface association, capsules are frequently the first bacterial structure encountered by the immune system upon infection. Therefore, in many bacteria, the capsule is required for evasion of the host immune system³⁷.

There is enormous structural diversity in capsular polysaccharides; nearly two hundred different polysaccharides are produced by *E. coli* alone. Mixtures of capsular polysaccharides, either conjugated or native are used as vaccines³⁸. More than 80 different capsule types are known in *E. coli*, and several are shared by other bacteria (e.g., *E. coli* K1 produce sialic-acid-containing capsules)³⁸. The capsular polysaccharide components have other important functional roles in the life of a bacterial cell. The capsular polysaccharides represent the first line of defence against bacteriophages. They prevent cell from drying out and permit bacteria to adhere to cell surfaces like in medical implants and catheters (first step in colonization). They also contain the major antigenic determinants that distinguish various serotypes of bacteria, which are sometimes correlated with disease. These components can also have effects on the mammalian host³⁸.

1.4 Exopolysaccharides [EPS]:

Bacterial polysaccharides that are synthesized and which are secreted into the external environment or are synthesized extracellularly by cell wall enzymes are known as exopolysaccharides (EPS). Exopolysaccharides are frequently composed of a repeating oligosaccharide structure and are categorized on the basis of this chemical structure, their functionality, their molecular weight (ranging from 0.5×10^6 – 2.0×10^6 Da) and type of linkages that they possess. On the basis of chemical composition, EPS may be composed of the same repeating monomeric units (homopolysaccharides) or of different repeating monomeric units (heteropolysaccharides), varying in size from disaccharides to heptasaccharides. Homopolysaccharides have been further divided into four groups: α -D-glucans, β -D-glucans, fructans and polygalactan³⁹.

On the other hand, the heteropolysaccharides include in their repeating units different combinations of the monosaccharides of D-glucose (D-Glc), D-galactose (D-Gal), L-rhamnose (L-Rha) and in some instance *N*-acetylglucosamine (NAG), *N*-

acetylgalactosamine (GalNAc) or glucuronic acid (GlcA). Each hexose can adopt the pyranose or furanose ring configuration, and be linked with the α - or β - anomeric configuration to other residues at several possible positions and also they can contain non-carbohydrate substituents like phosphate, acetyl, glycerol or pyruvate²⁷. Bonds between monomeric units in the back bone of the polymers are combinations of linkages 1,2; 1,3; 1,4; 1,6 and can also be 1,5- linked as in galactofuranoses. The quantity of EPS produced varies with bacterial species. However, the physicochemical factors playing crucial roles in the yield of these compounds include pH, temperature, incubation time and medium composition (carbon and nitrogen sources)⁴⁰. Exopolysaccharides allow bacteria to aggregate (bacterial communities grow on a living host by secreting polymers) and these aggregates are often referred to as biofilms. Researchers have estimated that 60-80% of microbial infections in the body are caused by bacteria growing as a biofilm. Dental plaque is an example of an external biofilm and the formation of kidney stone is one of the examples of internal biofilm.

Biofilms have been extensively studied, a summary of roles played by EPS in bacterial biofilms is listed in Table 1⁴¹ and some human diseases involving biofilms are summarized in Table 2⁴¹.

Table 1: Some of the roles ascribed to exopolysaccharides in biofilms (adapted from Nwodo *et. al*⁴¹)

Process	Functional relevance of exopolysaccharides (EPS) to biofilm
Adhesion	EPS makes provision for the initial steps in the colonization of bacterial surfaces.
Water retention	Hydrophilic EPS have high water retention ability thus maintain a hydrated microenvironment around a biofilm and thus lead to the survival of desiccation in water-deficient environments.
Cohesion of biofilms	Neutral and charged EPS form a hydrated polymer network mediating the mechanical stability of biofilms, determining biofilm architecture.
Nutrient source	EPS serves as source of carbon, nitrogen and phosphorus containing compounds for utilization by the biofilm community.
Protective barrier	EPS confers resistance to non specific and specific host defences during infection, confers tolerance to various antimicrobial agents
Export of cell components	Lipopolysaccharides mediate the release (cellular material) as a result of metabolic turnover.

Table 2: Some human disease associated with bacterial biofilms⁴⁴ (red: Gram +ve, blue: Gram –ve)
(adapted from Nwodo *et. al* ⁴¹)

Human Disease	Bacterial Biofilm responsible
Cystic fibrosis pneumonia	<i>P. aeruginosa</i> and <i>Burkholderia cepacia</i>
Periodontitis	Gram-negative anaerobic oral bacteria
Dental caries	Gram-positive cocci
Musculoskeletal infections	<i>Staphylococci</i> and other Gram-positive cocci
Bacterial prostatitis	Gram-negative bacteria
Urinary catheter cystitis	<i>E. coli</i> and other Gram-negative bacteria

Some of the extensively studied extracellularly synthesized bacterial EPSs with their molecular weight, main properties, applications and bacterial strains are tabulated in Table 3.

Table 3: Some of the extensively studied bacterial EPS (adapted from Nwodo *et. al* ⁴¹)

Bacterial EPS	Polysaccharide component	Charge	Molecular weight (Da)	Main properties	Main applications	Bacterial strains
Dextran	Glucose	Neutral	10^6 - 10^9	Non-ionic, Good stability, Newtonian fluid behaviour	Foods, pharmaceutical industry, chromatographic media	<i>L. mesenteroides</i>
Xanthan	Glucose Mannose Glucuronic acid Acetate Pyruvate	Anionic	$(2.0$ - $50.0) \times 10^6$	High viscosity, stable over a wide temp., pH and salt concentrations	Foods, petroleum industry, pharmaceuticals, cosmetics, agriculture	<i>Xanthomonas spp.</i>
Curdlan	Glucose	Neutral	5×10^4 - 2×10^6	Gel forming ability, water insolubility, edible and non-toxic	Foods, pharmaceutical industry, heavy metal remover and concrete additive	<i>Rhizobium meliloti</i> and <i>Agrobacterium radiobacter</i>

To date, polysaccharides recovered from plant, algae and animal sources are still the major contributors to the commercial hydrocolloid market mainly because of the higher prices of bacterial polysaccharides. Nevertheless, the research interest in bacterial production of polysaccharides is continuously growing, and is focused on using low-cost substrates.

1.4.1 Applications of EPS:

EPSs generated by Gram-negative bacteria have many more negative attributes than those produced by Gram-positive bacteria. On the other hand some Gram-positive bacteria have a number of positive attributes including GRAS (generally regarded as safe) status and can be used in applications involving human consumption and for this reason EPS from Lactic Acid Bacteria (LAB) are used increasingly in food preparations. EPS from Gram-positive bacteria are composed of branched repeating units consisting of mainly galactose, glucose and rhamnose, in different ratios. The discoveries of numerous types of EPS have been documented, but only a handful have been shown to have industrial relevance and commercial value⁴². The limitation of the applications of some of these bacterial polysaccharides has been largely due to cost of production. To minimize the cost, scientists are using cheaper substrates, trying to improve product yield by optimizing fermentation conditions and developing higher yielding strains via mutagenesis and/or genetic and metabolic manipulations⁶. Over the past decades, EPS from Gram-positive bacteria have found application in the improvement of the texture properties of fermented milk products and yoghurt^{43,26}. Problems like low viscosity and gel fracture, which are frequently encountered during yoghurt manufacture, can be solved by the application of EPS⁴⁴. Texture profile analysis showed that hardness, consistency, adhesiveness, chewiness and relaxation were significantly lower in cheese fermented by EPS-producing *Streptococcus thermophilus* and *Lactobacillus delbrueckii* sp. *Bulgaricus* culture⁴⁵. The increasing demand for healthy and consumer-friendly dairy products has motivated the food industry to better understand the effects of EPS on existing products and to search for new EPS-producing strains with different properties. There is a high consumer demand for products with low fat or sugar content and low levels of food additives especially stabilizers and thickeners; EPSs are a viable alternative^{46,47}. In dairy products EPSs are added to improve the functional properties of foods (yoghurt, cheese and bread) and in pharmaceuticals where they are used directly as biological active agents, i.e: as a probiotic. EPS produced by lactobacilli are also used in bread production, where they favourably influence bread properties like water absorption, the softness of the gluten content of the dough, improving the structure build-up, increasing specific volume of loaf and prolonging shelf life⁴⁸. Since the EPS stay longer in the gastrointestinal tract (GIT), they also

facilitate colonization of the tract by probiotic bacteria like bifidobacteria and lactobacilli⁴⁹. EPS have found extensive applications in pharmaceutical industries, e.g; to improve the effectiveness of drug release in colon cancer treatment, certain types of EPSs are used as drug conjugates, coatings and matrix agents which act as substrates for the colon microflora⁵⁰. Much of the recent research has been done to examine the probiotic activity of Lactic Acid bacteria and Bifidobacteria in order to determine the mechanism of their biology activity. An initial study suggests that the EPS play a significant role in generating the health benefits associated with EPS consumption. Whilst the sensory benefits of the exopolysaccharides of lactic acid bacteria are well established in dairy products and there is also evidence for the health properties, due to the direct consumption of EPS producing bacteria as probiotics. At present, the development of functional foods containing probiotic bacteria (defined as “live microbial food ingredients that are beneficial to health”⁵¹) is an expanding market.

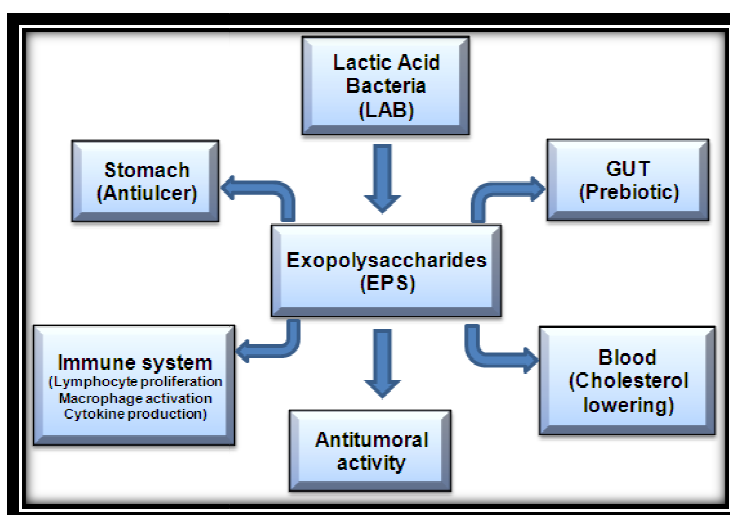


Figure 24: Possible health-promoting properties of EPS produced by LAB (adapted from Madiedo *et. al*)²⁶.

1.4.2 Negative attributes of EPS:

In some cases, the production of EPSs causes food spoilage. The synthesis of EPS by LAB during wine and cider fermentation renders undesirable rheological properties to the products. Dental plaque that leads to dental caries is due to EPS synthesis by LAB. The biofilm formation by LAB as a result of accumulation of EPS leads to biofouling⁵⁰.

1.4.3 EPS Biosynthetic pathway:

Most bacterial EPSs are synthesized intracellularly and exported to the extracellular environment as macromolecules^{52,53}. There are a few known exceptions (e.g. levans and dextrans) whose synthesis and polymerization occur outside the cells by the action of secreted enzymes that convert the substrate into the polymer in the extracellular environment⁵² (these will not be covered in the current work).

The biosynthetic pathway for EPS synthesis can be classified into four steps:

- (i) the reactions involved with sugar transport into the cytoplasm
- (ii) the synthesis of sugar-1-phosphates
- (iii) activation and coupling of sugars
- (iv) export of the EPS

Each of these steps is crucial and can be manipulated to modify the amount and composition of the EPS. The highest-producing strains of bacteria generate low gram per litre (2.0 g/L) quantities of polysaccharides⁵⁴. The biosynthesis starts with sugar transport. Depending on substrate type, it can be taken up by the cell either through a passive or an active transport system (Fig. 25a). It can be transported and oxidized through a direct oxidative periplasmic pathway (present in certain bacteria)⁵⁵. Both these systems have been reported in several EPS-producing bacterial strains and they can function simultaneously if there is enough substrate available⁵⁶. In the cytoplasm, the substrate is either catabolised through glycolysis (Fig. 25b) and the primary metabolites formed are used as precursors for the synthesis of small biomolecules (amino acids or monosaccharides) or are converted into activated sugars. Polysaccharide synthesis requires the biosynthesis of activated precursors that are energy-rich monosaccharides, mainly nucleoside diphosphate sugars (NDP-sugars), which are themselves derived from phosphorylated sugars (fig. 25c)^{53,57}.

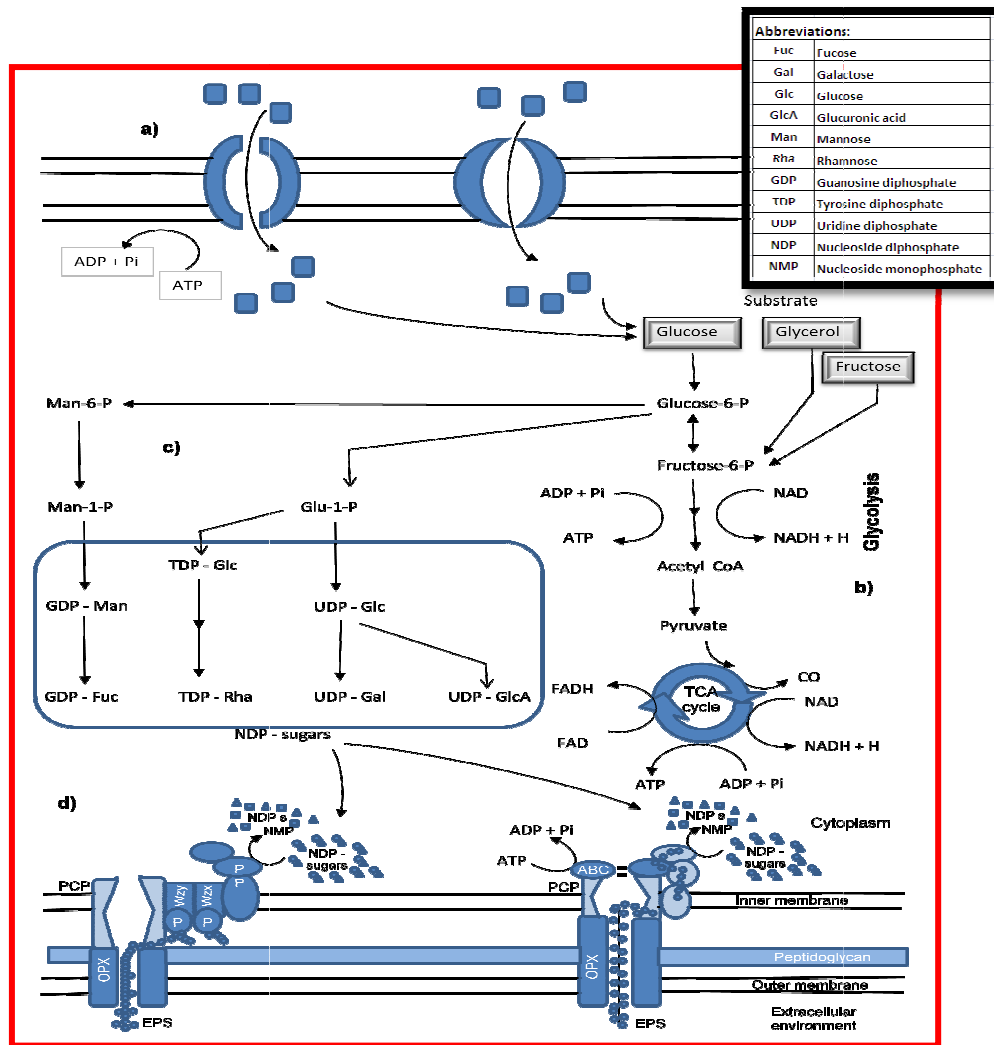


Figure 25: Processes for EPS biosynthesis (adapted from Freitas *et. al*⁵⁸)

Phosphorylated sugars are converted into energy-rich monosaccharides, mainly UDP-Gal and GDP-Man and are interconverted through reactions of epimerization, oxidation, decarboxylation, reduction and rearrangement to generate the different monosaccharides required in the repeat unit of the polysaccharides^{52,53}.

Polysaccharide synthesis and polymerization occurs through one of two mechanisms.

(i) In the Wzx–Wzy-dependent system (Fig. 25, bottom left), the repeat unit is synthesized by the sequential transfer of monosaccharides from NDP-sugars to a polyprenylphosphate lipid carrier. Mature repeat units are transported across the inner membrane by a presumed flippase (Wzx) to the periplasmic face {flippase are lipid transporter enzymes responsible for helping in the movement of phospholipid molecules between the cell's membrane}, where polymerization occurs by the

action of a polymerase (presumed Wzy). In many bacteria, the translocation pathway that spans the cell envelope is formed by a polysaccharide copolymerase (PCP) that determines polymer chain length, and an outer membrane polysaccharide export protein (OPX) that forms a channel^{52,59,60}.

(ii) In the ABC-transporter-dependent system (Fig. 25, right), the polysaccharide is polymerized at the cytoplasmic face of the inner membrane through the sequential addition of sugar residues to the nonreducing end of the polymer chain. The polymer is exported across the inner membrane through an ABC transporter, followed by its translocation across the periplasm and the outer membrane, through PCP and OPX proteins⁵⁹.

1.4.4 Extraction of EPS:

Before EPS can be characterized it is necessary to isolate them in a pure form. Recovery of extracellular microbial polysaccharides from the culture broth is commonly achieved by procedures that involve^{60,61,62,63}:

- (i) cell removal, usually achieved by centrifugation or filtration;
- (ii) polymer precipitation from the cell-free supernatant by the addition of a precipitating agent that consists of a water-miscible solvent in which the polymer is insoluble (e.g. methanol, ethanol, isopropanol or acetone);
- (iii) drying of the precipitated polymer, namely by freeze drying (laboratory scale) or drum drying (industrial scale).

In many procedures, the broth is subjected to heat treatment (up to 90–95 °C) at the end of the fermentation process, before cell removal⁶². This heat step is aimed at killing the bacterial cells and inactivation of enzymes that could cause polymer degradation in subsequent steps. Moreover, it also gently reduces broth viscosity. Cell removal is facilitated by dilution of the culture broth by addition of deionized water before centrifugation/filtration.

There is a large range of low-molecular-weight compounds, co-produced or added during the production processes, which end up as impurities in the final product (e.g. cell debris, salts and proteins)^{38,61,64}.

To obtain a higher purity grade polysaccharide, the polymer is additionally subjected to one or several of the following processes:

- (i) reprecipitation of the polymer from diluted aqueous solution (<math><1.0\text{ g/l}</math>);
- (ii) chemical deproteinization (e.g. salting out or protein precipitation with trichloroacetic acid⁶⁵ or using enzymatic methods (e.g. proteases⁶⁴) or membrane processes (e.g. ultrafiltration and diafiltration⁵⁸).

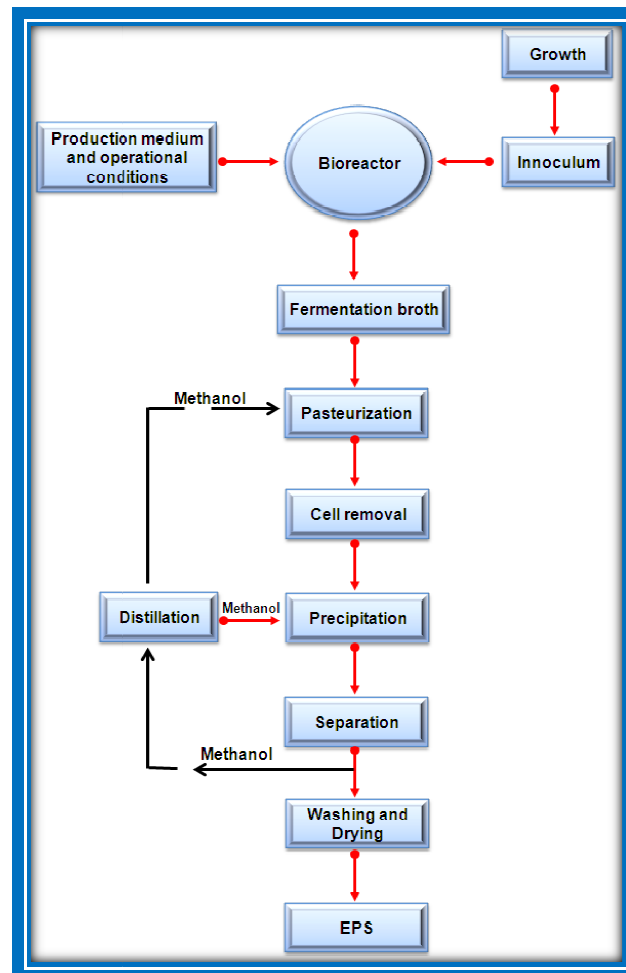


Figure 26: Schematic representation of EPS extraction process

Some of these purification procedures can decrease product recovery or have a negative impact on polymer properties, e.g. when protein removal is carried out with the addition of chemicals that might react with EPS components. Therefore, the choice of the most appropriate procedure must be made carefully as a compromise between product recovery, product purity, and its impact on polymer properties. As such, research is still needed, either for the improvement of the existing extraction and purification processes or for the development of new approaches that are focused on the specifications required for the final product.

1.4.5 Purification of EPS by Size Exclusion Chromatography (SEC):

The concept of size based separation chromatography was first speculated by Synge and Tiselius⁶⁶ based on the experimental observation on zeolites, that small molecules can pass through the small pores in zeolites (molecular sieves-first used by McBain⁶⁷) according to their molecular size. To describe this property of zeolites, it was subsequently used to describe the technique known as “size exclusion chromatography (SEC)”. SEC is known as a number of other names, such as exclusion chromatography, gel-filtration chromatography or gel permeation chromatography⁶⁸. Wheaton and Bauman⁶⁹ were the first to mention the separation of analytes on the basis of their size by using liquid chromatography in their work on ion exclusion chromatography. Similarly, Clark⁷⁰ separated sugar alcohols on a strong cation exchange resin. Lindqvist and Storgards⁷¹ reported the first separation of biomolecules by size exclusion process, where they separated peptides from amino acids on a starch-filled column.

Size exclusion chromatography (SEC) is used to analyse and purify molecules such as polysaccharides and proteins. SEC is the simplest chromatographic method, which is based on separation of particles with respect to their size⁷² using stationary phases (polystyrene divinylbenzene) with pore sizes capable of discriminating among the different sized analytes in a sample.

The column packing consists of particles containing various size pores and pore networks, so that molecules are retained or excluded on the basis of their size and shape. The sample is introduced into the flow of the mobile phase which passes through the column. Very large molecules cannot enter many of the pores, and they also penetrate less into the comparatively open regions of the packing, thus interacting less with the stationary phase than smaller molecules do.

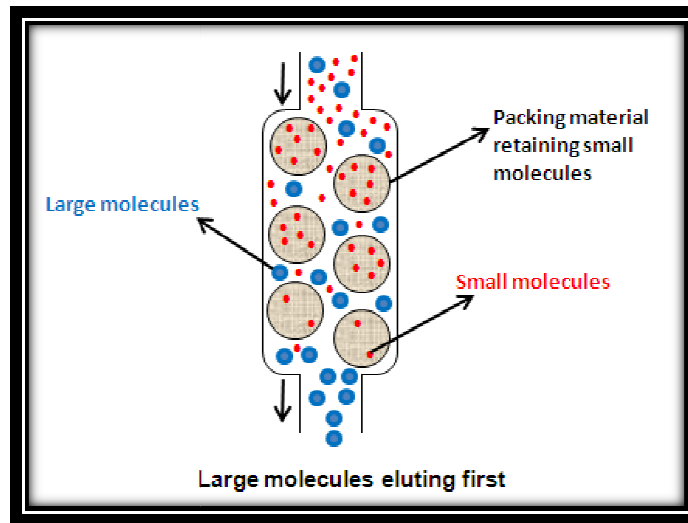


Figure 27: Schematic diagram of SEC

This means that the larger molecules elute faster than the smaller molecules, because very small molecules diffuse into all or many of the pores accessible to them. Between these two extremes, intermediate-size molecules can penetrate some passages, which delay their progress down the column, and exit at intermediate times.

1.4.6 Purification of EPS by Ion Exchange Chromatography (IEX):

Ion Exchange (IEX) chromatography is a technique that is frequently used to separate charged biomolecules. This technique was introduced in 1960s and is the most frequently used technique for the separation of proteins, due to its high capacity and simplicity, high resolution power and ability to separate molecular species that have very little charge difference. It uses stationary phases with charged functional groups⁷³. IEX separates molecules on the basis of differences in their net surface charge. Due to differences in charge, they interact differently with a charged chromatography medium. To bind all the charged molecules, the mobile phase that is used is a low conductivity solution. The interaction strength is determined by the number and location of charges on the molecule. By increasing the salt concentration, the molecules with the weakest ionic interactions start to elute first and molecules with stronger ionic interaction elute later (requires high salt concentration) from the column. So, it is better to use mobile phase with a linear salt gradient. Molecules exhibit different degrees of interaction with charged

chromatography media according to differences in their overall charge, charge density and surface charge distribution. The charged groups within a molecule that contribute to the net surface charge possess different pK_a values depending on their structure and chemical microenvironment. When the $pH > pI$ (isoelectric point – the pH at which a biomolecule has no net charge), the biomolecule has a net negative charge and binds to a positively charged anion exchanger and when the $pH < pI$, a biomolecule has a net positive charge and binds to a negatively charged cation exchanger. As such, IEX can be subdivided into cation exchange chromatography (positively charged ions bind to a negatively charged resin) and anion exchange chromatography (the binding ions are negative, and the immobilized functional group is positive). Anion exchangers are classified as strong (Quaternary amine-Q-resin) or weak (DiEthylAminoEthyl-DEAE-resin), depending on the ionization state of the functional groups in conjunction with pH .

A strong ion exchanger has the same charge density on its surface over a broad pH range, whereas the charge density of a weak ion exchanger changes with pH .

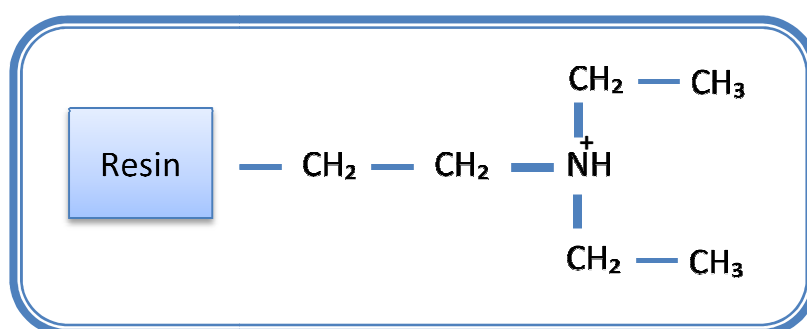


Figure 28: DEAE-anion exchanger

The Ion Exchange process can be separated into four basic stages: equilibration, application of sample, elution and regeneration. The equilibration stage involves setting up the desired starting conditions so that the system is ready for the ion exchange process. Then the sample is applied to the stationary phase. Only the samples carrying a charge opposite to the stationary phase will bind to it while those with the same charge or no charge will not bind. These unbound molecules will wash out during this stage. The elution step involves changing the buffer conditions in such a way that the analytes that are attached to the stationary phase can be removed. There are different methods used to remove the attached molecules, i.e.

change the pH of the buffer solution (buffer pH reaches the pI of the molecules, the molecules; net charge will be zero and they will be released and washed out) or to increase the salt concentration. The regeneration step involves simply removing all the bound analytes from the stationary phase (by using 1M NaCl buffer) so that it is ready for another process.

EPS contains a variety of negatively charged (carboxyl, phosphoric, sulphate and hydroxyl) and positively charged (amino) functional groups. Due to the presence of these charged functional groups, EPSs also serve as a naturally sticky ligand source for other charged particle and metal ions (calcium or magnesium)⁷⁴.

1.5 Characterisation of EPS:

Exopolysaccharides consist of monosaccharide units attached together through α - and β - glycidic linkages forming repeating oligosaccharide units. The two most important elements of the structural characterisation of exopolysaccharides are to determine the monosaccharide composition, in terms of identification of monomers and their relative ratio in the repeating unit and to determine how each monosaccharide is arranged (linked) in the repeating unit. The overall configuration of the repeating oligosaccharide sequence can then be deduced.

1.5.1 Monomer Analysis:

In the analysis, the first step is to know the type and amount of monosaccharide that are present. The most frequently used methods for determining the concentration of monosaccharides in a sample are based on analysis using gas chromatography (GC) and high performance liquid chromatography (HPLC). Unlike enzymatic methods, which tend to be specific for one type of monosaccharide only, as chromatographic techniques provide qualitative and quantitative information about one or several monosaccharides.

When the sample is a polysaccharide and monosaccharide analysis is required, the sample must be depolymerised. This is most commonly accomplished by using acid hydrolysis. The traditional method (Albersheim *et al.*⁷⁵, Blake *et al.*⁷⁶ and Gerwig *et al.*⁷⁷) which consists of acid hydrolysis followed by derivatization to alditol acetates which are assayed by gas chromatography (GC), has been gradually replaced by high pressure anion exchange chromatography with pulsed

amperometric detection (HP-AEC-PAD), which is a more straight forward method avoiding the derivatization step⁷⁸.

In the presence of a strong acid and heat, the glycosidic bond between monosaccharide residues in a polysaccharide is cleaved. During acid hydrolysis, the released monosaccharides are susceptible to degradation in the presence of hot concentrated acid. However, not all glycosidic linkages are cleaved at the same rate and the hydrolysis time must be sufficient to hydrolyze all linkages in the sample. Hydrolysis can be performed with acids like hydrochloric acid (HCl), trifluoroacetic acid (TFA) and sulphuric acid (H₂SO₄). It has been reported that sulphuric acid is superior to TFA for the hydrolysis of fibrous substrates such as wheat bran, straw and apples⁷⁹. However, sulphuric acid (H₂SO₄) can be difficult to remove post-hydrolysis and its presence can interfere with some analyses. TFA is volatile and can be easily removed prior to an HPLC analysis. Total or partial acid hydrolysis with TFA, HCl or H₂SO₄ is performed by heating the sample at 100 to 120 °C for 2 to 8 hours.

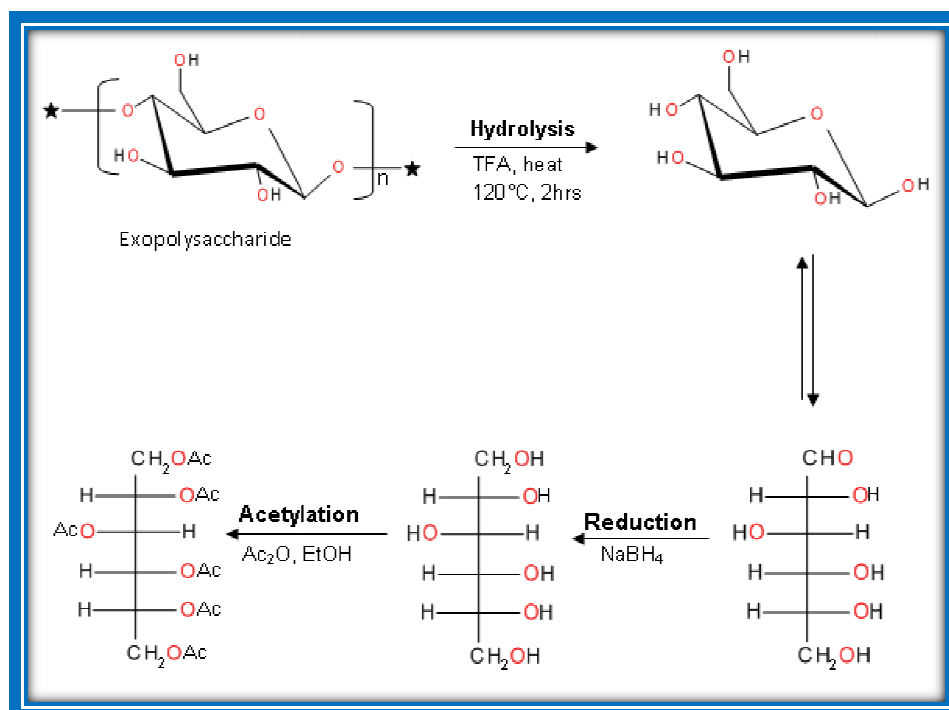


Figure 29: Monomer analysis reaction scheme

The qualitative monosaccharide composition of an EPS has been analyzed in the past by TLC^{80,81,82,83,84,85}, however this method has low discriminatory power and has been largely surpassed by more reliable liquid and gas chromatographic

techniques. In the past, the qualitative and quantitative determination of EPS monosaccharides by HPLC involves the separation of monosaccharides by anion-exchange columns and detection by refractive index (RI). Isocratic separations employed aqueous H₂SO₄ as eluent (2.5-5.0 mM) to analyze the monomer composition of EPS produced by *Lactobacillus rhamnosus*⁸⁶, *Lactobacillus delbrueckii* spp. *Bulgaricus*⁸⁶ and *Streptococcus thermophilus* strains⁸⁷. Isocratic elution with distilled water was used to determine the monosaccharide constituents of the EPS produced by *Lactobacillus helveticus* ATCC 15807⁸⁷.

1.5.2 High Performance Anion Exchange Chromatography with Pulsed Amperometric Detection (HPAEC-PAD) analysis:

A more modern technique used for the identification and quantification of mono- and oligosaccharides resulting from the partial hydrolysis of EPS combines high-performance anion-exchange chromatography with pulsed amperometric detection (HPAEC-PAD)^{83,84,85,88}.

HPAEC-PAD is a liquid chromatographic method that is very sensitive for the analysis of monosaccharides⁸⁹. Analysis by HPAEC-PAD has been reviewed by different authors^{89,90}, but the technique was first introduced by Rocklin *et al.*⁷⁸ Over the past few years HPAEC has proven invaluable in the analysis of carbohydrate-bound materials. This type of chromatography is based on the fact that carbohydrates in a strongly alkaline environment will ionize; thereby separation occurs on an ion exchange column.

Separation is made at high pH with strong alkaline solutions and detection is achieved by monitoring the change in the electric current due to the oxidation of the saccharides on the surface of a gold or platinum working electrode located in the pulsed amperometric detector (PAD)³⁴. The advantage of PAD is not only its low detection limits (in the picomole range)⁹¹ but also its suitability for gradient elution.

The main advantage of HPAEC is that the samples do not require derivatization and the analysis itself is usually quite fast. In the past, disadvantages of HPLC originated with detection systems, which for the most part were not very sensitive. Refractive index detectors have traditionally been the detector of choice, because more sensitive detectors (UV or fluorescence detectors) are not appropriate

for analyzing carbohydrates since carbohydrates do not possess chromophores that respond to these detection systems. HPAEC-PAD has overcome this disadvantage, enabling the separation and quantification of monosaccharides with low detection limits and using sodium hydroxide (NaOH) as eluent is inexpensive and relatively safe⁹¹.

In anion exchange chromatography, strong anions are retained on a positively-charged stationary phase through ion-pair formation. Similar series of anions such as monosaccharides will be present as oxy-anions with charge located primarily on the hydroxyl group attached to C2. The extent to which they will be retained will depend on their degree of ionization in the mobile phase eluent. The lower the pK_a of the hydroxyl ion the more ionized the monosaccharide will be and this will lead to their being retained on the column.

Table 4: Dissociation constants of some common carbohydrates⁹² (in water at 25⁰C)

Sugar	pKa
Fructose	12.03
Mannose	12.08
Xylose	12.15
Galactose	12.28
Glucose	12.39
Dulcitol	13.43
Sorbitol	13.60
α -Methyl glucoside	13.71

Examination of the pK_a values of the neutral monosaccharides shows that carbohydrates are in fact weak acids. At high pH, they are least partially ionized, and thus can be separated by anion exchange mechanisms.

1.5.3 Gas Chromatography (GC) Analysis:

The most extensively used technique for the analysis of the monomer composition of EPS is gas chromatography (GC) and gas chromatography-mass spectrometry (GC-MS). Compared to liquid chromatography, the main advantage of

GC is its much higher separation power. In GC many sugars can be detected in relatively short retention times. Although the resolution in GC is much better compared to other techniques, a derivatization step is required which can be seen as a drawback.

Due to their high polarity and low volatility, all sugars need to be converted into volatilizable and stable derivatives prior to GC or GC-MS analysis. Classical derivatization methods involve substitution of the polar groups of carbohydrates. The most popular derivatives for GC analysis of saccharides^{93,94,95} are methyl ethers, acetates, trifluoroacetates and trimethylsilyl^{77,96} ethers.

The essential elements of this derivatization procedure are the reduction of neutral sugars to alditols and their subsequent acetylation. The resulting alditol acetates are then dissolved in a suitable solvent (acetone) and injected onto a GC column⁷⁵.

1.5.4 Capillary Electrophoresis (CE):

Besides liquid and gas chromatography, a number of analytical methods are described using capillary electrophoresis (CE) as separation technique for the separation of sugars. CE utilizes an open tubular capillary, which can be rapidly flushed with fresh buffer directly after detection of interesting peaks.

Due to the high pK_a of monosaccharides (table: 4), they are negatively charged in strong basic running buffer and can be further separated under a fixed electric field. For improving the separation efficiency, some surface-active agents, such as sodium dodecyl sulphate (SDS or NaDS) can be added into the running buffer⁹⁷.

As was the case in HPLC, detection of sugars in CE is challenging because of the absence of chromophoric groups. There are different methods used for the detection of sugars by CE:

- (i) UV after derivatization^{98,99,100}
- (ii) Indirect UV detection^{101,102,103}
- (iii) Amperometric/electrochemical detection^{104,105,106}, a copper electrode¹⁰⁷ is used as working electrode for the determination of the sugars^{102,105,106}

1.5.5 Linkage Analysis:

The majority of the techniques used in this area were developed by Stellner *et al.*¹⁰⁸, and the main purpose is to find the linkage patterns in the repeating oligosaccharide. All the unsubstituted hydroxyl groups are methylated and then followed by hydrolysis, reduction of the methyl glycosides using sodium borodeuteride (NaBD₄) and acetylation, which provides *O*-acetyl group at linkage points. The methylated alditol acetate are then analyzed by GC-MS^{109,110}.

Per-*O*-methylation of carbohydrates is an essential step for determining the position of the glycosidic attachments¹¹¹. The first *O*-methylated sugar was prepared by Purdie and Irvine in 1903¹¹² by treating dry carbohydrates dissolved in methanol with methyl iodide (MeI) in the presence of silver oxide (Ag₂O). In 1913, Denham and Woodhouse¹¹³, treated aqueous carbohydrates with a solution of sodium hydroxide (NaOH) and dimethyl sulphate (Me₂SO₄). Both the methods gave *O*-methylated carbohydrates¹¹⁴.

The above two methylation methods with some modifications were used for preparative and analytical *O*-methylation of carbohydrates, e.g. Haworth in 1915 and Hirst & Percival in 1965 used NaOH_{aq} or aqueous potassium hydroxide (KOH_{aq}) with Me₂SO₄, whereas Purdie, Hirst & Percival in 1965 and Purdie & Irvine in 1965 used MeI and AgNO₃.

In 1964, Hakomori¹¹⁵, performed the per-*O*-methylation of polysaccharides in one step, by adding a solution of sodium methylsulfinyl carbanion (Na dimsyl or NaDMSO) and methyl iodide (MeI) to the carbohydrate dissolved in dimethyl sulfoxide (Me₂SO). This method was improved^{114,116,117} especially by using potassium dimysl and lithium dimysl. But the preparation of the dimysl reagent is still laborious and hazardous since moisture, air and carbon dioxide must be avoided during its preparation and storage, in order to minimize side reactions and to enhance the purity of the final analytical product. These conditions are viable when small amounts of polysaccharides are to be analyzed. Otherwise undermethylated products will be obtained. In order to obtain accurate results, full *O*-methylation is a prerequisite condition. However, a single treatment of complex carbohydrates with Na dimysl often results in incomplete methylation^{118,119,120}. These under-methylated materials are extracted and remethylated, but small amounts of undermethylated complex carbohydrates can still exist even after very considerable effort¹³⁴. Some of

these disadvantages are overcome by avoiding the presence of Na dimethyl sulfoxide in the reaction mixture by directly adding powdered sodium hydride (NaH) and methyl iodide (MeI)¹²¹ into the carbohydrate solution in dimethyl sulfoxide (DMSO). The per-*O*-methylation yields are higher and the products are cleaner. However, this methylation method was not widely used because of the dangers of working with alkali metal hydrides that are flammable and moisture-sensitive, and thus must be handled only in small quantities and with extreme care. Another method involves adding solid sodium hydride in small portions into the carbohydrate dimethyl sulfoxide solution^{122,123}, but the formation of Na dimethyl sulfoxide cannot be avoided.

Methylation of carbohydrates in dimethyl sulfoxide by treatment with powdered sodium hydroxide (NaOH) and methyl iodide was introduced by Ciucanu for per-*O*-methylation of carbohydrates^{121,124,125}, fatty acids and hydroxyl fatty acids¹²¹ and uronic acids¹²⁶. The method is not very sensitive to moisture and gives complete *O*-methylation in one step with high yields, no by-products and a very short reaction time. For this reason, this method has found widespread application. The methylated polysaccharide is hydrolysed to monosaccharides using trifluoroacetic acid (TFA). The partially methylated monosaccharides are subsequently converted to alditols by reduction with NaBD₄ and the products (methylated alditols) are acetylated with acetic anhydride (Fig. 30). The methoxy groups identify where a free hydroxyl group was present and the acetylated sites show where there was a glycosidic linkage to another monosaccharide or ring formation was present.

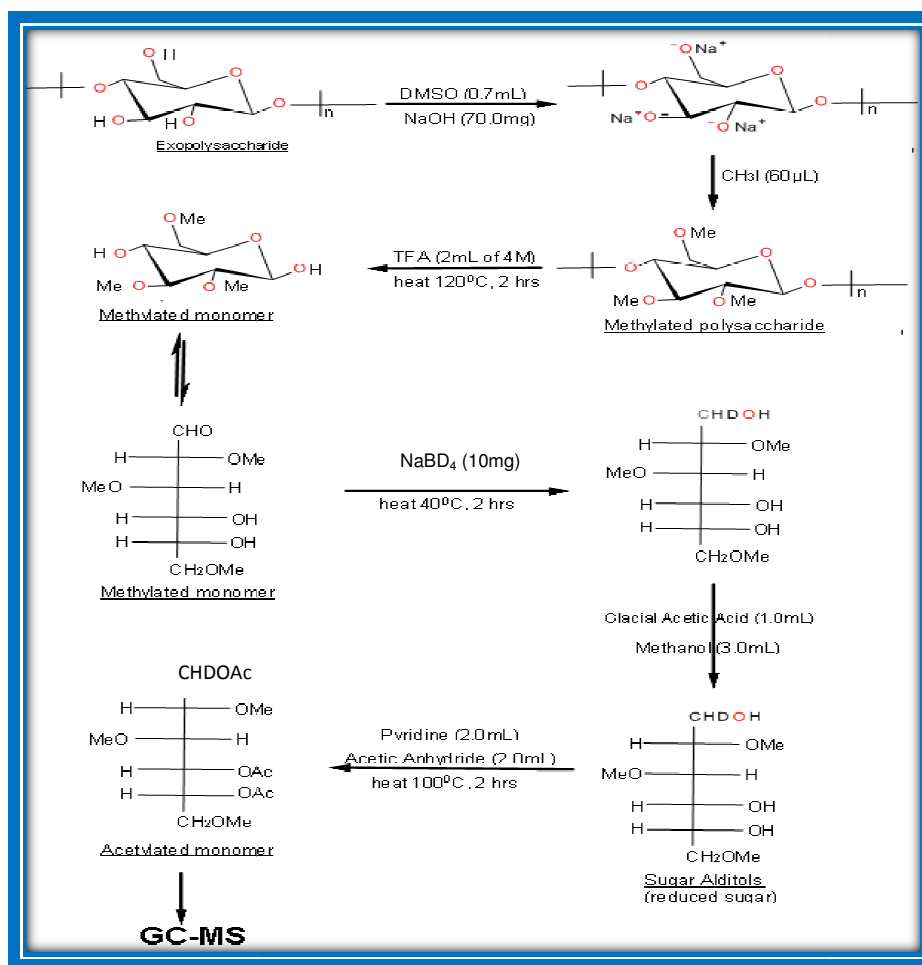


Figure 30: Linkage reaction scheme

1.5.6 NMR analysis of Exopolysaccharides:

NMR based exopolysaccharide analysis is often combined with data from mass spectrometry or chemical information like monosaccharide composition or methylation analysis¹²⁷. In characterisation of the repeat unit's structure carbohydrates normally have at least two NMR-active nuclei, ^{13}C and ^1H , but also less frequently used nuclei like ^2H , ^3H , ^{15}N , ^{17}O , ^{19}F and ^{31}P can be used for studies of natural or synthetic oligosaccharides^{128,129,130,131}. The dispersion of resonances in the carbon spectrum is favourable, but the amount of material needed to acquire such a spectrum is relatively high due to the low natural abundance¹³² of ^{13}C .

Doco¹³³ was the first to determine the structure of the repeating unit from an EPS, produced by *Streptococcus thermophilus*, using NMR spectroscopy. Since

Doco's initial NMR analysis, many structures have been published, that use the advances in 1D- and 2D- NMR spectroscopy^{134,135,136}.

The ¹H NMR spectra of polysaccharides are usually highly complex, due to the resonance overlap of the ring protons which are frequently crowded and are present in a narrow region (3.0 to 4.0 ppm). However, the anomeric protons are usually distinct from this region, with signals markedly downfield from the ring protons due to the electron-withdrawing effects of the neighbouring ring oxygen atoms. Integration of the anomeric signals gives a preliminary indication of the number of sugars in the repeat unit and the relative amounts of each type of monomer. Most of the α-anomeric protons will appear in region of 5 to 6 ppm and most of the β-anomeric protons will appear in the region of 4 to 5 ppm. In addition to the proton spectrum, vital information about the repeat unit can be obtained from the carbon spectrum. One of the most useful carbon spectra are ¹³C DEPT-spectrum (Distortionless Enhancement by Polarization Transfer).

In combination with 1D-NMR, selective 2D-NMR experiments can be used to determine the structure of the polysaccharide units. A 2D-NMR experiment shows the specific environment in which each carbon and hydrogen are positioned and by scalar connectivity the structure of complex oligosaccharides repeating units of EPS can be determined. Some of the 2D-NMR used are:

COSY-	Correlation Spectroscopy
TOCSY-	Total Correlation Spectroscopy
HSQC-	Heteronuclear Single Quantum Coherence
HMQC-	Heteronuclear Multiple Quantum Coherence
HMBC-	Heteronuclear Multiple Bond Correlation

A ¹³C DEPT135 NMR spectrum shows all carbons that are attached to a hydrogen in the sample (-CH, -CH₂ and -CH₃). The NMR signals are shown as positive peaks for -CH₃ and for -CH, where as signals are shown as negative peaks for -CH₂. For aldohexoses, the signals from -CH (C2-C5) in the DEPT135 spectra are observed between 65-85 ppm (with -OH substitution), whereas the C1 signal appears between 95-105 ppm (due to the neighbouring electron withdrawing oxygen in the heterocyclic ring). The C6 signal, is observed as -CH₂ (negative peak), is

generally located between 60-70ppm. Any $-\text{CH}_3$ (rhamnose) are observed at a lower ppm.

Polysaccharides are insoluble in common NMR solvents such as CDCl_3 and d_6 -DMSO, therefore deuterium dioxide (D_2O) is used. Unfortunately, D_2O gives a signal from the HOD in the solvent which can cover important signals from the polysaccharide. The signal can be reduced by repeated freeze drying of samples from D_2O solutions.

1.5.7 MultiAngle Laser Light Scattering (MALLS):

Multiangle Laser Light Scattering (MALLS) is one of the most direct and effective ways of obtaining absolute molar mass and the average size of particles in solution, by detecting their light scattering¹³². It has been used to determine the weight-average molecular weights of several bacterial exopolysaccharide structures^{137,138,65}.

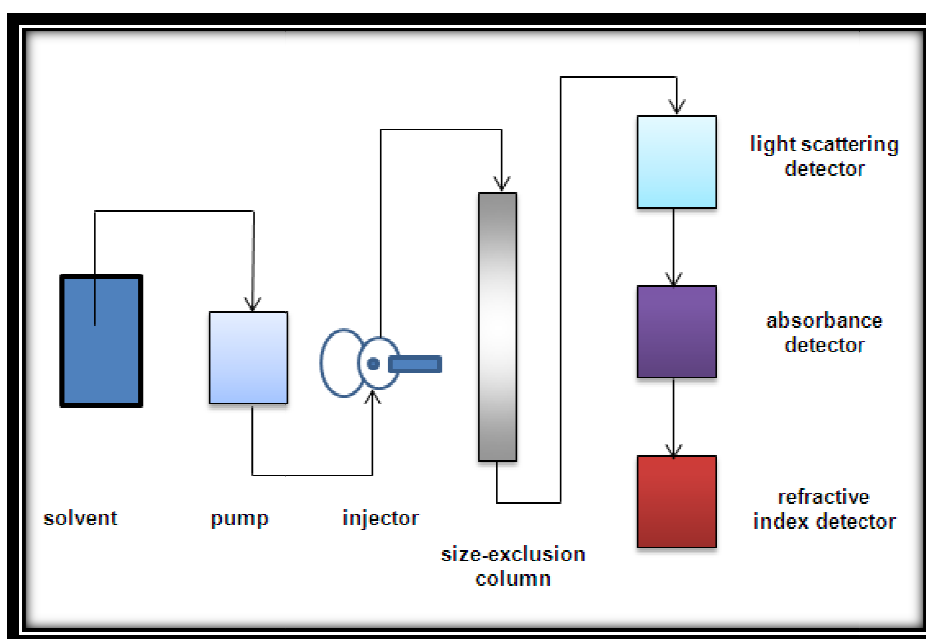


Figure 31: Laser light scattering scheme

The term multiangle refers to the detection of scattered light at different discrete angles by a single detector moving over a range or an array of detectors fixed at specific angular locations. In modern instruments, the laser beam is generally polarized, but the earlier work was performed with unpolarized sources, like Hg arc lamps¹³⁹.

1.5.8 Weight – Average Molecular Weight Determination

Polysaccharides have different molecular weight ranges and therefore they are polydispersed molecules (a polymer composed of macromolecules of differing molar masses). They are characterized by measuring their polydispersity, i.e: weight-average/molar mass dispersity (M_w/M_n) and degree of polymerization dispersity (X_w/X_n – size of polysaccharide can be expressed by the number of monosaccharide units)¹⁴⁰. The molar mass dispersity (M_w/M_n) is a ratio of weight average molecular weight divided by the number average molecular weight. A polymer is monodispersed if the M_w/M_n is equal to one.

1.5.9 Size Exclusion Chromatography – Multi Angle Laser Light Scattering (SEC – MALLS) Analysis of Exopolysaccharides

High performance chromatography systems have begun to replace the older technique of separating polysaccharides, which used gel permeation chromatography (GPC). GPC is now mostly used for sample purification because of the large volumes that can be loaded onto the column. Over the past two decades, absolute methods for the molecular mass determination of biological macromolecules have greatly improved, e.g, coupling of a multi-angle laser light scattering (MALLS) photometer to size exclusion chromatography (SEC-so-called SEC/MALLS), permitting on-line molecular mass determination by an absolute method¹⁴¹. HP-SEC-MALLS works on weight and size separation technique using smaller analytical columns^{142,143,144}. The sample is passed through an online ultraviolet (UV) light detector. After the UV, the flow passes through a differential refractive index (RI) detector for the determination of molecular mass of EPS. As MALLS is dependent on concentration, therefore SEC-MALLS must also be coupled to a separate detector for concentration determination. The widely used detectors are refractive index (RI) and ultra violet (UV) detectors. Oliva *et al.*¹⁴² compared the precision and accuracy of both SEC-MALLS/UV-Vis and SEC-MALLS/RI. The results were found to be having a high degree of correlation with the expected precision and accuracy for most proteins (12-480 kDa). The refractive index detector measures the concentration of the analytes eluting through references to the refractive index increment (dn/dc).

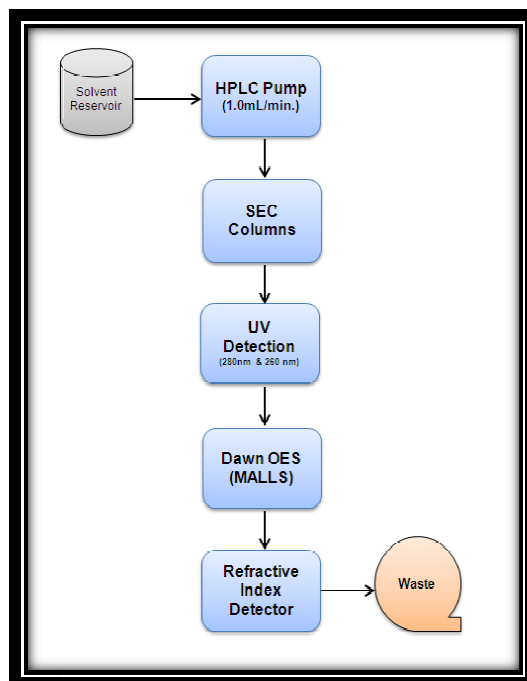


Figure 32: Schematic diagram for SEC-MALLS system

1.5.9.1 Refractive Index Increment (dn/dc)

The accuracy of molecular weight determination by MALLS is dependent on refractive index increment (dn/dc). The dn/dc value (refractive index increment) describes the refractive index changes in a polymer solution with respect to solute concentration. Polymers with larger values of dn/dc scatter more light at the same mass than those having smaller values. As dn/dc changes with wavelength, it is vital to measure it at the same wavelength as the light scattering apparatus. The refractive index detector requires a calibration constant so that the software can convert the signals to Rayleigh ratios and refractive index differences respectively. The calibration constant is measured by using toluene, due to its high and accurately determined Rayleigh ratio and also its refractive index is similar to the cell windows in the refractive index detector¹³².

The analysis of light scattering data can be processed using different mathematical equations. The most common equation used to derive M_w is using either the Debye plot, Zimm plot or Berry plot. By applying these different types of plots, more accurate results can be generated for different types of macromolecules.

Andersson¹⁴⁵ suggests that the Berry plot is superior, in terms of accuracy and robustness.

Refractive index increment is an essential parameter to several physical and analytical techniques that are based on optical measurements¹⁴⁶. It is important to know dn/dc :

- ✚ To characterize the shape, size and molecular weights of the polymers¹⁴⁷
- ✚ To calculate solute concentration based on refractive index measurements¹⁴⁸
- ✚ To obtain concentration and kinetics of molecules adsorbing on surfaces¹⁴⁹

Scientists are trying to make a refractometer having high precision (10^{-5} - 10^{-6} refractive index unit-RIU) and the capability of measuring dn/dc , led to the developments of differential refractometers (DRs). In fact most of the values that are present in the literature were measured using DRs¹⁴⁶.

1.5.9.2 SEC with Differential Refractometer:

Another technique which is sometimes used to determine M_w of polysaccharides was to use SEC in combination with a differential refractometer and comparison of the retention times of the analyte generated from a series of different M_w standards. An example of this has been reported by Beer and co-workers, who used a series of pullulan and dextran standards to determine the M_w of guar gum. This approach is acceptable for simple homopolysaccharides that have similar structures to the standards, but for exopolysaccharides that can be complex heteropolysaccharides the M_w determination is inaccurate, which is why M_w determination using dn/dc values is now the preferred technique.

1.5.10 Uronic acid determination:

In their natural environment, the extracellular polysaccharide frequently binds microbes to surfaces and causes physical modification of the microenvironment. The binding of EPSs to surfaces will be facilitated by the presence of charged groups in the repeating unit. The most frequently encountered charged monosaccharides are uronic acids and these are difficult to analyse using conventional monomer analysis methods (GCMS).

Quantitative measurement of uronic acid is commonly done using colorimetric methods after first hydrolyzing the polysaccharides with sulphuric acid (aq.)^{150,151}. But there is a problem with the older methods for determining uronic acid content. Neutral sugars and their degradation products from acid hydrolysis can interfere in the colorimetric determination of uronic acids¹⁵². Classical colorimetric methods include the phenol-sulfuric acid method¹⁵³ and the anthrone method¹⁵⁴ and these have been applied to the analysis of EPSs. However Sheng et al.¹⁵⁵ reported that these methods under-estimate uronic acids. When comparing standards, neutral sugars are frequently used to calibrate the UV-response (phenol/sulphuric- $\lambda=485$ nm) however uronic acids give small absorptions when treated in a similar manner (42% and 63%) so an underestimation of the total carbohydrate content is obtained. Colorimetric methods for the determination of uronic acids have also been developed. Early methods developed by Dische¹⁵¹ and Asboe¹⁵⁶ used carbazole or methoxydiphenyl (MHDP) as reagent. However, the accuracy of these was limited when uronic acids were present along with neutral sugars. A more up to date method, which was developed by Filisetti-Cozzi and Carpita¹⁵² overcame these problems by incorporating sulfamate/hydroxydiphenyl reagent to the reaction mixture with sodium tetraborate for the detection of D-mannuronic acid. With glucuronic acid as the standard, the protocol is frequently used to measure the glucuronic acid contents of xanthan and gellan gums¹⁵⁷.

1.6 AIM OF RESEARCH:

The **first aim** of this project was to analyse the structure of bacterial exopolysaccharides produced from bifidobacteria from a range of different sources. The samples were received from collaborators working in the Spanish Dairy Industry (Dr. Patricia-Ruas Madiedo). The main techniques used were, NMR, HPAEC-PAD (monomer analysis), GC-MS (monomer & linkage analysis), HP-SEC-MALLS (molecular weight), Preparative column (separation of different molecular weight EPSs) for determination of the repeating oligosaccharide structure. These are probiotic strains and that the EPS may be responsible for the biological act.

The **second aim** of this project was to analyze the EPS produced by pathogenic bacteria; i-e: *Campylobacter jejuni*. The samples were received from academics at University College, London, United Kingdom (Dr. Elaine Allan). The main techniques used were, NMR, HPAEC-PAD, GC-MS and HP-SEC-MALLS, for the determination of the repeating oligosaccharide structure. The academics at Cork are presently working on the biofilm/extracellular polymer matrix (EPM) that is produced by *C. jejuni*. These biofilms help the bacteria to survive in the environment. EPMs major component is polysaccharide, which is not yet characterized. The academics are trying to characterize the polysaccharide component secreted when *C. jejuni* is exposed to pancreatic α -amylase.

The **third aim** of this project was to analyze the EPS produced by *Bifidobacterium breve* different strains. The samples were received from the academics at University College, Cork, Ireland. The main techniques used were, NMR, HPAEC-PAD, GC-MS and HP-SEC-MALLS, for the determination of the repeating oligosaccharide structure.

2. EXPERIMENTAL

2. EXPERIMENTAL

2.1 General Reagents:

The general reagents used throughout the experiments were all purchased from either Sigma–Aldrich Co. Ltd (Gillingham, Dorset, UK), Fisher Scientific UK (Loughborough, Leicestershire, UK), VWR International Ltd (Lutterworth, Leicestershire, UK), Acros Organics (Part of Thermo Fisher Scientific, Loughborough, Leicestershire, UK), Goss Scientific Instruments Ltd (Nantwich, UK), Wilmad Labglass (Nantwich, Cheshire, UK) unless otherwise stated.

2.2 Exopolysaccharides:

EPS produced by *Streptococcus thermophilus* (referred as EU20) was kindly donated by the Department of Chemical and Biological Sciences, University of Huddersfield, UK. EPS produced from *Bifidobacterium* subspp. *animalis* (samples labelled as: A1 Batch 5, A1dOx Batch 9, A1dOx R, A1 Broth, A1dOx Broth, A1dOx R Broth) were kindly provided by Instituto de Productos Lacteos de Asturias – Consejo Superior de Investigaciones Cientificas (IPLA-CSIC), Villaviciosa, Asturias, Spain. β -Glucan was kindly donated by the Department of Food Science, University of Huddersfield, UK. EPS produced from *Campylobacter* subspp. *jejuni* (samples labelled as 11168H and KpsM) were provided by academics from University College, London, UK. EPS produced from *Bifidobacterium* subspp. *breve* (samples labelled as *B. breve* strain JCM7017, *B. breve* strain JCM7019, *B. breve* strain UCC2003, *B. breve* strain NCFB2258, *B. breve* UCC2003 POS NaOH, *B. breve* UCC2003 NEG NaOH, *B. breve* UCC2003 POS EDTA, *B. breve* UCC2003 NEG EDTA, *B. breve* UCC2003 EPS –ve, *B. breve* UCC2003 EPS +ve, *B. breve* UCC2003 (DEL) deletion mutant, *B. breve* UCC2003 Inversion strain) were provided by academics from University College, Cork, Ireland.

2.3 Structural Characterisation/Analysis of EPS:

2.3.1 Nuclear Magnetic Resonance (NMR):

All NMR spectra of the EPSs were run on either a Bruker Avance AV500 500.13 MHz spectrum with a 11.7 Tesla Ultra Shield™ magnet or on a Bruker DPX400 400.13 MHz unshielded magnet or Bruker AVIII 400.13 MHz with a 9.1 Tesla Ascend™ magnet. All EPS samples were prepared in deuterium oxide (D₂O) and were recorded at 70 °C or at room temperature. All one-dimensional NMR experiments (¹H and ¹³C DEPT 135) and two-dimensional NMR experiments (COSY, HMBC, HSQC, TOCSY, HSQC-TOCSY and NOESY) were run on different samples and standards of EPS. TOPSPIN version 3.1 was used for acquiring and analysis of NMR spectra. Chemical shifts were expressed in ppm relative to an internal standard of acetone.

2.3.2 Monomer analysis:

The monomer analysis process consists of 3 steps, namely hydrolysis, reduction and acetylation.

2.3.2.1 Hydrolysis:

For the hydrolysis of an EPS, trifluoroacetic acid (TFA–2.0 mL of 2M) was added to the EPS sample (3.0 mg) in a pressure tube. This was then heated at 120 °C for 2h. After 2h, the samples were cooled to room temperature and the cap of the pressure tube was removed. The solution was evaporated to dryness under a constant stream of nitrogen at 60 °C to give monomers which were used directly in the next step. To the dried residue, ultra pure water (3.0 mL-UPW) was added and 1.5 mL was used for HPAEC analysis and the other 1.5 mL was used in the reduction step.

2.3.2.2 Reduction:

In the reduction step, NaBH₄ (10.0 mg) was added to the pressure tube containing the hydrolyzed EPS (1.5 mL) in order to reduce the sugar monomers. The pressure tube was sealed and heated at 40 °C for 2h. After 2h, the cap of the pressure tube was removed and the solution was evaporated to dryness under a

constant stream of nitrogen at 60 °C. Glacial acetic acid (1.0 mL) was then added to the residue and the liquid evaporated to dryness under a stream of nitrogen. Methanol (3x1.0 mL) was then added and subsequently evaporated under nitrogen, in order to remove the borate complex and to give methylated sugar alditols.

2.3.2.3 Acetylation :

In the acetylation step, pyridine (2.0 mL) and acetic anhydride (2.0 mL) were added to the dried residue (sugar alditols) in a pressure tube, this was then heated at 100 °C for 2h. After 2h the solution was evaporated to dryness under a constant stream of nitrogen at 40 °C. The dried residue (acetylated monomers) was then suspended in UPW (5.0 mL) and was extracted with chloroform (3x10.0 mL). The total organic layer was then washed with UPW (2.0 mL). The combined organic layer was collected in a flask and anhydrous sodium sulphate (30.0 mg) was added and the sample left to stand for 30 minutes at 4 °C. The solution was then filtered and the liquid evaporated to dryness under a constant stream of nitrogen at 40 °C. The resulting residue was then dissolved in acetone (2.0 mL) and analyzed by GCMS.

2.3.2.4 High Performance Anion Exchange Chromatography –

Pulsed Amperometry Detection (HPAEC-PAD):

The HPAEC Instrument used was a Dionex ICS–3000 Ion Chromatography System (Dionex Corporation, CA, USA), which consists of Dionex AS (Auto Sampler), Dionex ICS 3000 EO (Eluent Organiser), Dionex ICS 3000 DC (Detector Chromatography), Dionex ICS 3000 DP–Dual Pump System, Dionex ICS 3000 EG–RFIC, (EG-Eluent Generator, RFIC-Reagent-Free Ion Chromatography). Chromeleon® Xpress software was used for the processing of the data.

<u>Typical Chromatographic Conditions</u>	
Instrument	Dionex ICS - 3000 Ion Chromatography System (Dionex Corp. CA, USA)
Pump	Dionex ICS-3000 DP-Dual Pump System
Column	CarboPac PA20 analytical column, 3x150 mm, 6.0 μm partical size
Mobile Phase	8mM NaOH
Flow Rate	0.45 mL / min
Injection Volume	25.0 μL
Temperature	30 $^{\circ}\text{C}$
Pressure	2815.4 psi
Run Time	20 min.

2.3.3 Linkage analysis:

The linkage analysis comprised methylation, hydrolysis, reduction and acetylation steps.

2.3.3.1 Methylation:

EPS (3.0 mg) was added to a pressure tube along with DMSO (0.7 mL) and the solution was stirred at room temperature until the formation of a slurry was observed. Dried and crushed sodium hydroxide (70.0 mg) was added with stirring along with methyl iodide (MeI) (60.0 μL). After 20 minutes, 1.0 mL of UPW was added in the resulting solution (methylated polysaccharide) and extracted with dichloromethane (1.0 mL). The dichloromethane (DCM) was then washed with UPW (3x5.0 mL). The resulting liquid was then evaporated to dryness under a constant stream of nitrogen at 40 $^{\circ}\text{C}$, to give the methylated polysaccharide as a solid which was used directly in the next step.

2.3.3.2 Hydrolysis:

TFA (2.0 mL of 2M) was added to the dried residue in the pressure tube, and was heated at 120 °C for 2h. After 2h, the samples were cooled to room temperature. Then the solution was evaporated to dryness under a constant stream of nitrogen at (60 °C) to give methylated monomers.

2.3.3.3 Reduction:

The dried residue (methylated monomers) was reconstituted with UPW (1.0 mL). Then NaBD₄ (10.0 mg) was added in order to reduce the sugar monomers; the sealed pressure tube was heated at 40 °C for 2h. After 2h, the solution was evaporated to dryness under a constant stream of nitrogen (60 °C). Glacial acetic acid (1.0 mL) was added to the dried residue and the solution was again evaporated to dryness under a constant stream of nitrogen. Methanol (3x1.0 mL) was then added and subsequently evaporated in order to remove the borate complex and to give methylated sugar alditols.

2.3.3.4 Acetylation:

Pyridine (2.0 mL) and acetic anhydride (2.0 mL) were then added to the dried residue (methylated sugar alditols) in the pressure tube, this was then heated at 100 °C for 2h. After 2h, the solution was evaporated to dryness under a constant stream of nitrogen at 40 °C. The dried residue (acetylated monomers) was then suspended in UPW (5.0 mL) and extracted with chloroform (3x10.0 mL). The combined organic layer was washed with UPW (2.0 mL). This was then dried with anhydrous sodium sulphate (30.0 mg) for 30 minutes. The solution was then filtered and the liquid evaporated to dryness under a constant stream of nitrogen at 40 °C. The resulting residue was then dissolved in acetone (2.0 mL) and analysis of the repeating unit linkages carried out by GCMS.

2.3.4 Gas chromatography-Mass spectrometry (GCMS):

The GCMS system consists of an Agilent 7890A GC system, Agilent 7683B Injector and Agilent 5975B Inert XL EI/CI MSD (Agilent Technologies, Edinburgh, UK). Agilent GCMS and Agilent MSD configuration was used the processing of the data.

<u>Typical Chromatographic Conditions</u>	
Instrument	Agilent 7890A GC system (Agilent Technologies, Edinburgh, UK)
Injector	Agilent 7683B
Mass Spectrometer	Agilent 5975B Inert XL EI/CI MSD
Column	Agilent 19091S-433, 30m \times 250 μ m \times 0.25 μ m
Carrier Gas	Helium
Mode	Split (split ratio of 10:1)
Flow Rate	1.0 mL / min
Injection Volume	0.25 μ m
Oven Temperature	140 $^{\circ}$ C
Front Inlet Temperature	250 $^{\circ}$ C
Pressure	12.775 psi
Run Time	38 min.

2.3.5 Size Exclusion Chromatography–Multi Angle Laser Light Scattering (SEC – MALLS)

The SEC-MALLS instrumentation consisted of a Shimadzu **HPLC** system (Shimadzu U.K. Ltd, Milton Keynes, UK), comprising a DGU-20 A₃–prominence degasser, LC-20AD–prominence liquid chromatograph system and an SPD-20 A–prominence UV/VIS detector, an injector port fitted with a Rheodyne 7125, a pump LC-20AD and with a detector (model SPD-20A).

All columns (see details below) were purchased from Polymer Laboratories, Ltd, Shropshire, UK (now ThermoFisher, UK). LC Real Time analysis software was used, for the analysis of chromatographs.

<u>Typical Chromatographic Conditions</u>	
Instrument	Shimadzu HPLC System (Shimadzu, UK, Ltd)
Injector	Rheodyne 7125
Pump	LC - 20AD
3 columns used that were attached in series	
Column 1	PL aquagel - OH 40 15µm, 300 x 7.5 mm (used for separating low molecular weight EPS- 10,000-200,000 Da)
Column 2	PL aquagel - OH 50 15µm, 300 x 7.5 mm (used for separating medium molecular weight EPS- 50,000-600,000 Da)
Column 3	PL aquagel - OH 60 15µm, 300 x 7.5 mm (used for separating high molecular weight EPS- 200,000->10,000,000 Da)
Guard Column	PL aquagel - OH Guard 15µm, 50 x 7.5 mm
Wavelength	280nm and 260nm
Mobile Phase	Ultra Pure Water
Flow Rate	1.0 mL / min
Injection Volume	25.0 µL
Pressure	450 psi
Run Time	100 min.

2.3.5.1 Malls light scattering detector and differential refractive index (dRI) detector for Molecular weight determination:

Molecular weight (Mw) and polydispersity (Mw/Mn) of the EPS were determined using HP-SEC-MALLS. Solutions (1.0 mg/mL) were prepared in deionised water and then filtered through a 0.2 µm PTFE syringe filter. Filtered samples were injected (using a 7125 injection port) onto an analytical size exclusion column. UPW was delivered by a HPLC pump (Prominence LC-20AD, Shimadzu) at 1.0 mL/min. The samples pass through a UV detector (Prominence SPD-20A, Shimadzu) with a wavelength set to 280 & 260 nm (to check the presence of protein & DNA in the samples). The concentration of the samples is then determined by a

refractive index (RI) detector (Optilab rEX) and finally the weight average molecular weight is measured using a multi-angle laser light scattering (MALLS) instrument.

The MALLS instrumentation consists of a Dawn EOS–enhanced optical system from Wyatt Technology which was used together with a refractive index detector–Wyatt Optilab rEX, Wyatt QELS (Wyatt Technology, Santa Barbara, CA, USA).

<u>Typical SEC-MALLS Conditions</u>	
Instrument	Dawn EOS (Wyatt Technology, Santa Barbara, CA, USA)
Detector	Wyatt Optilab rEX
Injector	Rheodyne 7125
Wavelength	280 nm and 260 nm
dn/dc value	0.148
Mobile Phase	Ultra Pure Water or 0.1 M NaOH
Flow Rate	1.0 mL / min
Injection Volume	25.0 μ L
Pressure	450 psi
Run Time	100 min.

2.3.6 Preparative size exclusion chromatography (SEC):

Preparative SEC was performed on a BioCAD Sprint FPLC System, attached to a preparative column from Pharmacia Biotech XK26/40 (26 mm is the inner diameter and 40 cm is the column length) with one adaptor and one base, purchased from Amersham Bioscience (GE Healthcare). Samples were detected using an ERMA ERC–7510 RI Detector with a chart recorder. The eluent reservoir used was 100 % A. BioCAD version 3.0 software was used for the processing of the data.

Solutions (5.0 mg/5.0 mL (1000 ppm)) were prepared in deionised water and were then filtered through a 0.2 μ m PTFE syringe filter. A glass column XK26/40 was filled with either Sephacryl S-500 HR (fraction range of 4×10^4 – 2×10^7 Da) having a matrix composed of allyl dextran and *N,N*-methylene bisacrylamide (average particle size 50 μ m) or Sephacryl S-200 HR (fraction range of 1×10^3 – 8×10^4 Da) having a

matrix composed of allyl dextran and *N,N*-methylene bisacrylamide (average particle size 50 μm) to separate different molecular weight EPSs. Filtered samples were injected (using a 7125 injection port) onto the BioCAD FPLC System. Mobile phase (0.1 M NaNO_3) was delivered by a BioCAD Sprint FPLC system, at 1.0 mL/min. The sample passes through the glass column (according to their molecular weight—high molecular weight EPS elute first) and entered into the RI detector and their presence was recorded on a chart recorder. Samples were collected according to the fraction collector settings (5.0 mL each sample or 2.0 mL each sample).

<u>Typical SEC Chromatographic Conditions</u>	
Instrument	BioCAD Sprint Perfusion Chromatography System (PerSeptive Biosystem, Incorporated, Massachusetts, USA)
Detector	ERMA ERC – 7510 RI (ERC International, Kawaguchi-City,, Saitma, Japan)
Chart Recorder	Amersham Pharmacia Biotech
Chart Recorder Sensitivity	32×10^{-5} (large peak) and 1/64 (small peak)
Chart speed	5 mm/min.
Glass Column	Pharmacia Biotech XK26/40 (with one adaptor and one base)
Injector	Rheodyne 7125
Wavelength	280 nm
Stationary Phase	Sephacryl S-500HR and Sephacryl S-200HR
Mobile Phase	0.1 M NaNO_3
Flow Rate	1.0 mL / min
Injection Volume	5.0 mL
Temperature	Room temperature
Pressure	6.89 bar
Run Time	180 min.

2.3.7 Preparative anion exchange chromatography (IEC):

Preparative IEX was performed using an AKTA PRIME FPLC system fitted with a glass column XK26/40 and employing an ERMA ERC-7510 RI Detector, UV detection at 254 nm, a fraction collector and a chart recorder.

Solutions of (5.0 mg/5.0 mL (1000 ppm)) were prepared in deionised water and then filtered through a 0.2 μm PTFE syringe filter. A glass column XK26/40, was filled with DEAE Sephacel-(fractionation range of approx. 1×10^6 Da, bead size range of 40–160 μm with an average particle size of 100 μm). A mobile phase (5.0 mM Tris-HCl with pH 7.2 and 1.0 M NaCl) was delivered by the FPLC system, at 1.0 mL/min., fraction collection was set at 5.0 mL each. Two methods were used for analysis: linear gradient increase in the mobile phase concentration and a constant mobile phase concentration. For the equilibration of the column, 5.0 mM Tris HCl was passed through the system for 60 min. Once the baseline was straight on the chart recorder, the sample was injected. The sample passes through the column eluting according to its charge and enters into the RI detector. From the chart recorder, the samples were collected according to the fraction collector settings (5.0 mL each sample or 2.0 mL each sample).

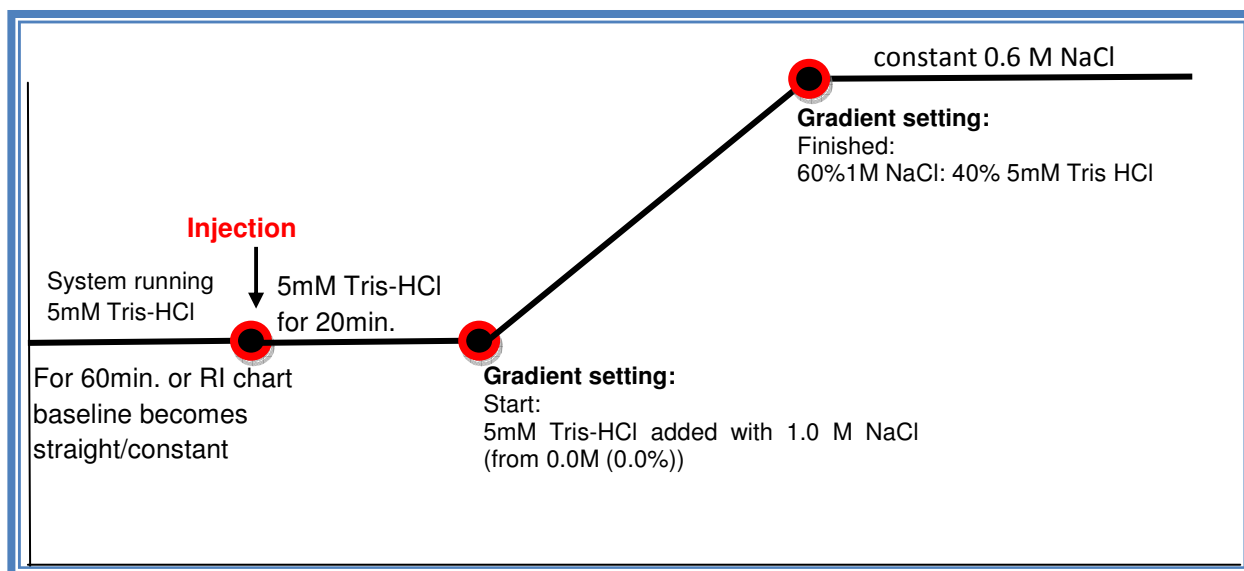


Figure 33: Gradient increase steps in anion exchange chromatography system

<u>Preparative IEX- Chromatographic Conditions</u>	
Instrument	AKTA PRIME FPLC System (Amersham Pharmacia Biotech)
Detector	ERMA ERC – 7510 RI (ERC International, Kawaguchi-City,, Saitma, Japan)
Chart Recorder	Amersham Pharmacia Biotech
Chart Recorder Sensitivity	32x10 ⁻⁵ (large peak) and 1/64 (small peak)
Chart speed	5 mm/min.
Glass Column	Pharmacia Biotech XK26/40 (with one adaptor and one base)
Injector	Rheodyne 7125
Wavelength	254 nm
Stationary Phase	DEAE - Sephacel
Mobile Phase	Tris–HCl (ph 7.2) and 1.0 M NaCl
Flow Rate	1.0 mL / min
Injection Volume	5.0 mL
Temperature	Room temperature
Pressure	6.89 bar
Run Time	380 min.

2.3.8 DIALYSIS:

Samples were dialyzed using cellulose membranes with an average flat width of 33.0 mm (1.3 in.) and having a molecular weight cut off (MWCO) of 12,500 Da (Sigma–Aldrich, Gillingham, Dorset, UK). For dialysis, the dialysis tubing was conditioned by adding lengths of (6.0–8.0 cm) tubing in boiling UPW (500 mL) containing ethylenediaminetetraacetic acid (0.186 g) and sodium hydrogen carbonate (10.0 g). The whole mixture was stirred for 10 mins., then the tubing was rinsed with cold UPW for 5 mins. After rinsing, the tubing was immersed again in boiling UPW for further 10 mins. After 10 mins. the tubing was rinsed again with cold UPW and stored at 4 °C in UPW for further use.

2.3.9 Uronic acid analysis:

As stated in the introduction, neutral sugars and their degradation products from acid hydrolysis can interfere in the colorimetric determination of uronic acids. For the present study, the Filisetti-Cozzi and Carpita method¹⁵² was employed for the analysis of uronic acid in EPS samples. Glucuronic acid was used as the standard by preparing different concentration of solutions (100 ppm-0 ppm).

The first step in uronic acid analysis was the hydrolysis of the EPS. EPS/standards (5.0 mg) were weighed out in to a pressure tube and conc. H₂SO₄ (1.0 ml) was added. The tube was placed in an ice bath and stirred (5 min.), a further portion of conc. H₂SO₄ (1.0 ml) was added to the tube and again stirred for further 5 min. in an ice bath. After 5min., UPW (0.5 mL) was added to the tube and the tube was stirred for additional 5 min. whilst being kept in an ice bath. The contents of the tube were diluted with UPW and were made upto 10.0 ml in a volumetric flask. The contents were transferred to a centrifuge tube (15.0 mL capacity) and centrifuged for 10.0 min at 2000xg (Beckman Coulter (USA)-Avanti J-26X PI High Performance Centrifuge with JSP F250 rotor, Piramoon Technologies), at room temperature to pellet any unhydrolysed material.

After the hydrolysis step, a sulfamic acid/potassium sulfamate solution (40µl of 4M, pH 1.6) was added to each of the standards and the EPS sample. After stirring the contents for 5 min., sodium tetraborate (2.40 ml of 75mM-prepared in sulphuric acid solution) was added to the tubes. The contents of the tubes were stirred vigorously for 10min., then the tubes were placed in a water bath at 100 °C for 20 min. After 20 min; the tubes were cooled by plunging them into an ice bath for 10min. A solution of 3-hydroxydiphenyl (0.15% 80 µL) was added to the tubes and the contents stirred for 15 min.). Finally then the contents of the tubes were heated at 100 °C for 5 min. over which time a pink colour develops (that shows the presence of uronic acids). After 10 min, each tube was analyzed at a wavelength of 520 nm using a UV/VIS spectrophotomer (Shimadzu-UV-160A, UV-Visible Recording Spectrophotometer, Shimadzu, Europa, GMBH).

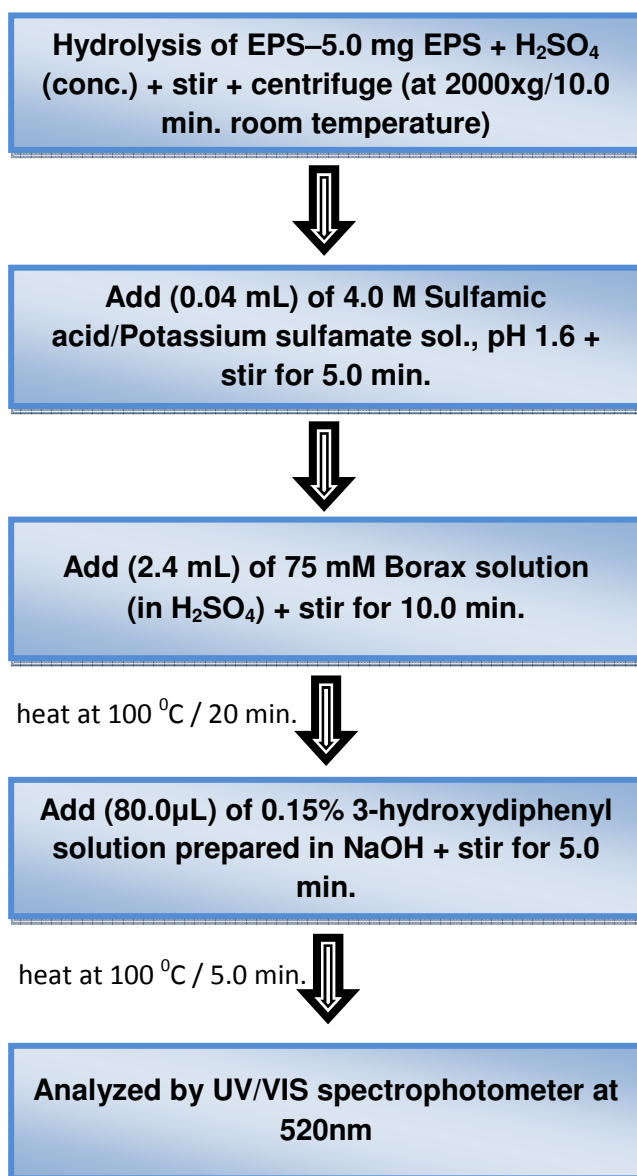


Figure 34: Uronic acid detection-Protocol

RESULTS AND DISCUSSION

*3. Analysis of the EPS recovered
from Campylobacter jejuni*

*4. Analysis of the EPS recovered
from Bifidobacterium animalis
subsp. lactis*

*5. Analysis of the EPS recovered
from Bifidobacterium breve strains*

*3. Analysis of the EPS recovered
from Campylobacter jejuni*

3. Analysis of the EPS recovered from *Campylobacter jejuni*

3.1 General Introduction:

The major gastrointestinal pathogen *Campylobacter spp.* was first discovered in 1886 by Theodor Escherich, from the colons of infants who had died of what he called “cholera infantum”¹⁵⁸. Later on, in 1906, it was identified in the uterine mucus of pregnant sheep by two British veterinary surgeons¹⁵⁹. The organism described was *Campylobacter fetus* (common cause of veterinary disease). In 1947, Vincent and his colleagues isolated *Campylobacter spp.* from the blood of three pregnant women. The organism was initially classified as *Vibrio spp.* because of their striking morphological similarity to the *Vibrio genus* and the type species now known as *Campylobacter fetus* was called *Vibrio fetus*¹⁵⁹. The term “*Campylobacter*” which is derived from two Greek words meaning “curved rod”, was first proposed by Sebald and Veron in 1963 as a new genus¹⁶⁰. The first report on a *Campylobacter spp.* outbreak dates back to 1938 in Illinois, when a milk-borne outbreak of diarrhoea was reported, now it is regarded as the first documented instance of human *Campylobacter enteritis*¹⁶¹. A milestone in the history of *Campylobacter spp.* came from Elisabeth King^{162,163} who made a systematic study of several *Vibrio spp.* and discriminated between *V. fetus* and the thermo-tolerant *V. jejuni* and *V. coli*¹⁶¹.

The analysis steps made by Elisabeth King¹⁶³ of *Vibrio spp.* continued till 1972, when *Campylobacter spp.* was isolated from human stools by Butzler and Dekeyser¹⁶⁴, and was based on the fact that *Campylobacter spp.* are small enough to pass through a filter that holds back other organisms¹⁵⁹. These discoveries received little attention until 1977 when Skirrow¹⁶⁵ described a method for isolating *Campylobacter spp.* from stools that eliminated the need to use the rather tedious filtration technique¹⁵⁹. The development of Skirrow’s selective medium enabled routine diagnostic microbiology laboratories to isolate *Campylobacter spp.* and to evaluate their clinical role. This brought to light the true dimension of *Campylobacter spp.* as the leading bacterial cause of human enteritis in the world¹⁶⁶.

Classification:

Kingdom	:	Bacteria
Phylum	:	Proteobacteria
Class	:	Epsilon Proteobacteria
Order	:	Campylobacterales
Family	:	Campylobacteraceae
Genus	:	Campylobacter
Species	:	<i>Campylobacter jejuni</i>

Today there is no doubt that *C. jejuni* is the commonest cause of bacterial-born diarrhoeal disease worldwide. In several developed countries, the number of reported *C. jejuni* cases currently exceeds 80 per 100,000 people¹⁶⁶. It is hyper-endemic in developing countries, owing to poor sanitation and close human contact with animals.

3.2 Campylobacter jejuni:

Campylobacter jejuni are small, curved, S-shaped (0.2–0.8 μm wide and 0.5–5.0 μm long¹⁵⁸) or spiral, motile (presence of single unsheathed flagellum at one or both poles¹⁶⁰) Gram-negative rods. The cell contains an outer membrane (consisting of lipopolysaccharide) and an inner membrane with a periplasmic space between the two membranes¹⁶⁷. They are microaerophilic, being neither truly anaerobic nor aerobic, but requiring an environment of reduced oxygen tension for optimal growth¹⁵⁹. Because of the requirement for reduced oxygen, they are very sensitive to stress (too much oxygen, acidic conditions, heating or drying) in the environment. They are motile with a corkscrew-like motion propelled via a polar unsheathed flagellum and occur as commensals in warm-blooded animals especially poultry¹⁵⁸.

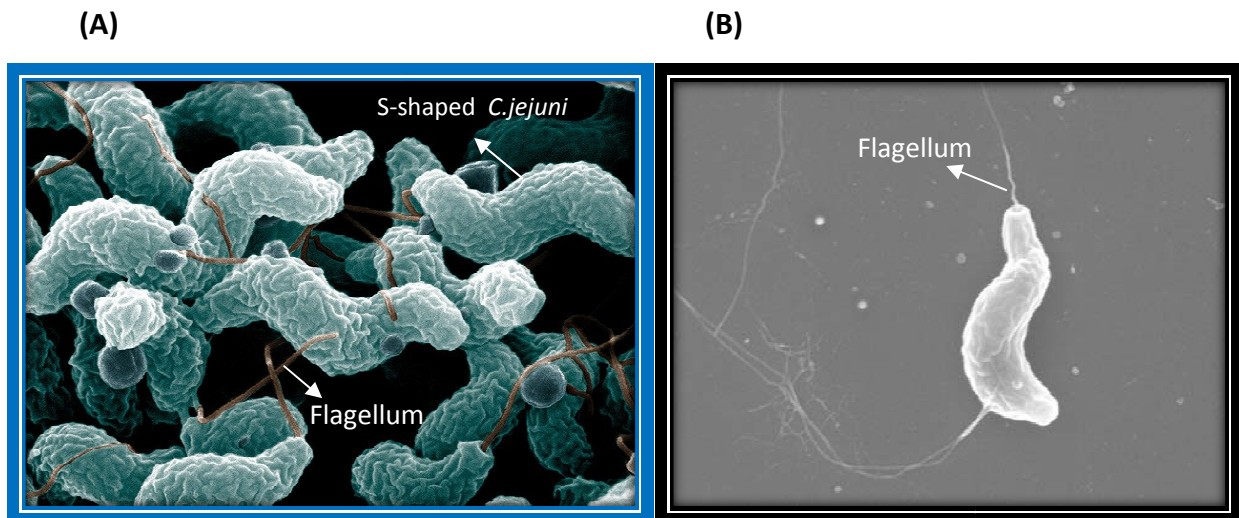


Figure 35: (A) Scanning Electron Microscopy Image of *Campylobacter jejuni*¹⁶⁸ – adapted from Pooley, C., Wood, D., USDA, Agricultural Research Service (ARS), United States Department of Agriculture, USA, (B) Single *Campylobacter jejuni*¹⁶⁹ -adapted from water scan images

Capsular polysaccharides (CPS) are a common feature on bacterial surfaces. As stated in the introduction they play an important role in bacterial survival. They can exhibit structural variation and provide resistance to phagocytosis¹⁶⁰. Production of CPS by *C. jejuni* remained unnoticed until the start of the analysis of the results of the first genome sequencing project in 1998. Identification of genes potentially involved in capsule biosynthesis during the sequencing resulted in a systematic genetic analysis of the corresponding locus and the identification of CPS in different strains of *C. jejuni*^{170,171}. Further experiments performed on *C. jejuni* also confirmed the presence of CPSs and also demonstrated the role of the capsule in serum resistance, epithelial invasion and diarrhoeal disease¹⁷². Further characterization led to visualization of the capsule by electron microscopy¹⁷². These experiments suggested that the previously labelled high molecular weight lipopolysaccharide of *Campylobacter jejuni* is in fact CPS¹⁶⁰. To date, the role of CPS in *Campylobacter jejuni* in protecting the bacterium against host innate defence remains limited¹⁶⁰.

Campylobacter jejuni has a relatively small genome of c. 1.6–1.7 Mbp of adenine and thymine rich DNA, whereas guanine and cytosine content ranges from 29–47 mol %¹⁷³. The small size of the genome is perhaps reflected in a requirement for a complex growth medium, no oxidation or fermentation of carbohydrates, no lipase or lecithinase activity and a lack of growth below pH 4.9¹⁵⁸.

Campylobacter spp. are present mostly in chickens and turkeys, wild birds also carry the organisms, but the birds are not associated with disease¹⁷⁴. It is also demonstrated that the *C. jejuni* can survive the commercial processing methods to which farmed chickens and turkeys are subjected^{175,176}.

3.2.1 *Campylobacter enteritis:*

The disease caused by *C. jejuni* is known as Campylobacter enteritis or gastroenteritis. The bacteria use their flagella at both poles for adhesion and invasion of the host¹⁶¹. The result of infection is severe diarrhoea and production of faecal leukocytes, combined with headaches, fever and muscle pain¹⁶¹. Although it is found in the intestines of many animals and humans, they travel through the whole intestine, which leads to diarrhoea. Clinical evidence suggested that the site of Campylobacter infection is likely to be the ileum and jejunum in the small intestines rather than in the large intestines¹⁷⁷. It is the leading cause of food-borne illness, but can be easily killed by cooking or heating. They can contaminate water, milk or undercooked meat (especially chicken)¹⁷⁷.

3.2.2 *Antibiotic resistance:*

Campylobacter jejuni is not known to produce any useful compounds or enzymes. It is mainly known as a pathogen that causes food – borne illness. However, *C. jejuni* produces an enzyme called beta-lactamase that is associated with its antibiotic resistance, mostly to ampicillin and penicillin¹⁷⁸. The mechanism of its beta-lactamase is still unknown, but effective antibiotics (erythromycin) have been developed to treat *C. jejuni* illnesses. In the past few years, a rapidly increasing proportion of *Campylobacter spp.* strains have been found to be fluoroquinolone resistant¹⁷⁹. Higher numbers of antimicrobial resistant *Campylobacter spp.* are found in developing countries, where antibiotic usage is unrestricted¹⁸⁰. The new antibiotics like azithromycin and clarithromycin, are effective against *C. jejuni* infections, but they are more expensive than erythromycin¹⁷⁹. Despite decades of usage, the rate of resistance of campylobacter to erythromycin remains relatively low, making erythromycin the ultimate drug for the treatment of *Campylobacter spp.* infection¹⁷⁹.

3.3 Present work on *Campylobacter jejuni*:

C. jejuni inhabits aerobic environments, but it is still difficult to explain the high incidence of infection. It has been suggested that *C. jejuni* survives in the environment by forming a biofilm¹⁸¹. Biofilms are commonly defined as matrix enclosed bacterial populations adherent to each other and/ or to surface or interfaces¹⁸², or a biofilm is a surface associated bacteria surrounded by an extracellular polymeric matrix (EPM)¹⁸³. Biofilm formation by *C. jejuni* has been reported but the EPM has not been characterized. It has recently been shown that exposure to concentrations of pancreatic α -amylase can increase biofilm formation however; there has been no attempt to characterise components of this biofilm. A major component of the EPM which provides a structural framework is polysaccharide¹⁸⁴. *C. jejuni* produces several surface associated carbohydrate structures like lipooligosaccharides (LOS) and capsular polysaccharides (CPS), but there is no evidence that these glycans contribute to biofilm formation^{183,185}. Although EPM has been visible by scanning electron microscopy in the biofilms¹⁸⁶, as stated earlier chemical and structural characterization has not been undertaken¹⁸³. McLennan *et al.*¹⁸⁵ reported a surface polysaccharide reactive with calcofluor white, up regulation of which increased biofilm formation, suggesting that this polysaccharide could be a component of the EPM¹⁸⁵.

3.4 Aim of the study:

The main aim of this study was to characterize the polysaccharide component secreted when *Campylobacter jejuni* has been exposed to pancreatic α -amylase. This work was performed in collaboration with the scientists at University College London, UK, who provided samples of biofilms.

3.5 Experimental:

3.5.1 General Reagents:

The general reagents used throughout the experiments were all purchased from either Sigma–Aldrich Co. Ltd (Gillingham, Dorset, UK), Fisher Scientific UK (Loughborough, Leicestershire, UK), VWR International Ltd (Lutterworth, Leicestershire, UK), Acros Organics (Part of Thermo Fisher Scientific, Loughborough, Leicestershire, UK), Goss Scientific Instruments Ltd (Nantwich, UK) and Wilmad Labglass (Nantwich, Cheshire, UK) or unless otherwise stated.

3.5.2 *Campylobacter jejuni* samples:

The two samples of polysaccharides derived from *Campylobacter jejuni* (referred as 11168H and KpsM) were kindly provided, by academics (Dr. Elaine Allan) from the Department of Microbial Diseases, UCL Eastman Dental Institute, University College London, London, UK.

3.6 Structural Characterisation/Analysis of EPS:

3.6.1 Nuclear Magnetic Resonance (NMR):

NMR spectra were run as described in the experimental section (2.3.1). All polysaccharide samples from *Campylobacter jejuni* were prepared in deuterium oxide (D₂O) and spectra were recorded at 70 °C. Spectra recorded included:

1D-NMR: ¹H and ¹³C DEPT,

2D-NMR: ¹H-¹H COSY, ¹H-¹³C HMBC, ¹H-¹³C HSQC, ¹H-¹H ROESY, ¹H-¹H NOESY

3.6.2 Monomer analysis using HPAEC-PAD:

Monomer analysis consists of 3 steps, namely hydrolysis, reduction and acetylation. All 3 steps have been discussed in detail previously at section 2.3.2.

3.6.3 Linkage analysis using GC-MS:

Linkage analysis of the EPS consists of methylation, hydrolysis, reduction and acetylation steps. All these steps have been discussed previously in section 2.3.3.

3.6.4 Gas chromatography–Mass spectrometry (GC-MS):

The GCMS system and experimental protocol used for the analysis have been discussed earlier in section 2.3.4.

3.7 Results and Discussions:

3.7.1 Structural analysis using NMR:

To determine the structure of the EPS repeat unit present in the *C. jejuni* samples, 11168H and kpsM, a series of 1D and 2D NMR experiments were carried out.

The first NMR experiment that was performed on the two samples was 1D-¹H NMR (proton NMR). The spectrum shows a signal from every proton in the repeating unit of the *C. jejuni* samples. The anomeric region (4.6–5.7 ppm) identifies the number of monosaccharides in the repeating unit.

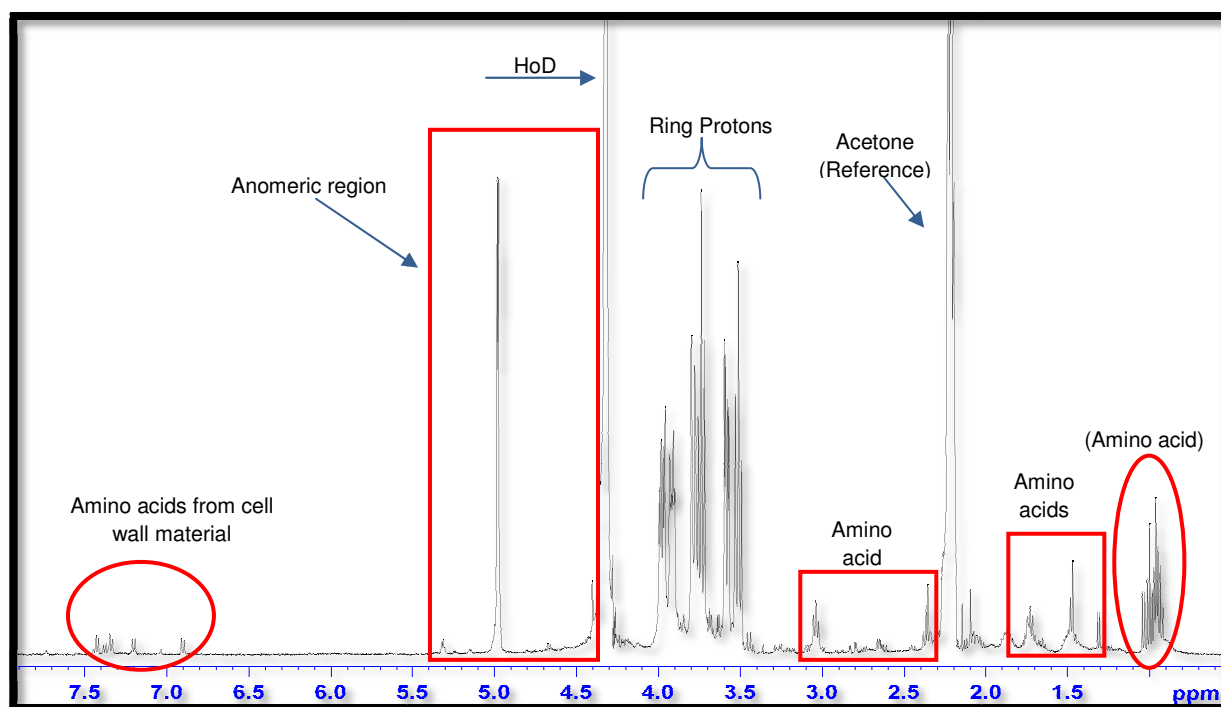


Figure 36: 11168H Crude Proton NMR spectrum

The ¹H NMR spectrum (Fig. 36) can be considered as being composed of two sets of signals: a group of intense resonances between 5.5 and 3.4 δ which are likely to be derived from a polysaccharide component of the biofilm and second set is a group of much weaker signals in the aromatic region (6.9–7.4 δ) and between 3.0

and 1.0 δ which are likely derived from peptides and amino acids that have been isolated as part of the biofilm.

Fig.37 represents the 1D- ^1H NMR of the second sample of EPS recovered from the *Campylobacter spp.* sample labelled as kpsM, which also shows the same profile as the 11168H sample.

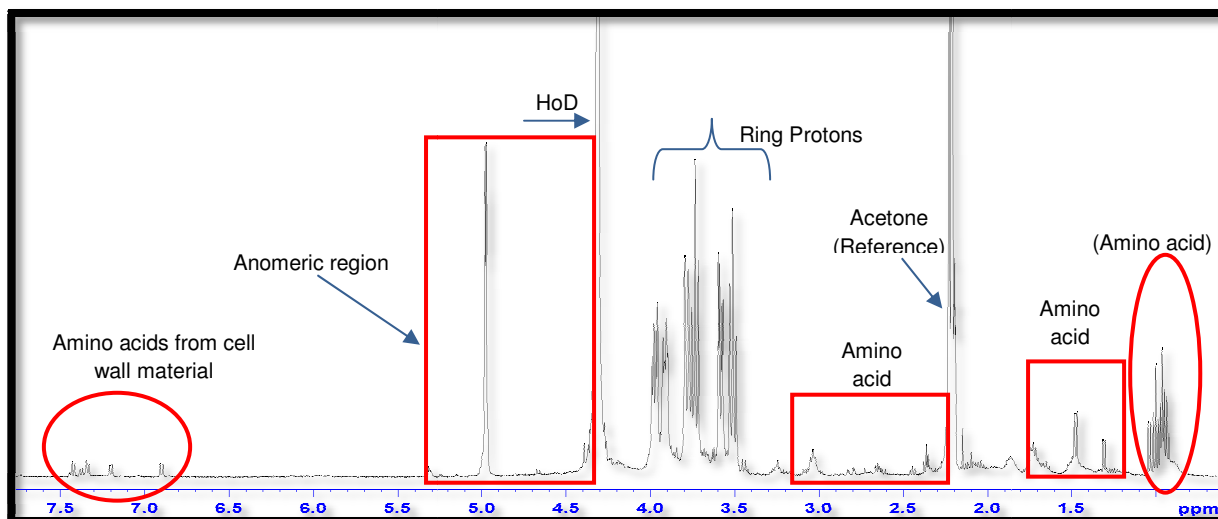


Figure 37: KpsM Crude Proton NMR spectrum

When polysaccharide signals from the two NMR spectra (11168H and kpsM), were compared closely (from 3.7–6.0 ppm), the main peaks from the two samples were very similar with a single anomeric resonance being observed at 5.4 δ .

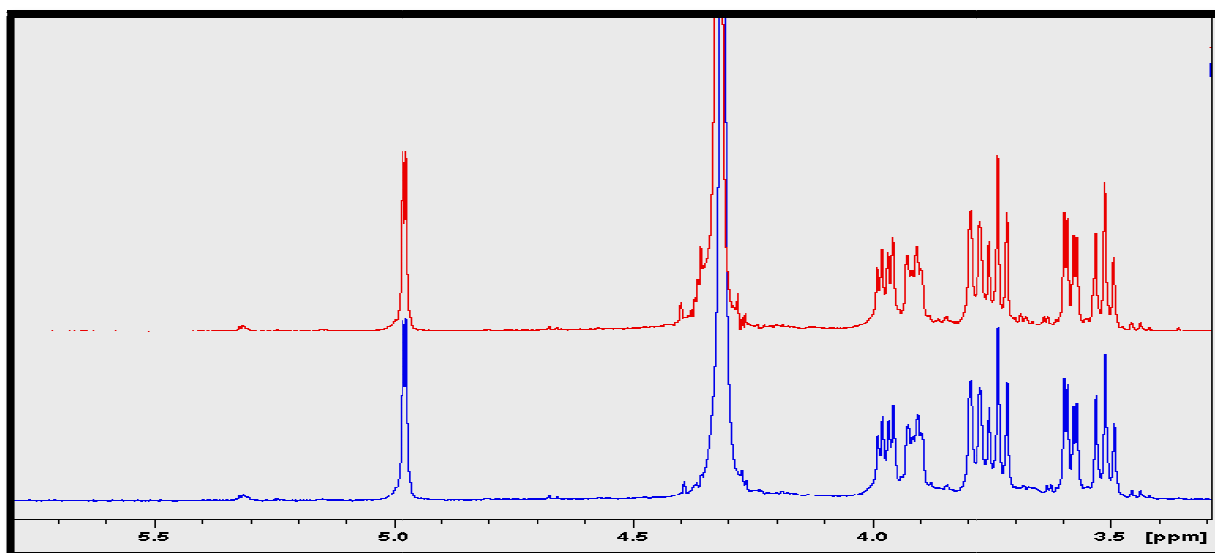


Figure 38: NMR spectra comparison of 2 samples of *Campylobacter jejuni* (blue spectrum – KpsM and red spectrum – 11168H).

The configuration of the anomeric protons were determined by the measurement of the $^3J_{1,2}$ coupling constant, the signal at 5.4 δ has a coupling constant of 6.5 Hz, representing a sugar having α -anomeric configuration. The signals between 4.4 and 3.8 δ represent those of ring protons and the integration, relative to that of the anomeric proton (1.6 δ), suggests that the polysaccharide is composed of a single monosaccharide and that this is a hexose, i.e: the EPS is a homopolysaccharide.

When the two samples of the *Campylobacter jejuni* were compared with the available NMR spectra of a series of glucans, the two samples looked to have a very similar spectrum to that of simple α -dextran. A dextran is a glucan (polysaccharide of D-glucose) composed of chains of varying lengths from 10 kD–150 kD, that are composed primarily of α -(1 \rightarrow 6) links with a small and varying amount of α -(1 \rightarrow 3) linked glucose units.

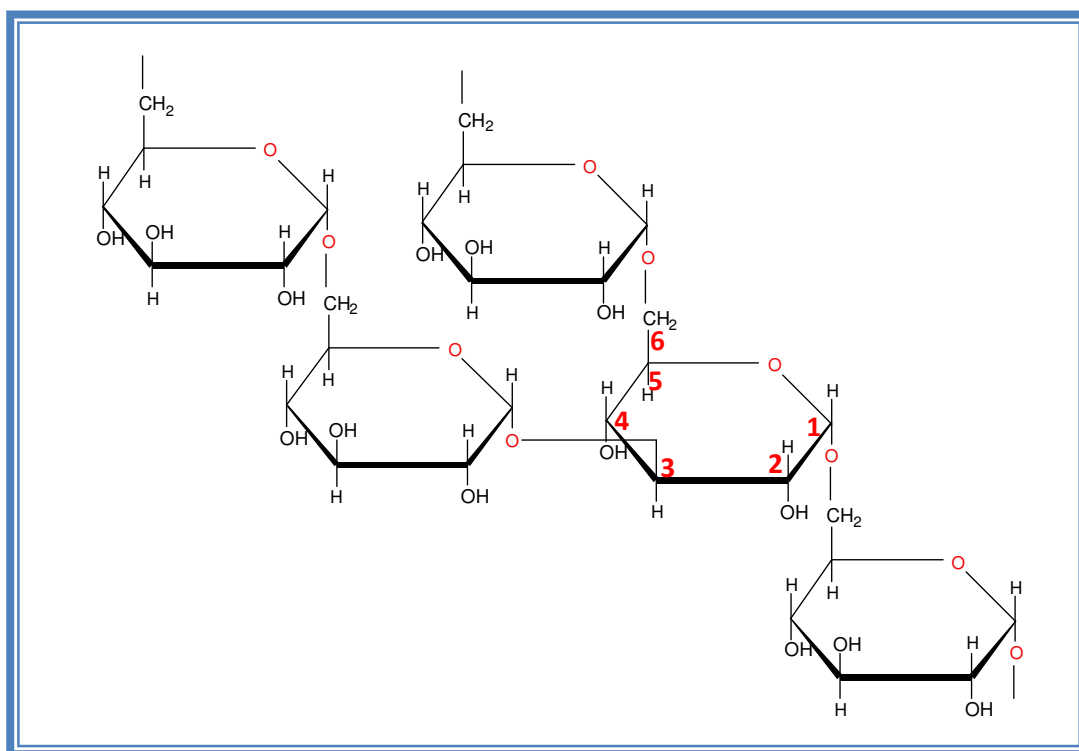


Figure 39: Structure of α -dextran, α -(1 \rightarrow 6) with α -(1 \rightarrow 3) branch

A spectrum was recorded for α -dextran under identical conditions and its appearance was exactly the same as that of the two samples of *Campylobacter jejuni*, i-e: 11168H and kpsM.

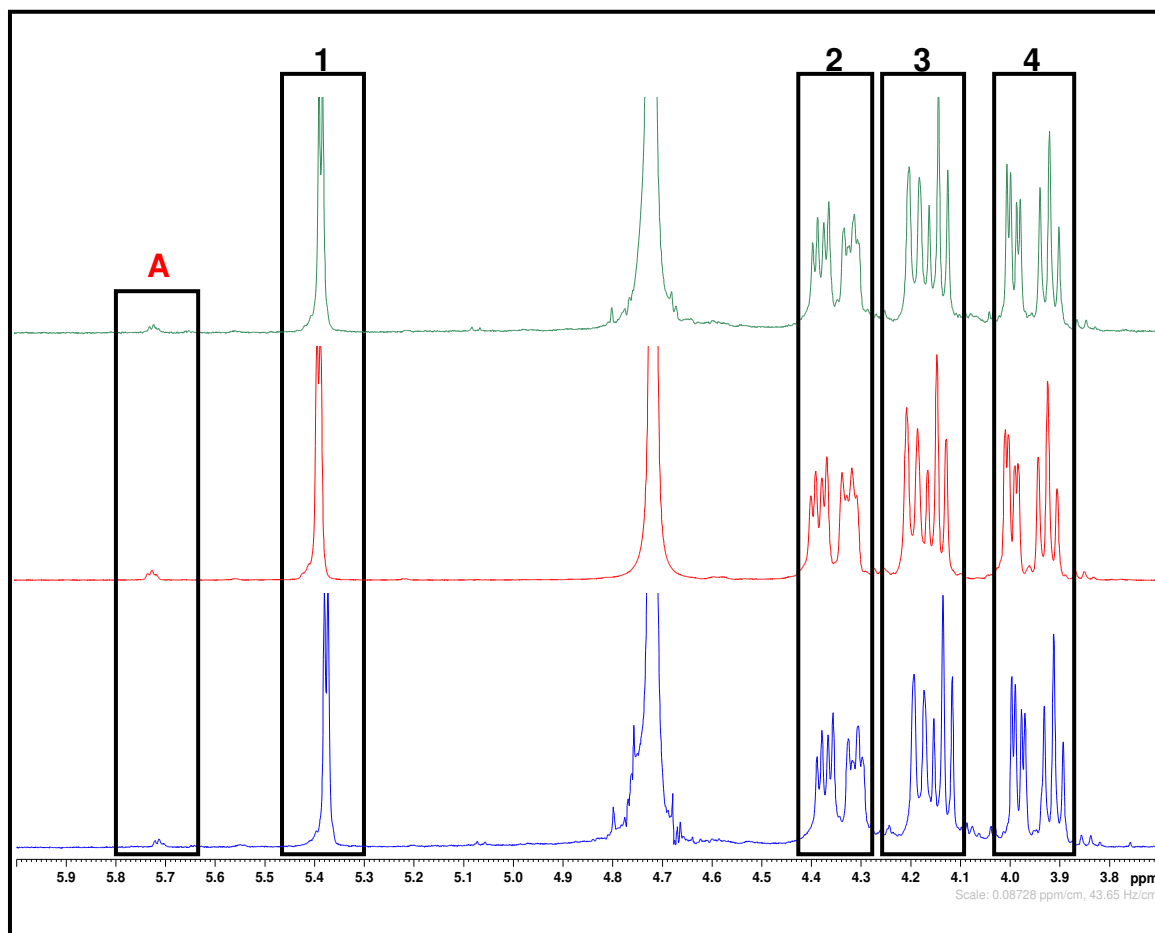


Figure 40: Comparison of 3 NMR spectra, blue = 11168H, red = α -dextran, green = kpsM

The above Fig. 40, represents the comparison of *Campylobacter jejuni* samples, 11168H (blue) and kpsM (green) with α -dextran (red). It is very clear from the comparison that the regions labelled **1**, **2**, **3** and **4** are identical, and the samples provided (11168H and kpsM) are also likely to be an α -dextran. Whereas the small signal at 5.7 ppm (labelled as **A**) represents the anomeric proton of the small amount of $\alpha(1,6)$ linked glucose.

After observing the 1D- ^1H NMR, a ^{13}C DEPT 135 spectrum was recorded (Fig.41) which shows CH and CH_3 as positive peaks (upwards) and CH_2 as a negative peak (downwards).

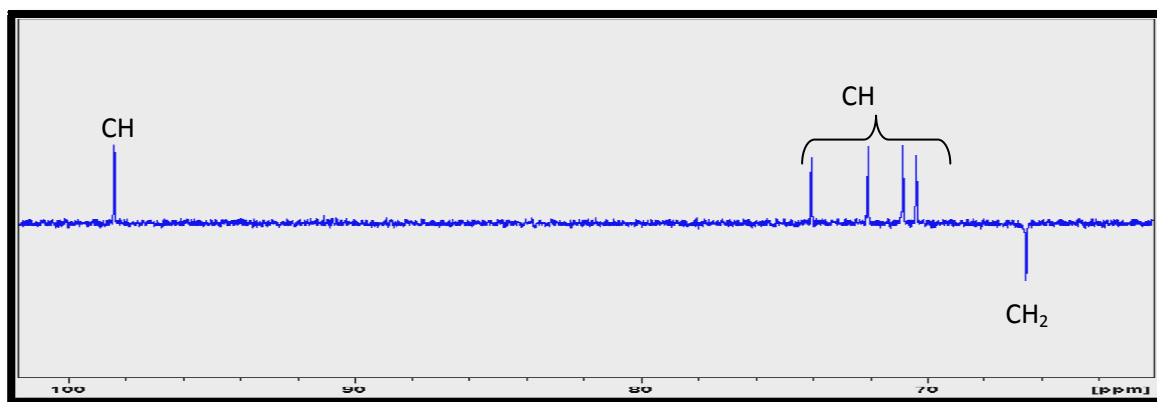


Figure 41: ^{13}C DEPT 135 NMR spectra of *Campylobacter jejuni*

From the observation of the ^{13}C DEPT 135 NMR spectrum above, the anomeric carbon signal appears at 99 ppm and the signals between 65–76 ppm identify the presence of ring carbon signals (due to neighbouring oxygen atom). There are 4 peaks located between 65–76 ppm that can be identified as CH, the negative peak at 66 ppm is from the CH_2 . Specific identification of the individual resonances has been based on the analysis of a series of 2D experiments.

When the ^{13}C DEPT 135 and ^{13}C DEPT 90 NMR spectra of the *Campylobacter jejuni* samples and that for an α -dextran were compared, again they were identical.

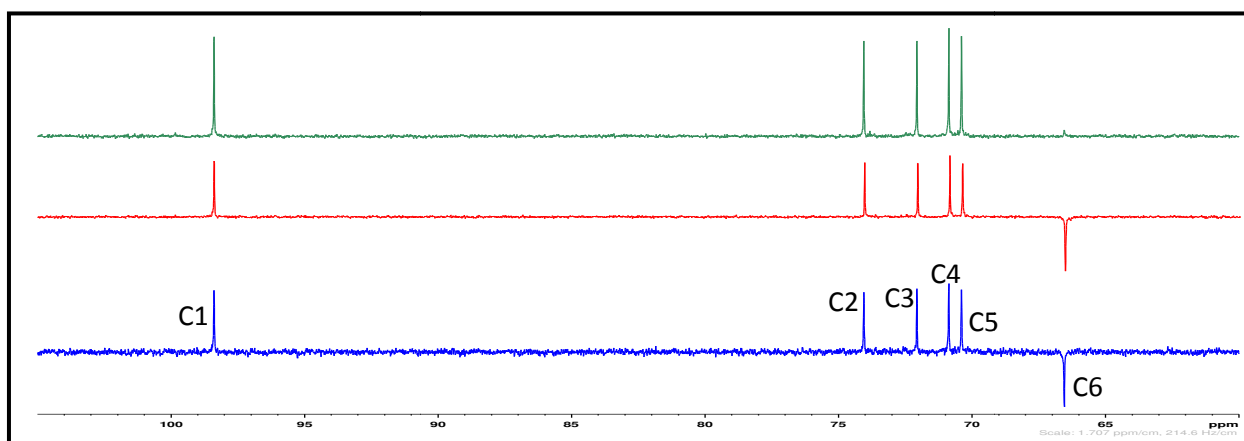


Figure 42: Comparison of *Campylobacter jejuni* sample 11168H ^{13}C DEPT 135 (blue), α -dextran ^{13}C DEPT 135 (red), α -dextran ^{13}C DEPT 90 (green)

To confirm the structure of the repeating unit of the EPS a ^1H - ^1H COSY experiment was performed on the *Campylobacter jejuni* samples as well as on the α -dextran sample. Both the experiment results were again identical.

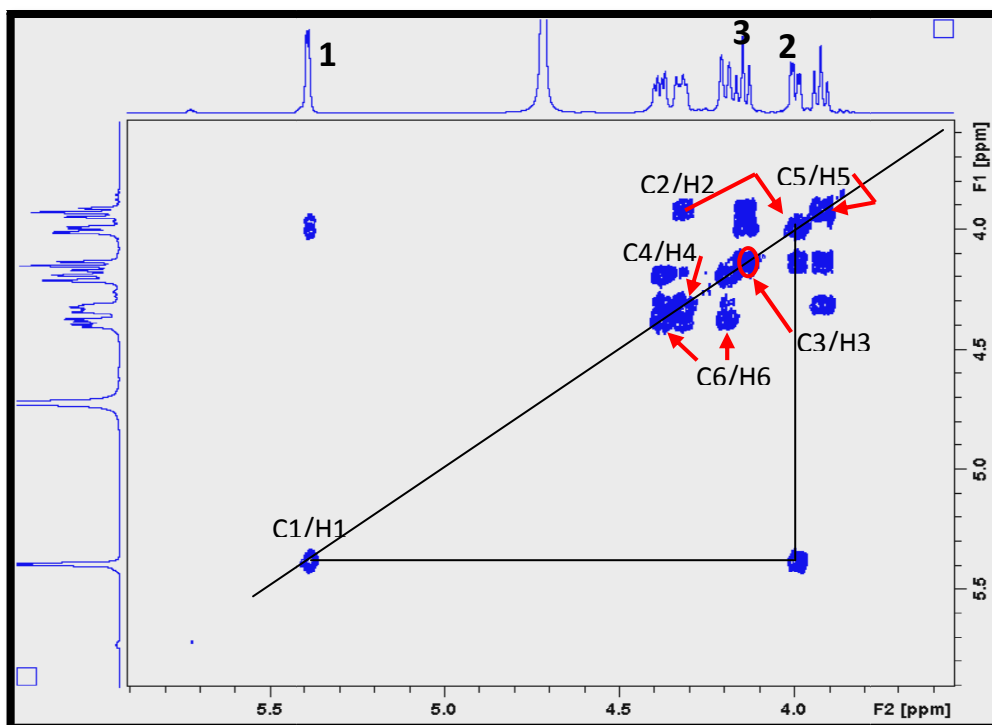


Figure 43: Comparison of ^1H - ^1H COSY spectrum of an α -dextran

The ^1H - ^1H COSY (Fig.43) shows protons attached to the adjacent carbon, the ^1H chemical shifts along both frequency axes are therefore correlated with each other. By drawing a diagonal cross, peaks can be identified for each of the monosaccharides ring protons H_2 - H_5 .

To locate the positions of the carbon resonances, a ^1H - ^{13}C decoupled HSQC 2D-experiment was performed. This spectrum contains a peak for each coupled ^{13}C . In the HSQC spectrum all six carbons can be identified (Fig. 44).

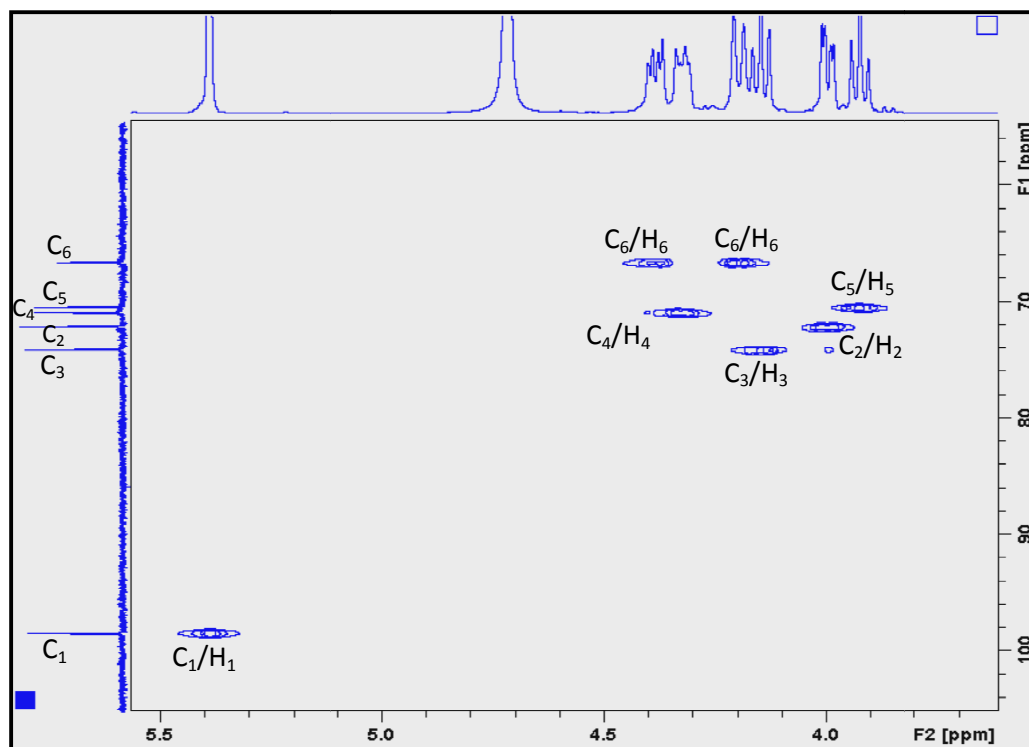


Figure 44: ^1H - ^{13}C HSQC spectrum of *Campylobacter jejuni* sample 11168H

From the above ^1H - ^{13}C HSQC spectrum, the protons can be assigned to their respective carbons, i-e: C_1/H_1 was identified at 98.76/5.38 ppm, C_2/H_2 was at 72.51/3.99 ppm, C_3/H_3 was at 74.52/4.15 ppm, C_4/H_4 was at 71.21/4.32 ppm, C_5/H_5 was at 70.75/3.99 ppm and C_6/H_6 was at 66.69/4.19 pm (table: 5).

Table 5: Chemical shifts of carbon and proton atoms

Carbon position	Chemical Shift (ppm)	Hydrogen position	Chemical Shift (ppm)
C1	98.76	H1	5.38
C2	72.51	H2	3.99
C3	74.52	H3	4.15
C4	71.21	H4	4.32
C5	70.75	H5	3.99
C6	66.69	H6	4.19

3.7.2 Structural analysis using GC-MS and HPAEC - PAD:

After getting the structural information from the NMR interpretation, monomer and linkage analysis were performed to confirm that the monomer was glucose and that the glucose monomers were joined by an $\alpha(1\rightarrow6)$ -linkage. GC-MS and HPAEC-PAD techniques were used to identify the monomers and the linkage present in the samples.

3.7.3 Monomer Analysis by HPAEC - PAD:

Monomer analysis by HPAEC – PAD is used frequently, as it has only one simple and quick step (acid hydrolysis) for analysis. The detailed procedure is discussed earlier in section 2.3.2.

The *Campylobacter jejuni* samples were processed using monomer analysis. The standards (glucose, galactose, rhamnose and mannose) were run, to identify the respective retention times of the monomers. Each standard was run in triplicate to minimize the variation in the retention times (table: 6). The peak's retention times (RT) give us the information of the presence of the respective monomers that were present in the sample.

Table 6: HPAEC – PAD retention times of standards

Standards	Average Retention Time (RT) (min.)	Standard Deviation (SD)
Rhamnose	4.92	0.003
Mannose	8.48	0.050
Galactose	6.32	0.013
Glucose	9.50	0.011

After acid hydrolysis of the two samples of *Campylobacter jejuni*, the samples were run on the HPAEC–PAD along with the standards. The two samples gave just one major peak, at an average RT of 9.5 min. (Fig.45 & 46). When the observed data was compared with the standards analysis chromatogram, the two samples were identical to glucose.

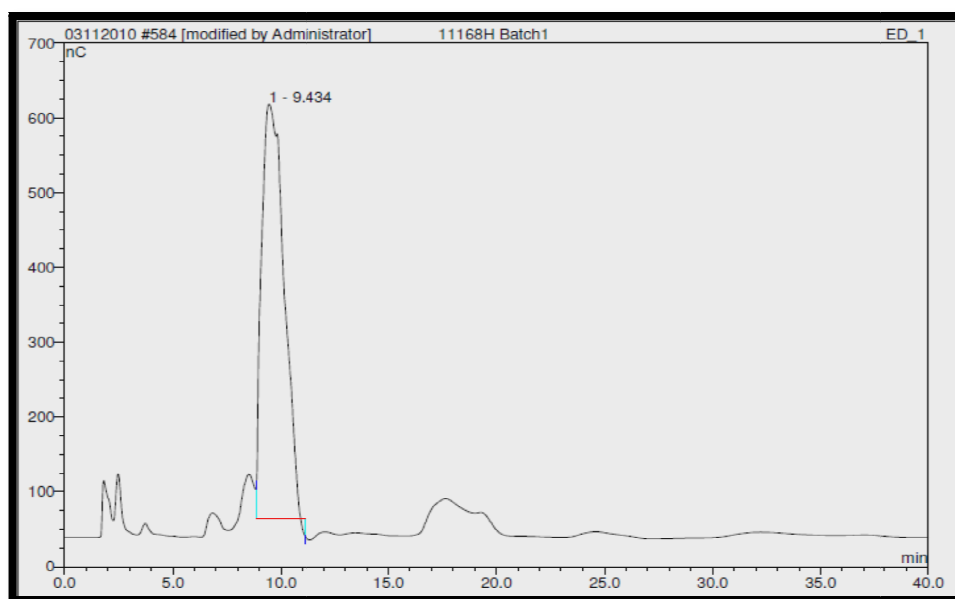


Figure 45: After hydrolysis - HPAEC-PAD chromatogram of *Campylobacter jejuni* sample 11168H

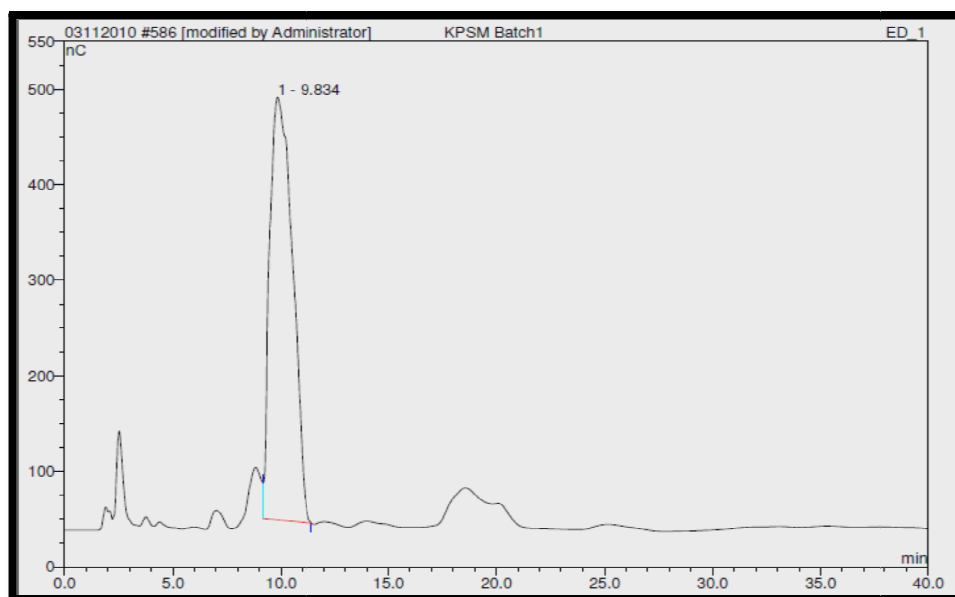


Figure 46: After hydrolysis - HPAEC-PAD chromatogram of *Campylobacter jejuni* sample kpsM

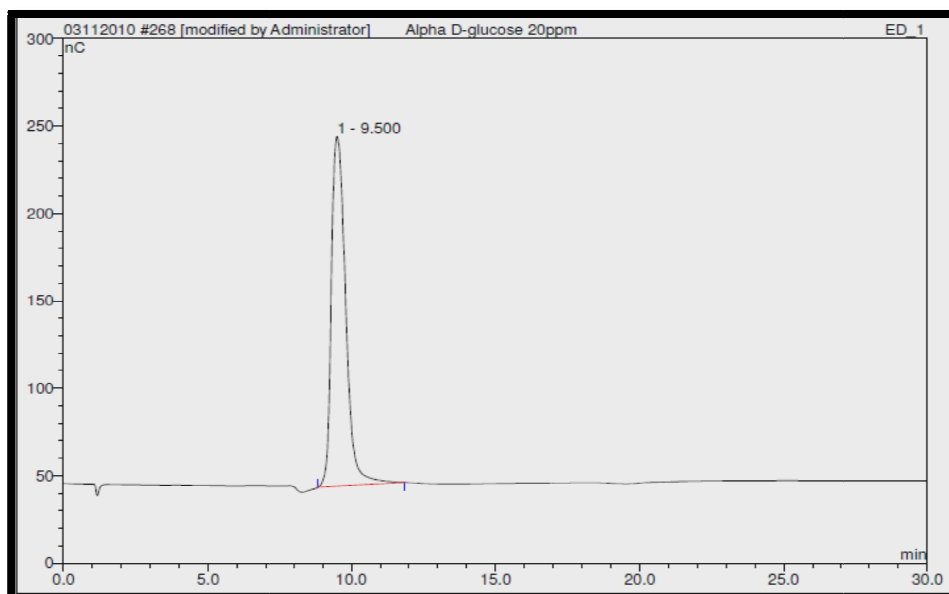


Figure 47: HPAEC – PAD chromatogram of Glucose

To gain further confirmation, the two samples of *Campylobacter* were spiked with glucose and the samples were run on the HPAEC–PAD, and the chromatogram, as expected, gave only one peak at a RT of 9.5 min, i-e glucose.

3.7.4 Monomer Analysis by GC - MS:

As the *Campylobacter* EPS samples were available in only a limited amount, it was decided to do monomer analysis on the kpsM sample and linkage analysis on the 11168H sample.

Monomers from the repeating unit of the *Campylobacter jejuni* samples, were analyzed by GC after converting them into their alditol acetates using the method described earlier in section 2.3.3. The acetylated monomers were then run on the GC–MS. The MS fragmentation patterns obtained from the GC-MS chromatogram, generated by each peak, were subsequently analysed and compared with the literature fragmentation patterns¹⁸⁷.

The GC trace of the *Campylobacter jejuni* sample kpsM is shown in Fig. 48 giving one major peak at 13.41min. with some minor peaks at 3.23 (6.70%), 6.57 (12.10%), 7.32 (3.40%) and at 13.70 (6.83%) min.

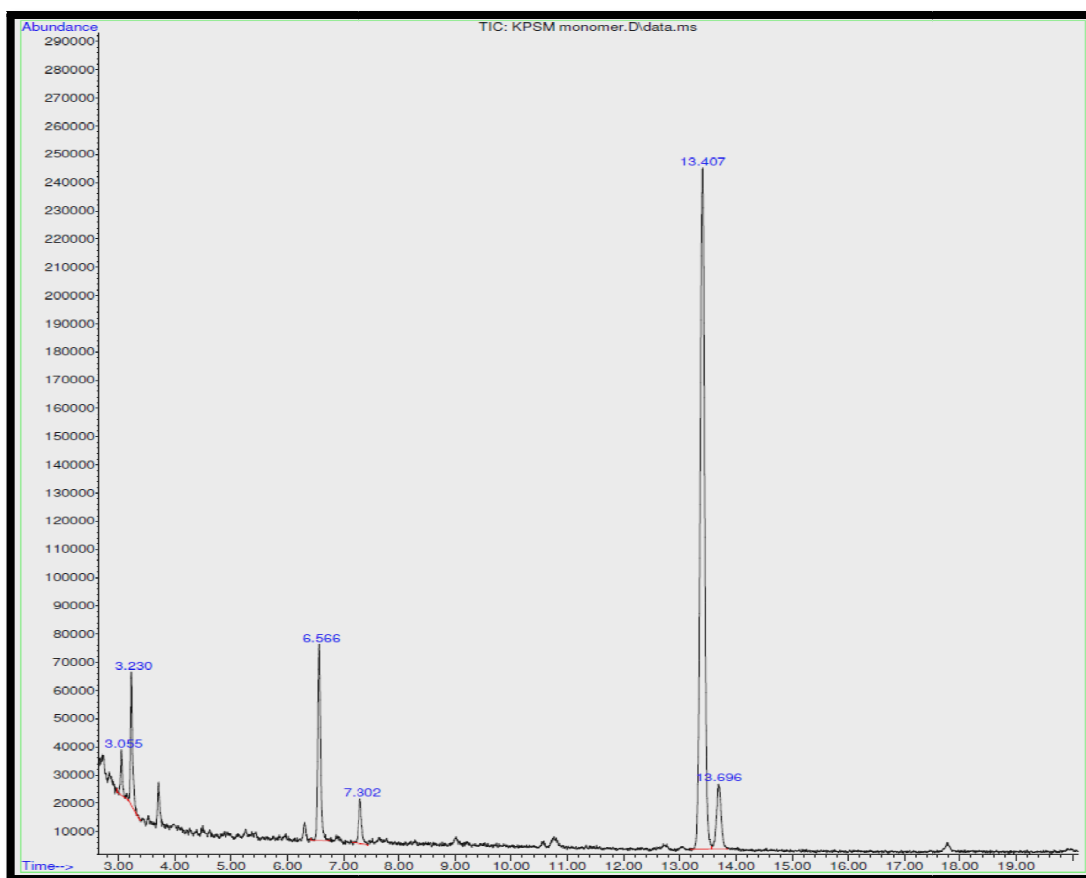


Figure 48: GC trace of monomer analysis of *Campylobacter jejuni* sample kpsM

To identify each peak, the MS was generated and then compared with the available MS of different monomers¹⁸⁷. The MS at 13.41 min. and at 13.70 min. were those of a hexose and the retention time of 13.40 is observed for glucose. A standard galactose sample gave a peak at retention time of 13.70 min. suggesting that the small peak appearing after glucose was a small amount of galactose.

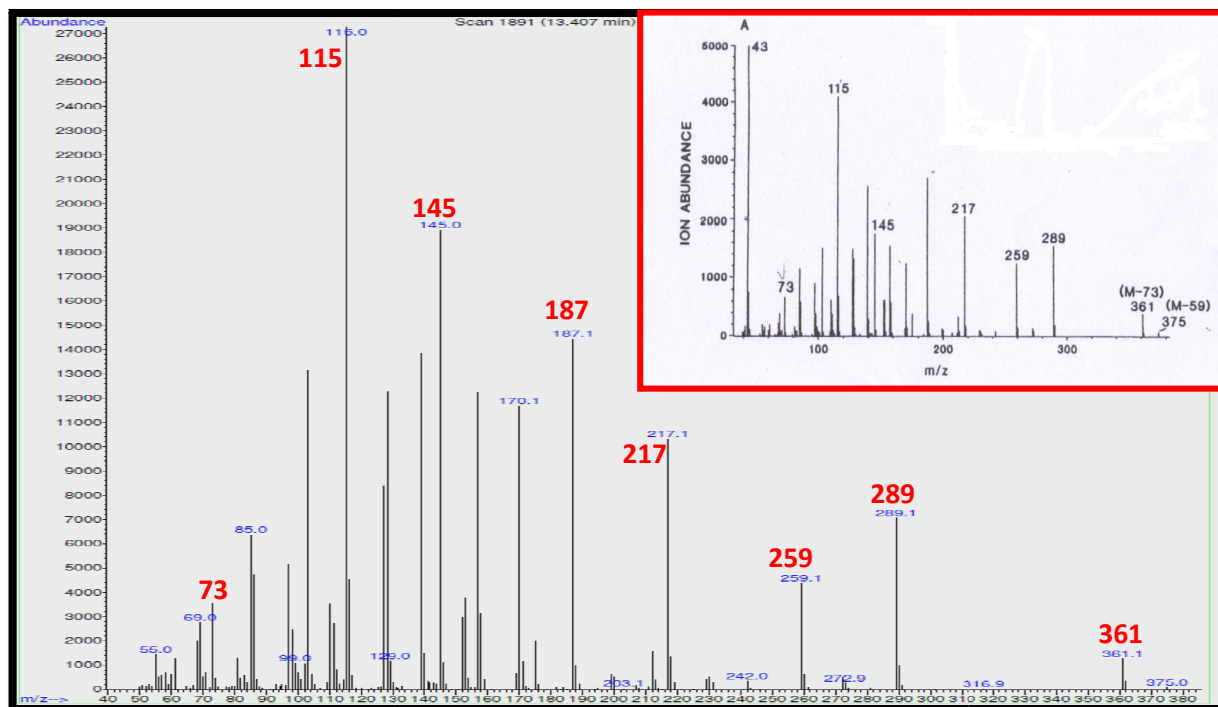


Figure 49: MS of *C. jejuni* sample kpsM at 13.413 min. (inset MS adapted from analysis of carbohydrates by GLC and MS¹⁸⁷)

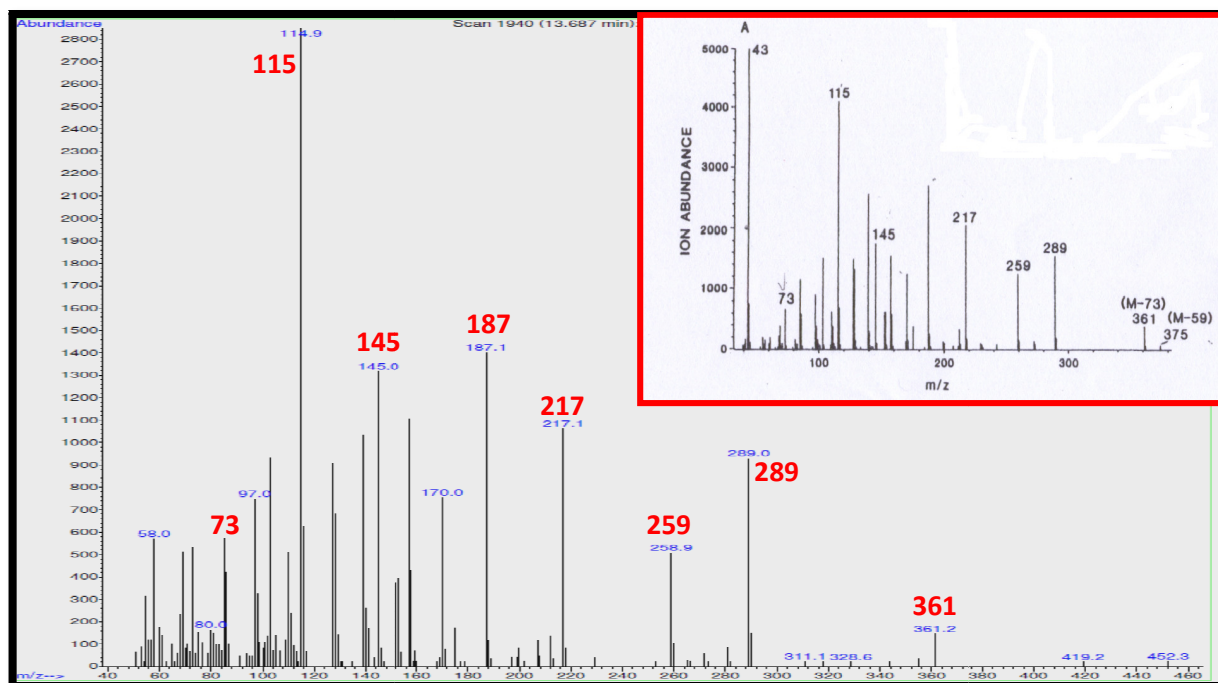


Figure 50: MS of *C. jejuni* sample kpsM at 13.687 min. (inset MS adapted from analysis of carbohydrates by GLC and MS¹⁸⁷)

3.7.5 Linkage analysis:

To find out how the monomers are linked with one another in an EPS repeating unit structure, linkage analysis has to be performed. To identify the linkage present in the sample of *Campylobacter jejuni* (11168H), linkage analysis was performed by derivatization of the EPS sample followed by analysis of the permethylated alditol acetate by GC–MS. The GC chromatogram shows a single major peak that was produced at a retention time of 16.351 min.

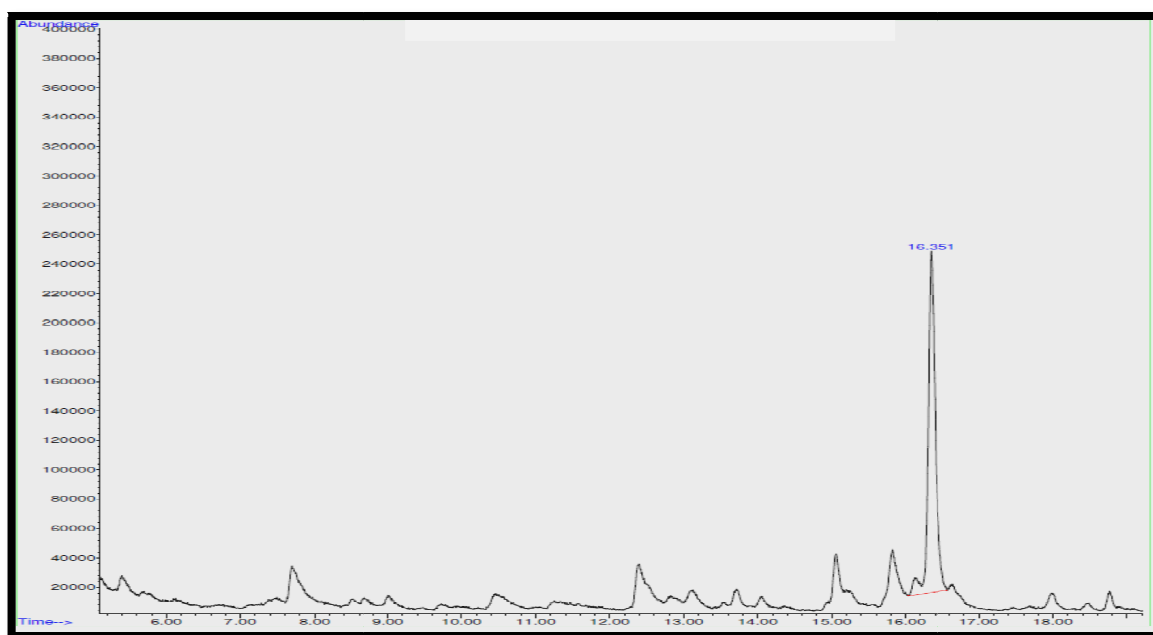


Figure 51: GC linkage chromatogram of *Campylobacter jejuni* sample 11168H

When the MS fragmentation of the peak at 16.351 min. was generated, it shows the characteristics of aldohexoses such as glucose, galactose or mannose in sugar alditol acetate form. The MS fragmentation obtained for the peak at 16.361 min. gives us fragment ions with m/z ratio of 43, 87, 102, 118, 128, 162, 189 and 233.

When the observed MS chromatogram was compared with the literature^{187,186} for a 1,6-linked sugar, it exactly matches with the 1,5,6 – tri-O-acetyl-(1-deuterio)-2,3,4-tri-O-methyl hexitol (Fig.52) confirming that the EPS is an α -dextran.

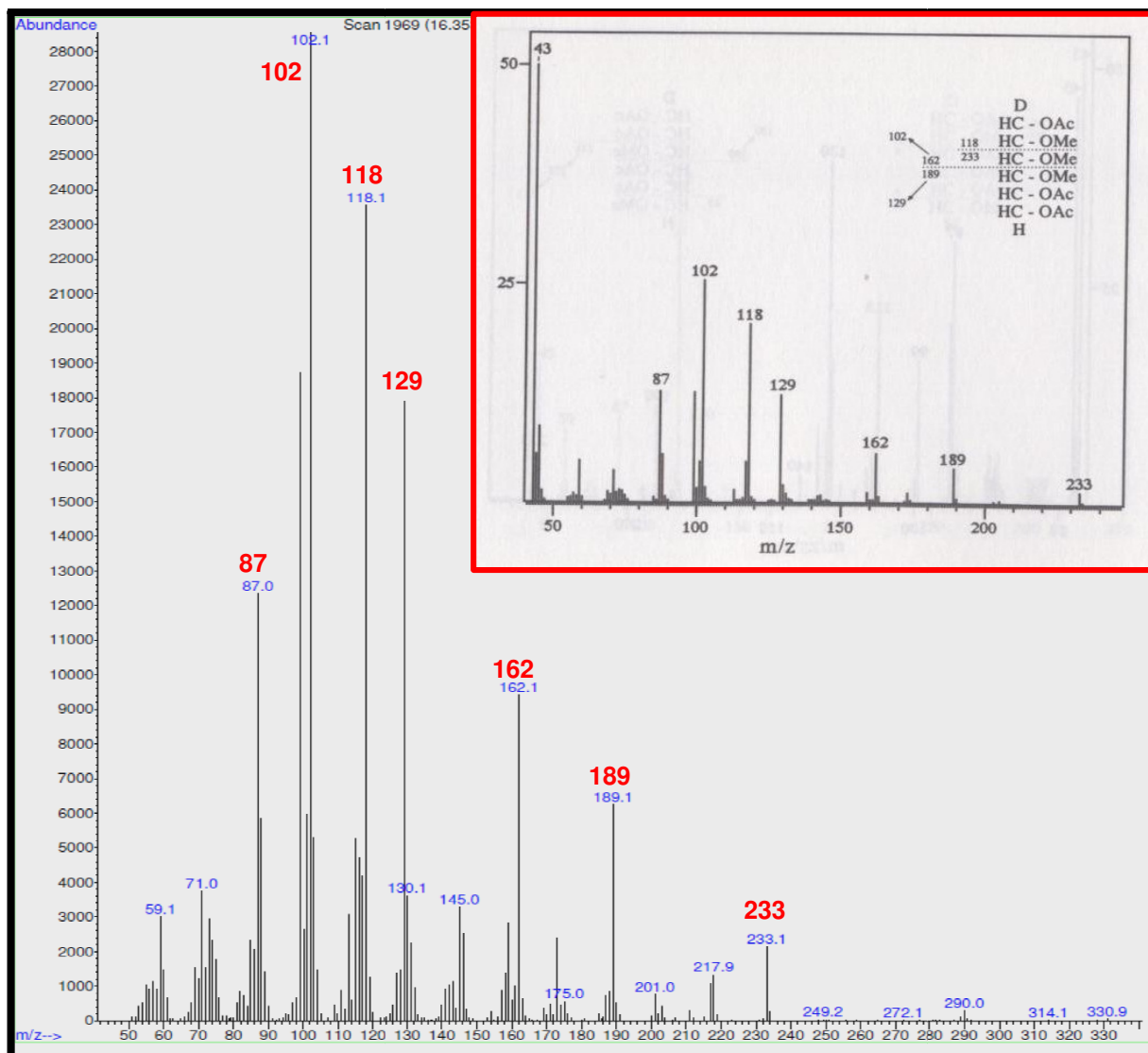


Figure 52: MS of the GC chromatogram at 16.353 min. of the sample (11168H) from *C. jejuni* (inset MS adapted from analysis of carbohydrates by GLC and MS¹⁸⁷)

Once it was established that the EPS sample from *Campylobacter jejuni* is an α -dextran, the standard α -dextran was used for monomer and linkage analysis. And as expected, α -dextran just gave one peak in both the monomer and linkage analysis. For the dextran linkage, the GC chromatogram (Fig. 53) gave one peak at 16.360 min. When the MS of the peak at 16.360 min. was generated, it was the same MS fragmentation as that of *Campylobacter jejuni* samples. MS chromatogram shows fragments that were exactly the same as the literature suggested¹⁸⁷.

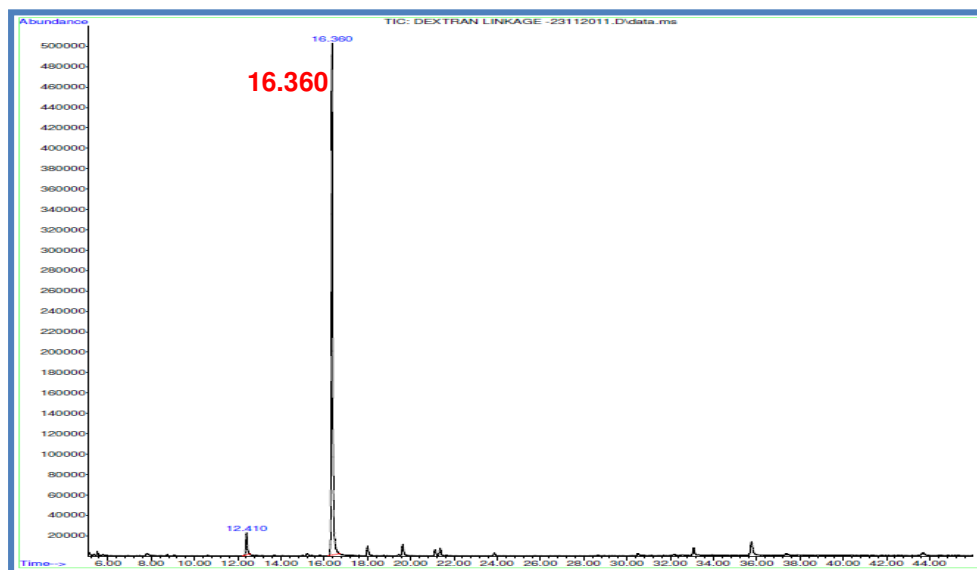


Figure 53: GC linkage chromatogram of an α -dextran

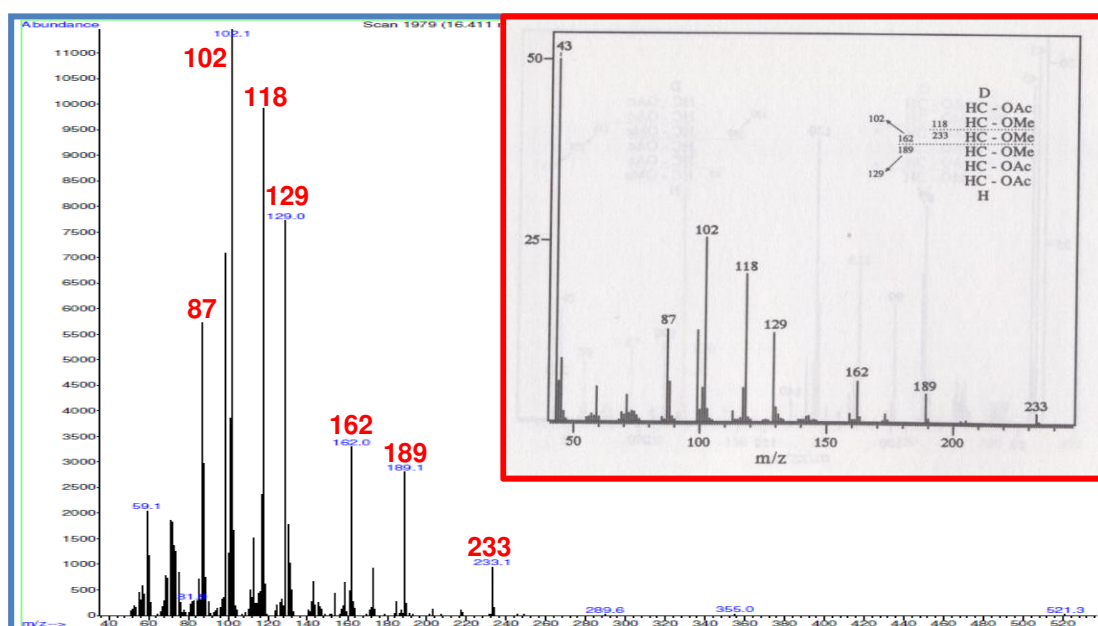


Figure 54: MS of the GC chromatogram at 16.411 min. of an α -dextran standard (inset MS adapted from analysis of carbohydrates by GLC and MS¹⁸⁷)

As far as the author of this thesis is aware, this is the first ever report of the characterisation of a biofilm component from *C. jejuni* and the results have been incorporated into a manuscript generated by co-workers at UCL and added as an appendix. The manuscript describes how the biofilm is generated in response to exposure of the bacterial cells to α -amylase. As a homopolysaccharide, α -dextrans have been produced by a number of Gram positive organisms including lactic acid bacteria such as *Leuconostoc mesenteroids*. In contrast, a number of Gram negative bacteria are known which are able to degrade dextrans and actively generate the dextran degrading enzyme dextranase.

In order to rule out the possibility that the dextran observed in the biofilm samples was being added along with the α -amylase a proton NMR spectrum of α -amylase was recorded (Fig. 55).

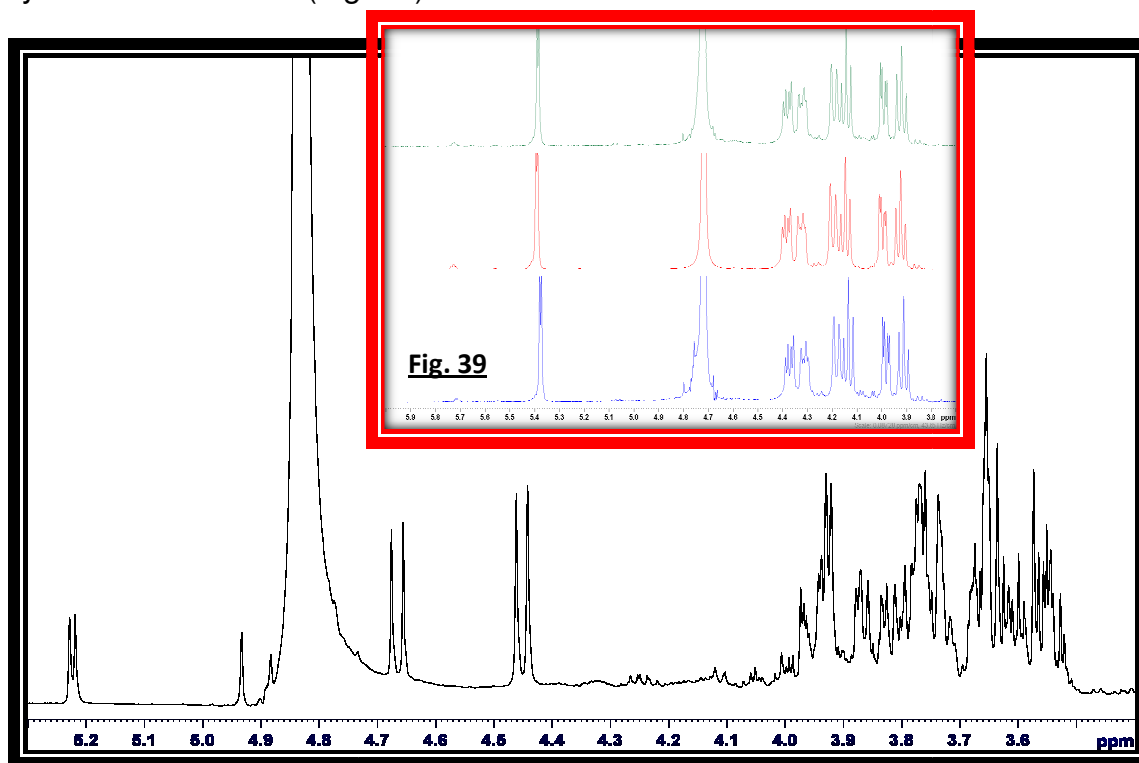


Figure 55: Proton NMR of α -amylase (spectrum recorded at room temperature)

Inspection of the NMR shows that the α -amylase contains a significant amount of carbohydrate as lactose. Lactose is listed as an ingredient; the spectrum of lactose was also recorded (Fig. 56-blue) and it is clear that lactose represents the bulk of the polysaccharide present in the α -amylase preparation.

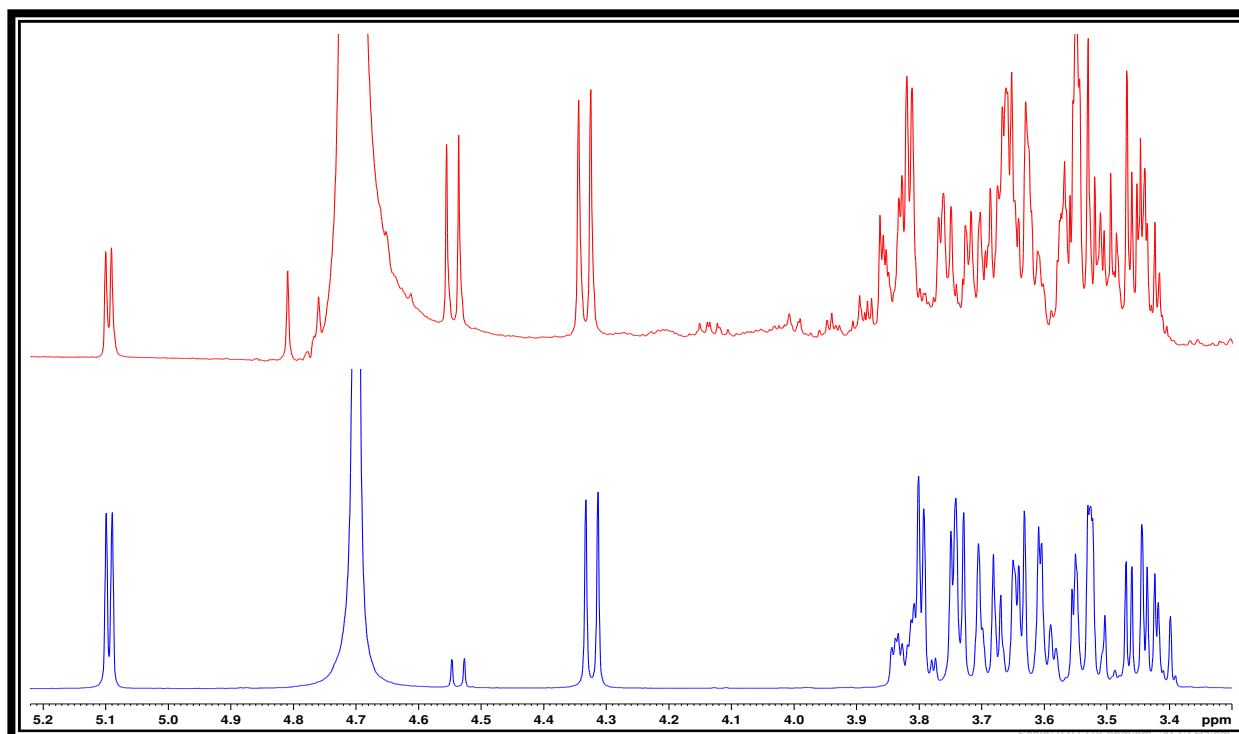


Figure 56: Proton NMR of α -lactose (blue) and α -amylase (red)

Lactose is added to stabilize the manufacture of the enzyme to increase the activity and stability of the product. Any lactose that was added with the enzyme to the *C. jejuni* cells would be expected to be removed during the exhaustive dialysis of the biofilm prior to NMR analysis. However, a small amount of contamination cannot be ruled out and this could explain the observation of a small galactose peak in the monomer analysis.

3.8 Conclusion:

NMR, monomer and linkage analysis of the two biofilm samples produced by the *C. jejuni* strains suggests that, in response to exposure by α -amylase, these bacterial systems produced an α -dextran as the main carbohydrate component of their biofilm.

*4. Analysis of the EPS recovered
from Bifidobacterium animalis
subsp. lactis*

4. Analysis of the EPS recovered from *Bifidobacterium animalis* subsp. *lactis*

4.1 Introduction - Bifidobacteria:

Bifidobacterium is an important genus of the human intestinal microbiota. They are among the first colonizers of the gastrointestinal tract (GIT) of newborns and represent the dominant genus of healthy breast-fed infants. *Bifidobacterium* spp. are Gram-positive, non-motile, non-gas producing, non-spore-forming anaerobic bacteria, that produce acetic acid and lactic acid (responsible for the decrease in pH in the intestines and inhibition of the growth of pathogenic bacteria¹⁸⁸) from carbohydrates without the generation of CO₂¹⁸⁹. Their morphology is generally referred to as bifid or irregular V- or Y- shaped rods¹⁹⁰. The actual reason for their morphology is still not clearly understood. However, a few studies have revealed that the absence or low concentrations of *N*-acetylamino-sugars, calcium ions or amino acids (alanine, aspartic acid, glutamic acid) in the growth media exclusively induce the bifid shape of *Bifidobacterium*¹⁹⁰.

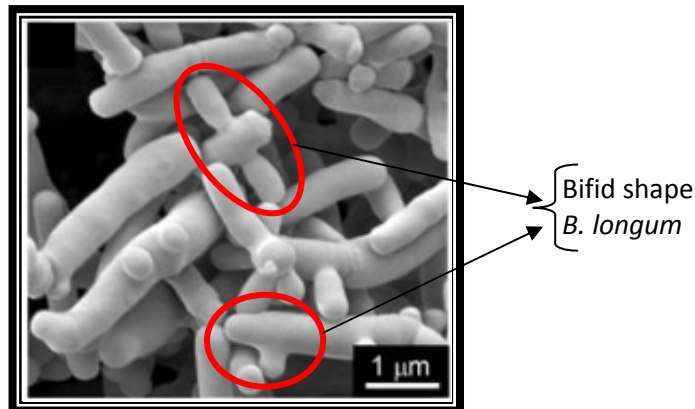


Figure 57: Scanning electron micrographs of *B. longum* NCC2705 cells. Bacteria grown in MRS medium under anaerobic conditions. rod or bifid or branched shaped form¹⁹¹.

Bifidobacteria were first isolated/discovered from the faeces of breast fed infants in 1899 by Henry Tissier who named them as “*Bacillus bifidus*”^{192,193}, (*bifidus*- due to bacterium’s Y-shaped morphology). In 1924, Orla-Jensen¹⁹⁴ proposed the genus *Bifidobacterium*, but they were classified into other taxonomic groups. Almost 50 years later, Poupard¹⁹⁵ in 1973 and subsequently in the 8th edition of Bergey’s Manual¹⁹⁶ in 1974, *Bifidobacterium* were reclassified as a separate taxon and designated the genus *Bifidobacterium*, consisting of 11 species¹⁹⁶. In 1986,

Scardovi¹⁸⁹, updated this to 24 species and currently there are 39 proposed species that have been isolated from the intestines of humans, animals and insects and also from human dental caries and raw milk¹⁹⁰. The complete genome of 21 bifidobacterial strains has been sequenced to date and made publicly available in the GenBank database. The genome size of bifidobacterium spp. ranges from about 2.0 to 2.8 Mb, with a G+C content of between 54 and 67%¹⁹⁰.

The genus *Bifidobacterium* spp. currently includes 39 characterized species¹⁹⁷ (table:7).

Table 7: Currently recongized *Bifidobacterium* species¹⁹⁷

Bifidobacterial species	Animal origin	Bifidobacterial species	Animal origin
<i>B. actinocoloniformis</i>	Bumblebee intestine	<i>B. longum</i>	Child and adult intestine, vagina
<i>B. adolsecentis</i>	Adult intestine	subsp. <i>infantis</i>	Infant intestine, vagina
<i>B. angulatum</i>	Human faeces, sewage	subsp. <i>suis</i>	
<i>B. animalis</i>		subsp. <i>longum</i>	Child and adult intestine, vagina
subsp. <i>animalis</i>	Chicken, rat, rabbit faeces, calf faeces, river	<i>B. magnum</i>	Rabbit faeces, sewage
subsp. <i>lactis</i>	Fermented milk	<i>B. merycicum</i>	Rumen
<i>B. asteroides</i>	Hindgut of honeybee	<i>B. minimum</i>	Sewage
<i>B. bifidum</i>	Adult intestine, human faeces, vagina	<i>B. mongoliense</i>	Fermented milk products
<i>B. bohemicus</i>	Bumblebee intestine	<i>B. pseudocatenulatum</i>	Child faeces
<i>B. bombi</i>	Bumblebee intestine	<i>B. pseudolongum</i>	
<i>B. boum</i>	Bovine rumen, piglet faeces	subsp. <i>globosum</i>	Pig, chicken, calf and rat faeces, rumen
<i>B. breve</i>	infant intestine, faeces, vagina	subsp. <i>pseudolongum</i>	Pig, chicken, calf and rat faeces, rumen
<i>B. catenulatum</i>	Child and adult intestine, vagina	<i>B. psychraerophylum</i>	Porcine caecum
<i>B. choerinum</i>	Pig faeces	<i>B. pullorum</i>	Chicken faeces
<i>B. coryneforme</i>	Hindgut of honeybee	<i>B. ruminantium</i>	Rumen
<i>B. crudilactis</i>	Raw milk, raw milk cheese	<i>B. saeculare</i>	Rabbit Faeces
<i>B. cuniculi</i>	Rabbit faeces	<i>B. scardovii</i>	Adult faeces
<i>B. dentium</i>	Human dental caries, faeces, human vagina	<i>B. subtile</i>	Sewage
<i>B. gallicum</i>	Adult intestine	<i>B. thermophilum</i>	Pig, chicken and calf faeces, bovine rumen
<i>B. gallinarum</i>	Chicken cecum	<i>B. thermacidophilum</i>	Anaerobic digester
<i>B. indicum</i>	Bees, river	<i>B. tsurumiense</i>	Hamster dental plaque

The genomes of 24 different strains representing 10 bifidobacterial species have been subjected to sequence analysis, but only 11 genomes (1.9 to 2.9 Mbp) have been completely annotated (table:8). These genome-scale analyses have provided suggestions as to how these bacteria colonize and adapt to the human gut^{198,199,200,201}, and to identify their protein products. The different complete genome sequences of some of the *Bifidobacterium* spp. are tabulated in table: 8.

Table 8: General features of completely sequenced some of the *Bifidobacterium* genomes¹⁹⁷

Species	Genome Size (bp)	GC Content (%)	Genes	Proteins	Source	GeneBank No.	Reference
<i>B. adolescentis</i> ATCC15703	2,089,645	59	1,701	1,631	Human GIT	NC_008618	Unpublished
<i>B. adolescentis</i> L2-32	2,385,710	59	2,499	2,428	Infant	NZ_AAXD000000000	Unpublished
<i>B. animalis</i> subsp. <i>lactis</i> HN019	1,915,892	60	1,632	1,578	Infant	NZ_ABOT000000000	Unpublished
<i>B. animalis</i> subsp. <i>lactis</i> DSM0140	1,938,483	60	1,629	1,566	French yogurt	NC_012815	Published
<i>B. animalis</i> subsp. <i>lactis</i> AD011	1,933,695	60	1,604	1,528	Infant faeces	NC_011835	Published
<i>B. animalis</i> subsp. <i>lactis</i> B1-04	1,938,709	60	1,631	1,567	Adult faeces	NC_012814	Published
<i>B. animalis</i> subsp. <i>lactis</i> Bb12	1,942,198	61	1,624	Not Available	Fermented milk	CP001853	Published
<i>B. angulatum</i> DSM20098	2,007,108	59	1,811	1,748	Human Faeces	NZ_ABYS000000000	Unpublished
<i>B. bifidum</i> NCIMB41171	2,186,140	62	1,888	1,833	Adult faeces	NZ_ABQP000000000	Unpublished
<i>B. bifidum</i> PRL2010	2,214,650	59	1,848	Not Available	Human GIT	CP001840	Published
<i>B. breve</i> UCC2003	2,422,684	59	1,854	1,590	Infant faeces	NC_020517	Published
<i>B. breve</i> DSM20213	2,297,799	58	2,309	2,251	Human faeces	NZ_ACCG000000000	Unpublished
<i>B. dentium</i> ATCC27678	2,642,081	58	2,500	2,430	Dental caries	NZ_ABIX000000000	Unpublished
<i>B. dentium</i> ATCC27679	2,633,776	58	2,402	2,336	Urogenital tract	NZ_AEEQ010000000	Unpublished
<i>B. dentium</i> Bd1	2,600,000	59	2,270	Not Available	Dental caries	NC_013714	Published
<i>B. longum</i> subsp. <i>longum</i> DJO10A	2,375,792	60	2,062	1,990	Human GIT	NC_010816	Published
<i>B. longum</i> subsp. <i>longum</i> NCC2705	2,256,640	60	1,798	1,727	Human GIT	NC_004307	Published
<i>B. longum</i> subsp. <i>longum</i> subsp. <i>infantis</i> ATCC15697	2,832,748	59	2,588	2,416	Infant GIT	NC_011593	Published
<i>B. longum</i> subsp. <i>longum</i> JDM301	2,477,838	59	2,035	1,958	Human Faeces	NC_014169	Unpublished
<i>B. longum</i> subsp. <i>infantis</i> ATCC55813	2,372,858	60	2,171	2,109	Infant GIT	NZ_ACHI000000000	Unpublished
<i>B. longum</i> subsp. <i>infantis</i> CCUG52486	2,453,376	59	2,296	2,240	Infant GIT	NZ_ABQQ000000000	Unpublished
<i>B. pseudocatenulatum</i> DSM20438	2,304,808	56	2,220	2,151	Human Faeces	NZ_ABXX000000000	Unpublished
<i>B. catenulatum</i> DSM16992	2,058,429	56	2,011	1,950	Human Faeces	NZ_ABXY000000000	Unpublished
<i>B. gallicum</i>	2,016,380	57	2,045	1,983	Human Faeces	NZ_ABXB000000000	Unpublished

It has now become clear that *Bifidobacterium* spp. also constitute one of the major organisms in the colonic flora of healthy children and adults²⁰². There are definite differences in the *Bifidobacterium* spp. isolated from humans of different age groups and these are different to those isolated from animals²⁰³. Most common *Bifidobacterium* spp. isolated from infants belong to *B. breve* and *B. infantis*, whereas *B. bifidum*, *B. longum* and *B. adolescentis* are occasionally isolated from infants²⁰³. The beneficial intestinal flora protects the intestinal tract from proliferation or infection by harmful bacteria. In Japan and more recently in Europe, *Bifidobacterium* spp. are used as dietary supplements or starter cultures for yoghurt production and other cultured milk products with the thought that such products may help the promotion of health²⁰³.

4.1.1 Physiology:

Human bifidobacterial strains grow at an optimal temperature of 36-38 °C²⁰⁴, but animal strains can grow at a higher temperature, approximately 41-43 °C²⁰⁴. Extreme temperatures are tolerated by *B. thermacidophilum*, which has been reported to grow at temperatures as high as 49.5 °C and *B. psychraerophilum* that can grow at 8.0 °C²⁰⁴. *Bifidobacterium* spp. are acid tolerant microorganisms and the optimum pH for growth of several bifidobacterial strains is between 6.5 and 7. No growth is recorded at pH lower than 4.5 (only *B. thermacidophilum* has a delayed growth at pH 4.0) and higher than 8.5²⁰⁵. *Bifidobacterium* spp. are generally described as strictly anaerobic, although some of them can tolerate limited amounts of oxygen. The sensitivity to oxygen is variable, with the fermented-milk adapted *B. animalis* subsp. *lactis*, the most aerotolerant^{189,206,207}. The capability to tolerate and survive in the presence of oxygen depends on the activity of some enzymes which are able to detoxify and remove reactive oxygen species. Genomic and functional analysis of bifidobacterium spp. revealed the presence of specific enzymes involved in these activities, in particular NADH oxidase¹⁹⁰.

The capability to adapt and tolerate salts (bile) and acidic stress is a characteristic shared by several members of the *Bifidobacterium* genus, although high variability has been detected among strains^{205,208}. Adaptation and tolerance to physiological concentrations of bile salts (below 5 mM) is an essential factor for bacterial survival and colonization of the human gastro-intestinal tract (GIT)²⁰⁹. Bile salts are detergent like compounds secreted into the intestine during digestion and are required for the emulsification and absorption of fats, but they exert also a strong antimicrobial activity²¹⁰. The ability to tolerate these compounds gives *Bifidobacterium* spp. a selective advantage in the gut ecosystem.

4.1.2 Hexose Metabolism:

The main difference which is unique to the sugar metabolism by *Bifidobacterium* spp. is the presence of fructose-6-phosphate phosphoketolase (F6PPK), a typical enzyme of the genus *Bifidobacterium*, that is responsible for the degradation of glucose and detection of this enzyme is a crucial test for the identification of such microorganisms¹⁸⁹.

Bifidobacterium degrade hexose monosaccharides (glucose and fructose) exclusively by fructose-6-phosphate phosphoketolase pathway, named according to its key enzyme or as “bifid shunt”^{211,212,197,213}. *Bifidobacterium* does not have the enzymes aldolase, phosphofructokinase and glucose-6-phosphate dehydrogenase, which are the main enzymes of homofermentative and heterofermentative lactic acid bacteria²¹³. Therefore, they are unable to ferment hexose monosaccharides through the Emden-Meyerhof-Parnas (EMP) pathway or 6-phosphogluconate/phosphoketolase pathway, respectively. However, the “bifid shunt” allows bifidobacterium to produce more ATP from glucose or fructose than the conventional homo or heterofermentative pathways used by lactic acid bacteria.

Bifidobacterium will initially cleave, by means of the key enzyme fructose-6-phosphate phosphoketolase, one mole of fructose-6-phosphate into one mole of erythrose-4-phosphate and one mole of acetyl-phosphate. In parallel, the combined action of a transaldolase and transketolase on the erythrose-4-phosphate and an additional fructose-6-phosphate results in the formation of two moles of xylulose-5-phosphate, which are subsequently converted into two moles of acetyl-phosphate and two moles of glyceraldehyde-3-phosphate by the action of a xylulose-5-phosphate phosphoketolase.

The three moles of acetyl-phosphate are further converted into three moles of acetate by the action of the acetate kinase, which results in the formation of three moles of ATP per two moles of glucose/fructose.

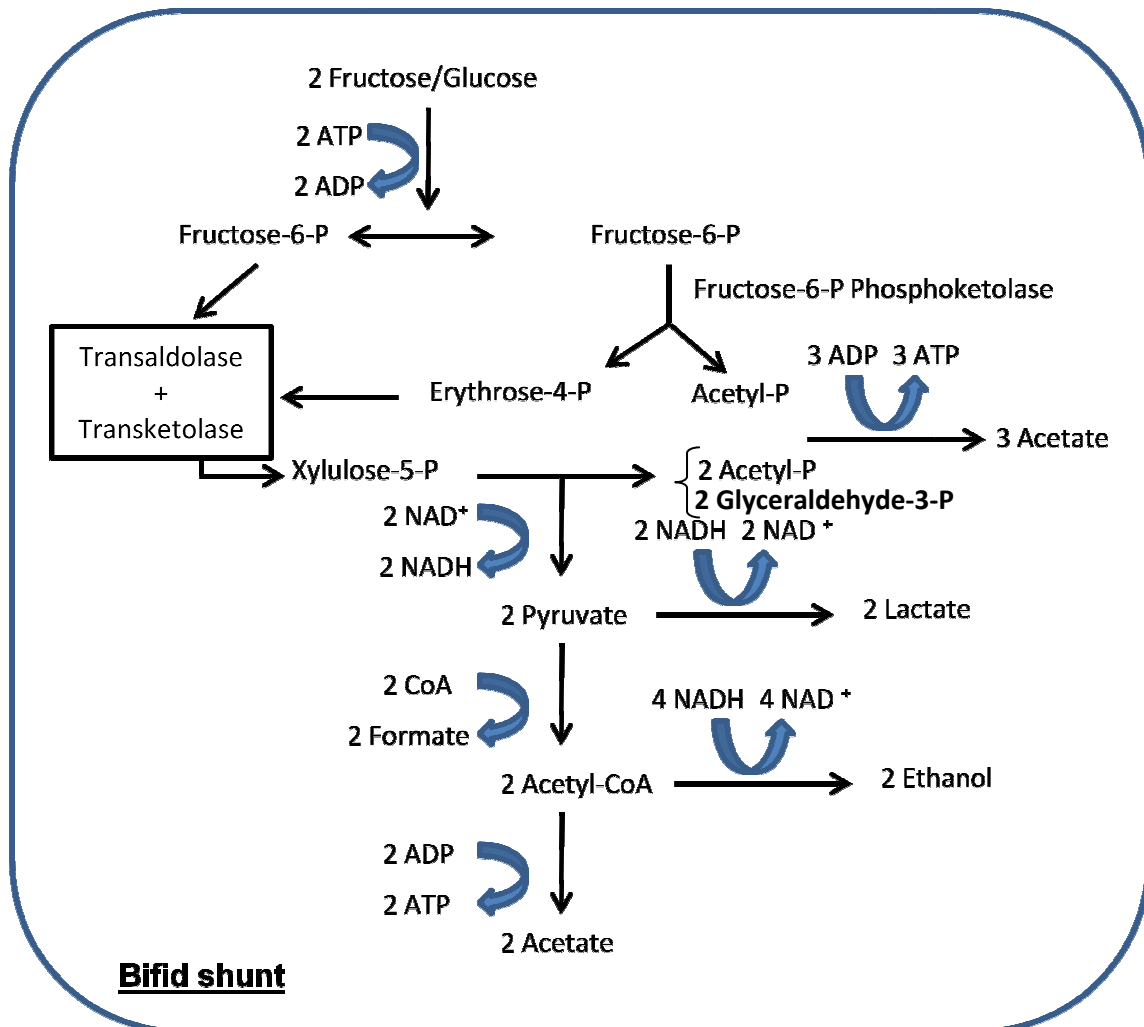


Figure 58: Hexose monosaccharides (glucose and fructose) through the fructose-6-phosphate phosphoketolase pathway or bifid shunt²¹³.

The two moles of glyceraldehyde-3-phosphate are oxidized into two moles of pyruvate that are further reduced to two moles of lactate by the action of enzymes that participate in the lower part of the EMP pathway, which results in the additional production of two moles of ATP per two moles of glucose or fructose. The reduction of pyruvate by means of a lactate dehydrogenase does not lead to the production of extra ATP but is necessary for NAD^+ recycling. Hence, in total, the fructose-6-phosphate phosphoketolase pathway theoretically yields three moles of acetate, two moles of lactate and five moles of ATP from two moles of hexose monosaccharides. However, the theoretical acetate : lactate production ratio of 3 : 2 is rarely seen, due to the different possible fates of pyruvate, depending on the available energy source and its consumption rate^{212,214,215}. Indeed, pyruvate can be converted into formate,

acetate and ethanol, which not only results in altered acetate/lactate production ratios but also influences the redox balances and ATP yields of the cell. Therefore, it is mainly the formation of formate and ethanol that determines the acetate/lactate production ratio. More importantly, the specific rate of sugar consumption plays a crucial role in the ratio of end-metabolites produced^{216,217}.

Bifidobacterium spp. produce large amounts of lactate and small amounts of acetate, formate and ethanol, when the energy source is consumed fast, whereas less lactate is produced and more acetate, formate and ethanol, when the energy source is consumed slowly. This enables *Bifidobacterium* spp. to produce more energy when high amounts of substrate are available to invest in growth and to save energy under starving conditions to avoid cell death^{215,216,217,218}.

4.1.3 *Bifidobacterium* spp. - as Probiotics:

The Human intestinal flora is composed of approximately 100 trillion bacteria, comprising more than 100 species, providing a variety of enzymes that perform extremely varied types of metabolism in the intestine. Thus, the intestinal flora can influence the host's health, including nutrition, physiological functions, drug efficacy, carcinogenesis, aging, immunological responses and resistance to infection. Within the intestine, bacteria are responsible for the conversion of various substances, resulting in the production of both beneficial and harmful products to the host. The beneficial intestinal flora protects the intestinal tract from proliferation of or infection by harmful bacteria, whereas the harmful bacteria increase pathogenicity when the host's resistance is decreased²⁰².

The concept of "probiotics" has started from the work of Metchnikoff²¹⁸ in 1908 who postulated that the apparent longevity of Balkan peasants was due to their ingestion of milk fermented with *Lactobacillus delbrueckii* subsp. *bulgaricus*. In 1965, the term was used by Lilley and Stilwell²¹⁹, in a different context to represent 'substances secreted by one organism which stimulate the growth of another'. In 1974, Parker²²⁰ described probiotics as 'organisms and substances which contribute to intestinal microbial balance'. In 1989, Fuller²²¹ proposed that 'probiotics were live microbial supplements which beneficially affect the host animal by improving its microbial balance'. Later on, in 1998, Salminen²²² defined probiotics as 'foods containing live bacteria which are beneficial to health'. Due to the increased research

in probiotics, in 2001, the United Nations Food and Agriculture Organization and the World Health Organization (FAO/WHO) defined probiotics as “live microorganisms which when administered in adequate amounts confer a health benefit on the host”²²³. Many “microbial types” are used around the world to ferment milk, two of the most widely known and characterized types are *Lactobacillus delbreuckii* subsp. *bulgaricus* and *Streptococcus thermophilus*²²⁴. *Lactobacillus acidophilus* and *Bifidobacteria animalis* subsp. *lactis* are the lactic acid bacteria that are most frequently used as probiotics. These bacteria grow slowly in milk because they lack essential proteolytic activity and for this reason they are usually combined with *Streptococcus thermophilus*. Thus, the use of these combinations allows dairy processors to produce fermented dairy products with the desired technological characteristics, as well as with potential nutritional and health benefits²²⁵. Whilst the properties of probiotic foods have been extensively explored, including their therapeutic properties²²⁶ and the effect of the ingredients on their viability²²⁷, only a few studies have investigated the molecular species responsible for their probiotic activity^{228,229}.

4.2 Exopolysaccharides (EPS) Samples:

In the food industry, one of the commonly used probiotic bacterial species is *Bifidobacterium animalis* subsp. *lactis* strain Bb12, which is available under different labels in dairy products and infant formulas. The taxonomy of *B. animalis* subsp. *lactis* has been controversial since its original description by Meile *et al.*²³⁰, in 1997. Several studies have investigated its similarity with the closely related species *Bifidobacterium animalis* subsp. *animalis*²³¹. *Bifidobacterium Bb12*, is a rod shaped bacterium and was first deposited in the cell culture bank of Chr. Hansen²³² in 1983. At isolation, Bb12 was considered to belong to species *Bifidobacterium bifidum*. By using the latest molecular techniques, it was reclassified as *Bifidobacterium animalis* and later to a new species *Bifidobacterium lactis*. Later on, the species *Bifidobacterium lactis* was included in *Bifidobacterium animalis* as a subspecies. Today, Bb12 is classified as *Bifidobacterium animalis* subsp. *lactis*²³².

The most important health benefit from *Bifidobacterium spp.* is that they are able to suppress tumours, provide resistance to harmful microbes, resist the digestion of acid, helpful in colon inflammation, stimulate the body’s immune

response, and prevent diarrhoea. In addition to many other health benefits, *Bifidobacterium* subsp. *lactis* is beneficial in preventing and treating eczema in children with food allergies¹⁹⁰.

The work described in this thesis is concerned with the EPS production by a number of *Bifidobacterium* systems. Researchers at Asturias, Spain (Patricia Ruas Madiedo and her group) have grown a variety of *Bifidobacterium* strains at 37 °C for 72 hours under anaerobic conditions on the surface of MRS agar containing 0.25% L-cysteine (MRSC agar) and supplemented with 2% glucose, fructose, lactose or sucrose added separately. They have observed 60+ putative EPS strains and after determination of their 16S rRNA gene sequence, it was revealed that out of 60, 35 EPS strains belong to genus *Bifidobacterium*. Out of the 35 *Bifidobacterium* strains, the agar plate was crowded with *B. pseudocatenulatum* (51%) and the least crowded was *B. adolescentis* (3%). Isolation, production, results and analysis of EPS, were discussed in detail by Madiedo *et al.*^{233,234} and Salazar *et al.*²³⁵. These strains have the potential to produce a variety of EPSs, the original native *Bifidobacterium* strain (labelled as A1) was when bile adapted (labelled as A1dOx) and one with ropy characteristics (labelled as A1dOxR²³⁶), they generate three EPSs, a high molecular weight EPS (HMw), medium molecular weight EPS (MMw) and a low molecular weight EPS (LMw). The LMw and MMw EPSs polymers have so far not been characterized.

Whilst there are a number of reports of EPS producing *Bifidobacterium* spp. very little work has been done to fully characterise the EPS repeating unit structure. The structures of the EPS produced by *B. bifidum* BIM B-46512²³⁷ and *B. longum* JBL0513²³⁸ (human origin), have recently been reported.

The aim of this study was to analyse the structure of the EPS produced by *B. animalis* subsp. *lactis*. The EPS samples were from *Bifidobacterium animalis* subsp. *lactis* labelled as A1-batch 5 (parental strain, isolated from fermented milk) and A1-dOx batch 9 (bile-adapted derivative).

4.3 *Results and Discussion:*

4.3.1 *NMR Analysis*

In order to determine the structure of the repeating oligosaccharide unit of the EPS samples, labelled as A1dOx-Batch 9 and A1-Batch 5, a series of 1D (Fig. 59 & 60) and 2D NMR experiments were carried out.

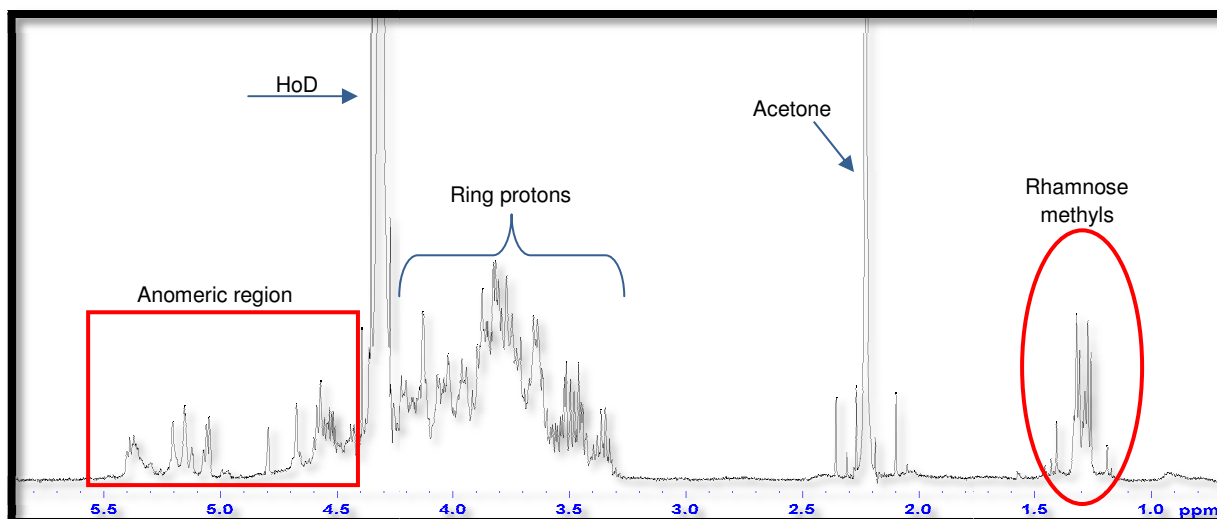


Figure 59: A1dOx-Batch 9, Crude Proton NMR

As can be seen from the ^1H spectrum (Fig.59) a lot of peaks are present in the ^1H NMR spectrum of the sample A1dOx-Batch 9 including: rhamnose methyls (1.00-1.28 ppm); ring protons (3.2-4.10 ppm) and monosaccharide anomeric resonances (4.20-5.30 ppm). The other signals are derived from acetone which was used as an internal standard at 2.225 ppm and the residual HOD signal at 4.35 ppm.

The ^1H NMR spectrum for the EPS derived from A1-Batch5 (Fig. 60) is very similar to that of A1dOx-Batch 9 and contains the same sets of peaks in approximately the same ratios.

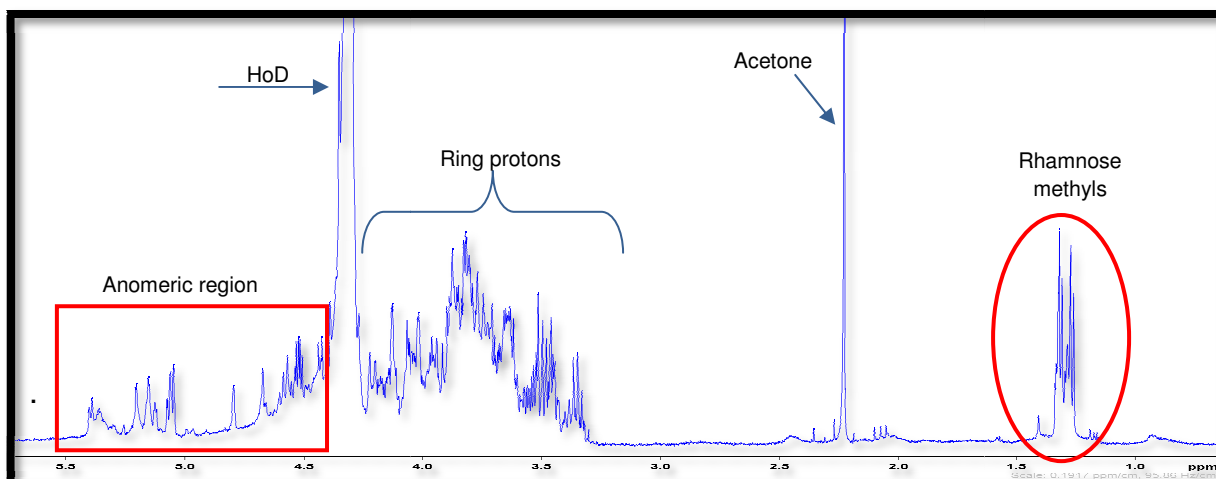


Figure 60: A1-Batch 5, Crude Proton NMR

When the anomeric regions of the ^1H NMR spectra of the two samples were compared, the location of signals was found to be almost identical (Fig. 61).

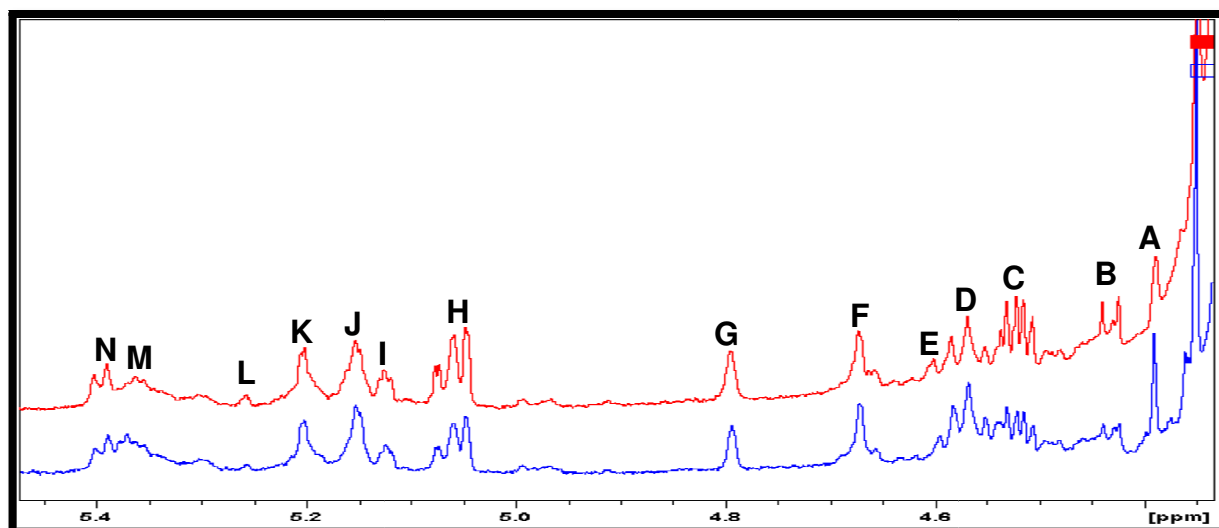


Figure 61: Comparison of ^1H NMR spectra of A1dOx-Batch 9 (blue) and A1-Batch 5 (red)

However, the relative intensities within each spectrum varied: as determined through analysis of the peak integrations which change from one spectrum to the next. These variations suggest that multiple components are present in both polysaccharide samples.

An attempt was made to identify how many components were present by passing dilute samples of the polysaccharide through an analytical Size Exclusion Chromatography system linked to a Multi-Angle Laser Light Scattering detector (SEC-MALLS).

4.3.2 Size Exclusion Chromatography – Multi Angle Laser Light Scattering (SEC – MALLS) Analysis of EPS:

Prior to the analysis of the EPS samples, the accuracy and precision of the SEC-MALLS instrument was evaluated using a pullulan standard (homopolysaccharide of glucose also known as α -(1 \rightarrow 6) linked maltotriose. It is secreted by a fungus *Aureobasidium pullulans*) of known molecular weight (M_w =790,000 g/mol) and having a low polydispersity (M_w/M_n = ~1.23) with a differential refractive index (dn/dc) value of 0.148 mL/g (dn/dc - the change in the refractive index of a solution for a given increment in concentration).

Table 9: SEC–MALLS results for Pullulan standard

Pullulan (796,000 M_w)	Average Molecular Weight (g mol^{-1})	Polydispersity (M_w/M_n)
Injection 1	808,000	1.020 \pm 0.048
Injection 2	800,000	1.021 \pm 0.16
Injection 3	798,000	1.010 \pm 0.12
Mean	802,000	1.017
SD	5291.50	0.006
RSD %	0.659	0.589

The results generated showed that the SEC-MALLS gave good accurate and precise results for the pullulan standard (Fig. 62). The M_w value obtained was similar to the known M_w and there was satisfactory agreement between repeat determinations.

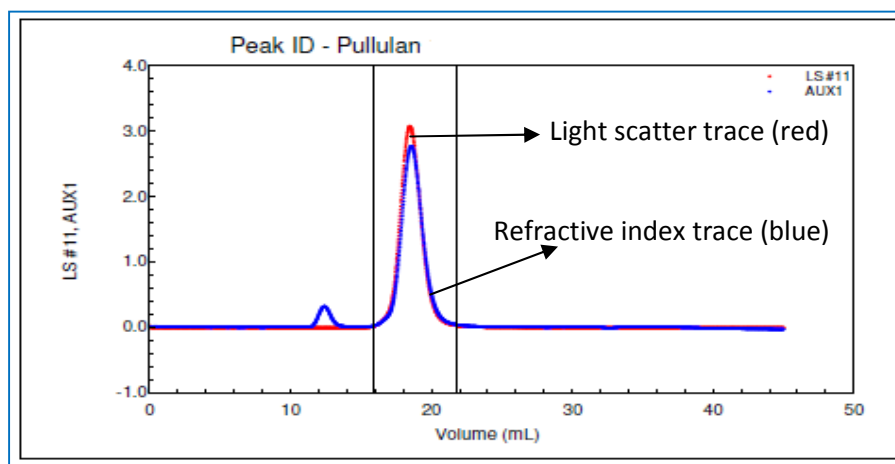


Figure 62: Pullulan 1000ppm, flow rate 0.45mL/min., mobile phase 0.1M NaNO₃, solvent RI 1.314, laser wavelength 690.0 nm, dn/dc 0.148 mL/g.

When the sample A1-Batch 5 was injected in to the SEC-MALLS, it gave a number of overlapping peaks (Fig. 63). The chromatogram shows that the sample comprises of a number of different molecular weight EPSs. The SEC-MALLS chromatogram trace shows 3 distinct peaks (red trace-light scatter), labelled as peak 1 with a molecular weight of 3.6×10^5 g/mol (5.8%), peak 2 with a molecular weight of 2.4×10^4 g/mol (27.3%) and peak 3 with a molecular weight of 6.8×10^3 g/mol (67.0%).

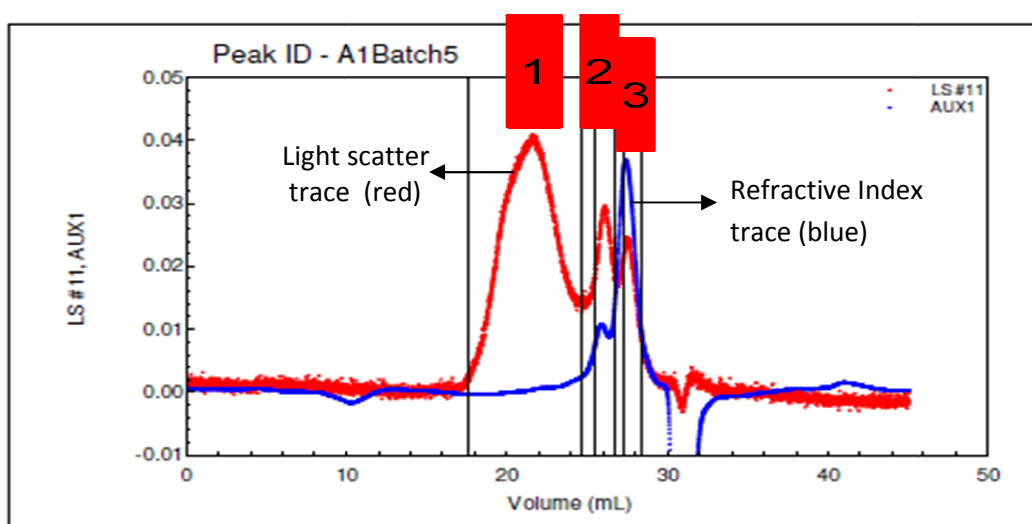


Figure 63: SEC-MALLS trace of A1-batch 5

As the above sample had previously been dialyzed using cellulose membrane (MWCO ~ 12,500 Da) the smallest peak (Fig. 63) was below the cut off value of the dialysis tubing and might indicate that this component is charged and is retained in the dialysis through absorption.

When the second sample A1dOx-Batch 9 was injected into the SEC-MALLS system, it also shows that a mixture of components was present (Fig.64).

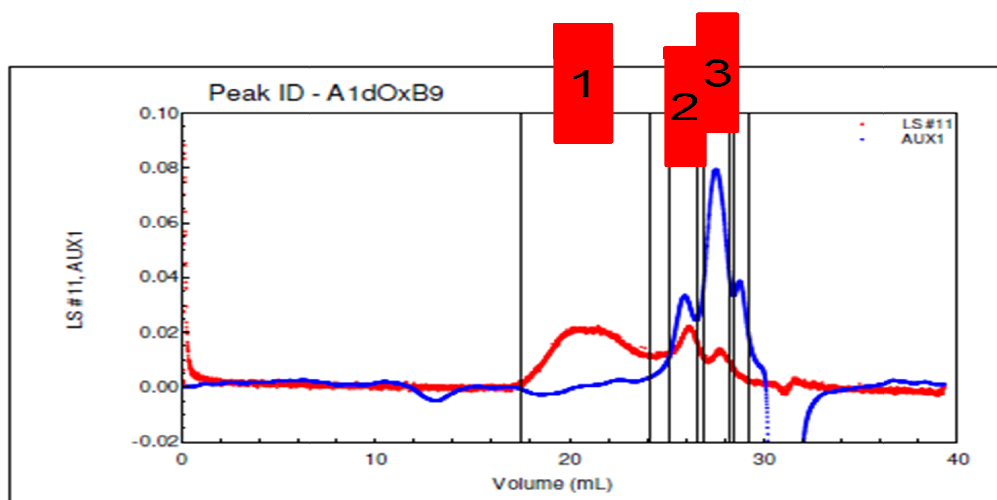


Figure 64: SEC-MALLS trace of A1dOx-Batch 9

Again the chromatogram (Fig. 64) shows that the sample comprises a number of different molecular weight EPSs. The SEC- MALLS chromatogram shows 3 distinct peaks: labelled as peak 1 with a molecular weight of 3.3×10^5 g/mol (0.86%); peak 2 with a molecular weight of 2.3×10^4 g/mol (31.17%) and peak 3 with a molecular weight of 6.2×10^3 g/mol (68.0%). From the SEC-MALLS traces (Fig. 62 and 63), it is clear that different molecular weight EPSs are present and these have been defined as a high molecular weight (HMw), medium molecular weight (MMw) and low molecular weight (LMw). Previous work²³⁶, demonstrated that the EPS sample contains three components, comprising of HM_w, MM_w and LM_w EPSs.

4.3.3 Preparative Size Exclusion Chromatography:

After analyzing the samples with SEC-MALLS, attempts were made to use preparative size exclusion chromatography, with the sample A1-batch 5, to separate the peaks. For the chromatographic conditions, please refer to the experimental section 2.3.5.

After analysing the chromatograph obtained, potentially two closely eluting peaks starting from fraction 18 and finishing at fraction 24 were visible (Fig. 65).

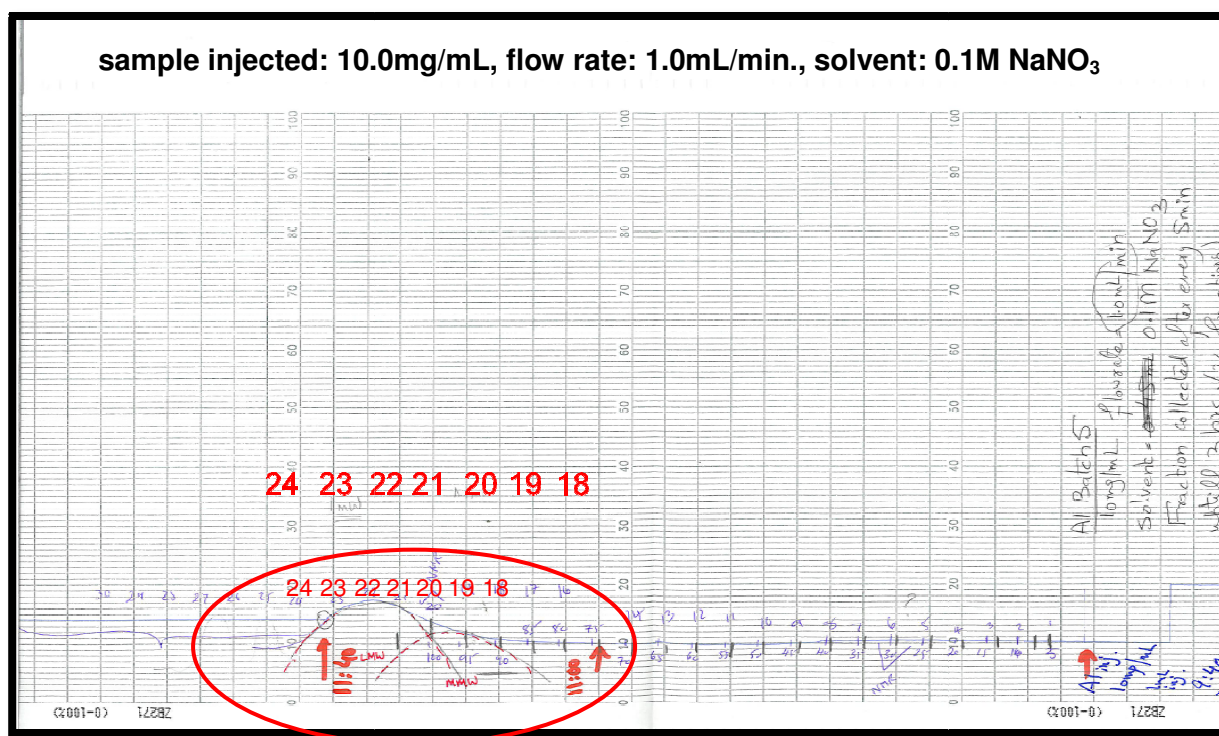


Figure 65: Chromatograph obtained after passing A1-batch 5, through the SEC column filled with Sephacryl S-500HR, showing the peaks from fractions 18 - 24

The peaks started to elute after 90 min. and completely eluted before 120 min. However, the small amount of sample that had been injected onto the column meant that the individual fractions were very dilute. Those fractions on either side of the peaks (fractions 1-17 and 25-30) were combined. Whereas fractions 18, 19, 20, 21, 22, 23, 24 were stored individually. Then all the fractions (1-17, 18, 19, 20, 21, 22, 23, 24 and 25-30) were dialysed for 18 hours (with 3 solvent changes), freeze dried (FD) and redissolved in deuterium oxide (D_2O) for NMR analysis, with special attention given to fractions 18 to 24. From the NMR analysis it was observed that the fractions 20-23 contained polysaccharide peaks.

When the different 1H NMR spectra of the sample were considered (Fig. 66), it was clear that there were two regions in which the peaks were visible. The regions are labelled as **A** and **B**. Region **A** is the anomeric region and the region **B** is where the signals from the rhamnose methyls are located.

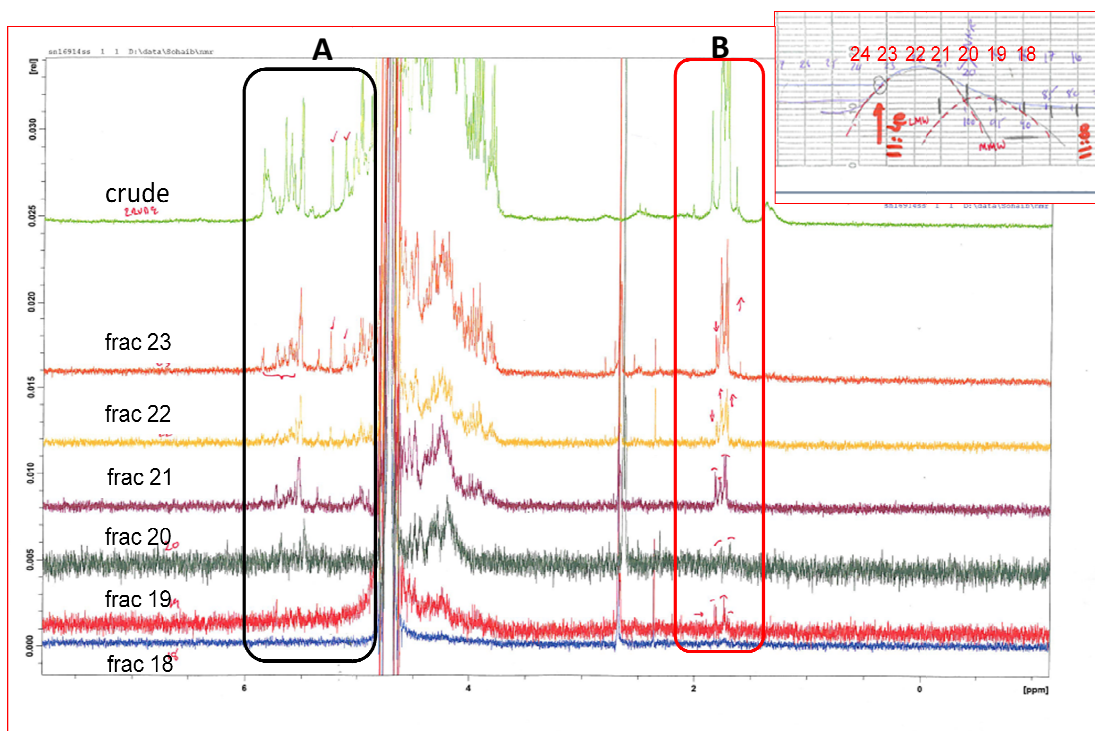


Figure 66: 1H NMR spectra comparison of fractions 18-24 with crude A1-batch 5

When the region **B** (Fig.67), was observed closely, it revealed that the fractions 21, 22 and 23 had the same peaks as that of the crude NMR spectrum of the sample.

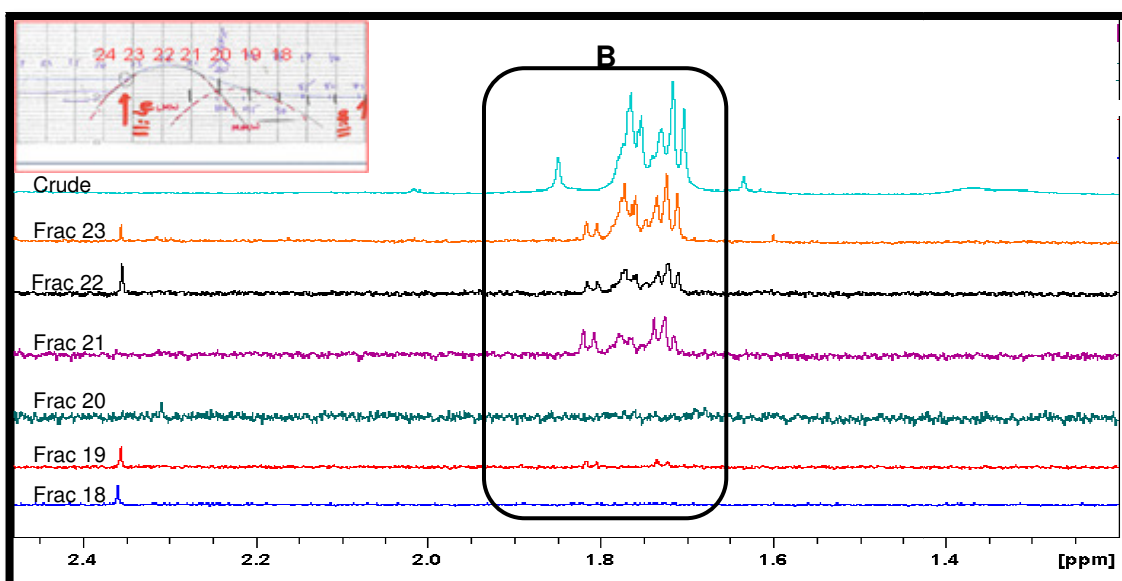


Figure 67: Region B, ¹H NMR spectra comparison of fractions 18-24 with crude A1-batch 5

When region **A** was observed closely, it revealed that a number of similar peaks were present in fractions 21, 22, 23 and which were also present in the crude NMR of the sample A1-batch 5. It is clear from inspection of the spectra (Fig. 67 & 68) that the polysaccharide is eluting from fractions 21 to 23, but also that there is only minimal separation of the peaks.

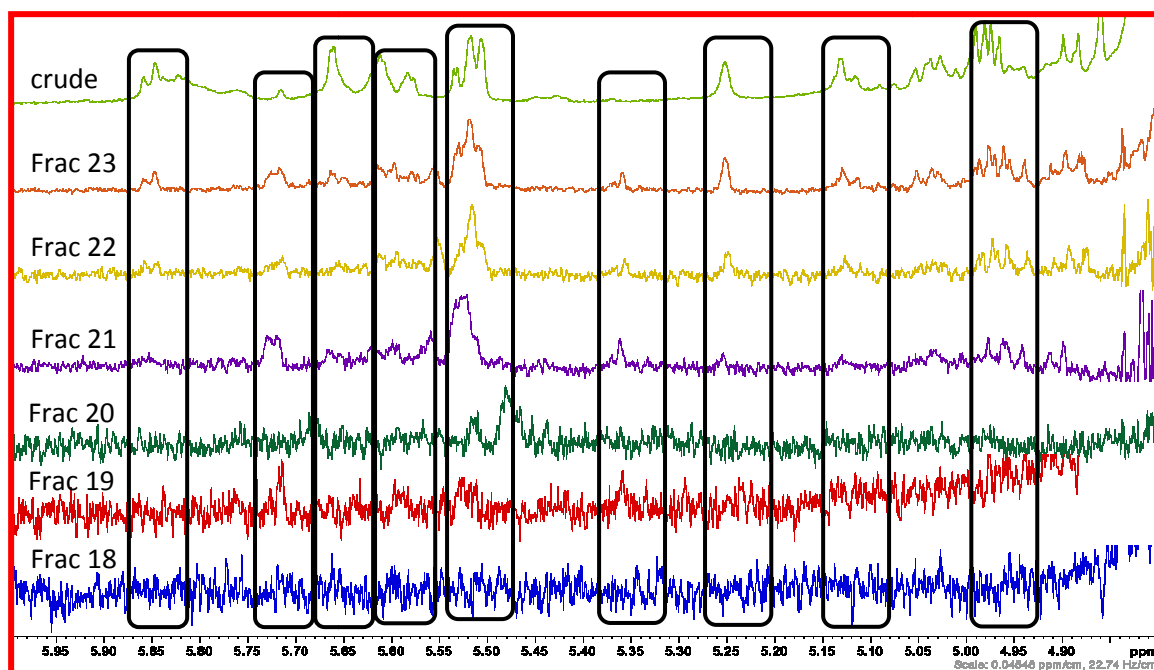


Figure 68: Region A, ¹H NMR spectra comparison of fractions 18-24 with crude A1-batch 5

When the second sample A1dOx-batch 9 was injected onto the SEC column (XK26/40) filled with Sephacryl S-500HR, a similarly weak set of signals was observed. The chromatograph showed a peak eluting after 90 min. The first fractions were collected over 20 min. until the peak was observed. Samples were collected after every 5 min. (overall 80 fractions were collected over a period of 6h & 40 min.). All the fractions collected were dialyzed, freeze dried and redissolved in D₂O for NMR analysis. Analysis of the NMR spectra revealed that all the spectra were the same as the previous sample (A1-batch 5) and it was concluded that the Sephacryl S-500HR was unable to separate the HMw, MMw and LMw EPSs. Therefore it was decided to use Sephacryl S-200HR (a size exclusion material with a smaller pore size—more details are discussed in the experimental section: 2.3.6) in an attempt to separate the polysaccharides.

To use Sephacryl S-200HR, another glass XK26/40 SEC column was filled with the stationary phase, and the sample was injected (20.7mg/5.0mL), overall 88 fractions (2 min. each fraction) were collected over a period of 3 hours. The chromatograph (Fig.69) shows four distinct regions, region A (fraction 24-31), region B (fraction 32-39), region C (fraction 42-50) and region D (fraction 51-72).

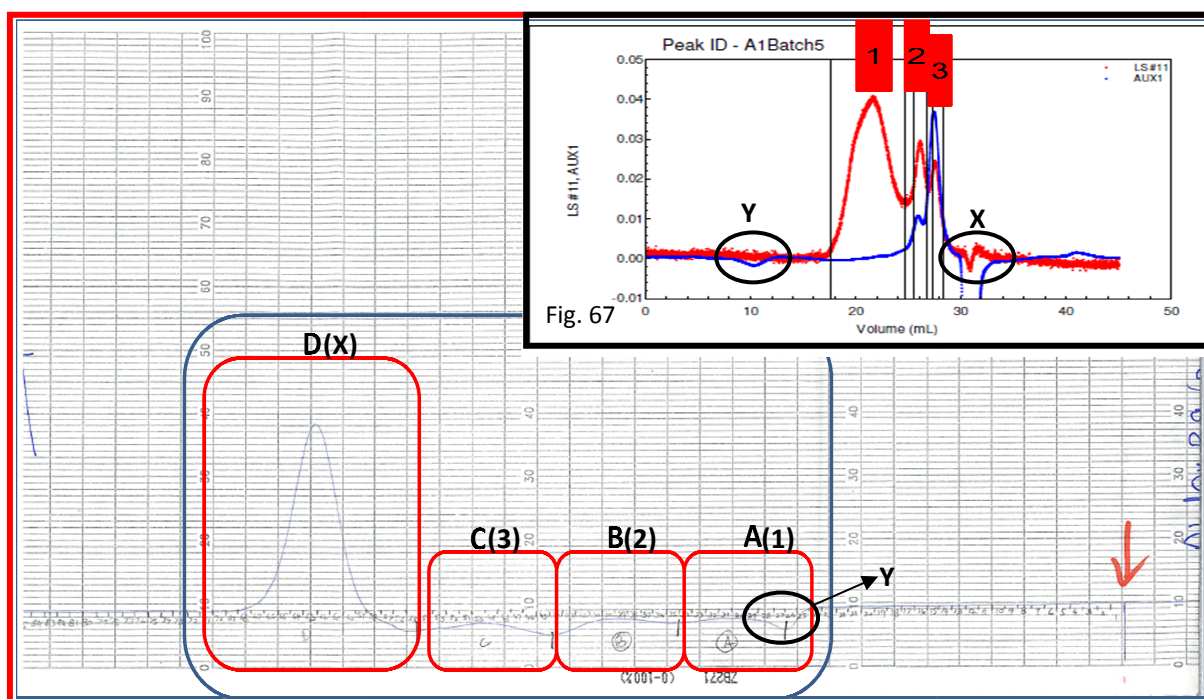


Figure 69: Chromatogram of A1dOx-batch 9, obtained after passing through the SEC column filled with Sephacryl S-200HR

These regions were expected to correlate with the MALLS traces (Fig. 64) with peak 1 (5.8%) of HMw (region **A/B**) that does not have a noticeable refractive index trace, followed by peak 2 (27.3%) of MMw (region **C**) and the late eluting peak 3 (67%) corresponding to LMw (region **D**). All the fractions collected were dialysed (24h with 3 solvent changes), freeze dried and redissolved in D₂O for NMR analysis.

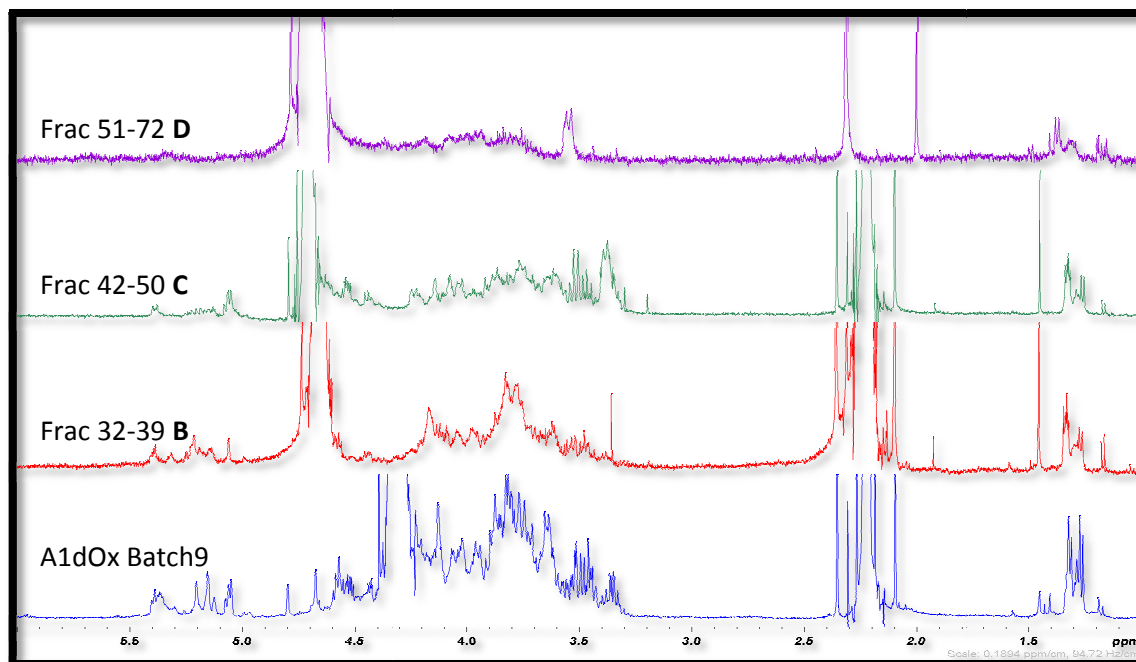


Figure 70: Comparison of 1D-1H NMR spectra of combined fractions with crude A1dOx batch9, obtained from SEC column filled with Sephacryl S-200HR

NMR analysis (Fig. 70-A1dOx batch9 (blue trace) was acquired at 70 °C, whereas the other three spectra (red, green & purple) were acquired at room temperature) shows very low quantities of EPS materials that were recovered and suggests that the main polysaccharides are being absorbed on the SEC column. Again, the NMR analysis does not show any real separation of peaks, even though the chart recorder shows some different height peaks labelled as A, B, C and D. Phosphorus (³¹P) NMR spectra were also recorded, but no significant peaks were visible in any of the fractions (that rules out the presence of phosphate group attached to the EPS backbone structure).

4.3.4 Monosaccharide analysis of EPS by GC - MS:

4.3.4.1 Sample: A1-batch 5

For the current monomer analysis, the procedure used for analysis was discussed in section 2.3.2. After hydrolysis of the EPS sample, reduction and acetylation were performed. On completion of the acetylation step, the sample was reconstituted in acetone and the sample analyzed by GC-MS. Before the samples were run, standards of alditol acetate were run to identify the monosaccharide peaks. The advantage of using alditol acetate is that each aldose sugar derivative will give only one peak on the chromatogram.

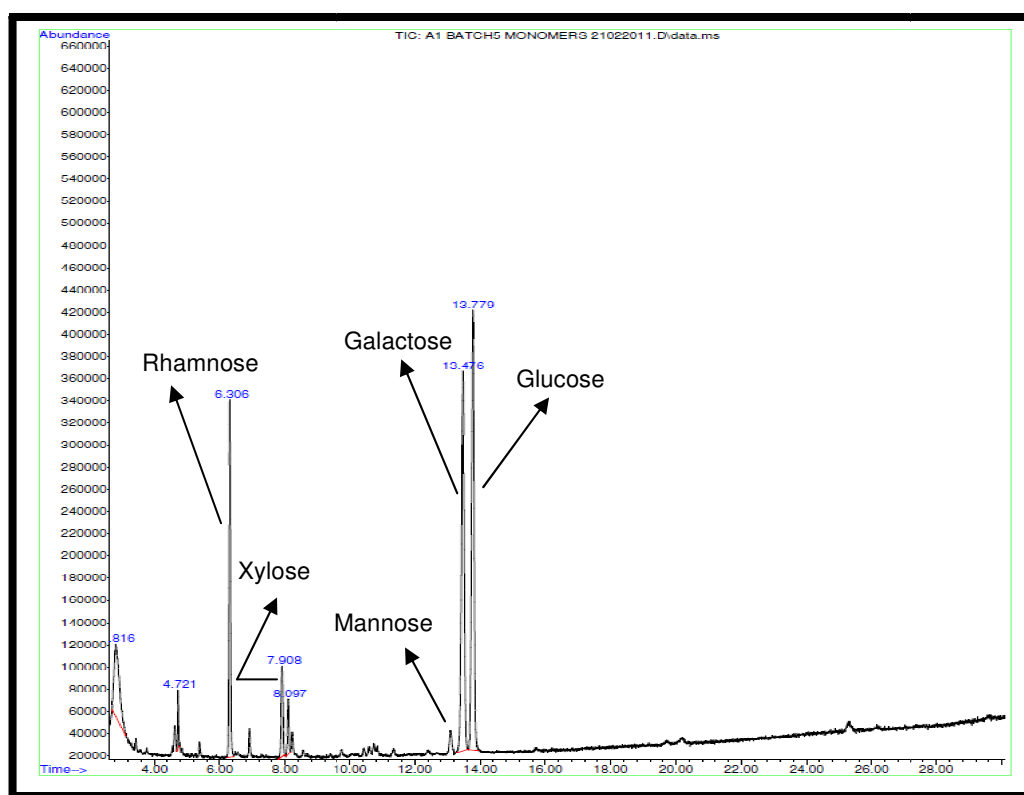
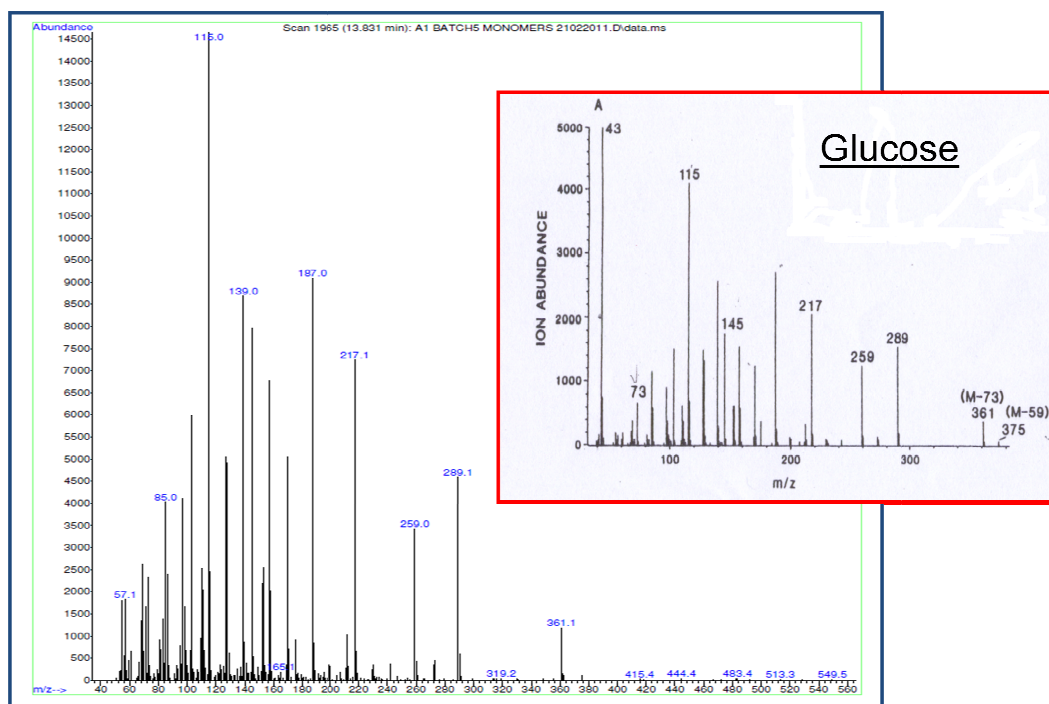


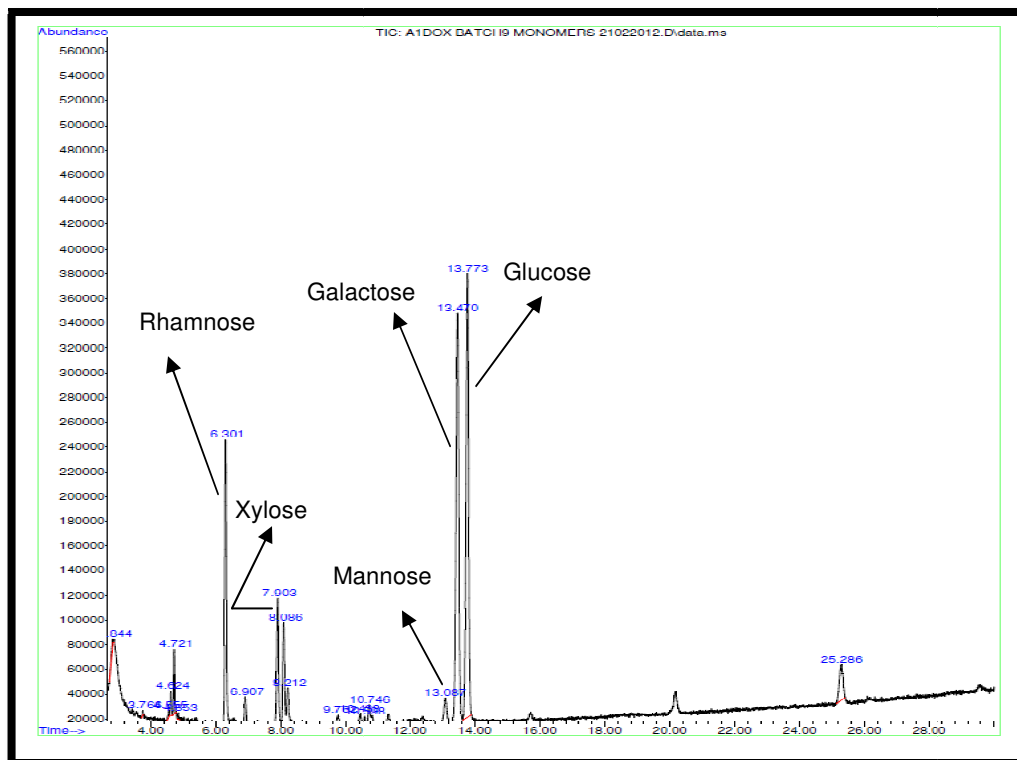
Figure 71: GC trace of A1-batch 5 (monomer analysis)

When the sample from A1-batch 5 was analysed, the GC chromatogram (Fig. 71) shows the presence of 3 major monosaccharide units. When the MS (Fig. 70) of these peaks were studied and compared with the literature spectra¹⁸⁷ and the retention times compared with those of the standards, the peaks were assigned the monosaccharide units, the constituents being rhamnose (12.78%), glucose (30.42%) and galactose (27.53%) and a number of minor peaks (xylose (4.09%), mannose (1.61%)) were also identified but were present in small amounts (< 5.0 %).



4.3.4.2 Sample: A1dOx-batch 9

The second sample, A1dOx-batch 9, was also used to identify monomers using GC-MS.



Again the GC chromatogram (Fig.73) shows the presence of 3 major monosaccharide units with constituents being rhamnose (10.33%), glucose (29.43%) and galactose (27.34%) and a number of minor peaks (xylose (5.76%), mannose (1.69%)) were present in small amounts (< 6.0 %). There were also some impurity peaks (4.7 mins, 8.08 mins) present in the chromatogram.

4.3.5 Monosaccharide analysis of EPS by HPAEC-PAD:

4.3.5.1 EPS sample: A1 batch5

It is well known that monomer analysis using GC-MS underestimates amino sugars (*N*-acetylglucosamine, *N*-acetylgalactosamine). The difficulties in the analysis of amino sugars have been overcome by the use of HPAEC-PAD. HPAEC-PAD is rapidly becoming the technique of choice for carbohydrate analysis due to the selectivity and sensitivity of the detection and its ability to analyze amino sugars.

Monomers have different response factors when they interact with the PAD in the HPAEC system (dependent on the pK_a of sugar monomers). So, in the present study, standard curves were obtained for rhamnose, mannose, galactose and glucose on the HPAEC-PAD to allow the quantification of the respective peaks, with both peak area and retention times being measured.

Table 10: Standards with their retention time by HPAEC-PAD

Standards	Retention time	Standard deviation
Rhamnose	7.52	0.003
Mannose	9.46	0.013
Galactose	11.54	0.050
Glucose	12.89	0.011

In monomer analysis using HPAEC-PAD, a hydrolysis step is required; after this step, the hydrolysed sample A1-batch 5 was run in HPAEC.

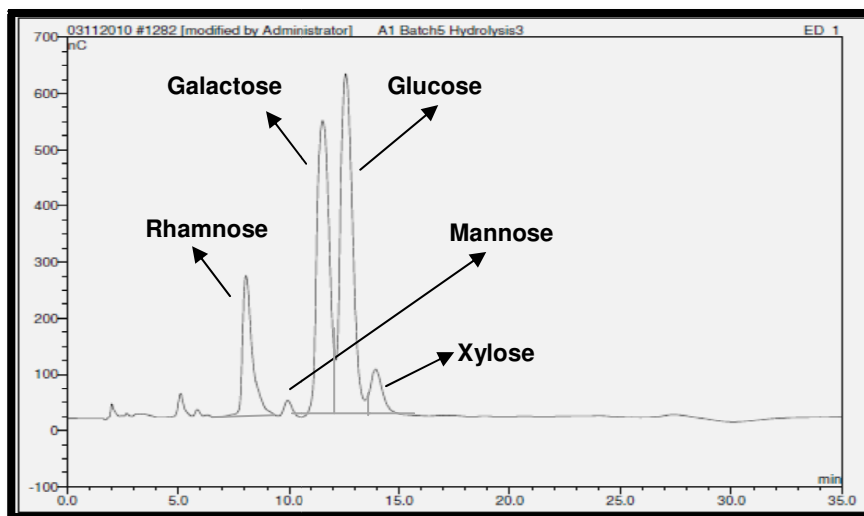


Figure 74: HPAEC chromatogram of A1-batch 5, after hydrolysis

The results of the HPAEC-PAD analysis (Fig. 74) shows the EPS from A1-batch 5 is composed of 3 major monosaccharide units. To identify the peaks observed in the HPAEC-PAD chromatogram, the EPS sample was spiked separately with the standard compounds. Peaks were identified as rhamnose (14.16%), mannose (5.55%), galactose (37.65%) and glucose (42.63%) with a molar ratio of 2.5 : 1 : 6.78 : 7.68.

When the monomer results from HPAEC-PAD and GC-MS were compared, it revealed that the EPS is composed principally of three monosaccharides: rhamnose, galactose and glucose. Each technique shows slightly different relative area percentage ratios for the monosaccharides and there is evidence for a smaller amount of rhamnose in the HPAEC than is recorded in GC-MS. And also it shows some evidence of the presence of *N*-acetyl amino sugars.

Table 11: Monosaccharide unit comparison of relative area percentage of GC-MS with HPAEC-PAD

Monosaccharide unit in EPS (A1-batch 5)	Relative area percentage (GC-MS)	Molar ratio	Relative area percentage (HPAEC)	Molar ratio
Rhamnose	12.78	1	14.16	1
Galactose	27.53	2.2	37.65	2.7
Glucose	30.42	2.4	42.63	3.0

4.3.5.2 *EPS sample: A1 dOx –batch 9:*

The second sample, A1dOx-batch 9, was also used to identify monomers by using HPAEC-PAD.

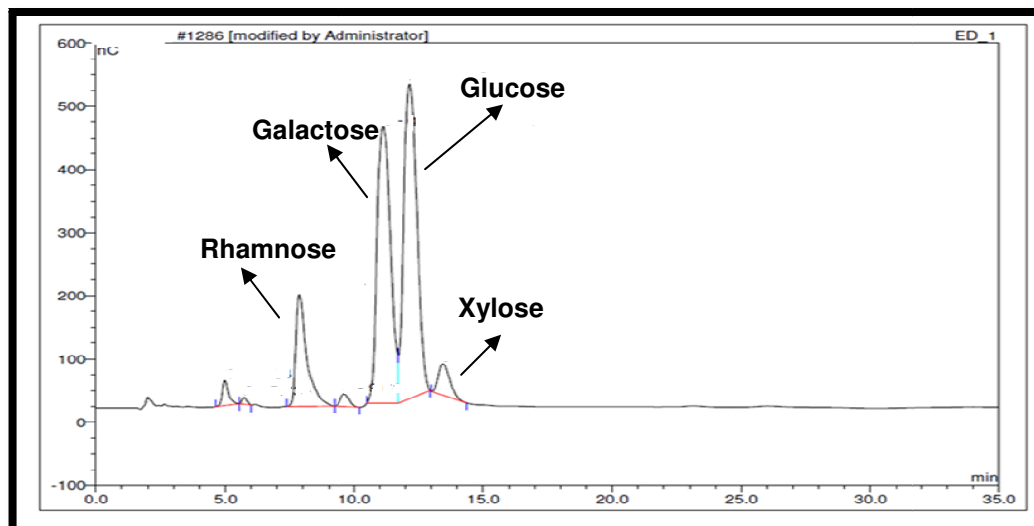


Figure 75: HPAEC chromatogram of A1-dOx batch 9 after hydrolysis

Again, the HPAEC-PAD generated a chromatogram containing 3 major peaks (Fig. 75); rhamnose, galactose and glucose in relative peak area percentages of 12.42%, 38.24% and 43.91% with a molar ratio of 1 : 3.1 : 3.5, with the presence of small amounts of xylose and mannose.

When the monomer results from HPAEC and GC-MS were compared, it revealed that the EPS is composed of three monosaccharide units; rhamnose, galactose and glucose.

Table 12: Monosaccharide unit comparison of relative area percentage of GC-MS with HPAEC-PAD

Monosaccharide unit in EPS (A1dOx-batch 9)	Relative area percentage (GC-MS)	Molar ratio	Relative area percentage (HPAEC)	Molar ratio
Rhamnose	10.33	1.0	12.42	1.0
Galactose	27.34	2.6	38.24	3.1
Glucose	29.43	2.8	43.91	3.5

Comparing the two batches, there appears to be slightly less rhamnose in A1dOx-batch 9 compared to that in A1-batch 5.

4.3.6 Uronic Acid Analysis:

In order to assess the likelihood of the presence of charged groups in an EPS sample, the monomer composition of the mixed EPS was investigated further to see if uronic acids could be identified. ^{31}P NMR already ruled out any sizeable amount of phosphates.

The first step in the procedure of uronic acid analysis, used by Filisetti-Cozzi and Carpita¹⁵², is to hydrolyse the EPS. The process used for the analysis of uronic acid is mentioned in the experimental section 2.3.9. In the colorimetric reactions of carbohydrates, two steps are involved:

- i) Formation of a chromogen from the sugar
- ii) The condensation of the chromogen with a specific reagent to develop a color.

The appearance of a chromogen relies on the reaction of the uronic acid with ether. Sulfuric acid has the ability to hydrolyze the glycosidic bonds that bind the polysaccharides. The step digests the polysaccharides into their component monosaccharides, of which the uronic acid components are then free to participate in the formation of the chromogen. In the Filisetti-Cozzi and Carpita¹⁵² method the development of a chromogen involves heating the uronic acid at 100 °C with a borax solution containing conc. sulphuric acid²³⁹. The free uronic acids then undergo a series of dehydration steps to generate 5-formyl-2-furan carboxylic acid. This chromogen then reacts with *m*-hydroxydiphenyl to give a conjugated system which can be quantified by UV-VIS spectroscopy.

A set of standards (D-galacturonic acid) were prepared and used to develop a calibration graph (Fig. 76).

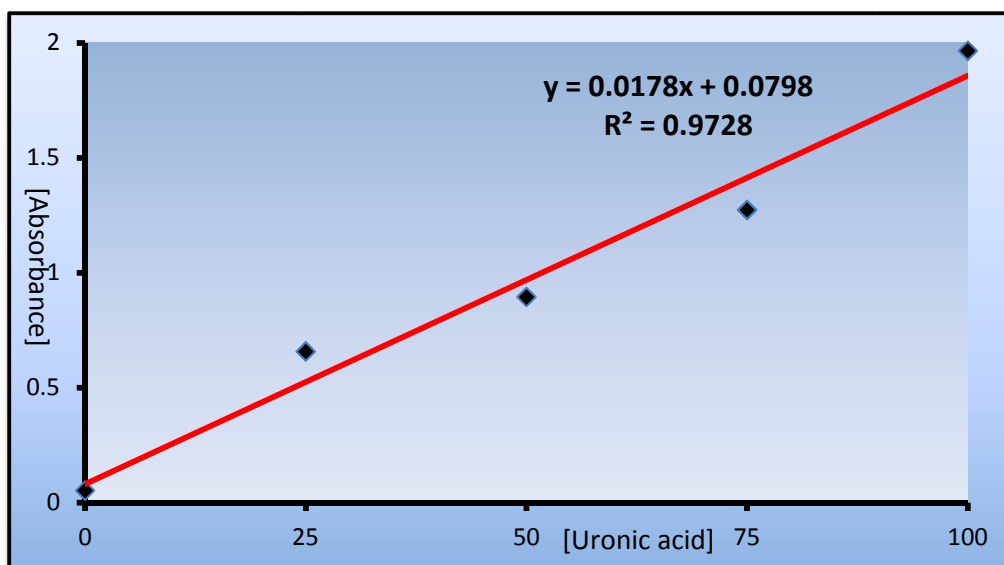


Figure 76: Calibration graph of uronic acid conc. vs. absorbance at 525nm

After the standards analysis, the EPS samples were analysed and it was observed that the EPS gave an absorption equivalent to 28ppm uronic acid which equates to 0.28mg of uronic acid in the 5.0mg sample (5% of uronic acid). The results suggest that small amounts of uronic acids are present in the EPS samples.

4.3.7 Linkage analysis of EPS by GCMS:

The results from the NMR and monomer analysis indicated a number of different sugars are present and the complexity of the NMR spectra suggested that a variety of different sugar linkages also exist. In order to confirm the different types of linkages between the monomers within the oligosaccharide repeat unit structure and any variation between the two samples, linkage analysis was performed by GC-MS.

Permethylated alditol acetates (PMAA) were prepared according to the procedure described in the experimental section 2.3.5. The symmetry introduced by converting sugars into alditols was avoided by introducing a deuterium (NaBD_4) at the C1 position during the reduction reaction. The deuterium atom in PMAA gives diagnostic fragments in the mass spectrum. However, some stereoisomeric PMAA give very similar mass spectra like glucose, galactose and mannose and make it impossible to distinguish between them on the basis of mass spectra. Fortunately,

the retention times in GC are significantly different for these 3 sugars and make identification easy.

The chromatograms obtained (Fig. 77 and 78) suggest that a very complex mixture of different sugars is present. The GC chromatogram shows the presence of several interesting peaks. The two EPS samples have the same peaks but present in different ratios, e.g. peaks A and B.

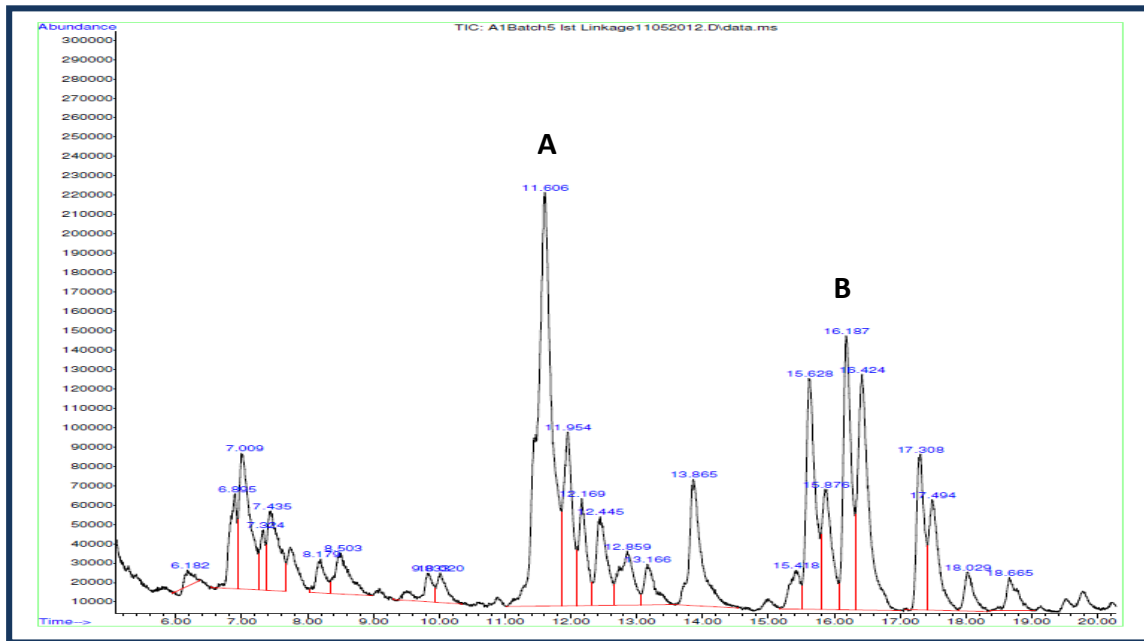


Figure 77: GC trace generated for the PMAA's derived during linkage analysis of A1-batch 5

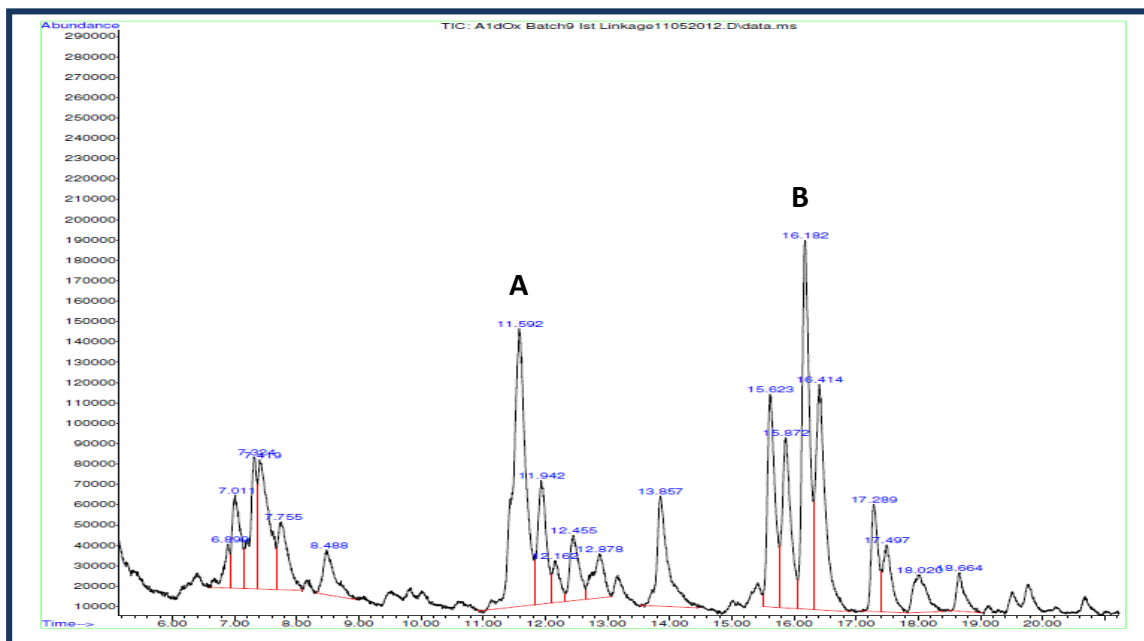


Figure 78: GC trace generated for the PMAA's derived during linkage analysis of A1dOx-batch 9

When each peak MS was studied and compared with the literature MS fragments¹⁸⁷, a number of different linkages could be identified (Fig. 79) these are tabulated in table: 13.

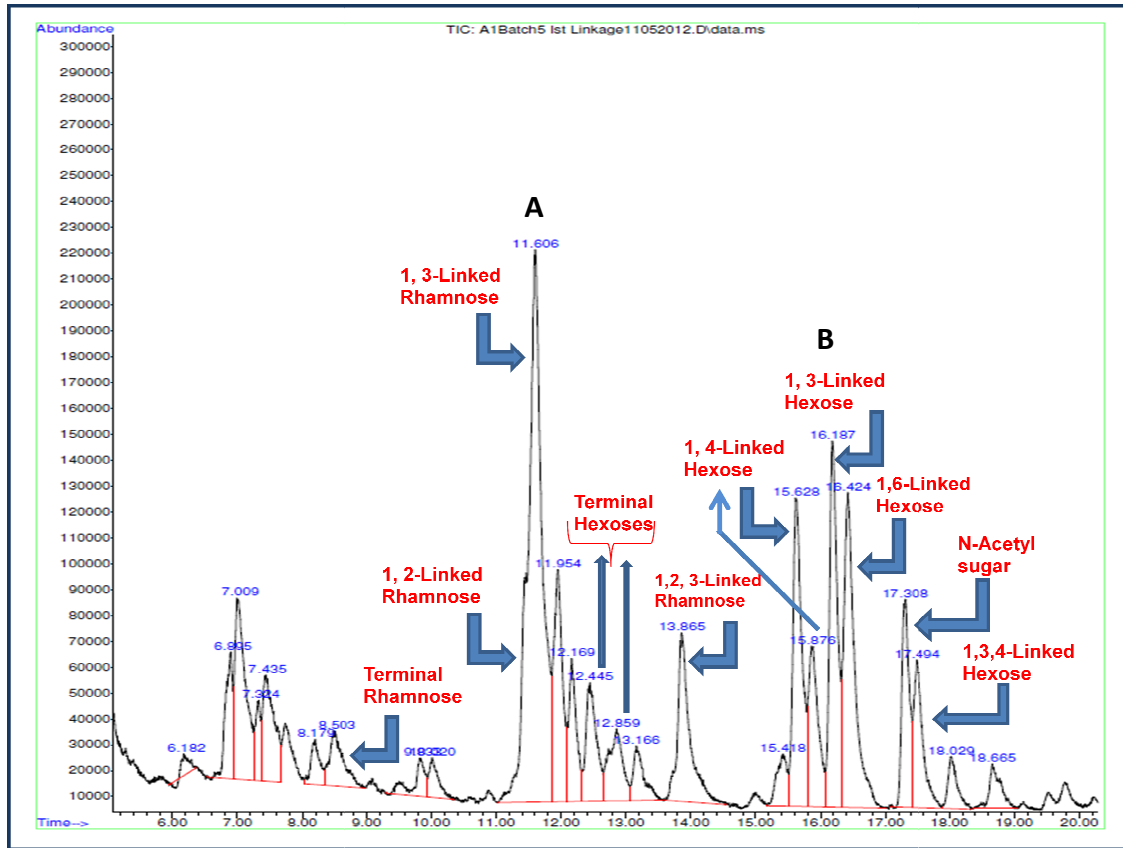


Figure 79: GC trace of linkage analysis of A1- batch 5 with linked hexoses

Table 13: Showing retention times of different linked hexoses

Retention times (min.)	Linked
8.48	Terminal Rhamnose
11.59	1, 2 – Linked Rhamnose
11.94	1, 3 – Linked Rhamnose
12.44, 12.87	Terminal Hexoses
13.85	1, 2, 3 – Linked Rhamnose
15.87	1, 4 – Linked Hexose
16.18	1, 3 – Linked Hexose
16.41	1, 6 – Linked Hexose
17.29	N – acetyl sugar
17.49	1, 3, 4 – Linked Hexose

Examples of the MS fragmentation patterns demonstrate how the different linkages are identified. Fig. 80 represents the fragmentation patterns observed for the terminal glucose and different linked hexoses.

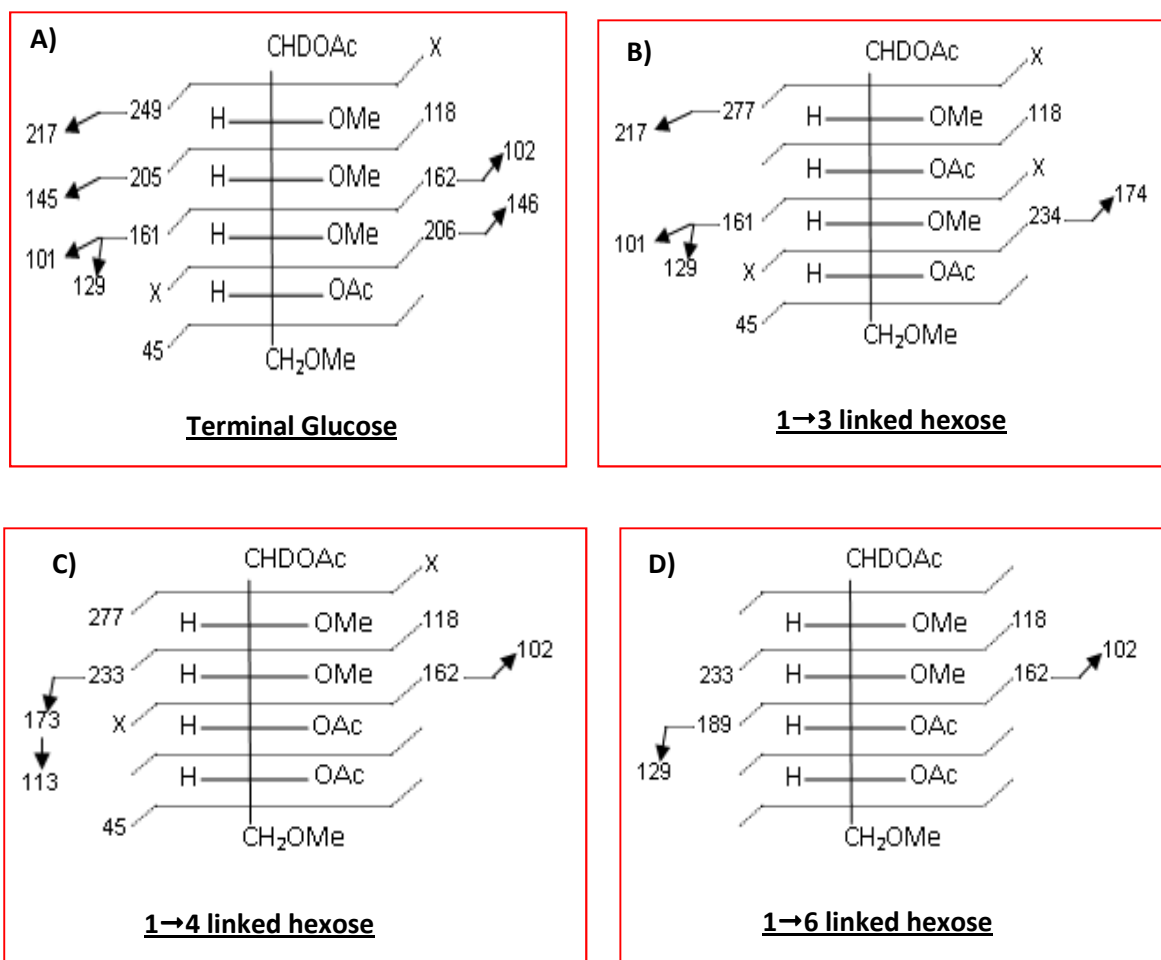


Figure 80: Mass spectra fragmentation: A) Terminal glucose, B) 1→3 Linked hexose, C) 1→4 linked hexose, D) 1→6 linked hexose

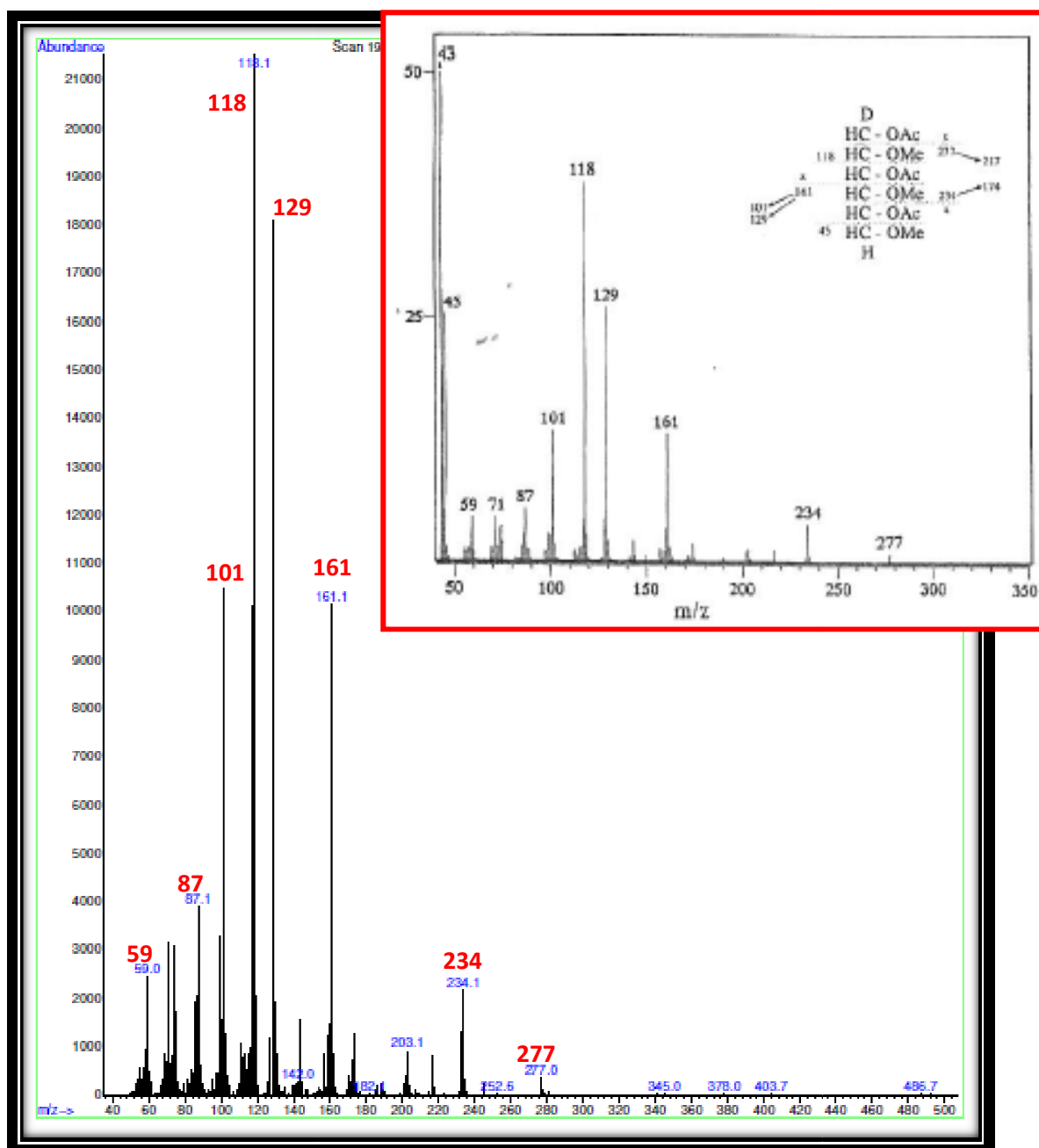


Figure 81: Mass spectra fragmentation (16.199 min-Peak B) of sample A1-batch 5, showing (1→3) linked hexose

Figure 81, represents MS at 16.199 min peaks (labelled as B in Fig. 79), representing (1→3) linked hexose, as linkage is confirmed from the literature spectrum¹⁸⁷.

4.3.8 Analysis of EPS by Ion Exchange Chromatography (IEX) - using DEAE – Sephacel:

All attempts to separate the different EPS components by SEC failed despite the fact that the SEC-MALLS results suggested that these components had different molecular weights. It was also apparent that a lot of the material added to the columns was not being eluted suggesting that adsorption onto the particular stationary phase being used in the study was occurring. The monomer results have suggested that there is a small but significant amount of charged groups present in at least one of the EPS; the charges being associated with the uronic acids. It was therefore decided to see if preparative anion exchange chromatography could be used to fractionate the different EPSs.

For the current study, DEAE-Sephacel was used, which is a weak anion exchanger based on beaded cellulose. The ion exchange group is a diethylaminoethyl (DEAE) group, which is charged at neutral pHs and maintains consistently high capacity. This medium is macroporous and has an exclusion limit of approximately 1,000,000 Da (for globular proteins) with an average particle size of 100 µm. The working pH of DEAE-Sephacel is taken as 7.2. As the sample contains EPSs with potentially varying charges, a gradient of different concentrations of salt with appropriate buffer was used. The column was packed with DEAE-Sephacel with tris-HCl as buffer which was used to equilibrate, wash and elute the column.

4.3.8.1 EPS (A1dOx-batch 9) analysis by IEX-DEAE Sephacel:

For the elution of the EPSs a linear salt gradient was used as a running buffer, starting from 0.0 M NaCl and changing to the final concentration of 0.6 M NaCl. Overall, 76 fractions were collected over a period of 6h 30 min. (see Fig. 82). The system was coupled to a refractive index detector and the chromatogram indicated the potential elution of three overlapping peaks.

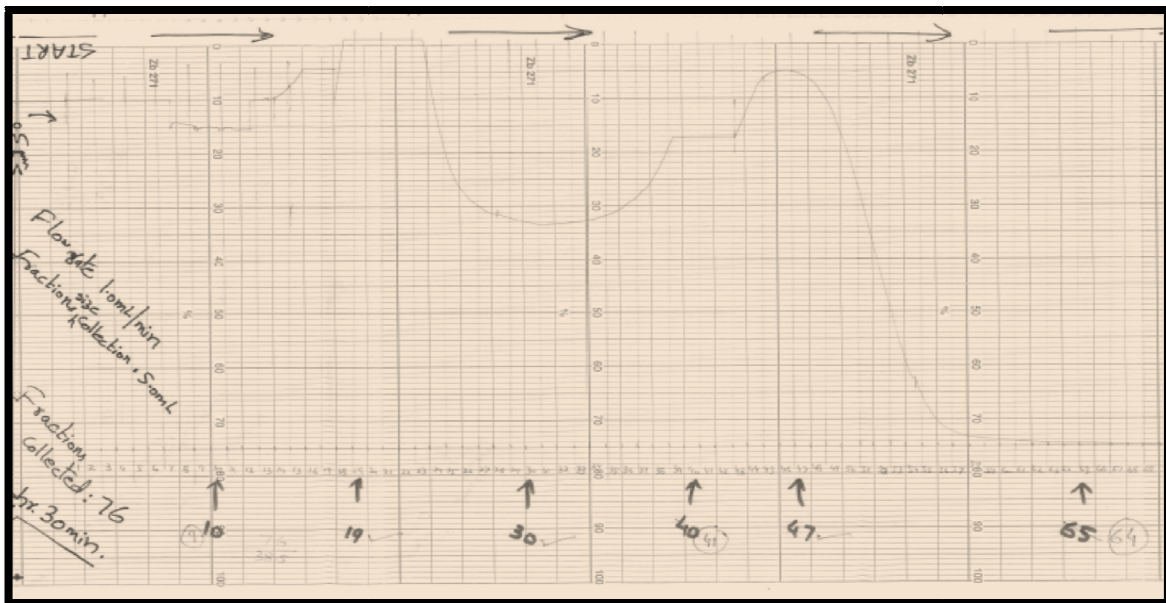


Figure 82: Chromatogram of A1dOx batch-9, obtained after passing through the IEX column filled with DEAE-Sephacel, showing different peaks (refractive index trace)

The UV trace shows 3 peaks (labelled as A, B, C in Fig. 83) between fractions 35-75. It shows that the EPS sample may contain proteins and or media material which are contamination that absorb UV.

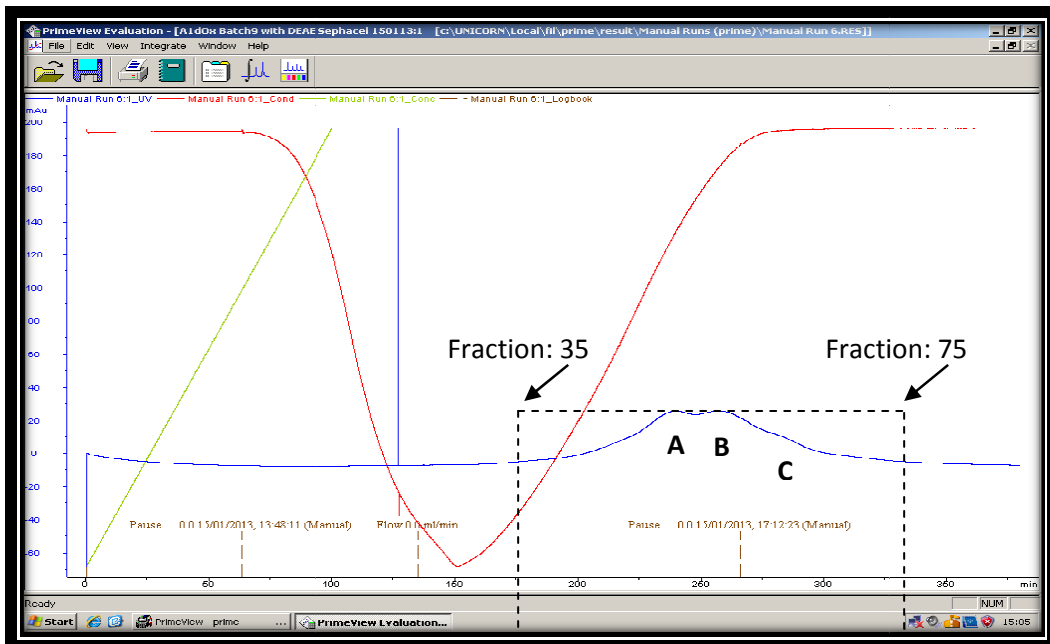


Figure 83: UV trace obtained from anion exchange chromatography, column filled with DEAE-Sephacel – green trace: buffer (1M NaCl), red trace: conductivity, blue trace: UV absorbance at 260nm

All the fractions collected were freeze dried. Those which showed positive responses on the UV and refractive index (RI) detectors were selected for NMR analysis. The freeze dried samples were dissolved in D₂O and NMR spectra were recorded at 70°C. Fractions 35 onwards up to fraction 39 showed the presence of polysaccharides, though the intensity of the signal was poor. Then it was decided to pool these fractions together, to get more concentrated signals. All the pooled fractions were again freeze dried and re-dissolved in D₂O for in depth study.

¹H NMR spectrum for the pooled fractions 35-39 (Fig. 84) shows the presence of a variety of anomeric signals (4.8-5.5 ppm) and sharp rhamnose methyl signals (1.75-1.85 ppm).

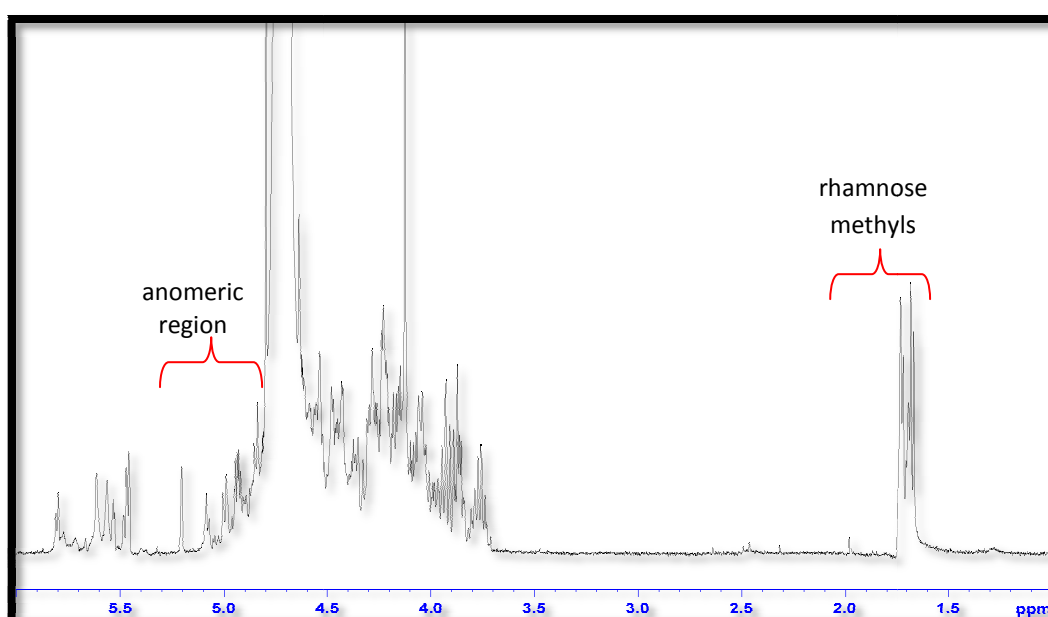


Figure 84: NMR spectrum of pooled fractions 35-39, showing some anomeric and rhamnose methyls signals

When the proton NMR spectra of fractions 35-39 (Fig. 84), crude A1dOx-batch9, and fractions 30-34 (Fig. 85-red spectrum) were compared (Fig. 85), the combined spectra show 4 clear regions (A, B, C and D) that have the same signal resonances with different percentage ratios, suggesting that there is only limited separation of the different polysaccharides.

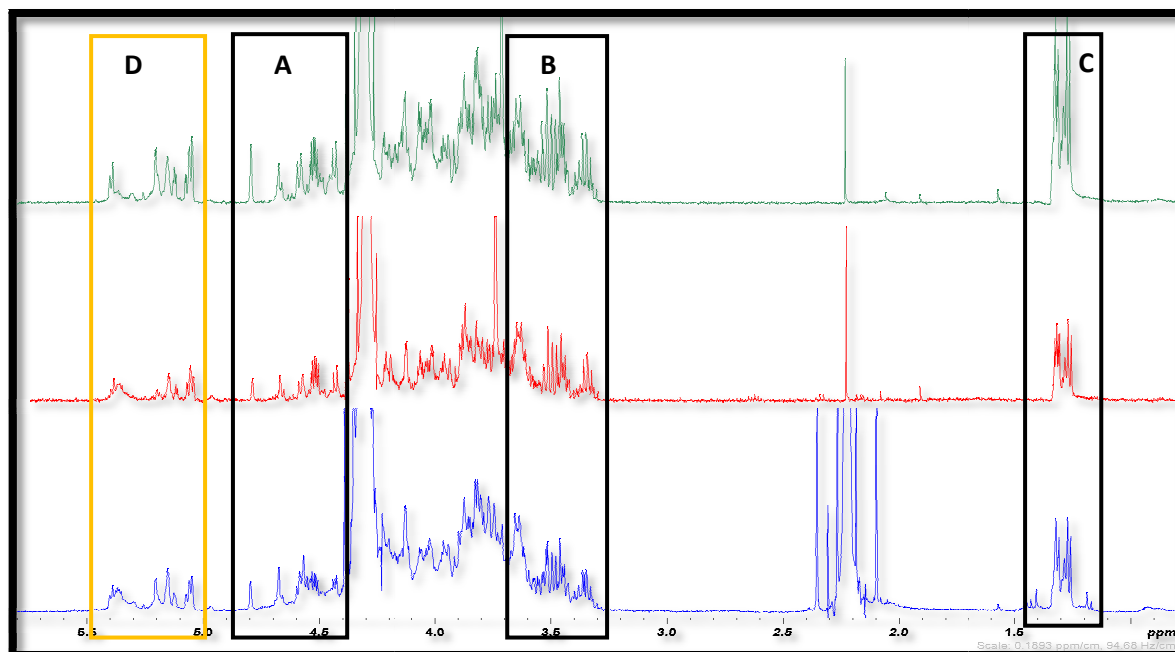


Figure 85: Comparison of NMR spectra showing some anomeric and rhamnose methyls signals—blue: crude A1dOx batch9, red: pooled fraction 30-34, green: pooled fraction 35-39

After failing to separate the polysaccharides it was decided to use 2D NMR analysis on the pooled fractions 35-39 for a more in depth analysis to determine if any evidence could be found for distinct patterns of signals (through comparison of signal intensities) which may belong to the individual polysaccharides.

4.3.8.2 2D-NMR analysis of the EPS recovered from *Bifidobacterium animalis* subsp. *lactis*:

2D-NMR analysis is used to provide additional information not obtainable from 1D-NMR experiments. The commonly used forms of 2D-NMR provide correlations between protons and other nuclei. In general, 2D-NMR can provide either through bond (COSY-scalar coupling) or through space (dipolar relaxation) coupling information.

At this point it was noticeable that one set of signals from *Bifidobacterium animalis* subsp. *lactis* was very similar to those observed in EPS extracted from the cell surface of the *Bifidobacteria breve* strains (discussed in chapter: 5).

The ^1H - ^1H COSY spectrum (Fig.86) shows protons attached to the adjacent carbon (linked by scalar coupling), the ^1H chemical shifts along both frequency axes are therefore correlated with each other.

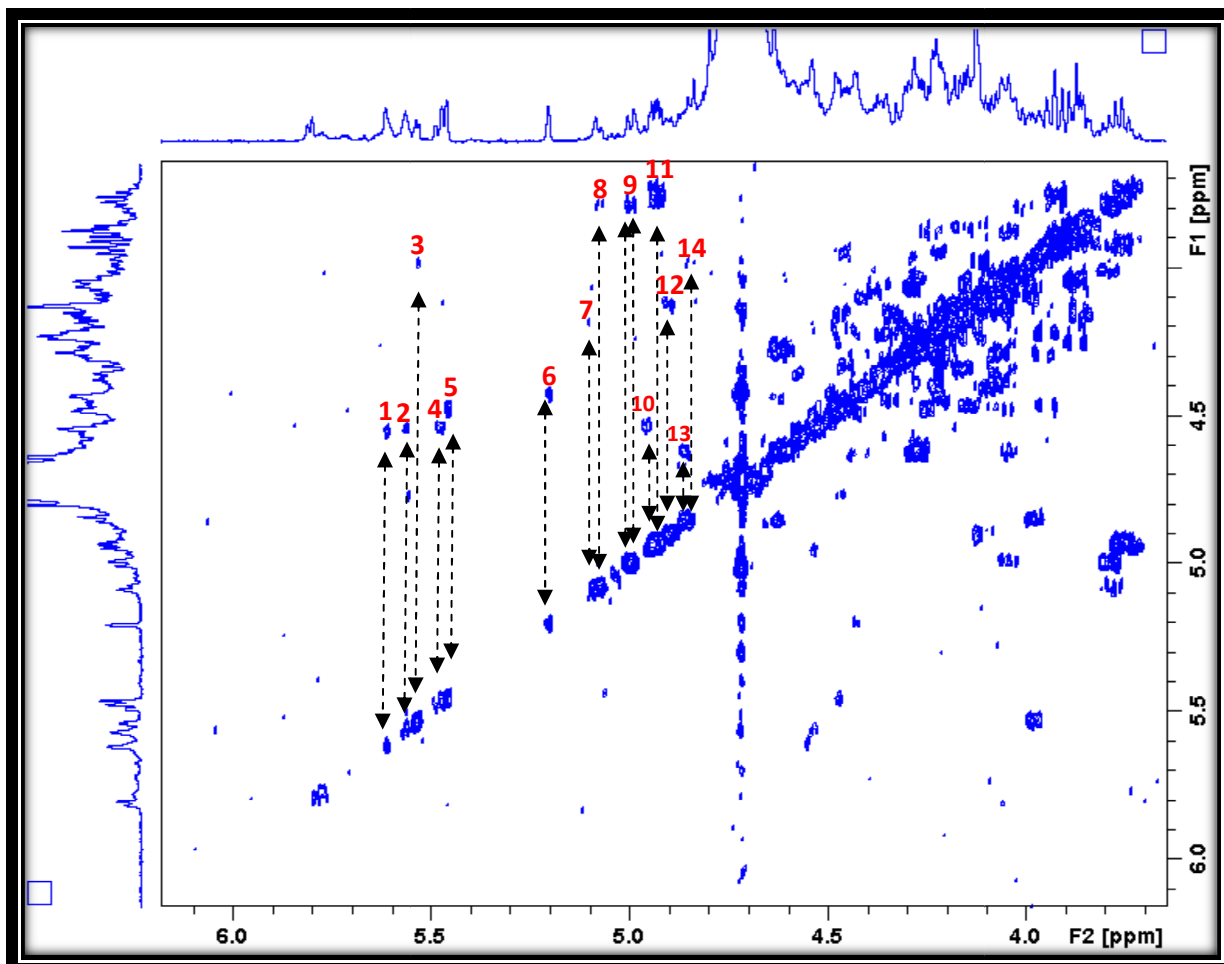


Figure 86: ^1H - ^1H COSY spectrum of pooled fractions: 35-39

The COSY spectrum (Fig. 86) confirms the large number of anomeric signals through their coupling to ring protons (> 14).

A TOCSY spectrum (mixing time 80ms-Fig.87) was also recorded. A TOCSY spectrum shows correlation between all protons within a given spin system. This is very useful for identifying protons on sugar rings. All protons on a given sugar ring will have a correlation with all other protons on the same ring but not with protons on different rings. Magnetization is transferred over 5 or 6 bonds, but the transfer can be disrupted by the presence of hetero-atoms, like oxygen.

A short mixing time (20 ms) will give only one-step transfers (spectrum will be like a COSY spectrum) and show only the sharp peaks, which are due to the protons on adjacent carbons. A long spin-lock time like 80 ms or 120 ms will give up to 5 or 6-step transfers and show less intense peaks that are due to the protons on the next but one carbon. Fig. 87 shows long spin-lock time of 80 ms to give 5 or 6-step transfers and it also shows extended coupling around the ring.

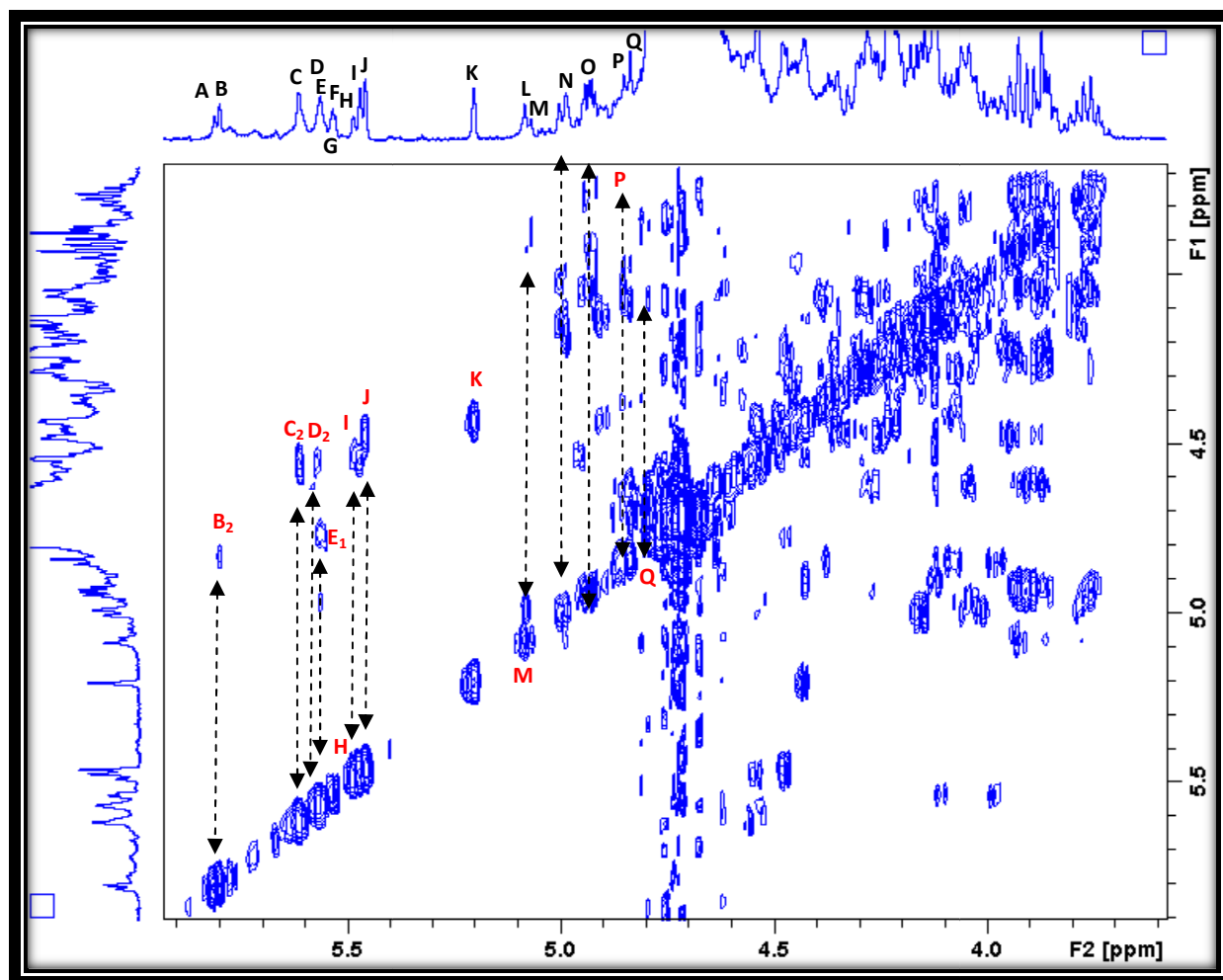


Figure 87: TOCSY (80ms) spectra of pooled fractions: 35-39

When the two 2D-NMR spectra (COSY and TOCSY) combine together (Fig. 88), they show the coupled protons exactly at the same resonance. The couplings over more than 4 bonds are highlighted by the resonance of blue contours without corresponding COSY (red contour).

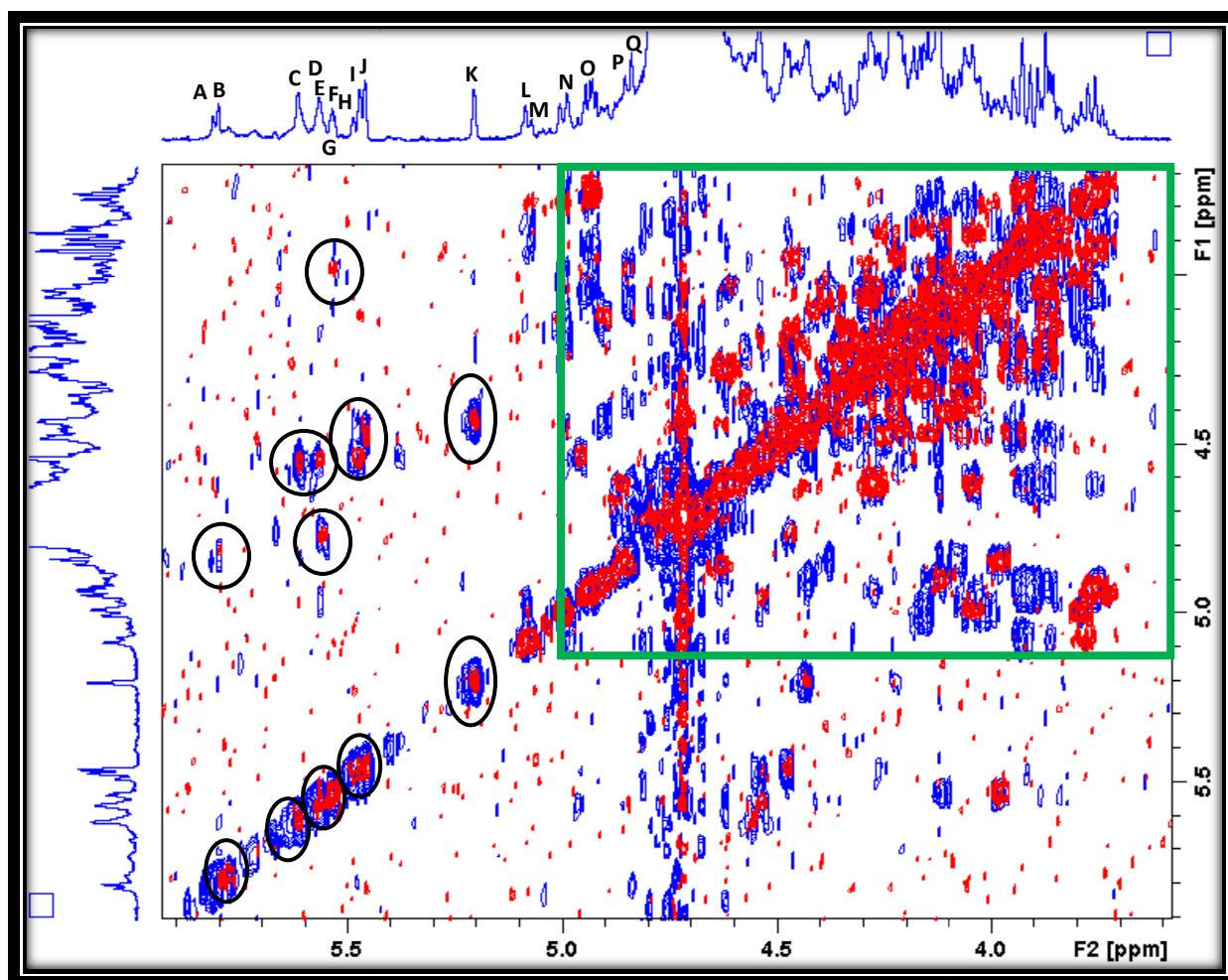


Figure 88: Combined COSY (red) and TOCSY (blue) spectra of pooled fractions: 35-39

In an attempt to assign the protons to their respective carbons a ^1H - ^{13}C HSQC spectrum (Fig. 89) was run on the sample (pooled fractions 35-39). Again the spectrum was complex but also showed signals that were observed in the *Bifidobacteria breve* samples (see chapter 5).

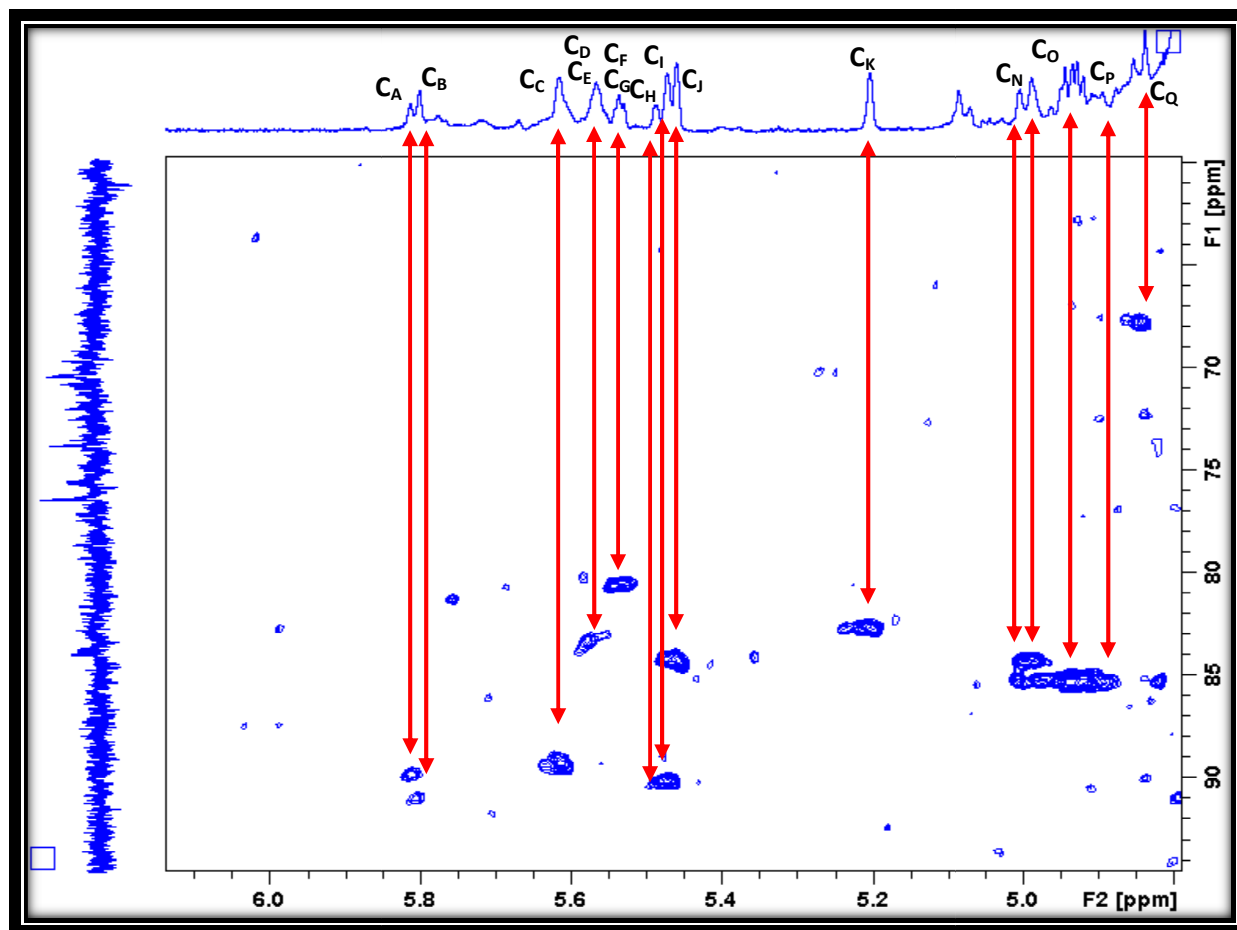


Figure 89: ^1H - ^{13}C HSQC spectra of pooled fractions: 35-39

^1H - ^{13}C HSQC (Fig. 89) shows protons that are attached to their respective carbons.

4.4 Conclusion:

Bifidobacterium animalis subsp. *lactis* two strains (A1dOx-batch 5 and A1dOx-Batch 9) were provided for analysis and characterization. In an attempt to characterise the novel EPSs produced by the *B. animalis* subsp. *lactis*, different analytical techniques were used. Monosaccharide analysis by HPAEC-PAD and with GC-MS showed that the repeating oligosaccharide structure consisted of mainly rhamnose, galactose and glucose with traces of mannose in an approximately (1: 2.7: 3.0) ratios. The linkage analysis by GC-MS showed that the EPS is a complex mixture of different sugars that are linked with a combination of 1→3, 1→4 or 1→6 linkages. SEC-MALLS also showed that the sample is composed of different molecular weight EPSs (HMw, MMw and LMw). Preparative size exclusion chromatography (Sephacryl S-500HR or S-200HR-used as stationary phases separately) was not able to separate the different molecular weight EPSs. To check whether the EPS is charged or not, uronic acid analysis was used, the results showed that in 5.0 mg of EPS only 0.28 mg of uronic acid was present. IEX (used DEAE-Sephacel as stationary phase) also failed to separate the different EPSs. The fractions collected from IEX were further analysed by 1D- and 2D-NMR. Data from 2D-NMR experiments showed the complex nature of this EPS that is produced by *B. animalis* subsp. *lactis* and provided evidence for the presence of a β (1→6) linked glucan, this polysaccharide has also been shown to be present in a number of *B. breve* strains, a point which will be expanded upon in the next section of this work.

4.5 Future work:

Further work is required to try and separate EPS samples, ideally this should involve molecular biology and biochemical techniques to find organisms and or fermentation conditions that provide single EPS structures in higher yields (this work is ongoing). More 2D-NMR experiments are required to determine the structure for the EPS produced by *Bifidobacterium animalis* subsp. *lactis*.

*5. Analysis of the EPS recovered
from Bifidobacterium breve strains:*

B. breve subsp. UCC2003,

B. breve subsp. JCM7017,

B. breve subsp. JCM7019,

5. Analysis of the Exopolysaccharides recovered from *Bifidobacterium breve* strains

5.1 Current work on *Bifidobacterium* spp.:

Bifidobacterium spp. are the most predominant species residing in the microbiota of the gastrointestinal tract (GIT) of a range of hosts; their presence is associated with a positive health status of the gut. However, very little is known about the exact molecular mechanisms that explain these probiotic effects²⁴⁰. As explained in the introduction of the last chapter, for this reason a significant amount of current research is directed at determining how these benefits are provided. In many cases, this research involves comparative and functional genome analysis. A number of *Bifidobacterium* spp. have been shown to have the capacity to produce exopolysaccharides (EPS) as part of a capsular layer²⁴¹ of polysaccharides. In recent years the EPS-encoding gene clusters of various Gram-positive bacteria including *Bifidobacterium* spp. have been identified and molecularly characterized^{242,243} including those of number of *Bifidobacteria breve* strains (see chapter: 4). To assess the chromosomal features of the members of *B. breve* species, researchers at Cork (Douwe Sinderen and Pauline Scanlan), analysed the genome sequences (in vivo) of thirteen different *B. breve* strains. Out of thirteen strains, eight (isolated from different human environments {table: 14}) were completely sequenced²⁴⁴ (table: 15).

Table 14: Bifidobacterial strain isolated from different human environments

Bifidobacterial strains	Isolated from
B. breve 689b	Infant faeces
B. breve NCFB 2258	
B. breve S27	
B. JCM 7017	
B. breve 12L	Human milk
B. breve 2L	
B. breve 31L	
B. breve JCM 7019	Adult faeces

Table 15: General features of eight complete genomes of *Bifidobacterium breve*

Feature	B. breve UCC2003	B. breve 527	B. breve 689b	B. breve NCFB 2258	B. breve JCM 7017	B. breve JCM 7019	B. breve 12L	B. breve ACS-071-V-Sch8b	Average value
Genome length	2,422,684	2,294,458	2,331,707	2,315,904	2,288,919	2,359,009	2,244,624	2,327,492	2,323,100
No. of genes	1854	1748	1821	1834	1770	1915	1765	1826	1817
Genes with assigned function	73%	73%	72%	74%	76%	73%	73%	80%	74%

Comparative genome hybridization (CGH) analyses on various *B. breve* strains have revealed the existence of a high level of sequence homology among same species members¹⁹⁹. They also found variable genetic functions that are related to bifidobacterial taxon¹⁹⁹. A number of these variable functions are associated with *Bifidobacterium* spp. adaptations to the host environment and defence against foreign DNA invasion including EPS synthesis genes.

5.2 Identifying the EPS gene cluster in *B. breve* UCC2003:

As stated above, significant efforts have been made to decode and analyze bifidobacterial genome sequences, aimed at the discovery of genetic determinants responsible for the adaptation of these microorganisms to the gastrointestinal tract (GIT) of their host^{198,201,245} including the ability to synthesize exopolysaccharides. One of the strains which has received the most attention is *Bifidobacterium breve* strain *UCC2003*.

Researchers at Cork are currently working on identifying EPS gene clusters of a number of *Bifidobacterium* subsp. *breve* strains including *B. breve* *UCC2003*. They found that the genome of *B. breve* *UCC2003* contains two putative EPS-encoding clusters. One cluster is believed to be responsible for the biosynthesis of a pellicle layer, a thin polysaccharide that is tightly associated with the peptidoglycan layer²⁴⁶. The second cluster is thought to be involved in the synthesis of a surface EPS (Fig.90)²⁴⁷. The majority of these genes are organized as two adjacent, oppositely oriented gene sets, designated *eps1* and *eps2* (Fig.90), which are flanked by two identical transposase-encoding sequences, similar to the organization seen in *Lactobacillus rhamnosus*²⁴⁷. The genes specifying several key components for EPS

biosynthesis, such as chain length regulation and the initiation of EPS subunit manufacture, are located at the extremities of the *eps* cluster. The predicted priming glycosyltransferase which initiates first step in EPS production and the phosphatase which is involved in chain length determination exhibit high identity to their counterparts in other bifidobacteria²⁴⁷.

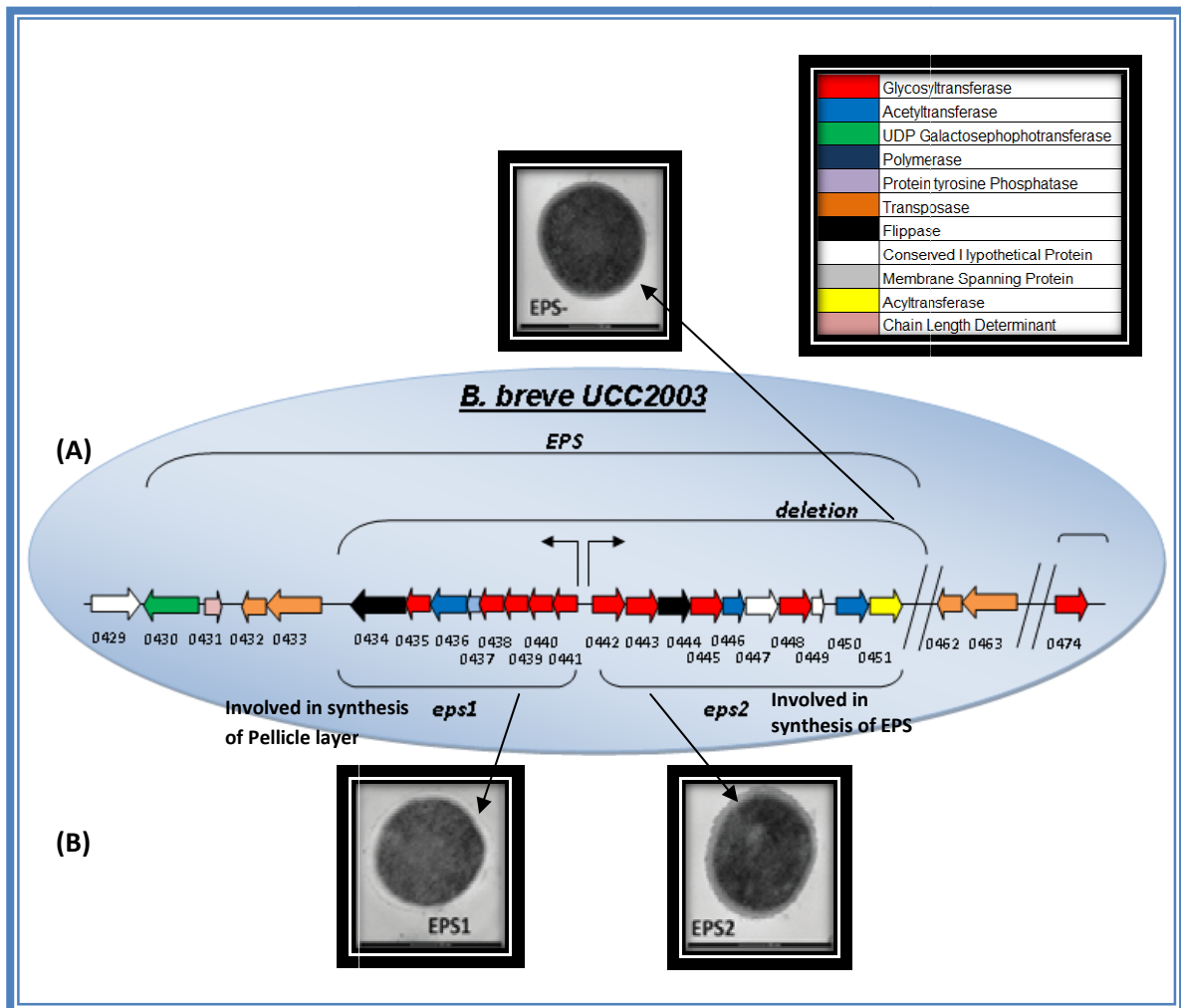


Figure 90: (A) Schematic diagram of the *eps* gene cluster of *B. breve* UCC2003. *-/-* represents a number of genes between Bbr_0451 and Bbr_0462 or between Bbr_0463 and Bbr_0474. The promoter swapping is indicated between Bbr_0441 and Bbr_0442 by arrows. (B) Transmission electron microscopy images show expression of EPS by the two transcriptional units of *B. breve* UCC2003 and a lack of EPS in the deletion strains²⁴⁷.

The two adjacent and oppositely oriented transcriptional units *eps1* and *eps2* were both reported to be involved in the production of EPS (variable EPS cluster). If the relative DNA is inverted, then the EPS polymer produced at any given time depends on the orientation of a single promoter. The researchers at Cork found that in the system there is high transcription of the *eps2* region and undetectable levels of the *eps1* region. In the inverted system, the transcriptional pattern suggested that the

variant was the result of DNA inversion that had reoriented the promoter located within the region between *eps1* and *eps2*. These findings, when correlated with HPAEC analysis²⁴⁷, suggest that the *eps* locus specifies two alternative EPS producing biosynthetic pathways which share a common priming glycosyltransferase and chain length determination.

In molecular biology, the standard method used to determine the function of predicted genes and establish which genes are essential under particular environment conditions is to disrupt the gene and determine the phenotypic change. Disruption of the priming glycosyltransferase in an EPS cluster has previously been shown to abolish EPS production in *L. lactis*^{247,248} which is consistent with the finding²⁴⁶ of EPS production being abolished in an insertional mutation of the gene encoding the priming glycosyltransferase.

Most of the work was done by the researcher at Cork (Douwe Sinderen), but so far very little is known about how similar mutation influences EPS structures in *B. breve* strain *UCC2003*. This is the starting point for our participation in this research. EPS biosynthesis (at Cork) was also abolished in a *B. breve strain UCC2003* carrying a deletion of the cluster. These EPS-negative (EPS⁻) strains were found to sediment quickly in liquid growth media relative to the wild-type EPS-producing strains and cells were found to aggregate substantially more when lacking the EPS layer.

5.3 Aim of the study:

The main aim of this research was to study the production of EPS by a variety of *Bifidobacterium breve* strains and to determine the effect of inversion and deletion mutants on the EPS that is synthesized.

5.4 Samples provided:

A number of EPS samples derived from *B. breve* UCC2003 strains were supplied and labelled as *B. breve* strain JCM7017 (isolated from infant faeces), *B. breve* strain JCM7019 (isolated from adult faeces), *B. breve* strain NCFB2258 (isolated from infant faeces), *B. breve* UCC2003 POS NaOH (extracted with NaOH), *B. breve* UCC2003 NEG NaOH (extracted without NaOH), *B. breve* UCC2003 POS EDTA (extracted with EDTA), *B. breve* UCC2003 NEG EDTA (extracted without EDTA), *B. breve* UCC2003 EPS -ve, *B. breve* UCC2003 EPS +ve, *B. breve* UCC2003 (DEL) deletion mutant (gene responsible for production of EPS have been deleted), *B. breve* UCC2003 Inversion strain (specific genes have been inverted). These samples were supplied by the academics from University College Cork (Douwe Sinderen and Pauline Scanlan) as freeze dried powder.

5.5 Analysis techniques used:

^1D (^1H , ^{13}C , ^{13}C DEPT) and ^2D -NMR (COSY, TOCSY, HSQC, HMBC, HSQC-TOCSY, NOESY) techniques were used for the analysis of the EPS samples that were derived from the cultures of the above bacteria grown on Agar and with a variety of sugars as substrates.

5.6 Results and Discussions:

5.6.1 NMR analysis of the crude sample:

A series of ^1D -NMR spectra were recorded on all the samples provided. Initial spectra were complicated as a number of signals associated with the media components (5.45–5.8 and 6.2-6.4 ppm) and some potential EPS anomeric resonances (4.7–5.4 ppm) (Fig. 91) were visible. Surprisingly, the other samples that were labelled as *B. breve* strain JCM7019 and *B. breve* strain NCFB2258, also gave identical NMR spectra, showing the same media peaks and a number of peaks related to the anomeric resonances of EPS.

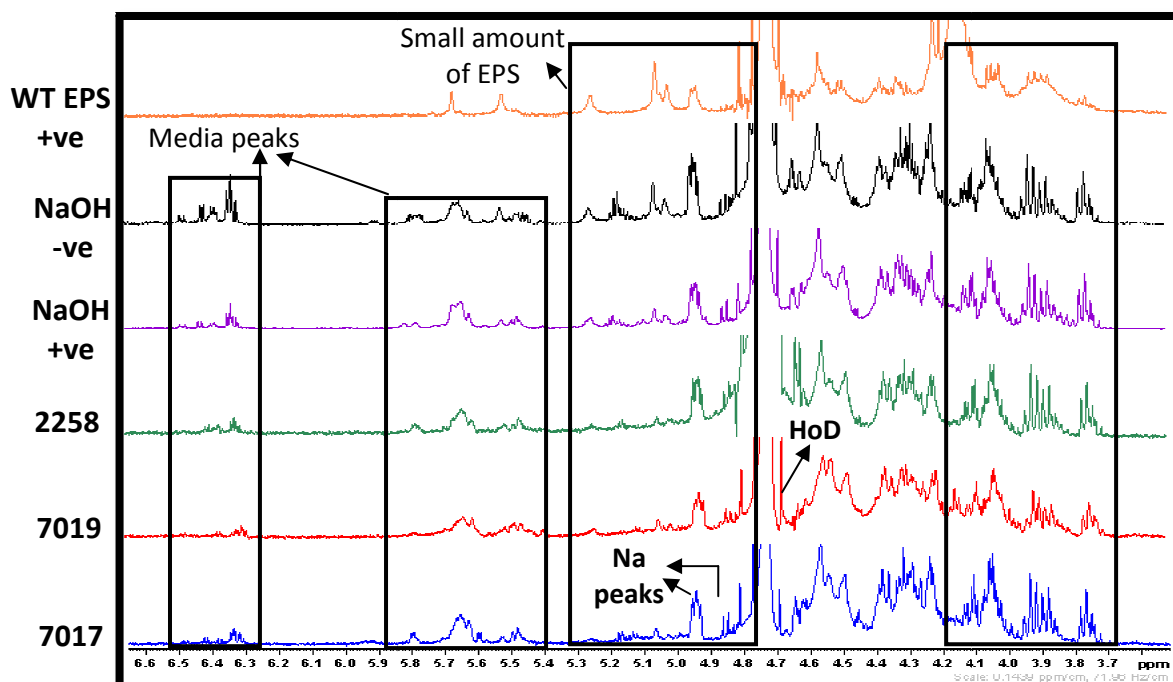


Figure 91: Comparison of NMR spectra of *B. breve* samples labelled as *B. breve* strain JCM7017(blue), *B. breve* strain JCM7019 (red), *B. breve* strain NCFB2258 (green), *B. breve* UCC2003 NaOH+ve (purple), *B. breve* UCC2003 NaOH-ve (black), *B. breve* UCC2003 WT-EPS+ve (orange).

Despite the differences in the EPS gene clusters, it is clear that some of the anomeric proton signals are identical in each of the samples. In a separate program of work, it has been shown that these peaks are only produced if NaOH is used in the isolation of polysaccharides from AGAR (used to provide a growth medium for bacteria) plates (Alhudhud-Huddersfield²⁴⁹).

After analysing ¹H-1D NMR, it was decided to run 2D-NMR spectra for each of the samples starting with the EPS from *B. breve* strain JCM7017. The analysis of the COSY spectrum (Fig. 92) identified the coupling between the ring protons and the anomeric protons for the signals that are present in the samples that were extracted from AGAR and which have been treated with sodium hydroxide.

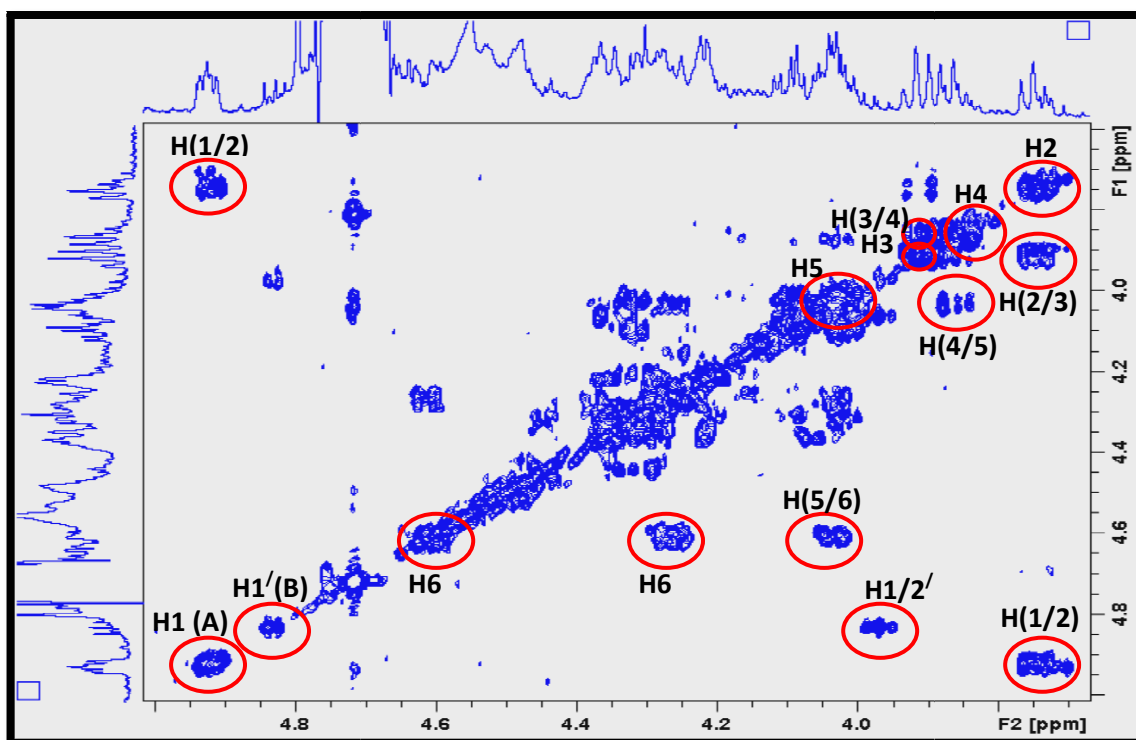


Figure 92: COSY spectrum of *B. breve* strain JCM7017

The COSY (^1H - ^1H) experiment (Fig. 92) showed coupling between protons attached to adjacent carbons (linked by scalar coupling), the ^1H chemical shifts along both frequency axes are therefore correlated with each other and it was possible to identify one full set of ring protons and a second partial set (H_1' at 4.82 ppm which is correlated to H_2' at 3.95 ppm). The following table (table: 16) shows the ^1H chemical shifts (in ppm) determined from the COSY spectrum of *B. breve* strain JCM7017 for the major anomeric resonance.

Table 16: ^1H NMR chemical shifts of *B. breve* strain JCM7017

Monosaccharide	^1H Chemical Shift (ppm)						
<i>B. breve</i> strain 7017	H1	H2	H3	H4	H5	H6	H6'
	4.92	3.74	3.91	3.84	4.01	4.59	4.6

After analyzing the COSY spectrum of *B. breve* strain JCM7017, it was decided to run a TOCSY spectrum to confirm the connectivities and to identify further couplings in the minor anomeric system. As TOCSY coupling depends on the length of mixing time (30-210 ms), it was decided to run a series of TOCSY experiment with longer mixing times to help identify less intense peaks.

When COSY and TOCSY spectra of *B. breve* strain JCM7017 were overlaid for analysis, the overlaid spectra (Fig. 93) show the positions of H1-H4 for the ring system at 4.9 δ where anomeric protons are present and a second set for a ring system with an anomeric proton at 4.8 δ . The H4' resonance appears at 4.38 ppm and no further coupling was observed; that is the indication of a D-galactose residue.

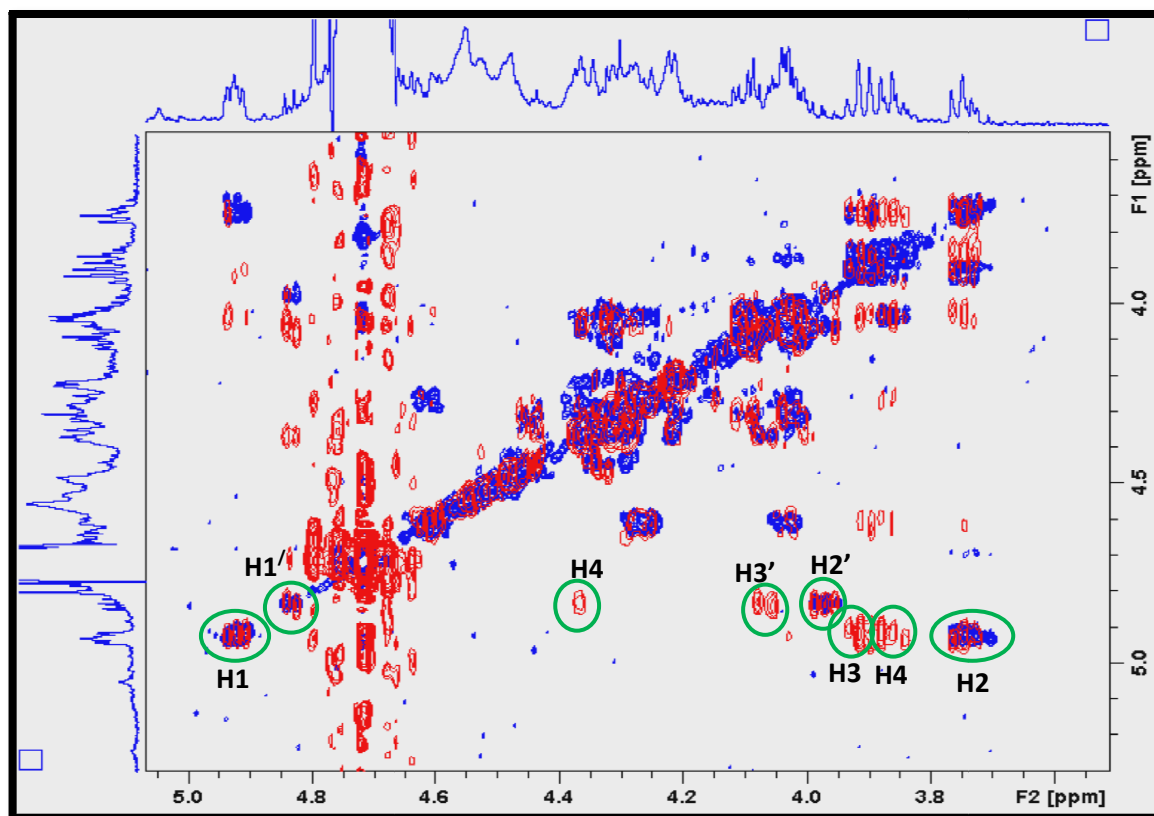


Figure 93: COSY and TOCSY overlaid spectra of *B. breve* strain JCM7017

To completely assign the proton signals with the connecting carbons, a ^1H - ^{13}C HSQC experiment was performed (Fig. 94). The spectrum contains cross peaks for each proton that is attached to ^{13}C . The ^{13}C chemical shifts are given in table:17.

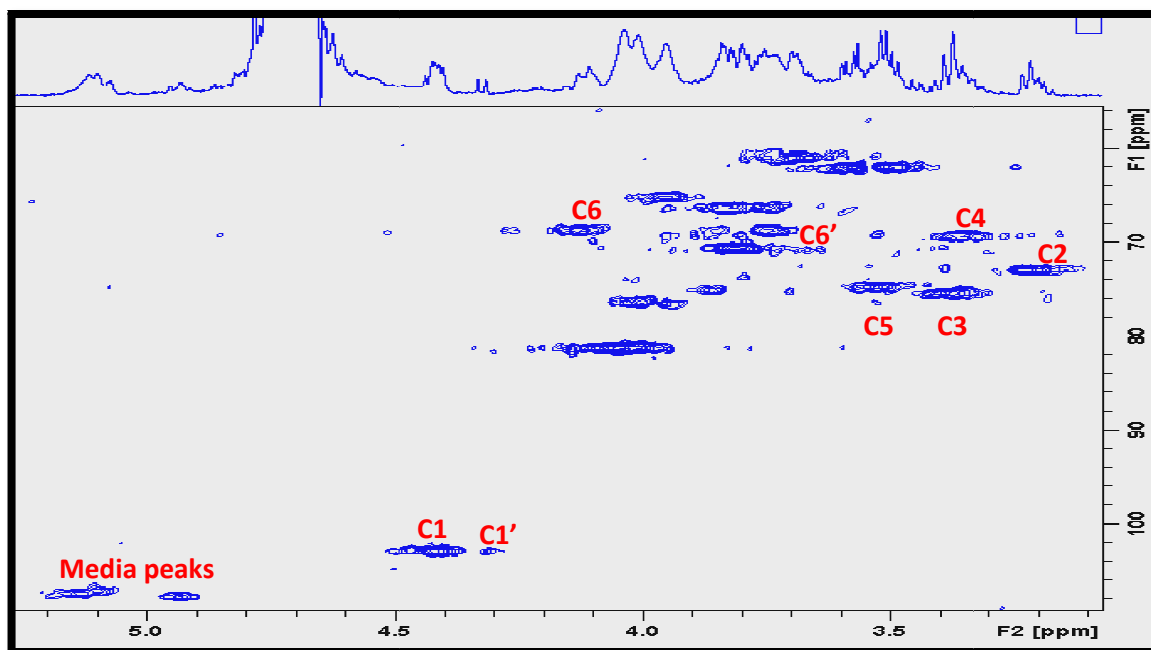


Figure 94: ^1H - ^{13}C HSQC spectrum of *B. breve* strain JCM7017

Table 17: ^1H - ^{13}C HSQC, Carbon chemical shifts of *B. breve* strain 7017

Monosaccharide	^{13}C Chemical Shift (ppm)							
	C1	C1'	C2	C3	C4	C5	C6	C6'
<i>B. breve</i> strain JCM7017	102.9	102.9	72.8	75.3	69.3	74.7	68.6	68.8

All the above spectra were recorded at 70 $^{\circ}\text{C}$, however, this places the residual HOD signal close to the anomeric signal from the monomer sugar peaks. So a number of spectra were recorded at room temperature in order to shift the HOD signal. The position of the resonances ^1H - ^{13}C are almost identical to those observed for β -(1 \rightarrow 6)-linked glucan, which was isolated from the cell walls of yeast²⁵⁰.

In Prof. Laws research group at the University of Huddersfield, a procedure was developed to grow bifidobacterial strains in broth cultures and to isolate the EPS without adding NaOH (Muhannad Alhudhud and Paul Humphreys²⁴⁹). The protocol was used by the researchers at Cork with the strain *B. breve* UCC2003 to produce a secreted EPS. Once the new sample of *B. breve* UCC2003 was received, it was dissolved in D₂O and a proton NMR spectrum was recorded (Fig. 95).

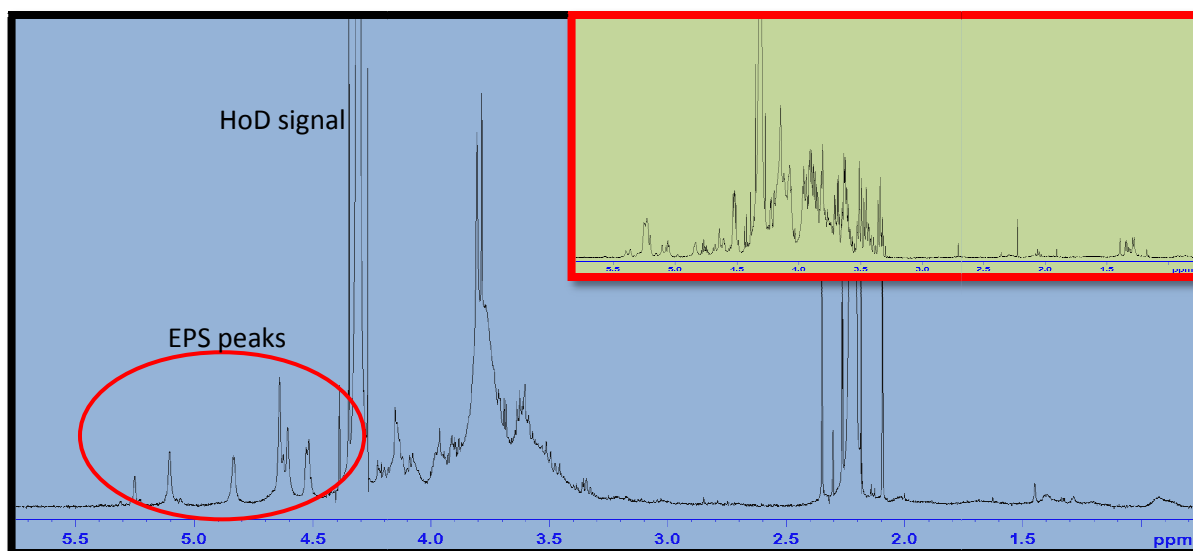


Figure 95: Comparison of *B. breve* UCC2003 EPS +ve sample showing only EPS peaks (blue) with NMR spectrum (green-Fig. 99) showing EPS and media peaks together

When the anomeric region of the above NMR spectrum was closely observed (Fig. 96), two things were noted: firstly that there was no evidence for any β -(1 \rightarrow 6) glucan and secondly it now shows resonances similar to those that are expected from a relatively clean EPS with anomeric resonances in the range of 4.39-5.29 ppm. The peaks are labelled for reference only.

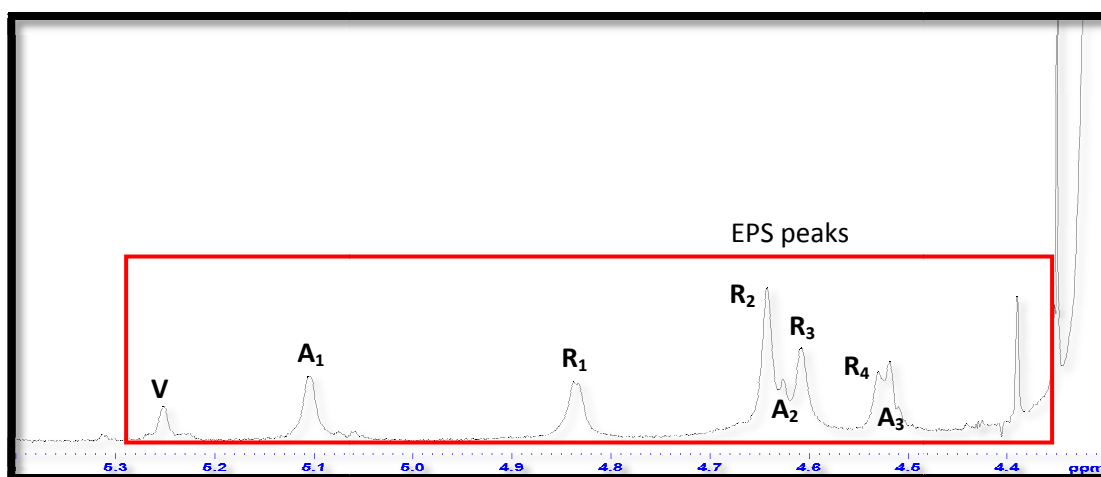


Figure 96: Expanded anomeric region of *B. breve* UCC2003 EPS +ve sample (V=Signal varies)

After observing the NMR spectrum of the crude samples, it appears that a series of *B. breve* UCC2003 systems have identical peaks including the EPS +ve and -ve strains which were treated with EDTA and therefore it is not clear if the extraction process is releasing EPS material.

When NMR spectra of the samples were compared, the regions labelled A1, B1, C1/D1, E1 and A2 are almost identical having constant peaks in all the samples whereas the strength of the most down-field signal varies in the different samples.

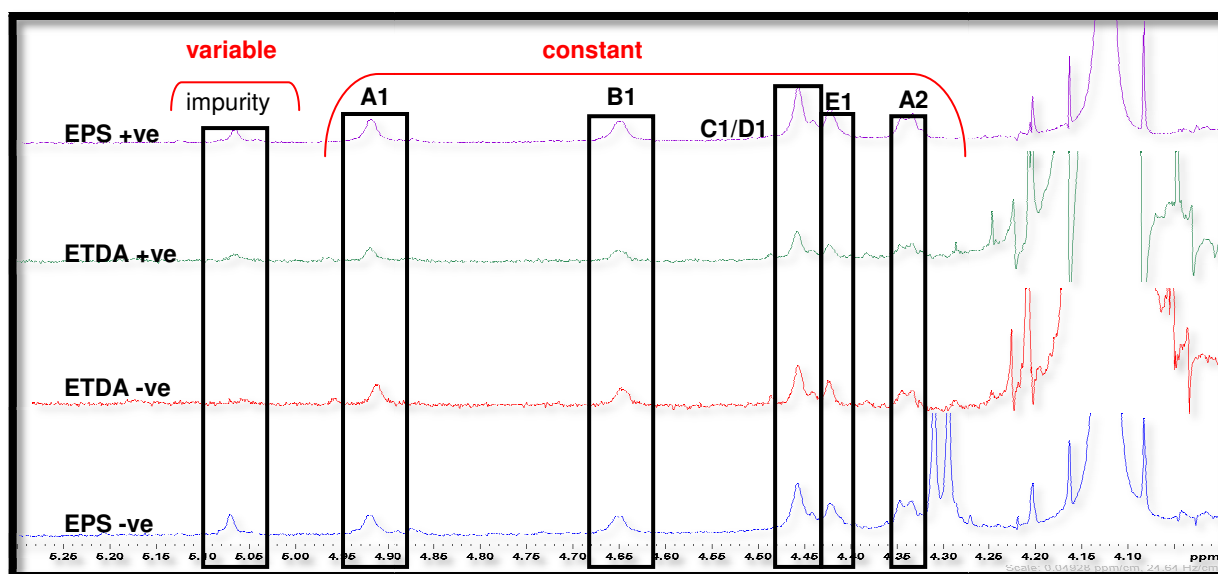


Figure 97: Comparison of the *B. breve* UCC2003 samples (EPS-ve {blue}, EDTA-ve {red}, EDTA+ve {green} and EPS+ve {purple})

In the EPS-ve sample, which is from the insertion mutant which should lack an active priming glycosyl transferase (no EPS should be formed), the same EPS signals were visible (Fig. 97-bottom trace-blue) but an intense anomeric resonance was also observed at 4.3 δ . A number of 2D-NMR spectra were recorded to gain an insight into the nature of this particular polysaccharide.

The ^1H - ^1H COSY spectrum (Fig. 98-{EPS-ve strain}) identified the presence of coupled protons by matching the chemical shifts on both frequency axes.

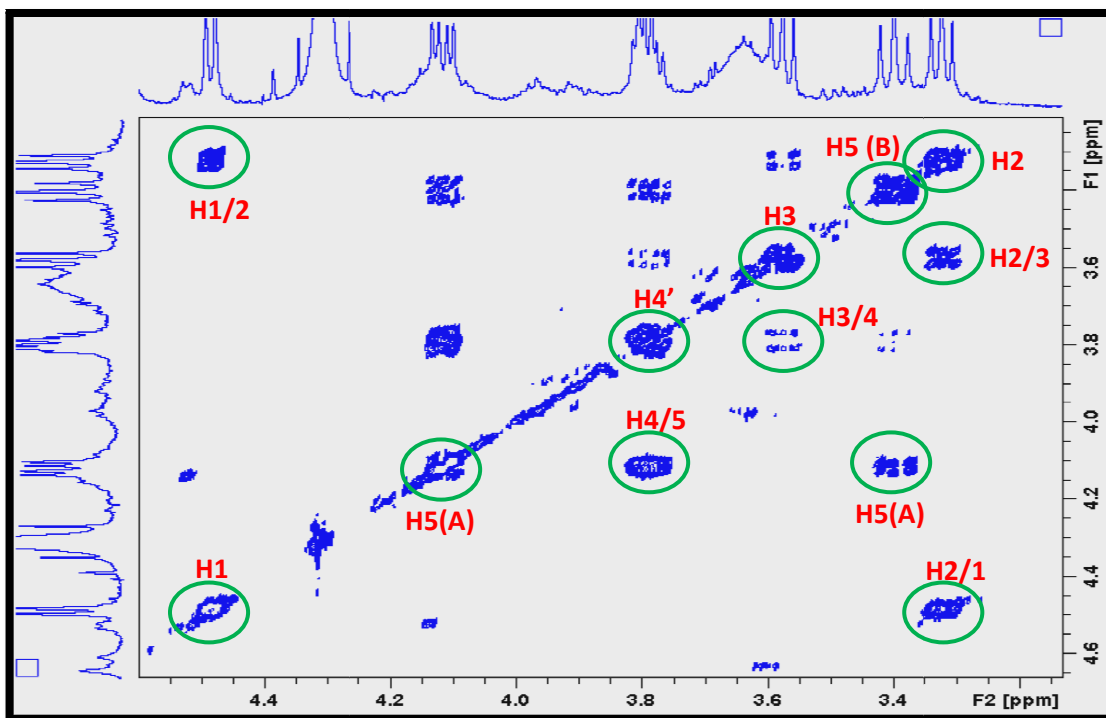


Figure 98: ^1H - ^1H COSY spectrum of *B. breve* UCC2003 EPS –ve strain, showing positions of protons

Table:18, shows the ^1H chemical shifts (in ppm) from the COSY spectrum of *B. breve* UCC2003 EPS-ve.

Table 18: Proton NMR chemical shifts of *B.breve* UCC2003 EPS-ve

Monosaccharide	^1H Chemical Shift (ppm)					
	H1	H2	H3	H4	H5(A)	H5(B)
<i>B. breve</i> UCC2003 EPS-ve	4.45	3.32	3.55	3.80	4.17	3.41

The corresponding ^1H - ^{13}C HSQC NMR spectrum (Fig. 99) of *B. breve* strain UCC2003 EPS -ve was used to identify the location of the corresponding C1, C2, C3, C4 and C5 carbons.

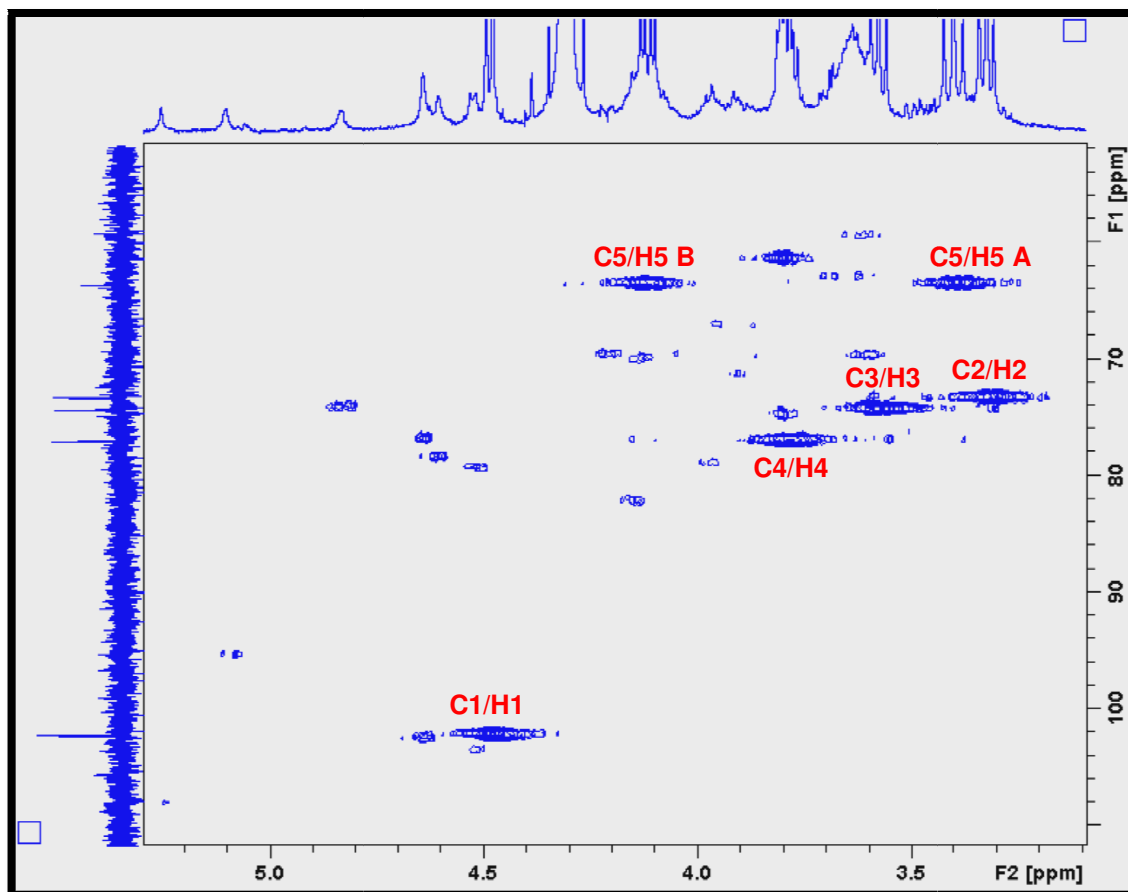


Figure 99: ^1H - ^{13}C HSQC spectrum of *B. breve* UCC2003 EPS -ve confirms the positions of carbons

The ^{13}C and ^1H chemical shifts of *B. breve* UCC2003 EPS-ve strain are provided in table: 19.

Table 19: Chemical shifts of ^{13}C and ^1H of *B. breve* UCC2003 EPS-ve

^{13}C chemical shifts		^1H chemical shifts	
C1	102.2	H1	4.47
C2	73.3	H2	3.30
C3	74.3	H3	3.56
C4	76.9	H4	3.78
C5	63.5	H5	3.37
C5	63.5	H5	4.11

By observing the values of ^1H and ^{13}C , it appears to confirm the presence of free ribose in the sample and it likely that this is derived from the carbon feed used to grow the culture²⁵¹.

5.6.1.1 *2D-NMR analysis of the EPS recovered from*
Bifidobacterium breve Strain UCC2003:

When the 2D-NMR spectra of the EPS +ve strains were studied (^1H - ^1H COSY {Fig. 100} and ^1H - ^{13}C HSQC {Fig. 101}), the analysis suggested that three of the signals are anomeric resonances (labelled as “A”) while four signals are ring protons.

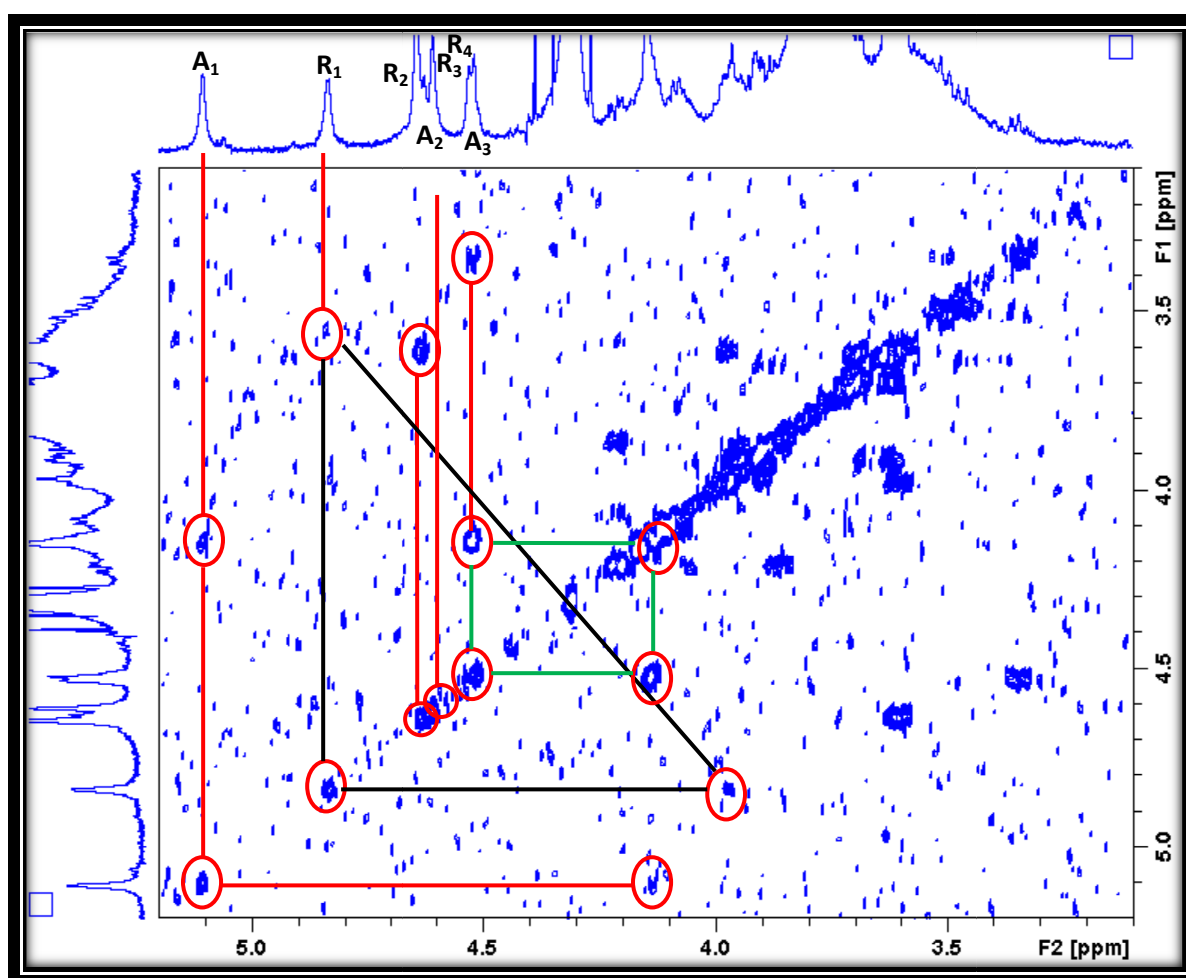


Figure 100: ^1H - ^1H COSY spectrum of *B. breve* UCC2003 EPS +ve with connectivity

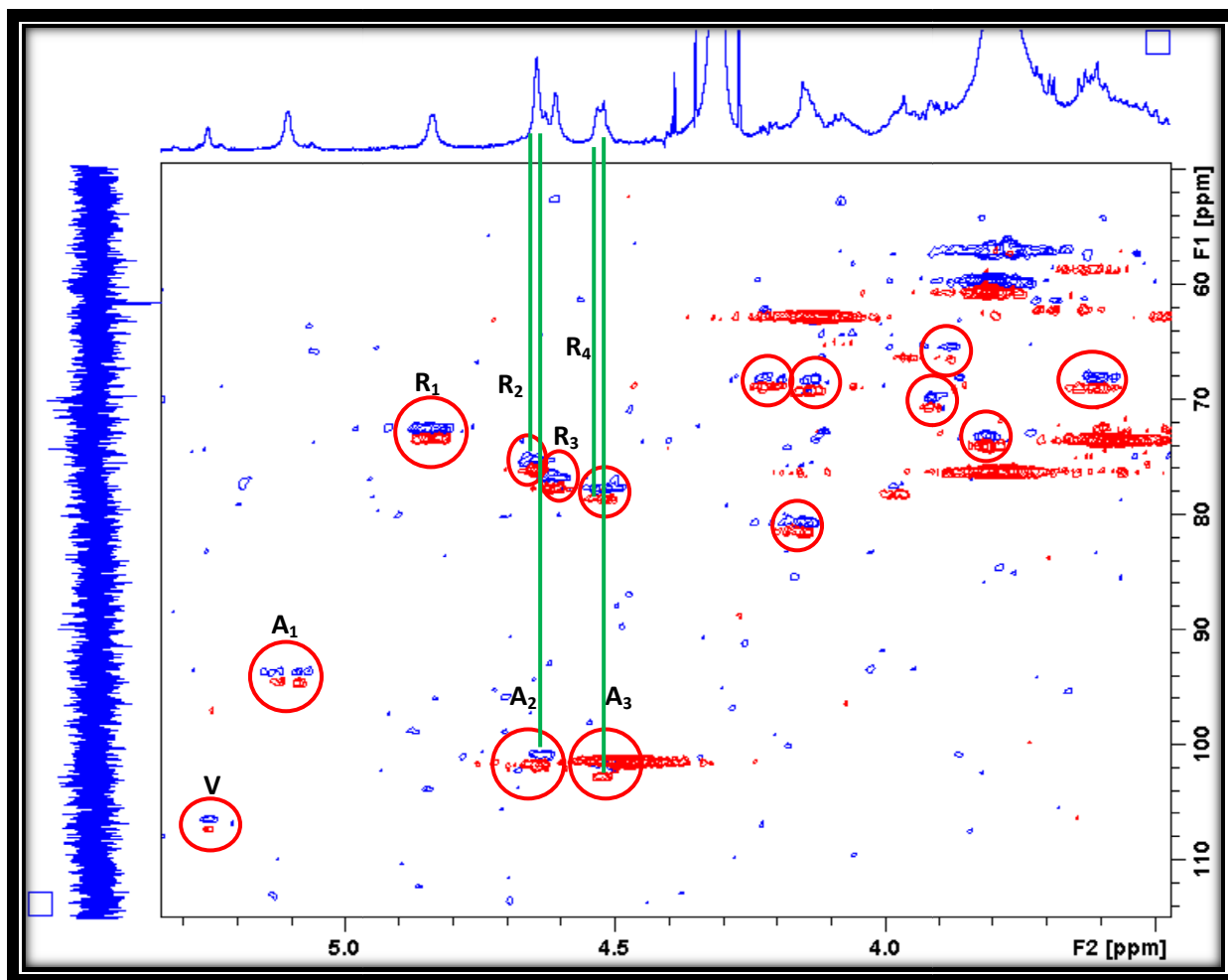


Figure 101: Comparison of ^1H - ^{13}C HSQC EPS +ve (blue) with EPS -ve (red)

The high field shift of these ring protons suggests that they may be associated with a furanose ring system. Unfortunately, due to the limited amount of material available it has not been possible to get any additional information about the structure of the EPS.

To extend this work further, the academics from University College Cork, sent samples labelled as *B. breve* UCC2003 (DEL) deletion mutant. In the deletion mutant, they have deleted the gene that produces EPS in *Bifidobacteria breve* UCC2003. To confirm the hypothesis, the crude proton NMR spectrum was run to check to see if EPS was being produced or not.

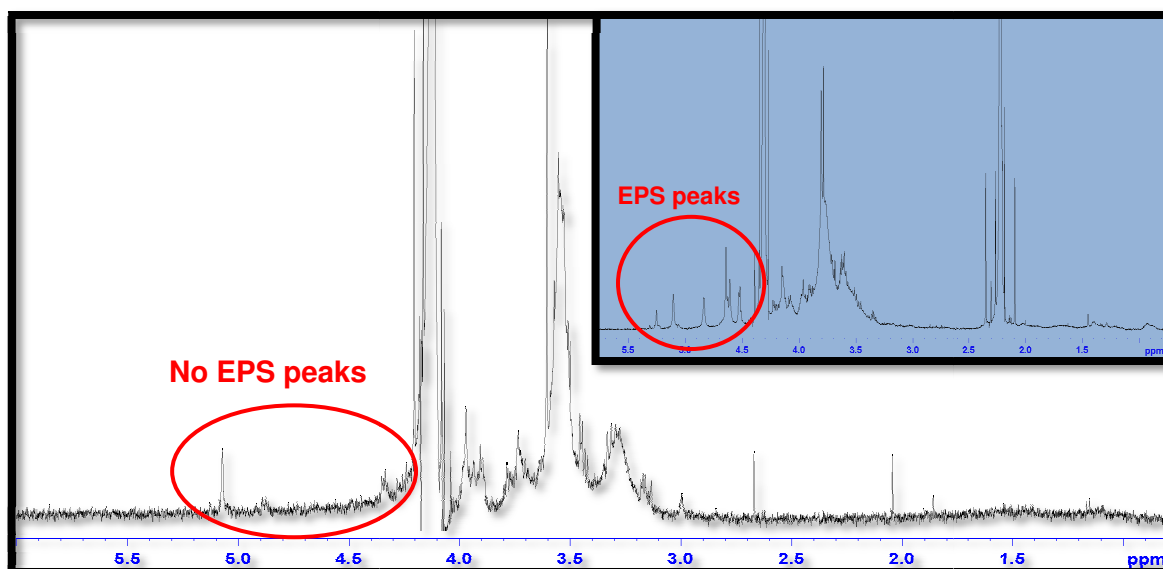


Figure 102: Proton NMR of *B. breve* UCC2003 (del) showing no EPS peaks, as compared to Fig. 95

After close observation of the *B. breve* UCC2003 (del) NMR spectrum (Fig. 102), it reveals that there were no anomeric peaks present at the region 4.2–5.2ppm and only the variable peaks can be detected.

5.7 Conclusion:

The samples from *B. breve* UCC2003 strain were analyzed by 1D and 2D-NMR experiments. The positions of the resonances from the ^1H - ^{13}C HSQC NMR experiment (fig. 99) suggested the EPS that was recovered from the *B. breve* strains is a β -(1 \rightarrow 6)-linked glucan (polysaccharides of D-glucose, linked by β -glycosidic bonds. These β -glucans are referred to as β -1,3/1,6 linked glucans²⁵² and are present in yeast (bakers' yeast) and mushrooms (shiitake), whereas β -1,3/1,4 linked glucans are present in oat and barley). It is anticipated that β -glucans are present in the EPS sample but with different percentages. The samples labelled as EPS +ve and EPS -ve shows some EPS peaks but due to the complex nature of the EPS and due to the limited amount of material available it has not been possible to fully characterize the EPS. Even though EPS -ve means it should not contain any EPS peaks, NMR spectra show some peaks that relate to EPS. Whereas, for the deletion mutant, it confirms the hypothesis, that once the gene that is associated with the production of EPS is altered/deleted, the *Bifidobacterium spp.* is not able to produce EPS.

5.8 Future Work:

To complete the structural determination of the EPS produced by *B. breve* UCC2003, detailed 2D-NMR experiments are required and this will only be possible once more sample is available. Researchers at Cork are currently undertaking large scale fermentations in order to generate large quantities of EPS.

6. CONCLUSIONS

6. Overall Conclusion:

Different analytical techniques (NMR, GC-MS, HPAEC-PAD, SEC-MALLS and Ion Exchange Chromatography) were used for the analysis of biofilmS produced by pathogenic and friendly bacteria. For the biofilm produced by the pathogenic bacterium i-e: *Campylobacter jejuni*, the bacterium produces an α -dextran on exposure to α -amylase. For the biofilm produced by friendly bacterium-*Bifidobacterium animalis* subsp. *lactis*, three main polysaccharides were observed and they are all consisted of rhamnose, galactose and glucose in different ratio. The linkage analysis showed that the EPS is a complex mixture of different sugars that are linked with 1 \rightarrow 3, 1 \rightarrow 4 or 1 \rightarrow 6 linkages. SEC-MALLS analysis showed that the EPS is composed of high molecular weight, medium molecular weight and low molecular weight EPS. NMR analysis shows the presence of a complex structure and provided evidence for the presence of a β (1 \rightarrow 6) linked glucan. The biofilm produced by *Bifidobacterium breve* UCC2003 were analysed by NMR and the results showed that the EPS is β (1 \rightarrow 6) linked glucan. These β -glucans are present in different percentages in different samples of *B. breve*. Incontrast for the deletion mutant (the gene that is associated with the production of EPS is altered/deleted) the *Bifidobacterium* spp. is not able to produced EPS.

6.1 Future work:

Due to the low quantity of available EPS and the complex nature of the EPS produced by *Bifidobacterium animalis* subsp. *lactis*, it was not possible to fully characterize the EPS. Further work is required to separate the EPS samples, this may be best achieved using either molecular biology or biochemical techniques or by adjusting the fermentation conditions to provide a single EPS structures in higher yields. Researchers at the University of Huddersfield (under the supervision and guidance of Prof. Andrew P. Laws) are undertaking large scale fermentations in order to generate large quantities of EPS for detailed structural analysis.

7. REFERENCES

7. References:

1. Flitsch, S., L., Ulijin R V. Sugars tied to the spot. *Nature* 2003;421:219–20.
2. Albert Lehninger, David Nelson MC. *Principles of Biochemistry*. 2nd ed. New York: Worth Publishers; 1992.
3. Campbell NJ. *Biology*. 4th ed. New York: 1996.
4. King MW. *Biochemistry of Carbohydrates* [Internet]. 1996 [cited 2011 Jul 13]; Available from: <http://themedicalbiochemistrypage.org/carbohydrates/html>
5. Linhardt, R. J., Hakim, A., Liu J. *Acidic Polysaccharides: Their modification and potential uses*. Iowa City:
6. Hancock IC. Bacterial cell surface carbohydrates: structure and assembly. *PubMed* 1997;25:183–7.
7. Berg, J. M., John, L. T., Lubert S. *Biochemistry*. 6th ed. New York: W. H. Freeman and Company; 2007.
8. Volhardt, k. P. C., Schore NE. *Organic Chemistry: Structure and Function*. 6th ed. New York: W. H. Freeman and Company; 2010.
9. Scrimgeour, M., Laurence, A., Horton, H., Robert H. *Biochemistry*. 2nd ed. Toronto: Prentice Hall; 1994.
10. Mathews, C. K., Van holde, K. E., Ahern KG. *Biochemistry*. 3rd ed. Prentice Hall; 1999.
11. Giraud, M. F., Naismith JH. The rhamnose pathway. *Curr Opin Struct Biol* 2000;10:687–96.
12. Chen, H. L., Lu, Y. H., Lin, J., Ko LY. Effects of fructooligosaccharide on bowel function and indicators of nutritional status in constipated elderly men. *Nutr Res* 2000;20:1725–33.
13. Mussatto, S. I., Mancilha IM. Non-digestible oligosaccharides: a review. *Carbohydr Polym* 2007;68:587–97.
14. Varki, A., Cummings, R., Esko J., Freeze, H., Stanley, P. Bertozzi, C., Hart, G., Etzler M. *Essentials of Glycobiology*. 2nd ed. Cold Spring Harbor Lab. Press; 2008.
15. Varki, A., Cummings, R., Esko, J., Freeze, J., Hart, G., Marth J. *Essentials of Glycobiology*. Cold Spring Harbor Lab. Press; 1999.
16. Gary, J. X., Rolfe BG. Exopolysaccharide production in *Rhizobium* and its role in invasion. *Mol Microbiol* 1990;4:1425–31.
17. Ielpi, L., Couso, R.O., Dankert MA. Xanthan gum biosynthesis: pyruvic acid residues are transferred from phosphoenolpyruvate to the pentasaccharides-P-P-lipid. *Biochem Biophys Res Commun* 1981;102:1400–8.
18. Isaac, D. H., Isaac DH. Bacterial Polysaccharides. In: *Polysaccharides: Topics in Structure and Morphology*. Weinheim, Germany: VCH Publishers; 1985.
19. Nic, M., Jirat, J., Kosata B. IUPAC, *Compendium of Chemical Terminology, The Gold Book*. 2nd ed. Oxford, UK: Blackwell Scientific Publications; 2006.
20. Romeo T. *Bacterial Biofilms, Current topics in Microbiology and Immunology*. Berlin: Springer; 2008.

21. Anderson, A. J., Haywood, G. W., Daws EA. Biosynthesis and composition of bacterial poly(hydroxyalkanoates). *Int J Biol Macromol* 1990;12:102–5.
22. Rehm, B. H. A., Valla S. Bacterial alginates: Biosynthesis and applications. *Appl Microbiol Biotechnol* 1997;48:281–8.
23. Cerning J. Production of exopolysaccharides by lactic acid bacteria and dairy propionibacteria. *Lait* 1995;75:463–72.
24. Rehm BHA. Bacterial polymers: Biosynthesis, modifications and applications. *Nat Rev Microbiol* 2010;8:578–92.
25. Sutherland IW. Bacterial Exopolysaccharides, In *Advances in Microbial Physiology*. New York: Academic Press; 1972.
26. Ruas-Madiedo, Hugenholtz, J., Zoon P. An overview of the functionality of exopolysaccharides produced by lactic acid bacteria. *Int Dairy J* 2002;12:163–71.
27. Sutherland IW. Novel and established applications of microbial polysaccharides. *Trends Biotechnol* 1998;16:41–6.
28. Otero, A., Vincenzini M. Extracellular polysaccharide synthesis by *Nostoc* strains as affected by N source and light intensity. *J Biotechnol* 2003;102:143–52.
29. Ruas – Madiedo, P. And Reyes-Gavilla'n CG d. I. Invited Review: Methods for the screening, Isolation and characterization of Exopolysaccharides produced by Lactic acid bacteria. *J Dairy Sci* 2005;88:843–56.
30. Baron S. *Medical Microbiology*. 4th ed. Texas: University of Texas, Galveston, Texas; 1996.
31. Knox, K.W., Wicken AJ. Immunological properties of teichoic acids. *Bacteriol Rev* 1973;37:215–57.
32. Garimella, R., Halye, J.L., Harrison, W., Klebba, P.E., Rice CV. Conformation of the phosphate D-alanine zwitterions in bacterial teichoic acid from nuclear magnetic resonance spectroscopy. *Biochemistry* 2009;48:9242–9.
33. Murray, P. R., Rosenthal, k. S., Kobayashi, G. S., Pfaller MA. *Medical Microbiology*. 4th ed. Michigan: Univesity of Michigan; 2002.
34. Madigan, M.T., Martinko, J.M. Parker J. *Brock Biology of Microorganism*. 10th ed. New Jersey: Prentice Hall; 2003.
35. Kroncke, K. D., Golecki, J. R., Jann K. Further electron microscopic studies on the expression of *Escherichia coli* group II capsules. *J Bacteriol* 1990;172:3469–72.
36. Willis, L. M., Whitfield C. Structure, biosynthesis and function of bacterial capsular polysaccharides synthesized by ABC transporter-dependent pathways. *Carbohydr Res* 2013;378:35–44.
37. Pelkonen, S., Hayrinen, J., Finne J. Polyacrylamide gel electrophoresis of the capsular polysaccharides of *Escherichia coli* K1 and other bacteria. *J Bacteriol* 1988;172:2646–53.
38. Kumar, A.S., Mody, K., Jha B. Bacterial exopolysaccharides – a perception, Review article. *J Basic Microbiol* 2007;47:103–17.
39. Stewart-Tull DES. The immunological activities of bacterial peptidoglycans. *Annu Rev Microbiol* 1980;34:311–40.
40. Heumann, D., Barras, C., Severin, A., Glauser, M. P., Tomasz A. Gram-positive cell walls stimulate synthesis of tumor necrosis factor alpha and interleukin-6 by human monocytes. *Infect Immun* 1994;62:2715–21.

41. Nwodo, U. U., Green, E., Okoh AI. Bacterial Exopolysaccharides: Functionality and Prospects. *Int J Mol Sci* 2012;13:14002–15.
42. Costerton, J. W., Stewart, P. S., Greenberg EP. Bacterial biofilms: A common cause of persistent infections. *Science* (80-) 1999;284:1318–22.
43. Cerning J. Exocellular polysaccharides produced by lactic acid bacteria. *Fed Eur Microbiol Soc Microbiol Lett* 1990;187:113–30.
44. De Vuyst, L. DB. Heteropolysaccharides from lactic acid bacteria. *Fed Eur Microbiol Soc Microbiol Rev* 1999;23:153–77.
45. Ahmed, N. H., El Soda, M., Hassan A. N., Frank J. Improving the textural properties of an acid-coagulated (Karish) cheese using exopolysaccharide producing cultures. *Food Sci Technol* 2005;38:343–7.
46. Jolly L. Exploiting exopolysaccharides from lactic acid bacteria. *Antonie Van Leeuwenhoek* 2002;82:367–74.
47. Robitaille, G., Tremblay, A., Moineau, S., St-Gelais, D., Vadeboncoeur, D., Britten M. Fat-free yoghurt made using a galactose-positive exopolysaccharide-producing recombinant strain of *Streptococcus thermophilus*. *J Dairy Sci* 2009;92:477–82.
48. Tiekink, M., Ganzle MG. Exopolysaccharides from cereal associated lactobacilli. *Trends Food Sci Technol* 2005;16:79–84.
49. Patel, S., Majumder, A., Goyal A. Potentials of exopolysaccharides from lactic acid bacteria. *Indian J Microbiol* 2012;52:03–12.
50. Azeredo, J., Oliveira R. The role of exopolymer in the attachment of *Sphingomonas paucimobilis*. *Biofouling* 2000;16:59–67.
51. Salminen S. Functional food science and gastrointestinal physiology and function. *Br J Nutr* 1998;80:147–71.
52. Rehm BHA. Microbial production of biopolymers and polymer precursors: applications and perspectives. Norfolk, UK: Caister Academic Press; 2009.
53. Ullrich M. Bacterial Polysaccharides: Current Innovations and Future Trends. Norfolk, UK: Caister Academic Press; 2009.
54. Macedo, M. G., Lacroix, C., Gardner, N. J., Champagne CP. Effect of medium supplementation on exopolysaccharide production by *Lactobacillus rhamnosus* RW-9595 M in whey permeate. *Int Dairy J* 2002;12:419–26.
55. Vanhooren, P. and Vandamme EJ. Biosynthesis, physiological role, use and fermentation process characteristics of bacterial exopolysaccharides. *Recent Res Dev Ferment Bioeng* 1998;1:253–300.
56. Schaechter M. The desk encyclopaedia of Microbiology. Elsevier Ltd; 2004.
57. Ruffing ACRR. Metabolic engineering of microbes for oligosaccharides and polysaccharides synthesis. *Microb Cell Fact* 2006;:05–25.
58. Freitas, F. , Alves, V. D., Torres, C. A. V., Cruz, M., Sousa, I., Melo, M., J., Ramos, A. M., Reis MAM. Fucose-containing exopolysaccharide produced by the newly isolated *Enterobacter* strain A47 DSM 23139. *Carbohydr Polym* 2011;:159–65.

59. Cuthbertson, L. Mainprize, i. L., Naismith, J. H., Whitfield C. Pivotal roles of the outer membrane polysaccharide export and polysaccharide copolymerase protein families in export of extracellular polysaccharides in Gram negative bacteria. *Microbiol Mol Biol Rev* 2009;73:155–77.
60. Rosalam, S., England R. Review of xanthan gum production from unmodified starches by *Xanthomonas campestris* sp. *Enzym Microb Technol* 2006;39:197–207.
61. Freitas, F., Alves, V. D., Pais, J., Costa, N., Oliveira, C., Mafra, L., Hilliou, L., Oliveira, R., Reis MA. Characterization of an extracellular polysaccharide produced by a *Pseudomonas* strain grown on glycerol. *Bioresour Technol* 2009;100:859–65.
62. Bajaj, I.B., Survase, S. A., Saudagar, P. S., Singhal RS. Gellan gum: fermentative production, downstream processing and applications. *Food Technol Biotechnol* 2007;45:341–54.
63. Pena, C., Millan, M., Galindo E. Production of alginate by *Azotobacter vinelandii* in a stirred fermentor simulating the evolution of power input observed in shake flasks. *Process Biochem* 2008;43:775–8.
64. Wang, X., Yuan, Y., Wang, K., Zhang, D., Yang, Z., Xu P. Deproteinization of gellan gum produced by *Sphingomonas paucimobilis* ATCC 31461. *J Biotechnol* 2007;128:403–7.
65. Ayala-Hernández, I., Hassan, A., Goff, H. D., Orduria, R. M. D. CM. Production, isolation and characterization of exopolysaccharides produced by *Lactococcus lactis* subsp. *cremoris* JFR1 and their interaction with milk proteins: Effect of pH and media composition. *Int Dairy J* 2008;18:1109–18.
66. Synge, R. L. M., Tiselius A. Fractionation of hydrolysis products of amylose by electrokinetic ultrafiltration in an agar-agar jelly. *Biochem J* 1950;41–2.
67. McBain, J. W., Kistler SS. Membranes for ultrafiltration of graduated fineness down to molecular sieves. *J Gen Physiol* 1928;12:187–200.
68. Hong, P., Koza, S., Bouvier ESP. A review: Size exclusion chromatography for the analysis of protein biotherapeutics and their aggregates. *J Liq Chromatogr Relat Techniques* 2012;35:2923–50.
69. Wheaton, R. M., Bauman WC. Non-Ionic separations with ion exchange resins. *Ann N Y Acad Sci* 1953;57:159–76.
70. Clark RT. Separation of glycerol from polyhydric alcohol mixture by nonionic exclusion. *Anal Chem* 1958;30:1676–8.
71. Lindquist, B., Storgards T. Molecular sieving properties of Starch. *Nature* 1955;175:511–2.
72. Barth, H.G., Boyes, B.E., Jackson C. Size exclusion chromatography. *Anal Chem* 1994;66:595–620.
73. Joachim Weiss J. *Hand book of Ion Chromatography*. 3rd ed. Germany: Wiley-VCH Verlag GmbH and Co; 2004.
74. Bhaskar, P. V., Grossart, H. P., Bhosle, N. B., Simon M. Production of macroaggregates from dissolved exopolymeric substances (EPS) of bacterial and diatom origin. *Fed Eur Microbiol Soc Microbiol Lett* 2005;53:255–64.
75. Albersheim, P, Nevins, D. J., English, P. D., Karr A. A method for the analysis of sugars in plant cell wall polysaccharides by gas liquid chromatography. *Carbohydr Res* 1967;5:375–87.
76. Blake, J. D., Richards GN. A critical re-examination of problems inherent in compositional analysis of hemicelluloses by gas liquid chromatography. *Carbohydr Res* 1970;14:375–87.

77. Gerwig, G. J., Kamerling, J. P. , Vliegthart JFG. Determination of the D and L configuration of neutral monosaccharides by high resolution capillary GLC. *Carbohydr Res* 1978;62:349–57.
78. Rocklin, R. D., Pohl, C. A. Determination of carbohydrates by anion exchange chromatography with pulsed amperometric detection. *J Liq Chromatogr* 1983;6:1577–90.
79. Bennek, J. A., Rolf, D., and Gray GR. 1,4-Anhydro-2,3,6-Tri-O-methyl-D-glucitol formed as an artefact in the reductive cleavage of permethylated 1,4-linked glucopyranosides. *J Carbohydr Chem* 1983;2:385–93.
80. Cerning, J., Buillanne, C., Desmazeaud, M. J., Landon M. Isolation and characterization of exocellular polysaccharide produced by *Lactobacillus bulgaricus*. *Biotechnol Lett* 1986;8:625–8.
81. Cerning, J., Buillanne, C., Desmazeaud, M. J., Landon M. Exocellular polysaccharide production by *Streptococcus thermophilus*. *Biotechnol Lett* 1988;10:255–60.
82. Cerning, J., Renard, C. M. G. C., Thibault, J. F., Bouillanne, C., Landon, M., Desmazeaud, M., Topisirovic, L. Carbon source requirements for exopolysaccharide production by *Lactobacillus casei* CG11 and partial structure analysis of the polymer. *Appl Environ Microbiol* 1994;60:3914–9.
83. Gruter, M., Leeflang, B. R., Kuiper, J., Kamerling, P., Vliegthart FG. Structure of the exopolysaccharide produced by *Lactococcus lactis* subspecies *cremoris* H414 grown in a defined medium or skimmed milk. *Carbohydr Res* 1992;231:273–91.
84. Gruter, M., Leeflang, B. R., Kuiper, J., Kamerling, P., Vliegthart FG. Structural characterization of the exopolysaccharide produced by *Lactobacillus delbrueckii* subspecies *bulgaricus* rr grown in skimmed milk. *Carbohydr Res* 1993;239:209–26.
85. Lemoine, J., Chirat, F., Wieruszkeski, J. M., Strecker, G., Favre, N., Neeser JR. Structural characterization of the exocellular polysaccharides produced by *Streptococcus thermophilus* Sfi39 and Sfi12. *Appl Environ Microbiol* 1997;63:3512–8.
86. Calsteren, V. M. R., Roblot, C. P., Begin, A., Roy D. Structure determination of the exopolysaccharide produced by *Lactobacillus rhamnosus* strains RW-9595M and R. *Biochem J* 2002;363:07–17.
87. De Vuyst, L., Vanderveken, F., Ven, S. V. D. DB. Production by and isolation of exopolysaccharides from *Streptococcus thermophilus* grown in a milk medium and evidence for their growth-associated biosynthesis. *J Appl Microbiol* 1998;84:1059–68.
88. Levander, F., Svensson, M., Radstrom P. Small scale analysis of exopolysaccharides from *Streptococcus thermophilus* grown in a semi-defined medium. *BMC Microbiol* 2001;1:01–23.
89. Cataldi, T. R. I. , Campa, C., Benedetto GED. Carbohydrate analysis by high performance anion exchange chromatography with pulsed amperometric detection: The potential is still growing. *Fresenius' J Anal Chem* 2000;368:739–58.
90. Lee YC. High performance anion exchange chromatography for carbohydrate analysis. *Anal Biochem* 1990;189:151–62.
91. Henshall A. High performance anion exchange chromatography with pulsed amperometric detection (HPAEC-PAD): a powerful tool for the analysis of dietary fiber and complex carbohydrates. New York: Marcel Dekker, Incorporated; 1999.
92. Lange, N. A., Dean JA. *Lange's Handbook of Chemistry*. 13th ed. New York: McGraw Hill; 1985.
93. Matute, A.I.R., Hernandez, O. H., Sanchez, S. R., Sanz, M. L., Castro M. Derivatization of carbohydrates for GC and GC-MS analyses. *J Chromatogr B* 2011;879:1226–40.

94. Medeiros, P. M., Simoneit BRT. Analysis of sugars in environmental samples by gas chromatography-mass spectrometry. *J Chromatogr A* 2007;114:271–8.
95. Gonzalez, S. G., Jimenez, J. R., Capote, F. P., Castro MDL. Quantitative and qualitative sugar profiling in olive fruits, leaves and stems by gas chromatography-tandem mass spectrometry (GC-MS/MS) after ultrasound assisted leaching. *J Agric Food Chem* 2010;58:12292–9.
96. Gerwig, G. J., Kamerling, Vliegthart JFG. Determination of the absolute configuration of monosaccharides in complex carbohydrates by capillary GLC. *Carbohydr Res* 1979;77:01–7.
97. Wang, Q., Fang Y. Analysis of sugars in traditional Chinese drugs. *J Chromatogr B* 2004;812:309–24.
98. You, J., Sheng, X., Ding, C., Sun, Z., Suo, Y., Wang, H., Li Y. Detection of carbohydrates using new labelling reagent 1-(2-naphthyl)-3-methyl-5-pyrazolone by capillary zone electrophoresis with absorbance (UV). *Anal Chim Acta* 2008;609:66–75.
99. Xia, L., Sun, Z. W., Li, G. L., Suo, Y. R., You JM. A sensitive analytical method for the component monosaccharides of the polysaccharides from a Tibetan herb *Potentilla anserina* L by capillary zone electrophoresis with UV detector. *Eur Food Res Technol* 2010;88:754–62.
100. Wang, T., Yang, X., Wang, D., Jiao, Y., Wang, Y., Zhao Y. Analysis of compositional carbohydrates in polysaccharides and foods by capillary electrophoresis. *Carbohydr Polym* 2012;88:754–62.
101. Gao, Q., Araia, M., Leak, C., Emmer A. Characterization of exopolysaccharides in marine colloids by capillary electrophoresis with indirect UV detection. *Anal Chim Acta* 2010;662:193–9.
102. Rizelio, V. M., Tenfen, L., Silveira, R. D., Gonzaga, L. V., Costa, A. C. O., Fett R. Fast determination of cations in honey by capillary electrophoresis. *Talanta* 2012;99:450–6.
103. Soga, T., Heiger DN. Simultaneous determination of monosaccharides in Glycoproteins by Capillary Electrophoresis. *Anal Biochem* 1998;261:73–8.
104. Hu, Q., Zhou, T., Hu, G., Fang Y. Determination of sugars in Chinese traditional drugs by CE with amperometric detection. *J Pharm Biomed Anal* 2002;30:1047–53.
105. Yang, Z., Wang, H., Zang, W., Wang, Q., He, P., Fang Y. Analysis of Neutral Sugars of *Asparagus officinalis* Linn. Polysaccharides by CZE with Amperometric Detection. *Chromatographia* 2012;75:297–304.
106. Cao, Y., Wang, Y., Chen, X., Ye J. Study on sugar profile of rice during ageing by capillary electrophoresis with electrochemical detection. *Food Chem* 2004;86:131–6.
107. Luo, P., Zang, F., Baldwin RP. Comparison of metallic electrodes for constant-potential amperometric detection of carbohydrate, amino acids and related compounds in flow systems. *Anal Chim Acta* 1991;244:169–78.
108. Stellner, K., Saito H., Hakomori, S. I. Determination of amino sugar linkages in glycolipids by methylation: Aminosugar linkages of ceramide pentasaccharides of rabbit erythrocytes and of Forssman antigen. *Arch Biochem Biophys* 1973;155:464–72.
109. Lama, L., Nicolaus, B., Calandrelli, V., Manca, M. C., Romana, I., Gambacorta A. Effect of growth conditions on endo- and exopolymer biosynthesis in *Anabaena cylindrical* 10 C. *Phytochemistry* 1996;42:655–9.
110. Poli, A., Anzelmo, G., Nicolaus B. Bacterial exopolysaccharides from extreme marine habitats: production, characterization and biological activities. *Mar Drugs* 2010;8:1779–802.

111. Lavery SB. Glycopeptides and related compounds. New York: Marcel Dekker, Incorporated; 1997.
112. Purdie, T., Irvine JC. The alkylation of sugars. *J Chem Soc* 1903;83:1021–37.
113. Denham, W.S., Woodhouse HJ. The methylation of cellulose. *J Chem Soc* 1913;103:1735–41.
114. Sandford, P. A., Conrad HE. The Structure of the *Aerobacter aerogenes* A3(S1) Polysaccharide. I. A Reexamination using improved procedures for methylation analysis. *Biochemistry* 1966;5:1508–17.
115. Hakomori S. A rapid permethylation of glycolipid and polysaccharide catalyzed by methylsulfinyl carbanion in dimethyl sulfoxide. *J Biochem* 1964;55:205–8.
116. Phillips, L. R., Fraser BA. Methylation of carbohydrates with dimethyl potassium in dimethyl sulfoxide. *Carbohydr Res* 1981;90:149–52.
117. Blakeney, A. B., Stone BA. Methylation of carbohydrates with lithium methylsulphinyll carbanion. *Carbohydr Res* 1985;140:319–24.
118. Needs, P. W., Selvendran RR. An improved methylation procedure for the analysis of complex polysaccharides including resistant starch and a critique of the factors which lead to undermethylation. *Phytochem Anal* 1993;4:210–6.
119. Harris, P. J., Henry, R. J., Blakeney, A. B., Stone BA. An improved procedure for the methylation analysis of oligosaccharides and polysaccharides. *Carbohydr Res* 1984;127:59–73.
120. Zahringer, U., Rietschel ET. 2-deoxy-1,3,4,5,6-penta-O-methyl-2-(N-methylacetamido)-D-glucitol and derivatives undergo C-methylation at the N-methylacetamido group on repeated hakomori methylation. *Carbohydr Res* 1986;152:81–7.
121. Ciucanu, I., Kerek F. A simple and rapid method for the permethylation of carbohydrates. *Carbohydr Res* 1984;131:209–17.
122. Brimacombe, J. S., Jones, B. D., Stacev, M., Willard JJ. Alkylation of carbohydrates using sodium hydride. *Carbohydr Res* 1966;2:167–9.
123. Anderson, D. M. W., Stefani A. The degradation of acidic polysaccharides during structural analysis involving permethylation. *Anal Chim Acta* 1979;105:147–52.
124. Ciucanu, I., Costello EC. Elimination of oxidative degradation during per-O-methylation of carbohydrates. *J Am Chem Soc* 2003;125:16213–9.
125. Ciucanu, I., Konig WA. Immobilization of peralkylated β -cyclodextrin on silica gel for high performance liquid chromatography. *J Chromatogr A* 1984;286:179–85.
126. Ciucanu, I. CL. Avoidance of degradation during the methylation of uronic acids. *Carbohydr Res* 1990;206:731–4.
127. Lindberg, B., Lonngren J. Methylation analysis of complex carbohydrates: general procedure and application for sequence analysis. *Methods Enzymol* 1978;50:03–33.
128. Basu, B. B., Zajicek, J., Bondo, G., Zhao, S., Kubsch, M., Carmichael, I., Serianni AS. Deuterium nuclear spin lattice relaxation times and quadrupolar coupling constants in isotopically labelled saccharides. *J Magn Reson* 2000;144.
129. Penglis AAE. Fluorinated Carbohydrates. *Adv Carbohydr Chem Biochem* 1981;38:195–285.
130. Csuk, R., Glanzer BI. NMR spectroscopy of fluorinated monosaccharides. *Adv Carbohydr Chem Biochem* 1988;46:73–177.

131. Michalik, M., Hein, M., Frank M. NMR spectra of fluorinated carbohydrates. *Carbohydr Res* 2000;327:185–218.
132. Wyatt PJ. Light scattering and the absolute characterization of macromolecules. *Anal Chim Acta* 1993;272:01–4.
133. Doco T. Structure of an exocellular polysaccharide produced by *Streptococcus thermophilus*. *Carbohydr Res* 1990;198:313–21.
134. Leeflang BR. Structural elucidation of glycoprotein glycans and of polysaccharides by NMR spectroscopy. *J Biotechnol* 2000;77:115–22.
135. Harding LP. Structural characterization of a perdeuteriomethylated exopolysaccharide by NMR spectroscopy: characterization of the novel exopolysaccharide produced by *Lactobacillus delbrueckii* subsp. *bulgaricus* EU23. *Carbohydr Res* 2003;338:61–7.
136. Maina NH. NMR spectroscopic analysis of exopolysaccharides produced by *Leuconostoc citreum* and *Weissella confusa*. *Carbohydr Res* 2008;343:1446–55.
137. Fisherman ML. Screening the physical properties of novel *Pseudomonas* exopolysaccharides by HPSEC with multi-angle light scattering and viscosity detection. *Carbohydr Polym* 1997;32:213–21.
138. Hwang HJ. Production and molecular characteristics of four groups of exopolysaccharides from submerged culture of *Phellius gilvus*. *J Appl Microbiol* 2003;94:708–19.
139. Zimm BA. Apparatus and methods for measurement and interpretation of the angular variation of light scattering; preliminary results on polystyrene solutions. *J Chem Phys* 1948;16:1099–116.
140. Gilbert, R. G., Hess, M., Jenkins, A. D., Jones, R. G., Kratochvil, P., Stepto RFT. Dispersity in polymer science (IUPAC Recommendations 2009). *Pure Appl Chem* 2009;81:351–3.
141. Churms SC. Recent progress in carbohydrate separation by HPLC based on size exclusion. *J Chromatogr A* 1996;720:151–66.
142. Oliva, A., Llabres, M., Farina JB. Comparative study of protein molecular weights by size exclusion chromatography and laser light scattering. *J Pharm Biomed Anal* 2001;25:833–41.
143. Folta-Stogniew, E., Williams KR. Determination of molecular masses of proteins in solution: Implementation of an HPLC size exclusion chromatography and laser light scattering service in core laboratory. *J Biomol Techniques* 1999;10:51–63.
144. Ritter, A., Schmid, M., Afflter S. Determination of molecular weights by size exclusion chromatography (SEC)-Results of Round Robin Tests. *Polym Test* 2010;29:945–52.
145. Andersson, M., Wittgren, B., Wahlund KG. Accuracy in multiangle light scattering measurements for molar mass and radius estimations: Model calculations and experiments. *Anal Chem* 2003;75:4279–91.
146. Tumolo, T., Angnes, L., Baptista MS. Determination of the refractive index increment (dn/dc) of molecule and macromolecule solutions by surface plasmon resonance. *Anal Biochem* 2004;333:273–9.
147. Kratochvil P. *Classical light scattering from polymer solutions*. New York: Elsevier Ltd; 1987.
148. Catalgil-Giz, Giz, A., Alb, A. M., Reed WF. Absolute online monitoring of acrylic acid polymerization and the effect of salt and pH on reaction kinetics. *J Appl Polym Sci* 2004;91:1352–9.

149. Feijter, J. A., Benjamins, J., Veer FA. Ellipsometry as a tool to study the adsorption of synthetic and biopolymers at the air-water interface. *Biopolymers* 1978;17:1759–72.
150. Ahmed, A. E. R., Labavitch JM. A simplified method for accurate determination of cell wall uronide content. *J Food Biotechnol* 1977;1:361–5.
151. Selvendran, R. R., March, J. R., Ring SG. Determination of aldoses and uronic acid contents of vegetable fiber. *Anal Biochem* 1979;96:282–92.
152. Filisetti-Cozzi, T. M. , Carpita NC. Measurement of uronic acids without interference from neutral sugars. *Anal Biochem* 1991;197:157–62.
153. Dubois, M., Gilles, K.A., Hamilton, J.K., Rebers, P.A., Smith F. Colorimetric method for determination of sugars and related substances. *Anal Chem* 1956;28:350–6.
154. Dreywood R. Qualitative test for carbohydrate material. *Ind Eng Chem Anal Ed* 1946;18:499.
155. Sheng, G.P., Yu, H.Q., Li XY. Extracellular polymeric substances (EPS) of microbial aggregates in biological waste water treatment systems: a review. *Biotechnol Adv* 2010;28:882–94.
156. Blumenkranz, N., Asboe Hansen G. New method for quantitative determination of uronic acid. *Anal Biochem* 1973;54:484–9.
157. Melton, L. D., Smith BG. Determination of the Uronic acid content of plant cell walls using a colorimetric assay, *Current Protocols in Food Analytical Chemistry. Cell Wall Polysaccharides* 2001;:E3.3.1–3.3.4.
158. Snelling, W.J., Matsuda, M., Moore, J.E., Dooley JSG. Under the microscope – *Campylobacter jejuni*. *Lett Appl Microbiol* 2005;41:297–302.
159. Sellu DP. *Campylobacter enterocolitis: general and surgical aspects*. *Post Grad Med J* 1986;62:719–26.
160. Zilbauer, M., Dorrell, N., Wren, B.W., Bajaj-Elliot M. *Campylobacter jejuni*-mediated disease pathogenesis: an update. *Trans R Soc Trop Med Hyg* 2008;102.
161. Engberg J. Contributions to the epidemiology of *Campylobacter* infections. *Dr Med Sci* 2006;53:361–89.
162. Elizabeth K. Human infections with *vibrio fetus* and a closely related *vibrio*. *J Infect Dis* 1957;101:119–28.
163. Elizabeth K. The laboratory recognition of *vibrio fetus* and a closely related *vibrio* isolated from cases of human vibriosis. *Ann N Y Acad Sci* 1962;98:700–11.
164. Butzler, J. P., Dekeyser, P., Detrain, M., Dehaen F. Related *vibrio* in stools. *J Pediatr* 1973;82:493–5.
165. Skirrow MB. *Campylobacter enteritis: a new disease*. *Br Med J* 1977;2:09–11.
166. Freidman, C., Neimann, J., Wegener, H., Tauxe RV. *Epidemiology of Campylobacter jejuni infections in the United States and other industrialized nations*. 2nd ed. Washington: ASM International; 2000.
167. Hunt, J. M., Abeyta, C., Tran T. *Campylobacter*. 8th ed. *Bacteriological Analytical Manual*; 1998.
168. Pooley, C., Wood, D. Scanning Electron Microscope Image No. K11505-1. *Agric Res Serv* 2006;
169. Virusi B. TEM image of *Campylobacter jejuni* [Internet]. 2009 [cited 2012 Jul 10]; Available from: [www.waterscan.rs/images/virusi-bakteriji/Campylobacter_jejuni B&W1.jpg](http://www.waterscan.rs/images/virusi-bakteriji/Campylobacter_jejuni_B&W1.jpg)

170. Karlyshev, A.V., Henderson, J., Ketley, J.M., Wren BW. Procedure for the investigation of bacterial genomes: random shot-gun cloning, sample sequencing and mutagenesis of campylobacter jejuni. *Biotechniques* 1999;26:50–6.
171. Karlyshev, A.V., Linton, D. Gregson. N.A., Lastovica, A.J., Wren BW. Genetic and biochemical evidence of a campylobacter jejuni capsular that accounts for penner serotype specificity. *Mol Microbiol* 2000;35:529–41.
172. Karlyshev, A.V., McCrossan, M.V., Wren BW. Determination of polysaccharide capsule in campylobacter jejuni using electron microscopy. *Infect Immune* 2001;69:5921–4.
173. Ketley JM. Pathogenesis of enteric infection by campylobacter. *Microbiology* 1997;143:05–21.
174. Fricker, C.R., Girdwood, R.W.A., Munro D. A comparison of procedures for the isolation of campylobacters from seagull faeces. *J Hyg Cambridge* 1983;91:445–50.
175. Simmons, N. A., Gibbs FJ. *Campylobacter* spp. in oven ready poultry. *J Infect* 1979;1:159–62.
176. Luechtefeld, N.A., Wang GWL. *Campylobacter fetus* subsp. *jejuni* in a turkey processing plant. *J Clin Microbiol* 1981;13:266–8.
177. Karmali, M.A., Fleming PC. *Campylobacter* enteritis. *Can Med Assoc J* 1979;120:1525–32.
178. Wright, E.P., Knowles MA. Beta – lactamase production by *Campylobacter jejuni*. *J Clin Pathol* 1980;33:904–5.
179. Allos BM. *Campylobacter jejuni* infections: update on emerging issues and trends. *Clinical Infect Dis* 2001;32:1201–6.
180. Field, P. I., Swerdlow MD. *Campylobacter jejuni*. *Clin Lab Med* 1999;19:489–504.
181. Buswell, C.M., Herlihy, Y.M., Lawrence, L.M., Mcguiggan, J.T., Marsh, P.D., Keevil, C.W., Leach SA. Extended survival and persistence of *Campylobacter* spp. in water and aquatic biofilm and their detection by immunifluorescent antibody and rRNA staining. *Appl Environ Microbiol* 1998;49:733–45.
182. Costerton, J.W., Lewandowski, Z., Caldwell, D.E., Korber, D.R., Lappin-Scot HM. Microbial biofilms. *Annu Rev Microbiol* 1995;49:711–45.
183. Jowiya, W., Hussain, H., Sadiq, S., Williams, L.K., Trantham, E.K., Stephenson, H., Wren, B.W., Elliott, M.B., Cogan, T.A., Laws, A.P., Wade, J, Dorrell, N., Allan E. Secretion of an α -dextran in response to host pancreatic α -amylase promotes biofilm formation and chicken colonisation by *Campylobacter jejuni*. 2014;
184. Sutherland IW. The biofilm matrix – an immobilized but dynamic microbial environment. *Trends Biotechnol* 2001;9:222–7.
185. McLennan, M.K., Ringoir, D.D., Fridrich, E., Svensson, S.L., Wells, D.H., Jarrell, H., Szymanski, C.M., Gaynor EC. *Campylobacter jejuni* biofilms upregulated in the absence of the stringent response utilize a calcofluor white reactive polysaccharide. *J Bacteriol* 2008;190:1097–107.
186. Joshua, G.W., Guthrie-Irons, C., Karlyshev, A.V., Wren BW. Biofilm formation in *Campylobacter jejuni*,. *J Bacteriol* 2006;152:387–96.
187. Biermann, C.J., McGinnis GD. *Analysis of Carbohydrates by GLC and MS*. CRC Press; 1989.
188. Ibrahim, S.A., Bezkorovainy A. Inhibition of *E. Coli* by *Bifidobacteria*. *J Food Prot* 1993;56:713–5.
189. Scardovi V. *Irregular nonsporing gram-positive rods: Genus Bifidobacterium*, Orla-Jensen 1924. 9th ed. Baltimore: Williams and Wilkins Co; 1986.

190. Lee, J.H., O'Sullivan D. Genomic Insights into Bifidobacteria. *Microbiol Mol Biol Rev* 2010;74:378–416.
191. Klijn, A., Mercenier, A., Arigoni F. Lessons from the genomes of Bifidobacteria. *Fed Eur Microbiol Soc Microbiol Rev* 2005;29:491–509.
192. Tissier H. Le bacterium coli et la reaction chromophile d' Escherich. *Criit Rev Soc Biol* 1899;51:943–5.
193. Tissier H. Recherches sur la flore intestinale des nourrissons (etat normal et pathologique. Thesis1900;
194. Orla-Jenson S. La classification des bacteries lactiques. *Lait* 1924;4:468–74.
195. Poupard, J. A., Husain, I., Norris RF. Biology of the Bifidobacteria. *Bacteriol Rev* 1973;37:136–65.
196. Bergey, D. H., Buchanan, R. E., Gibbons NE. *Bergey's manual of determinative bacteriology*. 8th ed. Baltimore: Williams and Wilkins Co; 1974.
197. Pokusaeva, K., Fitzgerald, G. F., Sinderen D V. Carbohydrate metabolism in Bifidobacteria. *Genes Nutr* 2011;6:285–306.
198. Ventura, M., Turrioni, F., Motherway, M.C., MacSharry, J., Sinderen D V. Host microbe interactions that facilitate gut colonization by commensal Bifidobacteria. *Trends Microbiol* 2012;20:467–76.
199. Motherway, M. C., Zomer, A., Leahy, S. C., Reunanen, J., Bottacini F. Functional genome analysis of *Bifidobacterium breve* UCC2003 reveals type of IVb tight adherence (Tad) pili as an essential and conserved host-colonization factor. In: *Proceedings of the National Academy of Sciences*. USA: 2011. page 11217–22.
200. Zomer, R. L., Motherway, M. C., Sinderen, D. V., Margolles A. Discovering novel bile protection systems in *Bifidobacterium breve* UCC2003 through functional genomics. *Appl Environ Microbiol* 2011;78:1123–31.
201. Ventura, M., Turrioni, F., Sinderen D V. Probiogenomics as a tool to obtain genetic insights into adaptation of probiotic bacteria to the human gut. *Bioeng Bugs* 2012;3:73–9.
202. Mitsuoka T. Bifidobacteria and their role in human health. *J Ind Microbiol* 1990;6:263–8.
203. Mitsuoka T. Taxonomy and Ecology of Bifidobacteria. *Bifidobact Microflora* 1984;3:11–28.
204. Simpson, P.J., Ross, R.P., Fitzgerald, G.F., Stanton C. *Bifidobacterium psychraerophilum* sp. nov. and *Aeriscardovia aeriphila* gen. nov., sp. nov., isolated from a porcine caecum. *Int J Syst Evol Microbiol* 2004;54.
205. Waddington, L., Cyr, T., Hefford, M., Hansen, L.T., Kalmokoff M. Understanding the acid tolerance response of Bifidobacteria. *J Appl Microbiol* 2010;108:1408–20.
206. Simpson, P.J., Stanton, C., Fitzgerald, G.F., Ross RP. Intrinsic tolerance of *Bifidobacterium* species to heat and oxygen and survival following spray drying and storage. *J Appl Microbiol* 2005;99:493–501.
207. Kawasaki, S., Mimura, T., Satoh, T., Takeda, K., Niimura Y. Response of the microaerophilic *Bifidobacterium* species, *B. boum* and *B. thermophilum*, to oxygen. *Appl Environ Microbiol* 2006;72:6854–8.
208. Sanchez, B., Champomier, M. C., Collado, C., Anglade, P., Baraige, F., Sanz, Y., Reyes, C. G., Margolles, A., Zagorec M. Low pH adaptation and the acid tolerance response of *Bifidobacterium longum* biotype *longum*. *Appl Environmental Microbiol* 2007;73:6450–9.

209. Sanchez, B., Champomier, M. C., Lauridsen, B., Madiedo, P. R., Anglade, P., Baraige, F., Reyes, C. G., Johansen, E., Zagorec, C, Margolles A. Adaptation and response of *Bifidobacterium animalis* subsp. *lactis* to bile: a proteomic and physiological approach. *Appl Environmental Microbiol* 2007;73:6757–67.
210. Bernstein, H., Payne, C.M., Bernstein, C., Schneider, J., Beard, S.E., Crowley CL. Activation of the promoters of genes associated with DNA damage, oxidative stress, ER stress and protein malfolding by the bile salt, deoxycholate. *Toxicol Lett* 1999;108:37–46.
211. Palframan, R.J., Gibson, G.R., Rastall RA. Carbohydrate preferences of *Bifidobacterium* species isolated from the human gut. *Curr Issues Intest Microbiol* 2003;4:71–5.
212. Sela, D.A., Price, N.P.J., Mills DA. *Metabolism of Bifidobacteria: In Bifidobacteria: Genomics and Molecular Aspects*. Norfolk, UK: Caister Academic Press; 2010.
213. De Vuyst, L., Moens, F., Selak, M., Riviere, A., Leroy F. Summer Meeting, Growth and physiology of *Bifidobacteria*, Review Article. *J Appl Microbiol* 2013;116:477–91.
214. Amaretti, A., Bernardi, T., Tamburini, E., Zanoni, S., Lomma, M., Matteuzzi, D., Rossi M. Kinetics and metabolism of *Bifidobacterium adolescentis* MB 239 growing on glucose, galactose, lactose and galactooligosaccharides. *Appl Environ Microbiol* 2007;73:3637–44.
215. Falony, G., Lazidou, K., Verschaeren, A., Weckx, S., Maes, D. , De Vuyst L. In vitro kinetic analysis of fermentation of prebiotic inulin-type fructans by *Bifidobacterium* species reveals four different phenotypes. *Appl Environ Microbiol* 2009;75:454–61.
216. Van der Meulen, R., Makras, L., Verbrugghe, K., Adriany, T. , De Vuyst L. In vitro kinetic analysis of oligofructose consumption by *Bacteroides* and *Bifidobacterium* spp. indicates different degradation mechanisms. *Appl Environ Microbiol* 2006;72:1006–12.
217. Van der Meulen, R., Adriany, T., Verbrugghe, K., De Vuyst L. Kinetic analysis of bifidobacterial metabolism reveals a minor role for succinic acid in the regeneration of NAD⁺ through its growth associated production. *Appl Environ Microbiol* 2006;72:5205–10.
218. Metchnikoff E. *Optimistic studies* New York. New York: Putman’s Sons; 1908.
219. Lilly, D. M., Stillwell RH. Probiotics: Growth promoting factors produced by microorganisms. *Science* (80-) 1965;147:747–8.
220. Parker RB. Probiotics, the other half of the antibiotic story. *Anim Nutr Heal* 1974;29:04–8.
221. Fuller R. Probiotics in man and animals. *J Appl Bacteriol* 1989;66:365–78.
222. Salminen, S., von Wright, A., Morelli, L., Marteau, P., Brassart, D., de Vos, W. M., Fonden, R., Saxelin, M., Collins, K., Mogensen, G., Birkeland, S. E., Mattila-Sandholm T. Demonstration of safety of Probiotics – a review. *Int J Food Microbiol* 1998;44:93–106.
223. FAO/WHO. Health and nutritional properties of probiotics in food including powder milk with live lactic acid bacteria. 2001;:01–134.
224. Oyetayo, V.O., Oyetayo FL. Potentials of probiotics as biotherapeutic agents targeting the innate immune system. *African J Biotechnol* 2005;4:123–7.
225. Candy, D. C. A., Heath, S. J., Lewis, J. D. N., Thomas L V. Probiotics for the young and the not so young. *Int J Dairy Technol* 2008;61:215–21.
226. Sharma, M., Devi M. Probiotics: A comprehensive approach toward health foods. *Crit Rev Food Sci Nutr* 2014;54:537–52.

227. Marafon, A. P., Sumi, A., Granato, D., Alcantara, M. R., Tamime, A. Y., Oliveira MN. Effects of partially replacing skimmed milk powder with dairy ingredients on rheology, sensory profiling and microstructure of probiotic stirred-type yogurt during cold storage. *J Dairy Sci* 2011;94:5330–40.
228. Saccaro, D. M., Tamime, A. Y., Pilleggi, A.N.A., Oliveira MN. The viability of three probiotic organisms grown with yoghurt starter cultures during storage for 21 days at 4 °C. *Int J Dairy Technol* 2009;62:397–404.
229. Vinderola, C. G., Mocchiutti, P., Reinheimer JA. Interactions among lactic acid starter and probiotic bacteria used for fermented dairy products. *J Dairy Sci* 2002;85:721–9.
230. Meile, L., Ludwig, W., Rueger, U., Gut, C., Kaufmann, P., Dasen, G., Wenger, S., Teuber M. *Bifidobacterium lactis*. sp. nov., a moderately oxygen tolerant species isolated from fermented milk. *Syst Appl Microbiol* 1997;20:57–64.
231. Aguilar, G. S., Dawson, H., Restrep., M., Andrews. K., Vinyard, B., Urban JF. Detection of *Bifidobacterium animalis* subsp. *lactis* (Bb12) in the intestine after feeding of sows and their piglets. *Appl Environ Microbiol* 2008;74:6338–47.
232. Jungersen, M., Wind, A., Johansen, E., Christensen, J.E., Lauridsen, B. S., Eskesen D. Review: The science behind the probiotic strain *Bifidobacterium animalis* subsp. *lactis* Bb12. *Microorganisms* 2014;2:92–110.
233. Madiedo, P. R., Moreno, J. A., Salazar, N., Delgado, S., Mayo, B., Margolles, A., Gavila'n CGR. Screening of exopolysaccharide producing *Lactobacillus* and *Bifidobacterium* strains isolated from the human intestinal microbiota. *Appl Environ Microbiol* 2007;92:4385–8.
234. Madiedo, P. R., Medrano, M., Salazar, N., Gavila'n, C. G. R., Perez, P. F., Abraham AG. Exopolysaccharides produced by *Lactobacillus* and *Bifidobacterium* strains abrogate in vitro the cytotoxic effect of bacterial toxins on eukaryotic cells. *J Appl Microbiol* 2010;109:2079–86.
235. Salazar, N., Prieto, A., Leal, J. A., Mayo, B., Gancedo, J. C., Gavila'n, C. G. R., Madiedo PR. Production of exopolysaccharides by *Lactobacillus* and *Bifidobacterium* strains of human origin and metabolic activity of the producing bacteria in milk. *J Dairy Sci* 2009;92:4158–68.
236. Leivers, S., Cantabrana, C. H., Robinson, G., Margolles, A., Madiedo, P. R., Laws AP. Structure of the high molecular weight exopolysaccharides produced by *Bifidobacterium animalis* subsp. *lactis* IPLA-R1 and sequence analysis of its putative *eps* cluster. *Carbohydr Res* 2011;346:2710–7.
237. Zdrovenko, E.L., Kachala, V.V., Sidarenka, A.V., Izhik, A.V., Kisileva, E.P., Shashkov, A.S., Novik, G.I., Knirel YA. Structure of the cell wall polysaccharides of probiotic bifidobacteria *Bifidobacterium bifidum* BIM B-46512. *Carbohydr Res* 2009;344:2417–20.
238. Kohno, M.; Suzuki, S.; Kanaya, T.; Yoshino, T.; Matsuura, Y.; Asada, M.; Kitamura S. Structural characterization of the extracellular polysaccharide produced by *Bifidobacterium longum* JBL0513. *Carbohydrate Polym* 2009;77:351–7.
239. Kunerth, W.H., Youngs VL. Modification of anthrone, carbazole, and orcinol reaction for quantification of monosaccharides. *Cereal Chem* 1984;61:344–9.
240. Ventura, M., O'Flaherty, S., Claesson, M. J., Turrone, F., Klaenhammer, T. R., van Sinderen, D., O' Tool PW. Genome scale analyses of health promoting bacteria: Probiogenomics. *Nat Rev* 2009;7:61–71.

241. Salazar, N., Madiedo, P. R., Kolida, S., Collins, M., Rastall, R., Gibson G. Exopolysaccharides produced by *Bifidobacterium longum* IPLA E44 and *Bifidobacterium animalis* subsp. *lactis* IPLA RI modify the composition and metabolic activity of human faecal microbiota in pH-controlled batch cultures. *Int J Food Microbiol* 2009;135:260–7.
242. Dan, T., Fukuda, K., Sugai-Bannai, M., Takakuwa, N., Motoshima, H., Urashima T. Characterization and expression analysis of the exopolysaccharides gene cluster in *Lactobacillus fermentum* TDS030603. *Biosci Biotechnol Biochem* 2009;73:2656–64.
243. Dabour, N., LaPointe G. Identification and molecular characterization of the chromosomal exopolysaccharides biosynthesis gene cluster from *Lactococcus lactis* subsp. *cremoris* SMQ-461. *Appl Environ Microbiol* 2005;71:7414–25.
244. Bottacini, F., Motherway, M. C., Kuczynski, J., Connell, K. J., Serafini, F., Duranti, S., Milani, C., Turrone, F., Lugli, G. A., Zomer, A., Zhurina, D., Riedel, C., Ventura, M., Sinderen D V. Comparative genomics of the *Bifidobacterium breve* taxon. *BioMed Cent* 2014;15:170.
245. Turrone, F., Sinderen, D. V., Ventura M. Genomics and ecological overview of the genus *Bifidobacterium*. *Int J Food Microbiol* 2011;3:420–5.
246. Chartier, M. P. C., Vinogradov, E., Sadovskaya, I., Andre, G., Mistou, M. Y., Cout, P. T., Furlan, S., Bidnenko, E., Courtin, p., Pechoux, C., Hols, P., Dufrene, y. F., Kulakauskas S. Cell surface of *Lactococcus lactis* is covered by a protective polysaccharide pellicle. *J Biol Chem* 2010;285:10464–71.
247. Fanning, S., Hall, L. J., Sinderen D V. *Bifidobacterium breve* UCC2003 surface exopolysaccharides production is a beneficial trait mediating commensal-host interaction through immune modulation and pathogen protection. *Gut Microbes* 2012;3:420–5.
248. Lebeer, S., Verhoeven, T. L. A, Francius, G., Schoofs, G., Lambrichts, I., Dufrene, Y., Vanderleyden, J., Sigrid, c. J. Keersmaecker, S. CJ. Identification of a gene cluster for the biosynthesis of a long, galactose-rich exopolysaccharide in *Lactobacillus rhamnosus* GG and functional analysis of the priming glycosyltransferase. *Appl Environmental Microbiol* 2009;75:3554–63.
249. Alhudhud, M., Humphreys, P., Laws P. Development of a growth medium suitable for exopolysaccharide production and structural characterization by *Bifidobacterium animalis* ssp. *Lactis* AD011. *J Microbiol Methods* 2014;100:93–8.
250. Kollar, R., Reinholds, B. B., Petrokova, E., Yeh, H. J. C., Ashwell, G., Drgonova, J., Kapteyn, J. C., Klis, F. M., Cabib E. Architecture of the yeast cell wall- β (1,6)-Glucan interconnects mannoprotein, β (1,3)-Glucan and Chitin. *J Biol Chem* 1997;272:17762–75.
251. Ruiz, L., Motherway, M. C., Lanigan, N., Sinderen DV. Transposon mutagenesis in *Bifidobacterium breve*: Construction and characterization of a Tn5 Transposon mutant library for *Bifidobacterium breve* UCC2003. *Plus One* 2013;8:e64699.
252. Miura, N. N. , Ohno, N. , Aketagawa, J. , Tamura, H. , Tanaka, S. , Yadomae T. Blood clearance of (1-3)-beta-D-glucan in MRL *Ipr/Ipr* mice. *Fed Eur Microbiol Soc Immunol Med Microbiol* 1996;13:51–7.

8. PUBLICATIONS

8. Publications:

1. Jowiya, W., Hussain, H., **Sadiq, S.**, Williams, L.K., Trantham, E.K., Stephenson, H., Wren, B.W., Elliott, M.B., Cogan, T.A., **Laws, A.P.**, Wade, J, Dorrell, N., Allan, E. Secretion of an α -dextran in response to host pancreatic α -amylase promotes biofilm formation and chicken colonisation by *Campylobacter jejuni*, in press.